INVESTIGATING PROTEIN-DNA INTERACTIONS AT REPLICATION FORKS BY PHOTO-CROSSLINKING

by

CAROL MICHELLE MANHART

B.S., University of Arizona, 2006

A thesis submitted to the

Faculty of the Graduate School of the

University of Colorado in partial fulfillment

of the requirement for the degree of

Doctor of Philosophy

Department of Chemistry and Biochemistry

2013

This thesis entitled:
Investigating protein-DNA interactions at replication forks by photo-crosslinking
written by Carol Michelle Manhart
has been approved for the Department of Chemistry and Biochemistry

Charles McHenry

Robert Kuchta

Date

The final copy of this thesis has been examined by the signatories, and we find that both the content and the form meet acceptable presentation standards of scholarly work in the above mentioned discipline

Manhart, Carol Michelle (Ph.D., Biochemistry)

Investigating protein-DNA interactions at replication forks by photo-crosslinking

Thesis directed by Professor Charles McHenry

During Okazaki fragment synthesis, the replicase must distinguish single-stranded from duplex DNA in advance of the polymerase to sense completion of a fragment and trigger release from the lagging strand. A hypothesis in the literature proposes that the τ subunit (of the DnaX complex) directly senses completion of an Okazaki fragment. An alternative model suggests that the polymerase subunit senses conversion of a gap to a nick. I show using a novel phenyldiazirine photo-crosslinker linked to the 5-position of thymidylate that the τ subunit is not in position to distinguish gapped DNA from nicked DNA. The α subunit (the polymerase) is positioned to serve as the processivity sensor. Upon encountering duplex DNA, the polymerase likely changes conformation triggering its release from the lagging strand and the β processivity clamp, modulating its own affinity.

Unrepaired replication forks dissociate from the helicase and suffer collapse. PriA recognizes stalled replication forks and initiates interactions to reload the helicase and activate a previously stalled fork. I used a FRET helicase assay to develop a PriA-dependent helicase loading system in *E. coli* and *B. subtilis* and to identify a minimal substrate to support a photo-crosslinking study also discussed here. I discovered that PriA's ATPase activity dictates substrate specificity. I also show that PriA serves as a checkpoint protein by blocking the replicase from binding to stalled replication forks distinguishing between an alternative model.

SPP1 is a bacteriophage that infects *B. subtilis*. It encodes its own initiation proteins (origin binding protein, primosomal proteins, helicase, and single-strand binding protein (SSB)) but requires its host's primase and major replicative polymerase to replicate its genome. Both host and phage SSBs can support a reconstituted SPP1 system, but phage SSB does not support a reconstituted *B. subtilis* system. Using the *B. subtilis* FRET helicase assay, I show that phage SSB can substitute for the host's SSB in helicase reloading. Therefore the defect in the reconstituted system is not at the level of helicase loading or function and must occur after the helicase is loaded. I also show an absolute requirement on all SPP1 components in helicase reloading, including the origin binding protein (in a non-origin-containing template), which suggests a new role for this protein.

In collaboration with Tim Lohman's lab at Washington University, I have contributed to a study into the functions of the C-terminal tails of SSB. SSB functions as a homotetramer whose four C-terminal tails interact with many other proteins necessary for DNA replication and repair. In an *in vivo* assay, an SSB variant that has two functional C-terminal tails supports viability in *E. coli*. An SSB variant that has one C-terminal tail is dominant lethal. In a reconstituted rolling circle *E. coli* replication system, there is a defect in coupled synthesis that causes a two-fold decrease in lagging strand synthesis relative to the leading strand using the variant with one C-terminal tail. This is significant, but does not sufficiently account for the lethality *in vivo*. Using the *E. coli* FRET helicase assay, I show that the variant with one C-terminal tail causes the PriA replication restart pathway to be inactive. Presumably, all replication forks suffer a collapse if leading and lagging strand synthesis are uncoupled. Thus, the replication

restart pathway becomes even more critical. The SSB variant with one C-terminal tail does not support this pathway, which provides an explanation for the lethality.

Photo-crosslinking is used to probe the dynamics of *E. coli* primosomal proteins on a replication fork in the replication restart pathway. Both the specific locations on the DNA where PriA and the other protein machinery are bound and how the proteins change position as the complex protein machinery is assembled are identified. I have determined the binding positions of SSB and revealed a novel interaction between a replication fork and SSB. I have also determined that PriA excludes SSB at the replication fork. When the DnaB helicase is loaded onto the lagging strand, it interacts with the displaced strand and diffuses at least three nucleotides into the duplex. Interestingly, DnaB is seen to only make weak contact with the lagging strand arm.

ACKNOWLEDGEMENTS

None of the work presented here would have been possible without the support and encouragement of my mentors, colleagues, friends, and family.

I would like to thank first and foremost my advisor Charles McHenry. He has provided countless hours of support, patience, and advice. I would also like to thank all of my labmates over the years. In particular, I thank Paul Dohrmann who has been a source of encouragement and wisdom throughout my years in the lab. Quan Yuan has been my labmate and classmate for the last 7 years and I am grateful for all of her support. Also, thanks to Diane Hager for all of her help in everything. Nothing would get done without her.

Teaching undergraduates has been a truly rewarding experience for me. Interacting with the students and helping them develop an interest and love of science has been a profound source of encouragement, enlightenment, and an important reality-check. Several individuals stand out as having made this a valuable experience. In particular, I am very grateful to Margaret Asirvatham, Veronica Bierbaum, Laurel Hyde-Boni, and Kristen Roy who have fostered my enthusiasm for teaching and supported me during my time as a TA. I have been lucky enough to have worked with these individuals and been given the chance to cultivate my own teaching style with their help.

I would like to thank my family for all of their love and encouragement throughout my entire life. My parents, Daryl Manhart and Marilyn Rice, have long supported my interest in science and have always pushed me forward. They have always been an unwavering source of comfort and support. I would also like to thank my brother,

Michael, for inspiring me and making sure that I stay up to date on pop culture. My grandparents Ross and Marie Rice and Jess and Dorothy Manhart have all contributed to my successes in life.

I would also like to thank the family I have gained while in Boulder. I thank my dog Murphy, who reminds me every day not to take anything too seriously. I also cannot adequately express how thankful I am to Zeb Kramer for not only supporting me and encouraging me throughout graduate school but also making me excited for what lies ahead.

CONTENTS

TABLE

FIGURE

CHAPTER 1

Introduction

1.1 BACKGROUND

All organisms must be able to replicate their genomes efficiently and accurately to survive. Replication begins at chromosomal origins where the DnaA origin-binding protein (working with a complex system of proteins) loads the helicase onto DNA to first establish a replication fork. At the fork, the helicase interacts with the primase (DnaG) which synthesizes primers on the lagging strand to be used in Okazaki fragment synthesis [1]. These primers are extended by the polymerase, which is a part of a large protein system collectively known as the replicase.

1.2 DNA POLYMERASE STRUCTURE AND FUNCTION

1.2.1 The Escherichia coli *system*

The major replicative enzyme that is responsible for the replication of the *Escherichia coli* (*E. coli*) chromosome is Polymerase III holoenzyme (Pol III HE or HE). This enzyme is comprised of ten subunits ($\alpha, \varepsilon, \theta, \beta, \tau, \gamma, \delta, \delta', \psi,$ and χ) [2–7]. The α, ε, and θ subunits form the core polymerase complex. The α subunit contains the catalytic site for polymerization [8], the ε subunit possesses 3' to 5' exonuclease activity [9], while

θ binds to and stabilizes the ε subunit [10–12]. The β subunit is a sliding clamp and processivity factor that tethers the polymerase to the DNA [13,14]. The DnaX complex, also known as the "clamp loader," typically consists of five protein subunits—two subunits of either τ or γ along with δ and δ' subunits [7,15–17]. The τ subunits dimerize Pol III and have ATPase activity necessary to load the β clamp [18,19]. γ has a similar function in terms of ATPase activity and β loading [16]. The δ subunit binds β during assembly as δ' creates a bridge between δ and the rest of the clamp loader complex [20,21]. ψ links the DnaX proteins to χ, while χ is involved in binding single-stranded binding protein (SSB) on the lagging strand during replication [22,23]. The arrangement of these subunits is depicted in Fig. 1.1.

The catalytic α subunit of Pol III HE uses three different domains in polymerization. The fingers domain interacts with an incoming nucleotide, while another domain (the palm) positions Mg^{2+} and is the catalytic site for nucleotide incorporation. The third domain, the thumb, interacts with the DNA substrate. In addition to domains involved in polymerization, the α subunit contains a histidinol phosphatase domain, an internal β binding domain, and a C-terminal domain that contains an oligonucleotide-binding (OB) fold, whose function remains mysterious [24,25].

It has been suggested that the OB fold might bind single-stranded template ahead of the 3'-end of the primer [24,25]. In a 4 Å resolution crystal structure of the α subunit bound to primer-template DNA, a region of electron density is observed near the OB fold, but the OB fold does not appear to be in position to interact with single-stranded template downstream of the primer [24]. This is more fully discussed in section 1.3.2 of this chapter and in Chapter 2.

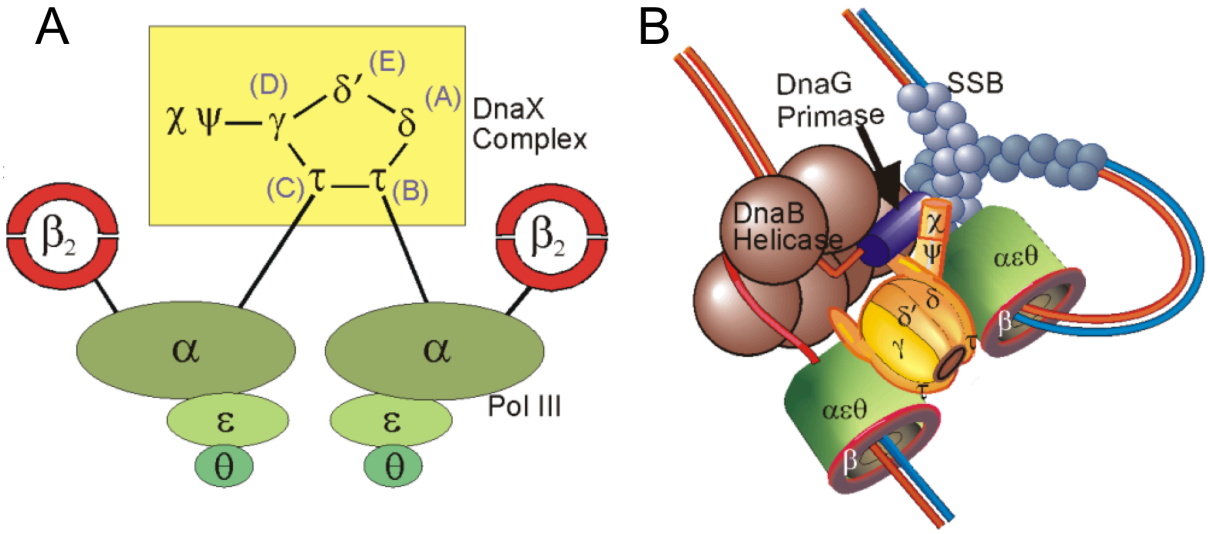

FIGURE 1.1
Proposed arrangement of Pol III HE subunits. (A) Known subunit interactions among Pol III HE proteins. (B) Cartoon depiction of Pol III HE on a replication fork with dimerized leading and lagging strand polymerases.

It was originally hypothesized that α has two β binding sites, a C-terminal site and an internal site. A study testing the importance of a suggested C-terminal β-binding site shows that when disrupted processive synthesis of DNA is unaffected, but interaction with the τ subunit is diminished [26]. Conversely, when the internal β binding site is mutated so that it no longer binds β, the reconstituted HE no longer synthesizes DNA processively, demonstrating the importance of this site for processivity [26]. A recent crystal structure reveals that the C-terminal domain of α interacts very closely with the C-terminal domain of τ [27], confirming the role of this domain in interacting with the clamp loader and excluding the possibility that β is interacting at this site.

1.2.2 The Bacillus subtilis *system*

In highly divergent, low G-C Gram-positive *Bacillus subtilis*, there are many conserved features compared to Gram-negative *E. coli*. In both systems, replication is initiated by a DnaA origin-binding protein, both systems have a replicase consisting of Pol III, β_2, and a DnaX complex [28], as well as a hexameric helicase that creates a replication fork [29].

In *E. coli*, Pol III HE is the only replicase. In *B. subtilis*, however, there are two Pol IIIs: PolC and DnaE [30]. DnaE in *B. subtilis* has the most in common with Pol III in *E. coli*, but it lacks a proofreading ε-type subunit. Both of these polymerases are required for a reconstituted replication system on a rolling circle template [31]. Lack of exonuclease proofreading activity, a slower than physiological elongation rate, and the ability to extend RNA primers (an activity not possessed by PolC) suggest DnaE has a

role more similar to Pol α in eukaryotes than Pol III in *E. coli* [31]. In eukaryotes, Pol α extends RNA primers before handing the substrate off to Pol δ to complete synthesis [32,33]. Such a handoff mechanism has been suggested in *B. subtilis* where DnaE is analogous to Pol α and PolC is analogous to Pol δ and ε in eukaryotes [31]. A genetic and functional comparison between *E. coli* and *B. subtilis* subunits is in Table 1.1.

1.3 CYCLING OF THE LAGGING STRAND POLYMERASE

During DNA replication, the new strand is synthesized in the 5' to 3' direction. The two template strands are antiparallel to one another and are read in the 3’ to 5’ direction. To preserve directionality, one of the DNA strands being synthesized is synthesized discontinuously (lagging strand), in short pieces known as Okazaki fragments, opposite replication fork movement.

1.3.1 Two non-exclusive models

E. coli’s Pol III HE can replicate more than 150 kilobases and possibly the entire chromosome before it dissociates [34,35]. During Okazaki fragment synthesis, however, the polymerase must be able to efficiently cycle to the next primer at the replication fork once Okazaki fragment is complete at a rate faster than Okazaki fragment production. The rate of fork progression in *E. coli* is approximately 600 nucleotides per second [36]. This is also the approximate rate at which the polymerase replicates on single-stranded template [37]. Most of the time is therefore spent

E. coli Gene	Subunit	Function	*B. subtilis* Gene
Elongation Components			
*dna*E	α	replicative polymerase (pol III type I)	*dna*E
	α + ε	replicative polymerase (pol III type II)	*pol*C
*dna*Q	ε	3'→5' proofreading exonuclease	*din*G
*hol*E	θ	no known function	not known
*dna*X	γ , τ	ATPase that loads β_2 onto DNA	*dna*X
*hol*A	δ	binds β, essential part of DnaX complex	*yqe*N
*hol*1B	δ'	essential part of DnaX complex	*hol*B
*hol*C	χ	non-essential, interacts with SSB	not known
*hol*D	ψ	non-essential, increases affinity of DnaX for δ'	not known
*dna*N	β	processivity factor	*dna*N
ssb	SSB	single stranded DNA binding protein	*ssb*
*dna*G	primase	RNA priming	*dna*G
Origin Initiation Proteins			
*dna*A		origin binding and initiation protein	*dna*A
*dna*B		replication fork helicase	*dna*C
*dna*C		accessory factor, loading DnaB helicase onto DNA	*dna*I
		interacts with DnaI in *B. subtilis* (helicase loading factor)	*dna*B
		interacts with DnaA and DnaB in *B. subtilis* (adaptor protein)	*dna*D
*pri*A		functions with DnaB and DnaD in *B. subtilis*, has helicase activity	*pri*A

TABLE 1.1
Comparison between *E. coli* and *B. subtilis* elongation components and origin initiation components.

elongating, and very little time remains for the polymerase to dissociate from the DNA, bind a new primer at the replication fork, and begin synthesis of a new Okazaki fragment. A processivity switch or sensor is needed to increase the rate of dissociation of the polymerase on the lagging strand.

Okazaki fragment synthesis requires the polymerase to rapidly dissociate to recycle to the next primer [38]. In this dissociation, HE subunits contacting DNA must dissociate from the DNA and from the β clamp which tethers the polymerase to the DNA [38].

There are two different, yet non-exclusive, models that describe the signal needed for the processivity switch. The first model is known as the signaling model. It is hypothesized that synthesis of a new primer at the replication fork causes the lagging strand to dissociate with or without having completed an Okazaki fragment [39]. A kinetic test of this model is discussed in Chapter 2. In the alternative model, it is proposed that the polymerase replicates to approximately the last nucleotide, thereby converting a gap to a nick, and collides with a completed Okazaki fragment triggering a communication circuit ultimately causing the lagging strand polymerase to dissociate and recycle to a new primer at the replication fork [38,40–42].

1.3.2 The processivity switch: the α versus τ debate

Intuitively, a processivity switch may sense the difference between gapped DNA and nicked DNA in order to modulate the affinity between the polymerase and the

lagging strand. There are many hypotheses available in the literature about which subunit or subunit element might be functioning as such a sensor.

The OB fold motif in the α subunit has been proposed to modulate processivity of the lagging strand polymerase [24,25]. In the structure of α bound to primer-template, the portion of the OB fold that commonly interacts with ssDNA (the β1-β2-β3 face) [43] is facing away from the template and is packed against a portion of the subunit that binds β [24]. The β1-β2 loop (a region known to contribute to ssDNA binding [43]) is accessible, however [24]. A study to test if this part of the OB fold is a processivity switch was performed where three basic residues in this loop were mutated to serine [44]. Upon mutation there was a reduced affinity of the polymerase for ssDNA [44]. Processivity was also diminished, but the effect was rescued by the τ subunit [44]. If a processivity switch were turned off by mutations, the polymerase should either dissociate from ssDNA immediately or remain bound even after encountering a primer, either way losing processivity. This suggests that the β1-β2 loop is likely not a processivity switch.

In comparing the apo and ternary structures of the α subunit, several elements undergo significant conformational changes. When primer-template is bound, the β binding domain rotates approximately 20º toward the DNA substrate [24]. This positions the β binding site near the duplex DNA ligand, where it can more productively interact with the β processivity clamp [24].

If the polymerase sensed the difference between gapped and nicked DNA, it follows that α would have an internal signaling pathway adjusting its own affinity for β. Evidence supporting this hypothesis shows that in the absence of DNA, α's active site

negatively regulates the β binding site [45], suggesting a communication channel between the catalytic site of α and the binding site for β [45]. A mutation study has shown that disrupting α's β binding site so that it no longer binds the β subunit, eliminates processive synthesis in a reconstituted HE assay [26]. This suggests that the α subunit is acting as a processivity sensor.

Despite evidence suggesting a direct role for α in modulating processivity, additional models have been suggested. A study asserts that τ's presence is required for the release of Pol III from β, but only when the primer has been extended to the last nucleotide, thereby creating a nick [40]. Using gel filtration data, it was observed that core polymerase elutes as a complex with τ in the presence of nicked DNA; with primed DNA, the core polymerase eluted as a complex with both τ and β [40]. A similar study claims that τ is the actual sensor for the completion of synthesis and that it binds DNA upstream of the replication fork in a mechanism where a one-nucleotide gap is distinguished from a nick [38].

Indeed a processivity switch likely contacts the primer terminus and a region on the DNA template immediately ahead of it in order to "feel" the difference between a gap and a nick. Previous work has shown the linear arrangement of subunits of HE along primer-template DNA [46]. The only verified contact of a DnaX protein (in that case γ) with the template was detected 13 nucleotides upstream of the primer terminus. So, it does not seem that τ is in the correct position to serve as a direct sensor. In Chapter 2, I identify the HE subunit that makes contact with single-stranded template ahead of the primer terminus and the 5'-end of a previously completed Okazaki fragment resolving this debate.

1.4 REPLICATION RESTART

1.4.1 Background

Damage to the genome occurs frequently under normal growth conditions, and unrepaired DNA can ultimately cause the helicase to dissociate and the replication fork to collapse. The ramifications of unrepaired forks can be catastrophic to the cell and pathways for repair and restart are crucial for complete and accurate replication [47]. In order to reactivate a collapsed fork, DNA recombination may occur and replication must be restarted in a process independent of the chromosomal origin [48]. Once a replication fork is repaired, the helicase needs to be reloaded onto the substrate prior to the re-initiation of the replicase. Since this process occurs in the absence of a chromosomal origin, it is thus independent of the origin-binding protein.

This pathway is dependent in both the *E. coli* and the *B. subtilis* systems on the PriA protein, which will be more fully described below. Null mutation studies have illustrated the importance of the PriA pathway *in vivo* [49,50]. In these studies, cells were viable, but they were extremely sick, underscoring the importance of the PriA-pathway in DNA replication [49,50].

1.4.2 The PriA-directed replication restart pathway in **E. coli**

A series of proteins known collectively as the primosome was first identified in ΦX174 bacteriophage replication [51,52]. It was later hypothesized that proteins of this

type participated at *E. coli* replication forks [1]. Genetic studies verified this hypothesis and also suggested the necessity of ΦX174-type primosomal proteins in DNA replication and in DNA repair and recombination pathways in *E. coli* [53–59].

PriA, PriB, PriC, DnaB, DnaC, DnaG, DnaT, and SSB are known to function at primosome assembly sites [51,52,60–62]. Of these, PriA, PriB, PriC, DnaT, DnaB, and DnaC are known as the preprimosome.

PriA recognizes stalled replication forks and directs a series of protein-protein interactions that reload the DnaB helicase and activate a previously stalled replication fork [63–65]. It has ATPase activity and can unwind duplex DNA in the 3' to 5' direction [66]. It is believed that this activity is used to unwind duplex DNA on the lagging strand arm to make a landing site for DnaB helicase [67].

A system dependent on PriA, PriB, and DnaT to restart a replication fork has been defined, while another pathway dependent on PriC coexists in *E. coli* [68]. Although many genetic studies have been performed determining the protein requirements for replication restart, and biochemical studies have illustrated interactions between the required proteins and DNA, the specific sequence of events that take place in restarting a stalled fork and how these proteins bind and function together at a replication fork are not yet well understood.

It is known that at replication forks, PriA interacts with SSB [69] and also interacts with PriB [70], a paralog of SSB [71–73]. PriB enables interaction between PriA and DnaT, which is a requirement for PriA-directed replication restart, yet its specific function is unknown [74,75]. DnaB (helicase) and DnaC (helicase loader) form a

complex in solution [76]. This complex is believed to then be recruited by the PriA, PriB, DnaT complex at the replication fork after a landing site is cleared by PriA [77].

1.4.3 The PriA-directed replication restart pathway in B. subtilis

The replication restart process in *B. subtilis* is even less understood. *B. subtilis* contains a PriA [78], SSB, and helicase (DnaC in *B. subtilis*), but does not have homologs of *E. coli* PriB or DnaT. Instead DnaB (not to be confused with the DnaB helicase in *E. coli*), DnaD, and DnaI proteins which are non-homologous to those required in *E. coli* are necessary to support replication restart [79].

In the replication restart process, there is a significant distinction between *E. coli* and *B. subtilis.* In order to re-load the helicase onto the lagging strand, *B. subtilis* uses two helicase loaders, as opposed to one in *E. coli* [80]. DnaI in *B. subtilis* shares some sequence similarity with DnaC in *E. coli*, but the specific function of DnaC in *E. coli* seems to be split between DnaB and DnaI in *B. subtilis* [80].

1.5 RESEARCH GOALS

Previous experiments that illustrate HE contacts with primer-template were performed by inserting photo-crosslinkers into a primer annealed to template DNA. The DNA was then bound to HE and subunits that contact at the probed positions were identified by electrophoretic mobility shift [46]. Experiments similar to these are performed in Chapter 2 to probe for transient interactions that occur between the HE

and the primer-template within model Okazaki fragments. Photo-crosslinkers are inserted at different positions ahead of the primer terminus in a gap and in the 5'-end of a blocking oligonucleotide. The subunit(s) involved in sensing gapped DNA is expected to crosslink to the primer terminus, a position ahead of the primer terminus, and the 5'-end of a preceding Okazaki fragment to distinguish gapped DNA from nicked DNA.

In Chapter 6, I also use photo-crosslinking and identification by electrophoretic mobility shift to probe the positions of the *E. coli* replication restart proteins on a model replication fork. Also using this method, the migrations of these proteins as the restart assembly is built up are determined.

In these experiments, the photo-reactive reagent used is a diazirine compound. These particular molecules, when irradiated with light at 350 nm, form a highly reactive carbene [81]. The carbene can subsequently insert itself into the side chain of any adjacent amino acid forming a covalent bond [82]. These have been shown to be highly effective reagents to sustain the types of studies presented here [83].

By incorporating these photo-reactive groups at positions in the DNA substrate, covalent bonds can form between the DNA and the protein where it makes contacts with the DNA. A distinctive benefit of using this photo-crosslinker is that negative data can be interpreted. Due to the lack of specificity of the carbene, if no photo-crosslink is seen to a particular protein, it can be interpreted that the protein is not making a direct contact at that probe position.

In optimizing a substrate to support photo-crosslinking studies of replication restart proteins, a FRET assay was used to monitor helicase efficiency. This assay was used to optimize a photo-crosslinking substrate, *E. coli* helicase loading conditions by

the PriA pathway, and *B. subtilis* helicase loading conditions by the PriA pathway (Chapter 3). This method and the optimized protein systems to monitor the replication restart process were used to provide contributions to two collaborative studies presented here (Chapters 4 and 5).

1.6 REFERENCES

1 Wu, C. A., Zechner, E. L. and Marians, K. J. (1992) Coordinated leading- and lagging-strand synthesis at the *Escherichia coli* DNA replication fork. I. Multiple effectors act to modulate Okazaki fragment size. The Journal of Biological Chemistry **267**, 4030–44.

2 McHenry, C. and Kornberg, A. (1977) DNA polymerase III holoenzyme of *Escherichia coli.* Purification and resolution into subunits. The Journal of Biological Chemistry **252**, 6478–84.

3 McHenry, C. S. and Crow, W. (1979) DNA polymerase III of *Escherichia coli*. Purification and identification of subunits. The Journal of Biological Chemistry **254**, 1748–53.

4 McHenry, C. S. (1982) Purification and characterization of DNA polymerase III'. Identification of τ as a subunit of the DNA polymerase III holoenzyme. The Journal of Biological Chemistry **257**, 2657–63.

5 Johanson, K. O., Haynes, T. E. and McHenry, C. S. (1986) Chemical characterization and purification of the β subunit of the DNA polymerase III holoenzyme from an overproducing strain. The Journal of Biological Chemistry **261**, 11460–5.

6 Maki, S. and Kornberg, A. (1988) DNA polymerase III holoenzyme of *Escherichia coli*. II. A novel complex including the γ subunit essential for processive synthesis. The Journal of Biological Chemistry **263**, 6555–60.

7 O'Donnell, M. and Studwell, P. S. (1990) Total reconstitution of DNA polymerase III holoenzyme reveals dual accessory protein clamps. The Journal of Biological Chemistry **265**, 1179–87.

8 Maki, H. and Kornberg, A. (1985) The polymerase subunit of DNA polymerase III of *Escherichia coli*. II. Purification of the α subunit, devoid of nuclease activities. The Journal of Biological Chemistry **260**, 12987–92.

9 Scheuermann, R. H. and Echols, H. (1984) A separate editing exonuclease for DNA replication: the ε subunit of *Escherichia coli* DNA polymerase III holoenzyme. Proceedings of the National Academy of Sciences of the United States of America **81**, 7747–51.

10 Studwell-Vaughan, P. S. and O'Donnell, M. (1993) DNA polymerase III accessory proteins. V. θ encoded by holE. The Journal of Biological Chemistry **268**, 11785–91.

11 Jonczyk, P., Nowicka, A., Fijałkowska, I. J., Schaaper, R. M. and Cieśla, Z. (1998) *In vivo* protein interactions within the *Escherichia coli* DNA polymerase III core. Journal of Bacteriology **180**, 1563–6.

12 Carter, J. R., Franden, M. A., Aebersold, R., Kim, D. R. and McHenry, C. S. (1993) Isolation, sequencing and overexpression of the gene encoding the θ subunit of DNA polymerase III holoenzyme. Nucleic Acids Research **21**, 3281–6.

13 LaDuca, R. J., Crute, J. J., McHenry, C. S. and Bambara, R. A. (1986) The β subunit of the *Escherichia coli* DNA polymerase III holoenzyme interacts functionally with the catalytic core in the absence of other subunits. The Journal of Biological Chemistry **261**, 7550–7.

14 Kong, X. P., Onrust, R., O'Donnell, M. and Kuriyan, J. (1992) Three-dimensional structure of the β subunit of *E. coli* DNA polymerase III holoenzyme: a sliding DNA clamp. Cell **69**, 425–37.

15 Maki, S. and Kornberg, A. (1988) DNA polymerase III holoenzyme of *Escherichia coli*. III. Distinctive processive polymerases reconstituted from purified subunits. The Journal of Biological Chemistry **263**, 6561–9.

16 Wickner, S. (1976) Mechanism of DNA elongation catalyzed by *Escherichia coli* DNA polymerase III, dnaZ protein, and DNA elongation factors I and III. Proceedings of the National Academy of Sciences of the United States of America **73**, 3511–5.

17 O'Donnell, M. E. (1987) Accessory proteins bind a primed template and mediate rapid cycling of DNA polymerase III holoenzyme from *Escherichia coli.* The Journal of Biological Chemistry **262**, 16558–65.

18 Studwell-Vaughan, P. S. and O'Donnell, M. (1991) Constitution of the twin polymerase of DNA polymerase III holoenzyme. The Journal of Biological Chemistry **266**, 19833–41.

19 Lee, S. H. and Walker, J. R. (1987) *Escherichia coli* DnaX product, the τ subunit of DNA polymerase III, is a multifunctional protein with single-stranded DNA-dependent ATPase activity. Proceedings of the National Academy of Sciences of the United States of America **84**, 2713–7.

20 Leu, F. P., Hingorani, M. M., Turner, J. and O'Donnell, M. (2000) The δ subunit of DNA polymerase III holoenzyme serves as a sliding clamp unloader in *Escherichia coli*. The Journal of Biological Chemistry **275**, 34609–18.

21 Stewart, J., Hingorani, M. M., Kelman, Z. and O'Donnell, M. (2001) Mechanism of β clamp opening by the δ subunit of *Escherichia coli* DNA polymerase III holoenzyme. The Journal of Biological Chemistry **276**, 19182–9.

22 Glover, B. P. and McHenry, C. S. (1998) The χψ subunits of DNA polymerase III holoenzyme bind to single-stranded DNA-binding protein (SSB) and facilitate replication of an SSB-coated template. The Journal of Biological Chemistry **273**, 23476–84.

23 Olson, M. W., Dallmann, H. G. and McHenry, C. S. (1995) DnaX complex of *Escherichia coli* DNA polymerase III holoenzyme. The χψ complex functions by increasing the affinity of τ and γ for δ.δ' to a physiologically relevant range. The Journal of Biological Chemistry **270**, 29570–7.

24 Wing, R. A, Bailey, S. and Steitz, T. A. (2008) Insights into the replisome from the structure of a ternary complex of the DNA polymerase III α-subunit. Journal of Molecular Biology **382**, 859–69.

25 Lamers, M. H., Georgescu, R. E., Lee, S.-G., O'Donnell, M. and Kuriyan, J. (2006) Crystal structure of the catalytic α subunit of *E. coli* replicative DNA polymerase III. Cell **126**, 881–92.

26 Dohrmann, P. R. and McHenry, C. S. (2005) A bipartite polymerase-processivity factor interaction: only the internal β binding site of the α subunit is required for processive replication by the DNA polymerase III holoenzyme. Journal of Molecular Biology **350**, 228–39.

27 Liu, B., Lin, J. and Steitz, T. A. (2013) Structure of the PolIIIα-τ_c-DNA Complex Suggests an Atomic Model of the Replisome. Structure (London, England : 1993).

28 Bruck, I. and O'Donnell, M. (2000) The DNA replication machine of a gram-positive organism. The Journal of Biological Chemistry **275**, 28971–83.

29 Bruand, C., Ehrlich, S. D. and Jannière, L. (1995) Primosome assembly site in *Bacillus subtilis*. The EMBO Journal **14**, 2642–50.

30 Koonin, E. V and Bork, P. (1996) Ancient duplication of DNA polymerase inferred from analysis of complete bacterial genomes. Trends in Biochemical Sciences **21**, 128–9.

31 Sanders, G. M., Dallmann, H. G. and McHenry, C. S. (2010) Reconstitution of the *B. subtilis* replisome with 13 proteins including two distinct replicases. Molecular Cell, Elsevier Ltd **37**, 273–81.

32 Nethanel, T. and Kaufmann, G. (1990) Two DNA polymerases may be required for synthesis of the lagging DNA strand of simian virus 40. Journal of Virology **64**, 5912–8.

33 Tsurimoto, T. and Stillman, B. (1991) Replication factors required for SV40 DNA replication *in vitro*. II. Switching of DNA polymerase α and δ during initiation of

leading and lagging strand synthesis. The Journal of Biological Chemistry **266**, 1961–8.

34 Mok, M. and Marians, K. J. (1987) The *Escherichia coli* preprimosome and DNA B helicase can form replication forks that move at the same rate. The Journal of Biological Chemistry **262**, 16644–54.

35 Mok, M. and Marians, K. J. (1987) Formation of rolling-circle molecules during ΦX174 complementary strand DNA replication. The Journal of Biological Chemistry **262**, 2304–9.

36 Breier, A. M., Weier, H.-U. G. and Cozzarelli, N. R. (2005) Independence of replisomes in *Escherichia coli* chromosomal replication. Proceedings of the National Academy of Sciences of the United States of America **102**, 3942–7.

37 Johanson, K. O. and McHenry, C. S. (1982) The β subunit of the DNA polymerase III holoenzyme becomes inaccessible to antibody after formation of an initiation complex with primed DNA. The Journal of Biological Chemistry **257**, 12310–5.

38 López de Saro, F. J., Georgescu, R. E. and O'Donnell, M. (2003) A peptide switch regulates DNA polymerase processivity. Proceedings of the National Academy of Sciences of the United States of America **100**, 14689–94.

39 Wu, C. A., Zechner, E. L., Reems, J. A., McHenry, C. S. and Marians, K. J. (1992) Coordinated leading- and lagging-strand synthesis at the *Escherichia coli* DNA replication fork. V. Primase action regulates the cycle of Okazaki fragment synthesis. The Journal of Biological Chemistry **267**, 4074–83.

40 Leu, F. P., Georgescu, R. and O'Donnell, M. (2003) Mechanism of the *E. coli* τ processivity switch during lagging-strand synthesis. Molecular Cell **11**, 315–27.

41 López de Saro, F. J., Georgescu, R. E., Goodman, M. F. and O'Donnell, M. (2003) Competitive processivity-clamp usage by DNA polymerases during DNA replication and repair. The EMBO Journal **22**, 6408–18.

42 Li, X. and Marians, K. J. (2000) Two distinct triggers for cycling of the lagging strand polymerase at the replication fork. The Journal of Biological Chemistry **275**, 34757–65.

43 Theobald, D. L., Mitton-Fry, R. M. and Wuttke, D. S. (2003) Nucleic acid recognition by OB-fold proteins. Annual Review of Biophysics and Biomolecular Structure **32**, 115–33.

44 Georgescu, R. E., Kurth, I., Yao, N. Y., Stewart, J., Yurieva, O. and O'Donnell, M. (2009) Mechanism of polymerase collision release from sliding clamps on the lagging strand. The EMBO Journal **28**, 2981–91.

45 Kim, D. R. and McHenry, C. S. (1996) Identification of the β-binding domain of the α subunit of *Escherichia coli* polymerase III holoenzyme. The Journal of Biological Chemistry **271**, 20699–704.

46 Reems, J. A., Wood, S. and McHenry, C. S. (1995) *Escherichia coli* DNA polymerase III holoenzyme subunits α, β, and γ directly contact the primer-template. The Journal of Biological Chemistry **270**, 5606–13.

47 Cox, M. M., Goodman, M. F., Kreuzer, K. N., Sherratt, D. J., Sandler, S. J. and Marians, K. J. (2000) The importance of repairing stalled replication forks. Nature **404**, 37–41.

48 Cox, M. M. (2001) Recombinational DNA repair of damaged replication forks in *Escherichia coli*: questions. Annual Review of Genetics **35**, 53–82.

49 Nurse, P., Zavitz, K. H. and Marians, K. J. (1991) Inactivation of the *Escherichia coli* priA DNA replication protein induces the SOS response. Journal of Bacteriology **173**, 6686–93.

50 Lee, E. H. and Kornberg, A. (1991) Replication deficiencies in priA mutants of *Escherichia coli* lacking the primosomal replication n' protein. Proceedings of the National Academy of Sciences of the United States of America **88**, 3029–32.

51 Wickner, S. and Hurwitz, J. (1974) Conversion of ΦX174 viral DNA to double-stranded form by purified *Escherichia coli* proteins. Proceedings of the National Academy of Sciences of the United States of America **71**, 4120–4.

52 Weiner, J. H., McMacken, R. and Kornberg, A. (1976) Isolation of an intermediate which precedes dnaG RNA polymerase participation in enzymatic replication of bacteriophage ΦX174 DNA. Proceedings of the National Academy of Sciences of the United States of America **73**, 752–6.

53 Lark, C. A., Riazi, J. and Lark, K. G. (1978) dnaT, dominant conditional-lethal mutation affecting DNA replication in *Escherichia coli*. Journal of Bacteriology **136**, 1008–17.

54 Masai, H., Bond, M. W. and Arai, K. (1986) Cloning of the *Escherichia coli* gene for primosomal protein i: the relationship to dnaT, essential for chromosomal DNA replication. Proceedings of the National Academy of Sciences of the United States of America **83**, 1256–60.

55 Masai, H. and Arai, K. (1988) Operon structure of dnaT and dnaC genes essential for normal and stable DNA replication of *Escherichia coli* chromosome. The Journal of Biological Chemistry **263**, 15083–93.

56 Masai, H., Asai, T., Kubota, Y., Arai, K. and Kogoma, T. (1994) *Escherichia coli* PriA protein is essential for inducible and constitutive stable DNA replication. The EMBO Journal **13**, 5338–45.

57 Sandler, S. J., Samra, H. S. and Clark, A. J. (1996) Differential suppression of priA2::kan phenotypes in *Escherichia coli* K-12 by mutations in priA, lexA, and dnaC. Genetics **143**, 5–13.

58 Sandler, S. J. (1996) Overlapping functions for recF and priA in cell viability and UV-inducible SOS expression are distinguished by dnaC809 in *Escherichia coli* K-12. Molecular Microbiology **19**, 871–80.

59 Kogoma, T., Cadwell, G. W., Barnard, K. G. and Asai, T. (1996) The DNA replication priming protein, PriA, is required for homologous recombination and double-strand break repair. Journal of Bacteriology **178**, 1258–64.

60 Lee, M. S. and Marians, K. J. (1989) The *Escherichia coli* primosome can translocate actively in either direction along a DNA strand. The Journal of Biological Chemistry **264**, 14531–42.

61 Allen, G. C. and Kornberg, A. (1993) Assembly of the primosome of DNA replication in *Escherichia coli*. The Journal of Biological Chemistry **268**, 19204–9.

62 Arai, K., Low, R., Kobori, J., Shlomai, J. and Kornberg, A. (1981) Mechanism of dnaB protein action. V. Association of dnaB protein, protein n', and other repriming proteins in the primosome of DNA replication. The Journal of Biological Chemistry **256**, 5273–80.

63 Sandler, S. J. (2000) Multiple genetic pathways for restarting DNA replication forks in *Escherichia coli* K-12. Genetics **155**, 487–97.

64 Jones, J. M. and Nakai, H. (2000) PriA and phage T4 gp59: factors that promote DNA replication on forked DNA substrates microreview. Molecular Microbiology **36**, 519–27.

65 Liu, J. and Marians, K. J. (1999) PriA-directed assembly of a primosome on D loop DNA. The Journal of Biological Chemistry **274**, 25033–41.

66 Lee, M. S. and Marians, K. J. (1987) *Escherichia coli* replication factor Y, a component of the primosome, can act as a DNA helicase. Proceedings of the National Academy of Sciences of the United States of America **84**, 8345–9.

67 Jones, J. M. and Nakai, H. (1999) Duplex opening by primosome protein PriA for replisome assembly on a recombination intermediate. Journal of Molecular Biology **289**, 503–16.

68 Heller, R. C. and Marians, K. J. (2005) The disposition of nascent strands at stalled replication forks dictates the pathway of replisome loading during restart. Molecular Cell **17**, 733–43.

69 Cadman, C. J. and McGlynn, P. (2004) PriA helicase and SSB interact physically and functionally. Nucleic Acids Research **32**, 6378–87.

70 Ng, J. Y. and Marians, K. J. (1996) The ordered assembly of the ΦX174-type primosome. I. Isolation and identification of intermediate protein-DNA complexes. The Journal of Biological Chemistry **271**, 15642–8.

71 Liu, J.-H., Chang, T.-W., Huang, C.-Y., Chen, S.-U., Wu, H.-N., Chang, M.-C. and Hsiao, C.-D. (2004) Crystal structure of PriB, a primosomal DNA replication protein of *Escherichia coli*. The Journal of Biological Chemistry **279**, 50465–71.

72 Shioi, S., Ose, T., Maenaka, K., Shiroishi, M., Abe, Y., Kohda, D., Katayama, T. and Ueda, T. (2005) Crystal structure of a biologically functional form of PriB from *Escherichia coli* reveals a potential single-stranded DNA-binding site. Biochemical and Biophysical Research Communications **326**, 766–76.

73 Lopper, M., Holton, J. M. and Keck, J. L. (2004) Crystal structure of PriB, a component of the *Escherichia coli* replication restart primosome. Structure (London, England : 1993) **12**, 1967–75.

74 Liu, J., Nurse, P. and Marians, K. J. (1996) The ordered assembly of the ΦX174-type primosome. III. PriB facilitates complex formation between PriA and DnaT. The Journal of Biological Chemistry **271**, 15656–61.

75 McCool, J. D., Ford, C. C. and Sandler, S. J. (2004) A dnaT mutant with phenotypes similar to those of a priA2::kan mutant in *Escherichia coli* K-12. Genetics **167**, 569–78.

76 Wickner, S. and Hurwitz, J. (1975) Interaction of *Escherichia coli* dnaB and dnaC(D) gene products *in vitro*. Proceedings of the National Academy of Sciences of the United States of America **72**, 921–5.

77 Lopper, M., Boonsombat, R., Sandler, S. J. and Keck, J. L. (2007) A hand-off mechanism for primosome assembly in replication restart. Molecular Cell **26**, 781–93.

78 Polard, P., Marsin, S., McGovern, S., Velten, M., Wigley, D. B., Ehrlich, S. D. and Bruand, C. (2002) Restart of DNA replication in Gram-positive bacteria: functional characterisation of the *Bacillus subtilis* PriA initiator. Nucleic Acids Research **30**, 1593–605.

79 Bruand, C., Farache, M., McGovern, S., Ehrlich, S. D. and Polard, P. (2001) DnaB, DnaD and DnaI proteins are components of the *Bacillus subtilis* replication restart primosome. Molecular Microbiology **42**, 245–55.

80 Velten, M., McGovern, S., Marsin, S., Ehrlich, S. D., Noirot, P. and Polard, P. (2003) A two-protein strategy for the functional loading of a cellular replicative DNA helicase. Molecular Cell **11**, 1009–20.

81 Fleming, S. A. (1995) Chemical Reagents in Photoaffinity Labeling. Tetrahedron **51**, 12479–12520.

82 Bayley, H. (1983) Laboratory techniques in biochemistry and molecular biology: Photogenerated reagents in biochemistry and molecular biology. Hagan Bayley, Volume 12, p 187, Elsevier.

83 Tate, J. J., Persinger, J. and Bartholomew, B. (1998) Survey of four different photoreactive moieties for DNA photoaffinity labeling of yeast RNA polymerase III transcription complexes. Nucleic Acids Research **26**, 1421–6.

CHAPTER 2[*]

The rate of polymerase release upon filling the gap between Okazaki fragments is inadequate to support cycling during lagging strand synthesis[†]

2.1 ABSTRACT

Upon completion of the synthesis of an Okazaki fragment, the lagging strand replicase must recycle to the next primer at the replication fork in under 0.1 s to sustain the physiological rate of DNA synthesis. We tested the collision model that posits that cycling is triggered by the polymerase encountering the 5'-end of the preceding Okazaki fragment. Probing with surface plasmon resonance, DNA polymerase III holoenzyme initiation complexes were formed on an immobilized gapped template. Initiation complexes exhibit a half-life of dissociation of approximately 15 min. Reduction in gap size to 1 nt increased the rate of dissociation 2.5-fold, and complete filling of the gap increased the off-rate an additional 3-fold ($t_{1/2}$ ~2 min). An exogenous primed template and ATP accelerated dissociation an additional 4-fold in a reaction that required complete filling of the gap. Neither a 5'-triphosphate nor a 5'-RNA terminated oligonucleotide downstream of the polymerase accelerated dissociation further. Thus, the rate of polymerase release upon gap completion and collision with a downstream

[*] My experimental work is the photo-crosslinking experiment presented in Fig. 2.3 of this chapter and described in sections 2.3.6, 2.3.7, and on pages 47-48. The remaining experimental work was performed by the co-authors of the corresponding publication [49].

[†] The contents of this chapter were published in [49] and are presented here with few modifications.

Okazaki fragment is 1000-fold too slow to support an adequate rate of cycling and likely provides a backup mechanism to enable polymerase release when the other cycling signals are absent. Kinetic measurements indicate that addition of the last nucleotide to fill the gap is not the rate-limiting step for polymerase release and cycling. Modest (approximately 7 nt) strand displacement is observed after the gap between model Okazaki fragments is filled. To determine the identity of the protein that senses gap filling to modulate affinity of the replicase for the template, I performed photo-crosslinking experiments with highly reactive and non-chemoselective diazirines. Only the α subunit crosslinked, indicating that it serves as the sensor.

2.2 INTRODUCTION

Cellular chromosomal replicases from all branches of life are tripartite. They contain a polymerase (Pol III in bacteria and Pol δ and ε in eukaryotes), a sliding clamp processivity factor (β_2 in bacteria and PCNA in eukaryotes), and a clamp loader (DnaX complex in bacteria and RFC in eukaryotes) [1–3]. The *Escherichia coli* replicase, the DNA polymerase III holoenzyme (Pol III HE), has the processivity required to replicate >150 kb [4,5], and perhaps the entire *E. coli* chromosome, without dissociation. Yet, the lagging strand polymerase must be able to efficiently cycle to the next primer synthesized at the replication fork upon the completion of each Okazaki fragment at a rate faster than that of Okazaki fragment production. The rate of replication fork progression in *E. coli* is about 600 nt/s at 30 °C [2], approximately the rate of replicase progression on single-stranded DNA (ssDNA) templates [6]. Thus, most of the time in

an Okazaki fragment cycle is spent on elongation, and little time (<0.1 s) remains for the polymerase to release, bind the next primer, and begin synthesis. A processivity switch must be present to increase the off-rate of the lagging strand polymerase by several orders of magnitude.

Upon complete replication of primed single strand DNA, Pol III* (a complex of Pol III and DnaX complexes containing the τ form of DnaX that binds Pol III) dissociates from a duplex and leaves the β_2 sliding clamp behind [7]. There are two competing but nonexclusive models for the signal that throws the processivity switch. The first, the signaling model, proposes that a signal is provided by synthesis of a new primer at the replication fork that induces the lagging strand polymerase to dissociate, even if the Okazaki fragment has not been completed [8]. The second, the collision model, originally proposed for T4 [9] and then extended to the *E. coli* system [10], posits that the lagging strand polymerase replicates to the last nucleotide [10] or until the Okazaki fragment is nearly complete, signaling polymerase dissociation [11]. A communication circuit that proceeds through the τ subunit has been proposed to sense the conversion of a gap to a nick, signaling release [10,12,13]. τ was proposed to act by competing with a C-terminal site on Pol III for binding to β. However, other work has shown the essential site required for β interaction to be internal within the Pol III α subunit [14–16]. Experiments designed to test whether the signaling or collision models are dominant have yielded equivocal results [17].

In the more fully characterized systems provided by the replication apparatus of bacteriophages T4 and T7, signaling through synthesis or the availability of a new primer appears to play an important role, with the collision pathway playing an apparent

backup function [18–20]. In T4, handoff of the nascent pentaribonucleotide primer occurs in a reaction that is facilitated by T4 ssDNA binding protein (T4 SSB) and the clamp and the clamp loader [21,22]. A proposal was made that the T4 clamp loader/clamp interaction with a new primer might be the key signal required for release of the lagging strand polymerase [22].

In this chapter, a kinetic assessment of the collision model is presented on templates constructed such that elongating Pol III HE encounters an oligonucleotide hybridized to the template that mimics the 5'-terminus of the preceding Okazaki fragment on the lagging strand of a replication fork. We compared the rate of Pol III* release with the rate of addition of the last nucleotide. To determine candidate holoenzyme subunits that could serve as a sensor for completion of lagging strand synthesis I identified the protein that contacts the template immediately ahead of the primer terminus and the 5'-end of the preceding Okazaki fragment.

2.3 MATERIALS AND METHODS

2.3.1 Oligonucleotides

The templates diagrammed in Fig. 2.1 were assembled from the following gel-purified oligonucleotides: template 81-mer, 5'-GCTAATGAATTCCCGGTTCTTGACTACATTACTCTTGATCAAGGTCAGCCAGCCTATGCGCGTGATCTGTACACCGTTCT(biotin)T-3' (T(biotin) represents T with biotin attached, via a linker, to the C5 position); primer 30-mer, 5'-

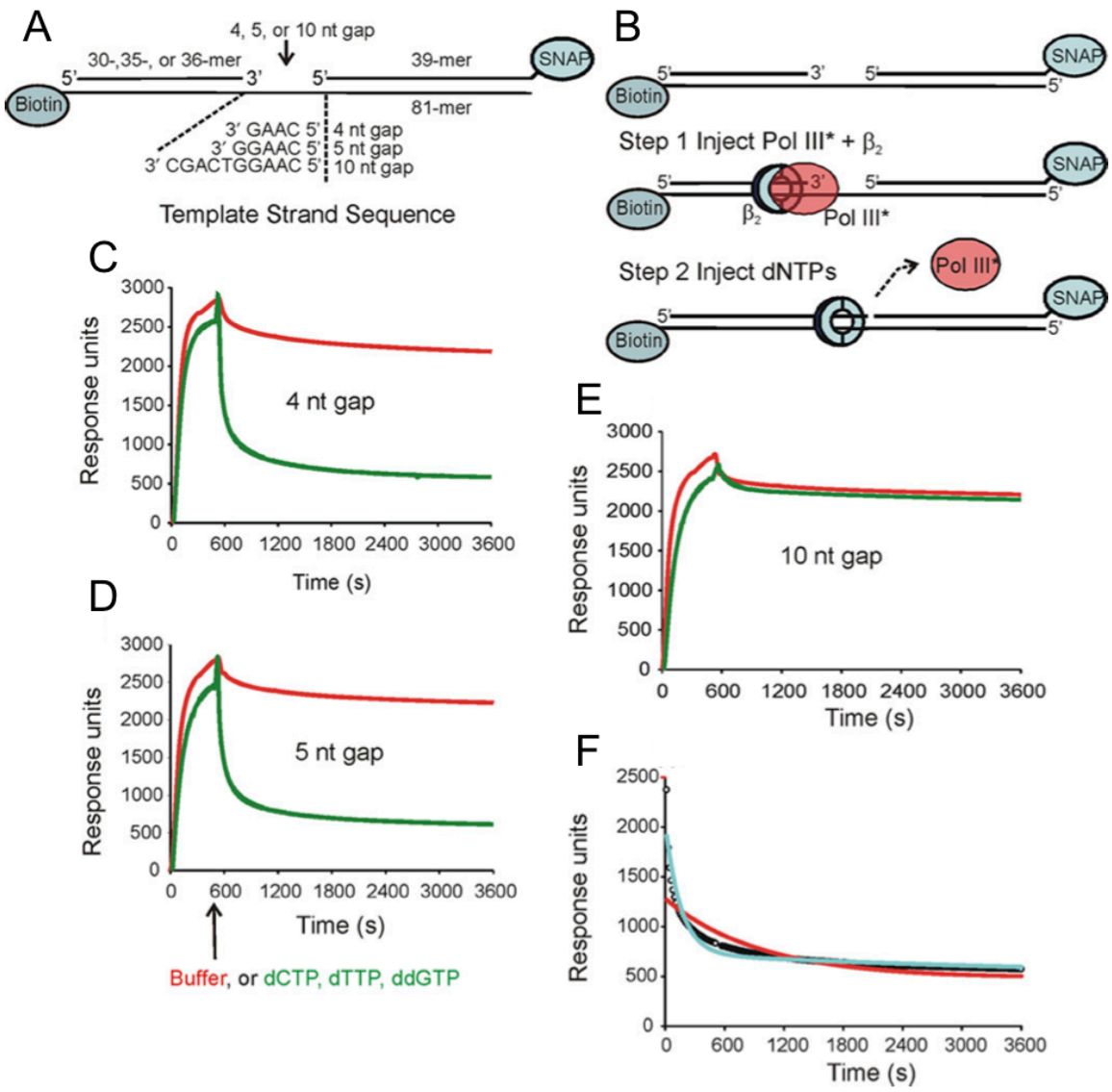

FIGURE 2.1

Pol III* does not release rapidly upon filling a gap. The dissociation of Pol III* from primed templates was measured using SPR. (A) Three primed templates containing 4, 5 and 10 nt gaps were anchored to the surface of a streptavidin-coated sensor chip using biotin-labeled oligonucleotides. The 3'-end of the blocking oligonucleotide was covalently linked to the SNAP protein to prevent β_2 from sliding off the end. (B) Initiation complexes were assembled onto the immobilized DNA primer–template by injecting Pol III*, β_2, and ATP. A second injection containing either buffer or a solution containing 40 μM dCTP, dTTP, and ddGTP (dNTPs) was made at 540 s. (C-E) Injection of either buffer (red) or dNTPs (green) over the 4 nt gapped template, 5 nt gapped template, and 10 nt gapped template, respectively. Dissociation was allowed to continue for 3 days. The data shown are only for the first hour after injection. (F) Curve-fit analysis is shown for the Pol III* dissociation in the presence of dNTPs over a 4 nt gapped template: data (open circles), curve fit to single-exponential decay (red), curve fit to double-exponential decay (cyan).

GAACGGTGTACAGATCACGCGCATAGGCTG-3’ (to make 10 nt gapped template); primer 35-mer, 5’-GAACGGTGTACAGATCACGCGCATAGGCTGGCTGA-3’ (to make 5 nt gapped template); primer 36-mer, 5’-GAACGGTGTACAGATCACGCGCATAGGCTGGCTGAC-3’ (to make 4 nt gapped template); blocking oligonucleotide 39-mer, 5’-ATCAAGAGTAATGTAGTCAAGAACCGGGAATTCATTAGC-SNAP-3’; blocking oligonucleotide 39-mer (5’-phosphate RNA_{12}/DNA_{27}), 5’-PO_4rArUrCrArArGrArGrUrArArUGTAGTCAAGAACCGGGAATTCATTAGC-SNAP-3’; and blocking oligonucleotide 39-mer (5’-triphosphate), 5’-triphosphate-ATCAAGAGTAATGTAGTCAAGAACCGGGAATTCATTAGCC-SNAP-3’. The exogenous primed template used to stimulate polymerase release (Table 2.1) was assembled by annealing a 20-mer primer (5’-TTGTTCAGATGAAGGCGCAT-3’) to a 70-mer template (5’-TAAAAAAAAAAAAAAAAAAGGATTACTGGATCCGAAGGTCAGCCAGCCTATGCGCCTTCATCTGAACAA-3’).

For experiments reported in Fig. 2.2, in addition to oligonucleotides described in this subsection, the following oligonucleotides were synthesized: blocking oligonucleotide 34-mer, 5’-GAGTAATGTAGTCAAGAACCGGGAATTCATTAG C-biotin-3’, and extended primer 45-mer, 5’-GAACGGTGTACAGATCACGCGCATAGGCTGGCTGACCTTGATCAA-3’.

Injection	4 nt gap template $t_{1/2}$ (s) [amplitude]	5 nt gap template $t_{1/2}$ (s) [amplitude]
5'-OH DNA_{39} blocking oligo	30 [86%]	40 [83%]
5' PO_4 RNA_{12}/DNA_{27} blocking oligo	60 [71%]	70 [68%]
5' Tri-PO_4 DNA_{39} blocking oligo	80 [51%]	90 [44%]

TABLE 2.1
RNA or a triphosphate on the 5'-terminus of the preceding Okazaki fragment does not contribute to the rate of Pol III* release.

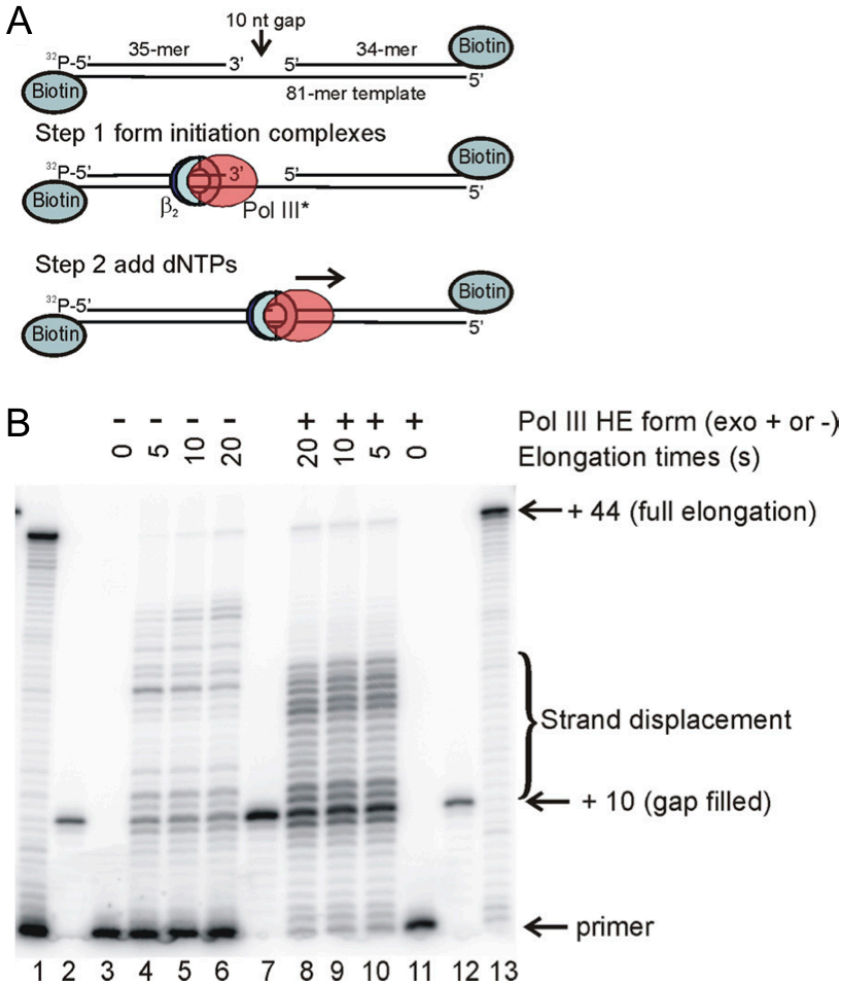

FIGURE 2.2

Pol III HE rapidly fills a 10 nt gap and partially displaces a blocking oligonucleotide. (A) 5'-^{32}P- end-labeled primer 35-mer was hybridized to a template 81-mer with a 10 nt gap in front of blocking oligonucleotide 34-mer. This primer–template was incubated with Pol III HE and ATP for 60 s to form initiation complexes, followed by addition of dNTPs to initiate primer elongation for the ^{32}P-labeled complexes. (B) Denaturing polyacrylamide gel analysis of the rate of nucleotide incorporation. The gel lanes were loaded with (1) unblocked primer–template fully extended by Pol III HE; (2) 5'-^{32}P- end-labeled 45-mer corresponding to a fully gap-filled product, annealed to the 81-mer template; (3) unextended 10 nt gap primer–template; (4) 10 nt gap primer–template after a 5 s extension time; (5) 10 nt gap primer–template after a 10 s extension time; (6) 10 nt gap primer– template after a 20 s extension time; (7) 45-mer annealed to the 81-mer template (4-fold more sample than loaded than in lanes 2 and 12); (8) 10 nt gap primer–template after a 20 s extension time; (9) 10 nt gap primer–template after a 10 s extension time; (10) 10 nt gap primer–template after a 5 s extension time; (11) unextended 10 nt gap primer–template; (12) 45-mer annealed to the 81-mer template; (13) unblocked primer–template fully extended by Pol III HE. The samples in lanes 1 and 4-6 were extended by exonuclease-deficient Pol III HE. The samples in lanes 8-10 and 13 were extended by wild-type Pol III HE.

2.3.2 Preparation of the SNAP-conjugated blocking oligonucleotides

A method [23] for attaching the Hexa-His-tagged O^6-alkylguanine-DNA-Transferase (SNAP-tag; New England Biolabs) to a DNA oligomer was adapted for our purposes. The blocking oligonucleotides (PAGE purified from Integrated DNA Technologies or Biosynthesis, Inc. for the 5'-triphosphate oligonucleotide) contained 3'-O-CH_2-CH_2-SH blocked by formation of a disulfide bond. Disulfide-blocked oligonucleotide (35 nmol) was reduced by incubation (1 h) at room temperature with 10 mM tris(2-carboxyethyl)phosphine hydrochloride (TCEP) (Pierce) in 500 μl TE buffer [10 mM Tris–HCl and 1 mM ethylenediaminetetraacetic acid (pH 8.0)] (Fig. A1.2). The solution was applied to a NAP5 (0.5 ml) gel-filtration column (GE Healthcare) with TE as the running buffer to remove TCEP and the 3-carbon thiol linker (Fig. A1.2). The most concentrated fractions, determined spectrophotometrically, were combined, giving a total of 800 μl. O^6-benzylguanine-maleimide (300 μl; New England Biolabs) (2.5 mM in dimethyl formamide) was added to the 800 μl of reduced 39-mer in a total volume of 1.1 ml, and the reaction mixture was allowed to proceed at room temperature (1 h) before application to a 2.5 ml NAP25 column to remove unreacted O^6-benzylguanine-maleimide. To verify attachment of the O^6-benzylguanine to the 3'-end of the 39-mer, we analyzed product (12,738 Da) on a 9% denaturing polyacrylamide gel using the unmodified 39-mer (12,316 Da) for comparison. Greater than 90% of the oligonucleotide was modified (Fig. A1.3). Unreacted/unmodified oligomer was removed in the next step.

The BG-modified-39-mer (33 nmol) was covalently attached to SNAP by incubating 1.5-fold excess of oligonucleotide over SNAP in [50 mM sodium phosphate (pH 8.0), 300 mM NaCl, 20% glycerol, 1 mM dithiothreitol, and 5 mM imidazole] for 1 h

at room temperature with gentle rotation of the tube in a final volume of 2 ml. The oligonucleotide-SNAP conjugate was applied to a 0.75-ml Ni^{2+}-NTA column (Qiagen) pre-equilibrated with wash buffer [50 mM sodium phosphate (pH 8.0), 300 mM NaCl, 20% glycerol, 1 mM dithiothreitol, and 5 mM imidazole]. All subsequent column procedures were performed at 0–4 °C. The column was washed with 10 column volumes of wash buffer [50 mM sodium phosphate (pH 8.0), 300 nM NaCl, 20% glycerol, 1 mM dithiothreitol, and 5 mM imidazole] to remove unreacted oligonucleotide. Protein was eluted with elution buffer [50 mM sodium phosphate (pH 8.0), 300 nM NaCl, 20% glycerol, 1 mM dithiothreitol, and 400 mM imidazole]. Eluted fractions containing the protein samples were detected by the Bradford method (Pierce). Analysis of the SNAP-tag-39-mer, monitored on a 4–20% gradient SDS-PAGE gel from its molecular mass shift (unmodified SNAP-tag, 22.2 kDa; modified SNAP-tag-39-mer, 34.9 kDa), indicated that approximately 90% of the SNAP-tag protein that eluted off the column contained a covalently attached 39-mer oligonucleotide (Fig. A1.3). The protein/oligo conjugate was frozen in small aliquots by flash freezing in liquid nitrogen.

2.3.3 DNA polymerase III holoenzyme components

Protein components were purified as described for Pol III [24], ε [25], τ [26], γ [26], δ [27], δ' [27], χ [28], ψ [28], β_2 [29], and SSB_4 [30]. Four different DnaX protein complexes with stoichiometries of $\tau_2\gamma\delta\delta'\chi\psi$, $\tau\gamma_2\delta\delta'\chi\psi$, $\tau_3\delta\delta'\chi\psi$, and $\gamma_3\delta\delta'\chi\psi$ were purified as described previously [31,32]. Unless otherwise noted, the ε subunit used in our

experiments was mutated at D12A and E14A to eliminate endogenous 3' to 5' exonuclease activity, which degrades the primer [33].

For experiments using Pol III* exhibiting a $\tau_2\gamma$ stoichiometry, complexes were assembled from purified sub-complexes of Pol III ($\alpha\varepsilon\theta$; 40 nM final) and DnaX complex ($\tau_2\gamma\delta\delta'\chi\psi$; 20 nM final). For experiments using Pol III* exhibiting γ_3 stoichiometry, complexes were assembled from purified sub-complexes of Pol III ($\alpha\varepsilon\theta$; 20 nM final) and DnaX complex ($\gamma_3\delta\delta'\chi\psi$; 20 nM final). For experiments using Pol III* exhibiting a $\tau\gamma_2$ stoichiometry, the Pol III* was isolated and purified first by cation-exchange chromatography over a Mono-S column [24,32,34]. DnaX complex ($\tau\gamma_2\delta\delta'\chi\psi$; 2 nmol) was incubated with Pol III ($\alpha\varepsilon$ D12A E14A, θ; 10 nmol) for 15 min at room temperature. The incubated mixture was applied to a 2.5 ml NAP25 (GE Healthcare) gel-filtration column to exchange the buffer [25 mM Hepes (pH 7.5), 5% glycerol, and 25 mM NaCl] prior to running the mixture over a 1 ml Mono-S column at 4 °C. The column was washed with 4 column volumes of wash buffer [25 mM Hepes (pH 7.5), 5% glycerol, and 25 mM NaCl]. Fractions (0.5 ml) were collected after application of a 150 mM NaCl step [in 25 mM Hepes (pH 7.5) and 5% glycerol]. The Pol III* fractions eluted approximately 5 column volumes after the 150 mM NaCl step. Purified Pol III* was injected over the Sensor chip SA at a final concentration of 50 nM.

2.3.4 Surface plasmon resonance

A BIAcore 3000 instrument was used to quantify and measure the release of Pol III from immobilized oligonucleotide templates. A flow rate of 5 μl/min in KCl-EDB buffer

[50 mM Hepes (pH 7.5), 125 mM KCl, 10 mM magnesium acetate, 0.005% Tween-20, and 10 μM TCEP] at 25 °C was used for all reactions. All buffers were filtered and degassed before use. The Sensor Chip SA (BIAcore), a sensor chip pre-immobilized with streptavidin for capture of biotinylated ligands, was pre-conditioned with three 1 min injections of 5 μl of 1 M NaCl/50 mM NaOH prior to attachment of DNA primer–templates. Three different DNA primer–templates were immobilized. The 81-mer template annealed to the 30-mer primer was attached to flowcell 1 of the Sensor Chip SA. The template 81-mer annealed to the 35-mer and the template 81-mer annealed to 36-mer were attached to flowcells 2 and 3, respectively. Flowcell 4 was not derivatized and was used as a control for background subtraction.

DNA primer–templates were assembled in two steps. First, duplex DNA containing the template oligonucleotide 81-mer (500 pmol) and the binding oligonucleotide 30-mer (or 35-mer or 36-mer) (5 nmol) was annealed *in vitro* in [10 mM Tris–HCl (pH 8.0), 300 mM NaCl, and 30 mM sodium citrate] in a volume of 250 μl. The sample was heated to 95 °C for 10 min and allowed to cool slowly to 23 °C at 1 °C/min. The sample was diluted 1000-fold to a concentration of 2 fmol/μl, with respect to the 81-mer, in KCl-EDB buffer and aliquoted. To prepare the flowcell with the DNA primer–template, a total of ca 50 μl of the annealed DNA primer–template was injected over the surface of an individual flowcell on the sensor chip SA, which resulted typically in an increase of ca 270–300 response units. Second, SNAP-tag-39-mer was diluted to a final concentration of 80 fmol/μl in KCl-EDB buffer, and 300 μl was injected over all four flowcells simultaneously. The SNAP-tag-39-mer does not bind to the underivatized flowcell. Complete annealing to the DNA templates on the remaining flowcells was

observed for the SNAP-tag-39-mer by determining the binding signal after injection. Since the output obtained from the BIAcore is directly proportional to the mass bound, stoichiometries could be calculated. Complete annealing was observed for the SNAP-tag-39-mer.

Pol III* complexes were injected over the DNA primer–template at concentrations determined empirically for each individual assembly. To determine the optimum concentration for binding, we injected a series of different concentrations ranging from 5 nM to 80 nM Pol III* complex. Concentrations were chosen that gave maximum stoichiometry of binding. In a typical experiment, Pol III*, β_2 (300 nM), and ATP (1 mM) were injected over all four flowcells of the SA sensor chip simultaneously in a 45 μl injection. The “KINJECT” command was used for measuring dissociation of Pol III complexes in the presence of buffer alone. Data were collected for 3 days following the injection to allow the dissociation of complexes to come to baseline. The long dissociation time was required to gather data for 10 half-lives for the slow, non-physiological second phase. Having a complete time course for the slow phase proved essential for a proper kinetic fit for accurate determination of the fast phase. To measure the dissociation of Pol III* in the presence of dNTPs and/or other additional components, we used the “COINJECT” command. The COINJECT command introduces a second sample injection (45 μl was used) immediately upon completion of the first. The following components were used either individually or in combination to determine the requirements for full recycling: dNTPs (40 μM each, final), ddNTPs (40 μM final), ATP (1 mM final), ATPγS (1 mM final), β_2 (0.5 μM final), SSB_4 (0.5 μM final), and 20-mer/70-mer (0.5 μM final). All were diluted in KCl-EDB running buffer. Pol III*

failed to bind to DNA primer–templates using control reactions that lacked β_2 or ATP in the first injection, demonstrating dependence on both for binding.

The rate of Pol III*/β_2 dissociation from DNA primer–templates was determined using nonlinear regression analysis using SigmaPlot software. The dissociation data were then fit to several models for exponential decay. All models tested included an offset value that defined the point at which the decay curve leveled out. To help assess whether a term was necessary to generate a good fit, we determined a "dependency" value for each parameter in the fitting equation. The simplest model that best fit our data was double-exponential decay.

2.3.5 Kinetics of filling the gap within model templates

A primer–template system similar to the SPR experiments was used, with an identical primer 35-mer and template 81-mer. Blocking oligonucleotide 34-mer was used to generate a 10 nt gap on the template. The primer 35-mer was 5'-^{32}P end-labeled using T4 polynucleotide kinase. The construct was annealed by combining 200 nM 5'-^{32}P-labeled primer 35-mer, 250 nM template 81-mer, and 300 nM blocking oligonucleotide 34-mer (to ensure complete capture of the primer by a fully blocked template) and heating to 95 °C for 10 min and cooling to 23 °C at 1 °C/min. An unblocked control sample was prepared by the same procedure but omitting the blocking oligonucleotide 34-mer. A marker for the expected product resulting from primer extension by 10 nt to fully fill the gap was prepared by annealing 200 nM 5'-^{32}P-extended primer 45-mer with 250 nM template 81-mer.

Primer elongation assays were conducted at ambient temperature in a buffer containing 50 mM Hepes (pH 7.5), 100 mM potassium glutamate, 10 mM magnesium acetate, 0.20 mg/ml bovine serum albumin, 10 mM dithiothreitol, 2.5% (v/v) glycerol, and 0.02% (v/v) Nonidet P40 detergent. Initiation complexes were generated by preincubating 10 nM ^{32}P-labeled 10 nt gap containing primed template with 30 nM streptavidin and then combining this mixture with 25 nM $\tau_2\gamma$ DnaX complex, 25 nM Pol III, 100 nM β_2, 200 μM ATP, and 1 μM hexokinase and incubating for 60 s. For experiments with wild-type Pol III, this initiation complex formation reaction included 20 μM dATP, enabling the polymerase to replace the 3'-terminal nucleotide of the primer 35-mer if digested by the 3'-5' exonuclease. Initiation complex formation was terminated, and primer elongation was initiated by adding an equal volume of 0.25 mg/ml activated calf thymus DNA (a cold trap for unassociated Pol III HE), 10 mM glucose (to activate the hexokinase ATPase activity), and 40 μM dNTPs [35]. The total volume of each gap filling reaction was 40 μl. All concentrations above are the final values after initiating gap filling. Primer elongation reactions were quenched after varying reaction times with 40 μl 50 mM ethylenediaminetetraacetic acid. To ensure a high yield of the full-length product, we conducted the primer elongation reaction for the unblocked primer–template for 30 s in the absence of calf thymus DNA and glucose. All other control DNA samples were not exposed to Pol III HE. All reactions and control samples were ethanol precipitated, and the air-dried pellets were each dissolved in 40 μl 75% formamide and 17 μl loaded onto 10% polyacrylamide/8.0 M urea/12% formamide sequencing gels to resolve the products. The gels were visualized using a Storm 840 Phosphor Imager and analyzed using ImageQuant 5.2.

2.3.6 Attachment of phenyldiazirine to oligonucleotides

In the absence of ambient light, 4-[3-(trifluoromethy)-diazirin-3-yl]benzoate N-hydroxysucinimide (custom synthesized by BioSynthesis, Inc.) was dissolved in anhydrous dimethyl formamide (0.5 M final concentration). A 4.4 μmol sample was combined with 20 nmol of oligonucleotide (Integrated DNA Technologies) containing amino-modified C2 dT from Glen Research in a 0.1 M sodium tetraborate buffer (pH 8.5) (final volume, 50 μl). This reaction mixture was incubated in the dark at room temperature overnight. The derivatized product was HPLC purified using a Waters XBridge OST C18 column (4.6 mm x 50 mm, pore size of 2.5 μm). The sample was applied in 0.1 M triethylammonium acetate (pH 7.0) at a flow rate of 1.0 ml/min and eluted with a gradient changing to acetonitrile at 1.54%/min. The column was run at 60 °C, and absorbance was monitored at 265 nm and 350 nm. Approximately 15 nmol of photoreactive oligonucleotide was recovered. The presence of photo-crosslinker in the oligonucleotide was verified by observing peaks at 260 nm and 350 nm and by a shift in chromatographic mobility from the unreacted oligonucleotide.

2.3.7 Photo-crosslinking oligonucleotides

Oligonucleotides (Fig. 2.3A) were combined with proteins and nucleotides at room temperature in a buffer containing 50 mM Hepes (pH 7.5), 10 mM magnesium acetate, 10 mM dithiothreitol, 20% (v/v) glycerol, 0.02% (v/v) Nonidet P40 detergent, and 100 mM potassium glutamate (unless otherwise indicated) in siliconized Pyrex

tubes covered in Parafilm and irradiated at 350 nm in a Rayonet photochemical reactor for 1 h at room temperature. The samples were quenched in 2x SDS-PAGE sample buffer [0.25 M Tris–HCl (pH 6.8), 5% SDS, 0.02% β-mercaptoethanol, and 0.2% glycerol]. Samples were analyzed by 4–11% gradient SDS-PAGE containing 4 M urea.

For experiments in Fig. 2.3C, initiation complexes were generated by pre-incubating 4 nM ^{32}P-labeled primed template (Fig. 2.3A) with 40 nM streptavidin and then combining with 16 nM τ_3 complex, 16 nM Pol III, 200 nM β_2, and 0.8 mM ATP prior to irradiation.

2.4 RESULTS

Most measurements assessing pathways that trigger Pol III* release and cycling have been performed using equilibrium binding measurements. While a decreased affinity of Pol III* for the template might be consistent with a role in accelerating release, the relevant issue is whether the lagging strand is triggered to release in less than 0.1 s upon collision with the preceding Okazaki fragment. To provide a method for quantitative assessment of the kinetics of Pol III* release, we set up a surface plasmon resonance (SPR) assay in which primers were placed on a surface-immobilized template a set number of nucleotides from an oligonucleotide that models the 5'-end of the preceding Okazaki fragment (Fig. 2.1A). Initiation complexes are mobile on DNA, and unless bulky blocking agents flank the complex, it rapidly slides off the ends of the template [36]. We placed biotin near the 3'-end of the template to permit attachment to a streptavidin-covered surface for SPR measurements. The other end of the construct

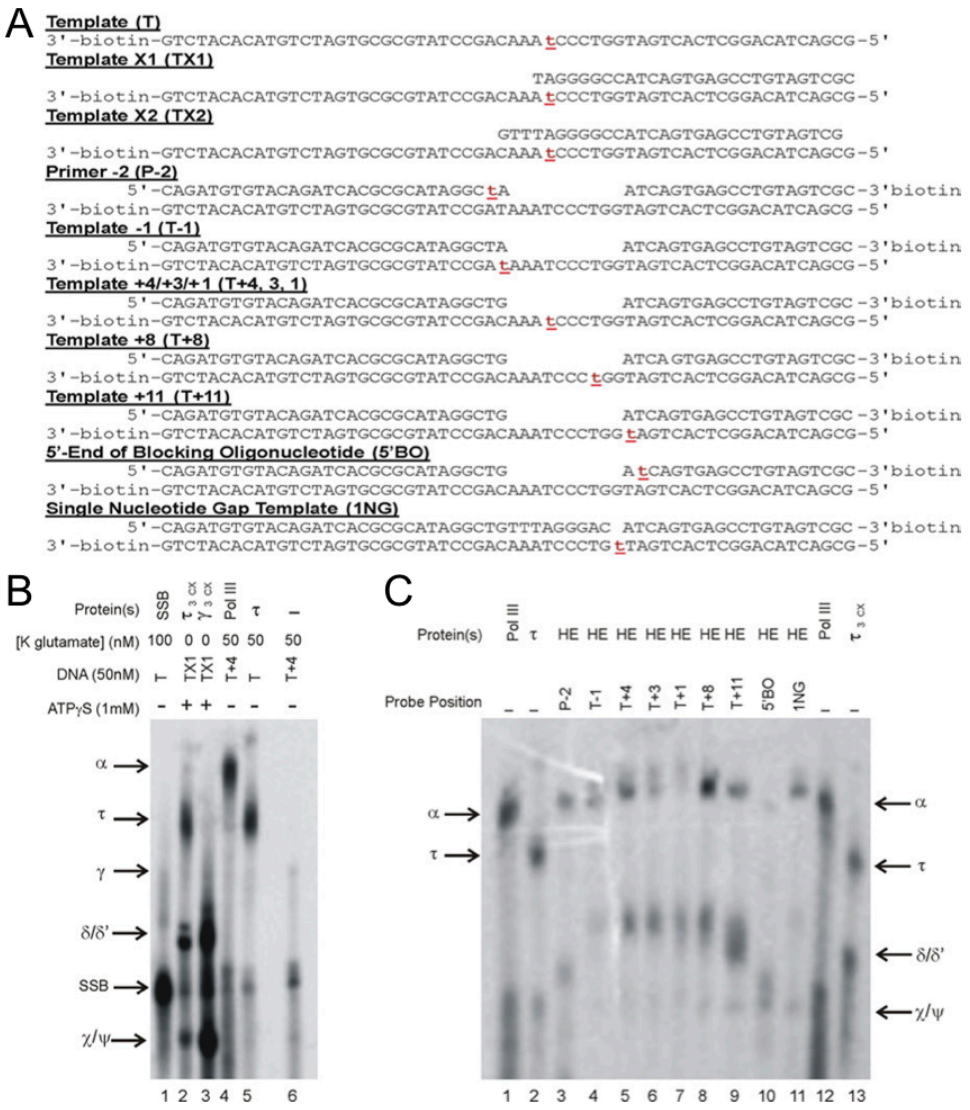

FIGURE 2.3

The Pol III α subunit and not τ is positioned to serve as the sensor for the completion of Okazaki fragment synthesis. (A) DNA constructs used to determine Pol III HE contacts with model templates. The position of the phenyldiazirine photo-cross-linker is indicated by red lowercase t. The oligonucleotide containing the photo-cross-linker was labeled with ^{32}P on the 5'-end prior to annealing. Template T+4 also served as Templates T+3 and T+1 by the addition of 10 μM ddTTP or dTTP, respectively. (B) Denaturing polyacrylamide gel analysis of Pol III HE subunit standards. Generation of lanes 1–3 is described in Fig. A1.4. Pol III (0.62 μM final concentration) used to generate lane 4 and τ (2 μM) used to generated lane 5. (C) Identification of protein contacts with model templates. Photo-cross-linking took place within initiation complexes formed with the designated model templates. The gel lanes were loaded with approximately equal counts of radioactivity. Lanes 1, 2, 12, and 13 are identical with lanes 4, 5, 4 and 2, respectively, in (B).

was blocked by covalently attaching the 3'-terminus of the blocking oligonucleotide to His_6-tagged O^6-alkylguanineDNA-transferase (SNAP-tag) [23]. The sequence of the template downstream of the primer was designed to permit controlled advancement of the elongating Pol III HE by a subset of dNTPs.

We observed stabile association of Pol III HE with each primer–template to form an initiation complex that dissociated with a half-life of 10–15 min (Fig. 2.1C–E). Addition of the full complement of dNTPs required for conversion of the gap to a nick greatly increased the amount of the Pol III* released (Fig. 2.1C and D) and modestly (3- to 8-fold) increased the dissociation rate (Table 2.2). However, the half-life of polymerase release (~2–5 min) is approximately 1000-fold slower than that expected to support the physiological rate of cycling upon completion of an Okazaki fragment. We observed that addition of any nucleotide, independent of whether the nucleotides present were able to fill the gap completely, led to an increase in the amount of Pol III* that dissociates (amplitude column in Table 2.2), but complete gap filling is needed to achieve the maximal rate.

Kinetic analysis was complicated by a second, more slowly dissociating component that required analysis using a double-exponential decay equation (Fig. 2.1F). The second component dissociated with a half-life of 1–5 h. This required each dissociation experiment to be run for up to 3 days to acquire a data set that allowed for complete decay (10 half-lives) for an accurate curve fit. In this chapter, we refer to the presumably biologically relevant fast dissociating component and present the full data under Tables A1.1–A1.3.

Recognizing that simple conversion of a gap to a nick did not provide an adequate rate of Pol III* release to achieve a physiologically relevant rate of cycling for Okazaki fragment synthesis, we sought external effectors that might stimulate dissociation. We found that the presence of ATP and an exogenous template–primer accelerates dissociation approximately 4-fold (Fig. 2.4 and Table 2.3). Raising the exogenous primed template concentration in the analyte solution did not further increase the rate. ATPγS will not substitute in this reaction, suggesting that ATP hydrolysis is required. The rate enhancement by these factors is only fully achieved when a gap has been filled. SSB and exogenous β_2 are not required to accelerate Pol III release (Table 2.3).

The blocking oligonucleotide used in our assay to mimic the preceding Okazaki fragment contained a 5'-hydroxyl group. The preceding fragment in cells would be expected to contain a 5'-triphosphate to be composed of RNA for ca 10 nt at the 5'-end. To determine whether either of these factors led to more rapid polymerase release, we had blocking oligonucleotides synthesized that contained either a 5'-triphosphate or a mixed RNA/DNA oligonucleotide with 12 RNA nucleotides at the 5'-end and a single 5'-phosphate. Neither of these modifications led to acceleration of release (Table 2.1). The experiments described so far were conducted using Pol III HE with the presumed physiological Pol III* composition: Pol III_2-$\tau_2\gamma\delta\delta'\chi\psi$ [1]. To ensure that a dimeric polymerase was not the cause of slow release, we also prepared an assembly with a Pol III-$\tau\gamma_2\delta\delta'\chi\psi$ composition. Upon addition of dNTPs on the 4 and 5 nt gapped templates, polymerase dissociated with half-lives of 140 and 130 s, respectively—similar to the 110 s observed with the dimeric polymerase assembly. We observed a

Injection	4-nt gap template $t_{1/2}$ (s) [amplitude]	Gap size	5-nt gap template $t_{1/2}$ (s) [amplitude]	Gap size
Buffer	860 [12%]	4	620 [10%]	5
dCTP	390 [69%]	3	360 [70%]	3
ddCTP	660 [25%]	3	380 [26%]	4
dCTP, dTTP	210 [62%]	1	190 [63%]	1
dCTP, ddTTP	370 [36%]	2	350 [37%]	2
dCTP, dTTP, dGTP	290 [55%]	0	180 [57%]	0
dCTP. dTTP. ddGTP	110 [64%]	0	110 [63%]	0

TABLE 2.2
Filling a gap completely is required to achieve the maximal rate of Pol III* release

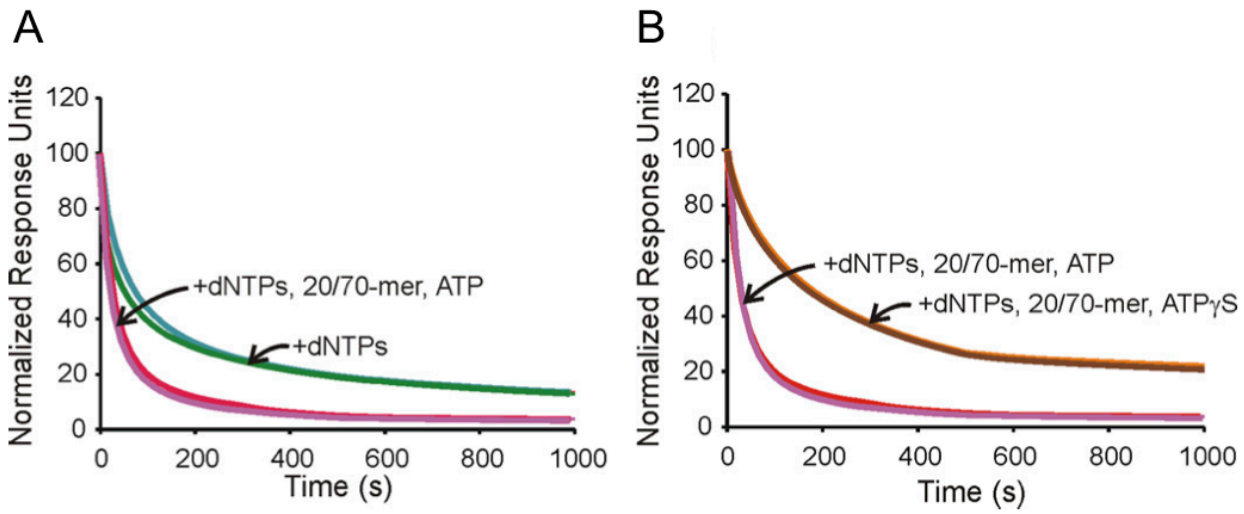

FIGURE 2.4

An exogenous primed template and ATP accelerate Pol III* release from templates with filled gaps. The dissociation of Pol III* from primed template was measured using SPR following a second injection of dNTPs (40 μM dCTP, dTTP, and ddGTP) alone or dNTPs plus additional components (+1 mM ATP or ATPγS and 0.5 μM exogenous 20/70-mer). Data shown are normalized response units versus time for the first 1000 s of dissociation. (A) Curves shown are for dNTPs alone with a 4 nt gapped template (green) and a 5 nt gapped template (teal) or for dNTPs + 20/70-mer +ATP with 4 nt gapped template (magenta) and 5 nt gapped template (red). (B) The slowly hydrolyzed ATP analog ATPγS decreases the off-rate of Pol III* in the presence of dNTPs and exogenous 20/70-mer. Curves shown are for dNTPs +20/70-mer +ATP with a 4 nt gapped template (magenta) and a 5 nt gapped template (red) or dNTPs +20/70-mer + ATPγS with a 4 nt gapped template (brown) and 5 nt gapped template (dark orange). The curves for the 4 nt and 5 nt gapped templates are coincident and not resolved at most times shown.

Injection	4-nt gap template $t_{1/2}$ (s) [amplitude]	5-nt gap template $t_{1/2}$ (s) [amplitude]
ATP	990 [60%]	920 [62%]
dNTPs	110 [64%]	110 [64%]
dNTPs, 20/70-mer, ATP	30 [86%]	40 [83%]
dNTPs, ATP	60 [75%]	60 [77%]
20/70-mer, ATP	330 [52%]	340 [51%]
dNTPs, 20/70-mer	60 [80%]	70 [77%]
dNTPs, 20/70-mer, ATP, SSB_4	50 [77%]	50 [73%]
dNTPs, 20/70-mer, ATP, SSB_4, β_2	30 [64%]	30 [59%]
dNTPs, 20/70-mer, ATPγS	130 [68%]	130 [67%]

TABLE 2.3
Exogenous primed template and ATP stimulate Pol III* release from completed Okazaki fragments

similar dissociation rate ($t_{1/2}$ = 140 s) upon the addition of dNTPs to allow gap filling for Pol III HE with a Pol III_3-$\tau_3\delta\delta'\chi\psi$ composition.

The rate of polymerase release that we observe is much slower than the rate of less than or equal to (0.5 s^{-1}; $t_{1/2}$ ~1.4 s) reported previously [10]. However, reanalysis of the published data yielded a fit to a single exponential with a half-life of 14 s (0.05 s^{-1}), too slow to support the rate of *in vivo* Okazaki fragment synthesis, albeit faster than the rates we observe in this work (Fig. A1.1).

Our results are consistent with gap completion providing a signal for cycling, but with release slower than would be expected for cycling during Okazaki fragment synthesis. We wanted to determine whether the slow rate of polymerase release was due to a slow process after Okazaki fragment completion such as a conformational change or whether the rate of incorporation of the final nucleotide(s) to complete the fragment was slow. To enable these measurements, we constructed templates similar to those used for the SPR experiments with 5'-^{32}P-labeled primers. This permitted monitoring of the rate of primer elongation and gap completion using high-resolution polyacrylamide gel electrophoresis. After formation of initiation complexes with Pol III HE on the primer–template, elongation reactions were initiated by addition of dNTPs. The majority (79%) of primer–templates are completely gap filled before the first manually sampled time point could be taken (5 s), a timescale faster than Pol III* dissociation (Fig. 2.2). Thus, dissociation is not limited by the rate of gap filling. The nicked duplex represents 22% of all elongated products. Interestingly, most of the elongation product (57% for wild-type Pol III HE) corresponds to a modest level of displacement of the blocking oligonucleotide. The wild-type Pol III HE forms significant

products up to 14 nt beyond the blocking oligonucleotide, and the average strand displacement is approximately 7 nt.

Previous models have proposed roles for either τ or α to serve as the sensor for conversion of a gap to a nick upon completion of Okazaki fragment synthesis, serving as a trigger for accelerated polymerase release [10,11,37,38]. To determine the proteins that contact the template and blocking oligonucleotide immediately ahead of the primer terminus, I performed crosslinking experiments. A phenyldiazirine linked to the 5-position of thymidylate was placed at a unique position in a series of templates that mimicked those used in the SPR experiments (Fig. 2.3A). I chose diazirines because, when irradiated, they generate carbenes that efficiently insert into C–H bonds of all amino acids [39]. This permits interpretation of negative results with certainty—if a protein does not crosslink, it is not bound to the template position to which the diazirine is linked.

To enable assignment of crosslinked proteins by their electrophoretic mobility I forced template–protein contacts with high concentrations of single or simple subsets of Pol III HE subunits to generate standards (Fig. A1.4 and Fig. 2.3B). Control experiments were performed with the phenyldiazirine placed at the penultimate (−2) position at the 3'-end of the primer terminus and at the template position opposite the 3'-primer terminus. As expected from previous work [37,40], α was observed to crosslink. Crosslinking at template positions 1, 3, 4, and 8 nt ahead of the primer and at the template position opposite the 5'-nucleotide of the blocking oligonucleotide led to the crosslinking of the α subunit of Pol III and not τ (Fig. 2.3C). I also observed a crosslink to single-stranded template positions that may correspond to either δ or δ'. In a control

experiment, where the material in lane 8 of Fig. 2.3C was mixed with lane 2, the τ and δ/δ' cross-links were clearly distinguishable (data not shown). These species may represent two binding states−one with Pol III bound to the primer terminus and another with DnaX complex bound. Crosslinks to α were also observed to the nucleotide in the gap for templates containing a single nucleotide gap (Fig. 2.3C). When phenyldiazirine was placed at the penultimate 5'-position of the blocking oligonucleotide, a very low yield of crosslinks to α was observed, consistent with the strand displacement observed upon completion of synthesis (Fig. 2.2). This result suggests that displaced blocking oligonucleotide does not maintain contact with Pol III. Thus, α and not τ is the only protein positioned to function as the sensor for gap completion.

2.5 DISCUSSION

To permit a kinetic evaluation of the rate of polymerase release upon completing Okazaki fragment synthesis, we immobilized model templates on a surface, assembled initiation complexes, and monitored polymerase release upon nucleotide addition by SPR. We found that conversion of a gap to a nick accelerates release, but the rate is far too slow to support the physiological rate of Okazaki fragment synthesis. The differences from other published models likely arise from their derivation from equilibrium measurements and ours from kinetic determinations.

In a search for factors that accelerate collision-induced dissociation, we found that a mixture of ATP and an exogenous primed template accelerates dissociation 4-fold. ATPγS will not substitute in this reaction, suggesting that ATP hydrolysis is

required. These findings partially reconcile previous models and observations pertaining to the requirement for gap completion [10], the availability of a new template–primer [8], and the requirement for τ [10]. A series of switches may exist, all of which must be accommodated for maximal cycling. Gap completion may put the Pol III HE in a state in which a signal can be received from the associated τ-containing DnaX complex that involves binding of a new primer–template and ATP hydrolysis. Additional acceleration might be derived from other factors or their arrangement/interaction at the fork, or the collision mechanism might only be a backup, with the primary signal provided by events associated with new primer generation. The Pol III HE is involved in mismatch repair and other repair reactions where large stretches of DNA need to be copied [41]. The collision mechanism might provide a means for dissociating Pol III* once it has completed its task in repair reactions. Previous reports describe that gaps need to be completely filled [10] or only mostly filled [11] before polymerase release is triggered. These measurements were made primarily by equilibrium binding measurements. Our kinetic experiments support the conclusion that gaps need to be completely filled before the maximal rate of release is induced, but this rate is too slow to support chromosomal replication.

Our experiments were performed on a DNA substrate that mimicked the gap in the final stages of Okazaki fragment synthesis. True replication forks contain additional interactions, including two coupled leading and lagging strand polymerases that are bound to the replicative helicase. It is possible that the polymerase could switch to a state where it could more rapidly dissociate in the presence of these additional potential

allosteric effectors. Nevertheless, our substrates are similar to those used to initially formulate the collision hypothesis.

Measurement of the rate of gap filling indicates that the reaction is complete before the first time point (5 s) was taken. Thus, the rate of gap filling is fast relative to the rate of polymerase dissociation. For a majority of primer–templates, filling of the gap is followed by a strand displacement of approximately 7 nt on average. This value is less than the processivity of 300 nt observed in a strand displacement reaction that benefitted from a stabilizing interaction of χ with SSB [42]. Comparison of these results suggests that the χ –SSB interaction increases the processivity of strand displacement approximately 40-fold. The fact that most of the product observed involves strand displacement argues against exact gap filling to form a nick providing the signal for Pol III* release. If the signaling model is dominant, many Okazaki fragments may end before the gap between their terminus and the primer, for the following Okazaki fragment, is filled. However, if the lagging strand polymerase is sufficiently fast relative to the leading strand polymerase, complete gap filling will occur. In that case, strand displacement is likely to occur. DNA polymerase I is recognized as an enzyme that fills any remaining gaps between Okazaki fragments and removes RNA primers with a duplex-specific 5'-3' exonuclease activity, providing a nick that can be sealed by DNA ligase [43,44]. If there is a portion of the product that arises from strand displacement, another repair enzyme would be required to excise the displaced single-stranded flap, analogous to the function of the flap endonuclease FEN1 in eukaryotes [45].

I applied diazirine-based photo-crosslinking to identify which proteins contact a uniquely reactive position within model templates. The advantages of the method

include high yields, irradiation at wavelengths (350 nm) far removed from chromophores present in proteins or nucleic acids, and the ability of the carbene formed upon irradiation to insert into all amino acids. The efficiency and lack of chemical specificity permit negative results to be interpreted with confidence. Using this method, I have identified that α, and not τ, contacts the template and blocking oligonucleotide in front of the primer, making it the candidate for sensing conversion of a gap to a nick, presumably triggering change to a conformation that more rapidly releases from DNA[‡].

In a structure of Pol III α complexed to DNA, an OB fold was located close to the primer terminus [37]. Because OB folds commonly bind to ssDNA, a proposal was made that the OB fold could be part of the sensing network [37,38]. Consistent with this hypothesis, the ssDNA-binding portion of Pol III was localized to a C-terminal region of α that contains the OB-fold element [46]. A test of the importance of the OB fold motif was made using a mutant in which three basic residues located in the β1–β2 loop were changed to serine [11]. No ssDNA binding was observed in the mutant, indicating diminution in affinity. However, even the wild-type polymerase bound ssDNA extremely weakly, near the limit of detection in the assays used (K_d ~8 μM); thus, a modest decrease in affinity would appear to be a null result. The processivity of the mutant polymerase was decreased by the β1–β2 loop mutations, an effect that was rescued by the presence of the τ complex [11]. The latter observation would seem to suggest that although the OB fold contributes to ssDNA affinity and processivity, it is not the

[‡] After the initial writing of this chapter, a structure of an α-τ C-terminal domain-DNA complex was published [50]. This structure reveals that the C-terminal domain of α interacts very closely with the C-terminal domain of τ. The τ subunit is not in position to interact with ssDNA ahead of the primer terminus, substantiating the photo-crosslinking results presented here.

processivity sensor, or at least the residues mutated are not the key interactors. The OB fold might act in concert with other binding changes as part of a more complex signaling network.

In our view, the entire polymerase active site is likely the processivity switch. Wing *et al.* have elegantly demonstrated a conformational change induced by substrate binding in which several elements move, one of the results of which is to place the β_2 binding domain in a position where it can productively interact with the β_2 clamp on DNA [37]. Follow-on studies with a Gram-positive polymerase suggest that this observation may be general [47,48]. The geometry and spatial constraints around the active site when the exiting template is double stranded might make insertion of the last nucleotide and ensuing strand displacement energetically unfavorable. Thus, these products may have decreased affinity for the active site, triggering a reversal of the conformational changes that occurred upon primer–template and dNTP binding, causing the β_2 binding domain to be pulled away, and switching the polymerase to a low-processivity mode. The presence of a polymerase domain that is not bound to DNA serves to decrease the affinity of the C-terminal domains of Pol III α for β_2 [14], which is consistent with this model.

Our results demonstrate that the collision of the Pol III HE with the downstream elongated primer of the preceding Okazaki fragment is inadequate to support the rapid release required for cycling to the next primer at the replication fork. The only alternative explanation in the literature is provided by the signaling model, originally proposed by Ken Marians [8]. We have shown that providing a competing primer in the presence of ATP only modestly stimulates dissociation. Thus, the function of primase in the

signaling model must be more than just providing a competing primer. One possibility is that primase, upon primer synthesis, sends a signal to the Pol III HE through the replicative helicase to which both are bound. Another possibility is that the competing primer is provided in a special context created by the molecular interactions at the replication fork.

Methodologies have been developed in the T4 and T7 systems [18–20] that might enable a more rigorous test of the signaling mechanism in *E. coli*. If the signaling model proves correct, an understanding of the specific reaction steps and molecular interactions that throw the processivity switch and direct the replicase to the next primer will be the next challenge. This remains a critical deficit in our understanding of all DNA replication systems.

2.6 REFERENCES

1 McHenry, C. S. (2011) DNA replicases from a bacterial perspective. Annual Review of Biochemistry **80**, 403–36.

2 Breier, A. M., Weier, H.-U. G. and Cozzarelli, N. R. (2005) Independence of replisomes in *Escherichia coli* chromosomal replication. Proceedings of the National Academy of Sciences of the United States of America **102**, 3942–7.

3 Masai, H., Matsumoto, S., You, Z., Yoshizawa-Sugata, N. and Oda, M. (2010) Eukaryotic chromosome DNA replication: where, when, and how? Annual Review of Biochemistry **79**, 89–130.

4 Mok, M. and Marians, K. J. (1987) Formation of rolling-circle molecules during ΦX174 complementary strand DNA replication. The Journal of Biological Chemistry **262**, 2304–9.

5 Mok, M. and Marians, K. J. (1987) The *Escherichia coli* preprimosome and DNA B helicase can form replication forks that move at the same rate. The Journal of Biological Chemistry **262**, 16644–54.

6 Johanson, K. O. and McHenry, C. S. (1982) The β subunit of the DNA polymerase III holoenzyme becomes inaccessible to antibody after formation of an initiation complex with primed DNA. The Journal of Biological Chemistry **257**, 12310–5.

7 Stukenberg, P. T., Turner, J. and O'Donnell, M. (1994) An explanation for lagging strand replication: polymerase hopping among DNA sliding clamps. Cell **78**, 877–87.

8 Wu, C. A., Zechner, E. L., Reems, J. A., McHenry, C. S. and Marians, K. J. (1992) Coordinated leading- and lagging-strand synthesis at the *Escherichia coli* DNA replication fork. V. Primase action regulates the cycle of Okazaki fragment synthesis. The Journal of Biological Chemistry **267**, 4074–83.

9 Alberts, B. M., Barry, J., Bedinger, P., Formosa, T., Jongeneel, C. V and Kreuzer, K. N. (1983) Studies on DNA replication in the bacteriophage T4 *in vitro* system. Cold Spring Harbor symposia on quantitative biology **47 Pt 2**, 655–68.

10 Leu, F. P., Georgescu, R. and O'Donnell, M. (2003) Mechanism of the *E. coli* τ processivity switch during lagging-strand synthesis. Molecular Cell **11**, 315–27.

11 Georgescu, R. E., Kurth, I., Yao, N. Y., Stewart, J., Yurieva, O. and O'Donnell, M. (2009) Mechanism of polymerase collision release from sliding clamps on the lagging strand. The EMBO Journal **28**, 2981–91.

12 López de Saro, F. J., Georgescu, R. E. and O'Donnell, M. (2003) A peptide switch regulates DNA polymerase processivity. Proceedings of the National Academy of Sciences of the United States of America **100**, 14689–94.

13 López de Saro, F. J., Georgescu, R. E., Goodman, M. F. and O'Donnell, M. (2003) Competitive processivity-clamp usage by DNA polymerases during DNA replication and repair. The EMBO Journal **22**, 6408–18.

14 Kim, D. R. and McHenry, C. S. (1996) Identification of the β-binding domain of the α subunit of *Escherichia coli* polymerase III holoenzyme. The Journal of Biological Chemistry **271**, 20699–704.

15 Dalrymple, B. P., Kongsuwan, K., Wijffels, G., Dixon, N. E. and Jennings, P. A. (2001) A universal protein-protein interaction motif in the eubacterial DNA replication and repair systems. Proceedings of the National Academy of Sciences of the United States of America **98**, 11627–32.

16 Dohrmann, P. R. and McHenry, C. S. (2005) A bipartite polymerase-processivity factor interaction: only the internal β binding site of the α subunit is required for processive replication by the DNA polymerase III holoenzyme. Journal of Molecular Biology **350**, 228–39.

17 Li, X. and Marians, K. J. (2000) Two distinct triggers for cycling of the lagging strand polymerase at the replication fork. The Journal of Biological Chemistry **275**, 34757–65.

18 Hamdan, S. M., Loparo, J. J., Takahashi, M., Richardson, C. C. and Van Oijen, A. M. (2009) Dynamics of DNA replication loops reveal temporal control of lagging-strand synthesis. Nature **457**, 336–9.

19 Lee, J.-B., Hite, R. K., Hamdan, S. M., Xie, X. S., Richardson, C. C. and Van Oijen, A. M. (2006) DNA primase acts as a molecular brake in DNA replication. Nature **439**, 621–4.

20 Pandey, M., Syed, S., Donmez, I., Patel, G., Ha, T. and Patel, S. S. (2009) Coordinating DNA replication by means of priming loop and differential synthesis rate. Nature **462**, 940–3.

21 Manosas, M., Spiering, M. M., Zhuang, Z., Benkovic, S. J. and Croquette, V. (2009) Coupling DNA unwinding activity with primer synthesis in the bacteriophage T4 primosome. Nature Chemical Biology **5**, 904–12.

22 Yang, J., Nelson, S. W. and Benkovic, S. J. (2006) The control mechanism for lagging strand polymerase recycling during bacteriophage T4 DNA replication. Molecular Cell **21**, 153–64.

23 Jongsma, M. A. and Litjens, R. H. G. M. (2006) Self-assembling protein arrays on DNA chips by auto-labeling fusion proteins with a single DNA address. Proteomics **6**, 2650–5.

24 Kim, D. R. and McHenry, C. S. (1996) *In vivo* assembly of overproduced DNA polymerase III. Overproduction, purification, and characterization of the α, α-ε, and α-ε-θ subunits. The Journal of Biological Chemistry **271**, 20681–9.

25 Wieczorek, A. and McHenry, C. S. (2006) The NH_2-terminal php domain of the α subunit of the *Escherichia coli* replicase binds the ε proofreading subunit. The Journal of Biological Chemistry **281**, 12561–7.

26 Dallmann, H. G., Thimmig, R. L. and McHenry, C. S. (1995) DnaX complex of *Escherichia coli* DNA polymerase III holoenzyme. Central role of τ in initiation complex assembly and in determining the functional asymmetry of holoenzyme. The Journal of Biological Chemistry **270**, 29555–62.

27 Song, M. S., Pham, P. T., Olson, M., Carter, J. R., Franden, M. A., Schaaper, R. M. and McHenry, C. S. (2001) The δ and δ' subunits of the DNA polymerase III holoenzyme are essential for initiation complex formation and processive elongation. The Journal of Biological Chemistry **276**, 35165–75.

28 Olson, M. W., Dallmann, H. G. and McHenry, C. S. (1995) DnaX complex of *Escherichia coli* DNA polymerase III holoenzyme. The χψ complex functions by increasing the affinity of τ and γ for δ.δ' to a physiologically relevant range. The Journal of Biological Chemistry **270**, 29570–7.

29 Johanson, K. O., Haynes, T. E. and McHenry, C. S. (1986) Chemical characterization and purification of the β subunit of the DNA polymerase III holoenzyme from an overproducing strain. The Journal of Biological Chemistry **261**, 11460–5.

30 Griep, M. A. and McHenry, C. S. (1989) Glutamate overcomes the salt inhibition of DNA polymerase III holoenzyme. The Journal of Biological Chemistry **264**, 11294–301.

31 Pritchard, A. E., Dallmann, H. G. and McHenry, C. S. (1996) *In vivo* assembly of the τ-complex of the DNA polymerase III holoenzyme expressed from a five-gene artificial operon. Cleavage of the τ-complex to form a mixed γ-τ-complex by the OmpT protease. The Journal of Biological Chemistry **271**, 10291–8.

32 Glover, B. P. and McHenry, C. S. (2000) The DnaX-binding subunits δ' and ψ are bound to γ and not τ in the DNA polymerase III holoenzyme. The Journal of Biological Chemistry **275**, 3017–20.

33 Fijalkowska, I. J. and Schaaper, R. M. (1996) Mutants in the Exo I motif of *Escherichia coli* dnaQ: defective proofreading and inviability due to error catastrophe. Proceedings of the National Academy of Sciences of the United States of America **93**, 2856–61.

34 Pritchard, A. E., Dallmann, H. G., Glover, B. P. and McHenry, C. S. (2000) A novel assembly mechanism for the DNA polymerase III holoenzyme DnaX complex: association of δδ' with DnaX(4) forms DnaX(3)δδ'. The EMBO Journal **19**, 6536–45.

35 Downey, C. D., Crooke, E. and McHenry, C. S. (2011) Polymerase chaperoning and multiple ATPase sites enable the *E. coli* DNA polymerase III holoenzyme to rapidly form initiation complexes. Journal of Molecular Biology **412**, 340–53.

36 Kaboord, B. F. and Benkovic, S. J. (1993) Rapid assembly of the bacteriophage T4 core replication complex on a linear primer/template construct. Proceedings of the National Academy of Sciences of the United States of America **90**, 10881–5.

37 Wing, R. A, Bailey, S. and Steitz, T. A. (2008) Insights into the replisome from the structure of a ternary complex of the DNA polymerase III α-subunit. Journal of Molecular Biology **382**, 859–69.

38 Lamers, M. H., Georgescu, R. E., Lee, S.-G., O'Donnell, M. and Kuriyan, J. (2006) Crystal structure of the catalytic α subunit of *E. coli* replicative DNA polymerase III. Cell **126**, 881–92.

39 Tate, J. J., Persinger, J. and Bartholomew, B. (1998) Survey of four different photoreactive moieties for DNA photoaffinity labeling of yeast RNA polymerase III transcription complexes. Nucleic Acids Research **26**, 1421–6.

40 Reems, J. A., Wood, S. and McHenry, C. S. (1995) *Escherichia coli* DNA polymerase III holoenzyme subunits α, β, and γ directly contact the primer-template. The Journal of Biological Chemistry **270**, 5606–13.

41 Modrich, P. (1989) Methyl-directed DNA mismatch correction. The Journal of Biological Chemistry **264**, 6597–600.

42 Yuan, Q. and McHenry, C. S. (2009) Strand displacement by DNA polymerase III occurs through a τ-ψ-χ link to single-stranded DNA-binding protein coating the lagging strand template. The Journal of Biological Chemistry **284**, 31672–9.

43 Kornberg, A. (1992) DNA Polymerase II of *E. coli*. In DNA Replication, p 167, W.H. Freeman and Company New York, NY.

44 Konrad, E. B. and Lehman, I. R. (1974) A conditional lethal mutant of *Escherichia coli* K12 defective in the 5' leads to 3' exonuclease associated with DNA

polymerase I. Proceedings of the National Academy of Sciences of the United States of America **71**, 2048–51.

45 Liu, Y., Kao, H.-I. and Bambara, R. A. (2004) Flap endonuclease 1: a central component of DNA metabolism. Annual Review of Biochemistry **73**, 589–615.

46 McCauley, M. J., Shokri, L., Sefcikova, J., Venclovas, C., Beuning, P. J. and Williams, M. C. (2008) Distinct double- and single-stranded DNA binding of *E. coli* replicative DNA polymerase III α subunit. ACS Chemical Biology **3**, 577–87.

47 Evans, R. J., Davies, D. R., Bullard, J. M., Christensen, J., Green, L. S., Guiles, J. W., Pata, J. D., Ribble, W. K., Janjic, N. and Jarvis, T. C. (2008) Structure of PolC reveals unique DNA binding and fidelity determinants. Proceedings of the National Academy of Sciences of the United States of America **105**, 20695–700.

48 Wing, R. A. (2010) Structural studies of the prokaryotic replisome, Yale University.

49 Dohrmann, P. R., Manhart, C. M., Downey, C. D. and McHenry, C. S. (2011) The Rate of Polymerase Release upon Filling the Gap between Okazaki Fragments Is Inadequate to Support Cycling during Lagging Strand Synthesis. Journal of Molecular Biology, Elsevier Ltd **414**, 15–27.

50 Liu, B., Lin, J. and Steitz, T. A. (2013) Structure of the PolIIIα-τ_C-DNA Complex Suggests an Atomic Model of the Replisome. Structure (London, England : 1993).

CHAPTER 3[*]

The PriA replication restart protein blocks replicase access prior to assembly and directs template specificity through its ATPase activity[†]

3.1 ABSTRACT

The PriA protein serves as an initiator for the restart of DNA replication on stalled replication forks and as a checkpoint protein that prevents the replicase from advancing in a strand displacement reaction on forks that do not contain a functional replicative helicase. I have developed a primosomal protein-dependent fluorescence resonance energy transfer (FRET) assay using a minimal fork substrate composed of synthetic oligonucleotides. I demonstrate that a self-loading reaction, which proceeds at high helicase concentrations, occurs by threading of a preassembled helicase over free 5'-ends, an event that can be blocked by attaching a steric block to the 5'-end or coating DNA with single-stranded DNA binding protein. The specificity of PriA for replication forks is regulated by its intrinsic ATPase. ATPase-defective PriA K230R shows a strong preference for substrates that contain no gap between the leading strand and the duplex portion of the fork, as demonstrated previously. Wild-type PriA prefers substrates with larger gaps, showing maximal activity on substrates on which PriA K230R is inactive. I demonstrate that PriA blocks replicase function on forks by blocking its binding.

[*] I performed the entirety of the experimental work presented in this chapter.
[†] The contents of this chapter were published in [46] and are presented here with few modifications.

3.2 INTRODUCTION

In bacteria, DNA replication initiates at a unique chromosomal origin directed by sequence-specific binding of multiple copies of DnaA with ensuing loading of the replicative helicase by a helicase loader [1,2]. Once replication forks are established, they often encounter a block before they reach DNA replication termination points, roughly 2 mega base pairs away on the *Escherichia coli* chromosome [3]. Once the replisome dissociates, DnaA no longer functions to re-establish the replication fork. This reaction is driven by the PriA protein in both Gram-negative and Gram-positive model organisms, *E. coli* and *Bacillus subtilis* [4,5].

In *E. coli*, several proteins are thought to act sequentially in building up the apparatus that can attract the helicase loader and assemble an active replication fork. Gel shift assays indicate that PriA binds initially, followed by PriB and then DnaT [6]. The resulting complex recruits the *E. coli* helicase loader/helicase (DnaC/DnaB), leading to helicase assembly in the presence of ATP [6].

Thus, PriA appears to be the lead protein that directs assembly of the restart primosome. This is consistent with its substrate specificity in binding to D loops, but not bubbles, and three-stranded structures that provide models for replication forks [7,8]. PriA contains an intrinsic 3’ to 5’ helicase that has been suggested to function to clear an annealed lagging strand product from the replication fork, creating a site for primosome assembly and helicase loading [9,10]. However, PriA mutants that are defective in helicase activity remain active and are even more effective than their wild-type counterparts on substrates containing single-stranded lagging strands [11]. This

has been proposed to be due to the mutant form remaining resident at the fork and not migrating away. PriA has also been shown to be a checkpoint protein that blocks the intrinsic strand displacement activity of DNA polymerase III holoenzyme (Pol III HE) on forks before an active replicative helicase has been assembled [12,13].

Early in the primosome assembly reaction, a handoff mechanism has been proposed, sequentially, between PriA, PriB and DnaT. Weak PriA-PriB and PriB-DnaT interactions are strengthened in the presence of single-stranded DNA. The binding sites on single-stranded DNA are partially shared by PriA, PriB, and DnaT. It has been suggested that the primosome assembly process is a dynamic one in which these proteins hand off the fork substrate to one another, culminating with DnaT binding to PriB and displacing it from DNA to provide a landing site for the helicase loader and helicase [14].

A replication restart protein-initiated rolling circle replication system has been established for *E. coli* that recapitulates the rate observed for replication forks *in vivo* [15,16]. Using this system, many of the basic principles of fork dynamics have been established, including the reversible association of primase with the replicative helicase, regulating Okazaki fragment length [16,17] and the association of the τ-subunit of the Pol III holoenzyme with the replicative helicase. The latter association tethers a dimeric replicase containing both leading and lagging strand polymerases to the helicase, binding all components active in DNA replication together at the fork in one large replisome assembly [18].

In the evolutionarily distant Gram-positive bacterium *B. subtilis*, conserved PriA proteins and the replicative helicase (termed DnaC in *B. subtilis*) participate in the

replication restart primosome, but novel proteins, DnaD and DnaB, which are not homologs of *E. coli* primosomal proteins, intervene between PriA and association with the helicase/helicase loader. The *B. subtilis* helicase loader, DnaI, is also poorly conserved, so *B. subtilis* and other low GC Gram-positive bacteria may follow a novel pathway for primosome assembly. An ordered assembly mechanism (PriA-DnaD-DnaB-DnaI-DnaC) has been proposed [19]. Another important difference between the *E. coli* and *B. subtilis* replication processes is that the proteins that act at intermediate stages between PriA and the helicase loader also participate in DnaA/origin-dependent initiation [20].

Our group established a fully functional *B. subtilis* rolling circle replication system on mini-circular templates that recapitulate the known *in vivo* replication rate and the genetically defined protein requirements [21]. This system allowed the function of two discrete Pol IIIs (DnaE and PolC) to be established. The PolC HE (PolC, τ-complex, and β_2) serves as the replicase for both the leading and lagging strands. Unlike in *E. coli*, the major replicase cannot efficiently elongate a primer provided by the DnaG primase. Instead, a protein functionally analogous to DNA polymerase α in eukaryotes, DnaE, extends the RNA primer a short distance and hands off the product to the PolC HE.

Both the *E. coli* and *B. subtilis* rolling circle replication systems require an extensive preincubation in a reaction where the helicase is recruited and assembled before elongation is initiated. This is necessary to isolate the elongation events so they can be studied without the kinetic complications of a rate-limiting initiation. Thus, a well defined system amenable to convenient acquisition of kinetic data is needed to study PriA-dependent assembly of the restart primosome.

FRET assays have been developed using synthetic forks that permit monitoring helicase function [22,23]. In this report, I adapt this FRET assay and show that blocking the 5'-end of the lagging strand template sterically precludes self-assembly of the helicase and makes the reaction dependent on PriA and the other components of the replication restart primosome. I use this system to reveal that PriA specificity for replication fork structure is determined by the PriA ATPase. I also explore the mechanism by which PriA acts as a checkpoint protein, blocking the intrinsic strand displacement activity of the Pol III HE on incompletely assembled replication forks.

3.3 MATERIALS AND METHODS

3.3.1 Oligonucleotides

All oligonucleotides were obtained from Biosearch Technologies. Substrates used in all FRET experiments and strand displacement reactions carried out in solution were assembled from the HPLC-purified oligonucleotides listed in Fig. 3.1E.

Substrates for fluorescent helicase assays and strand displacement reactions in solution were assembled by combining 1 μM fluorescent leading strand template, 1 μM quenching lagging strand template, and 1 μM of the appropriate leading strand primer (or no primer) in a final volume of 25 μl in a buffer containing 10 mM Tris-HCl (pH 7.75),

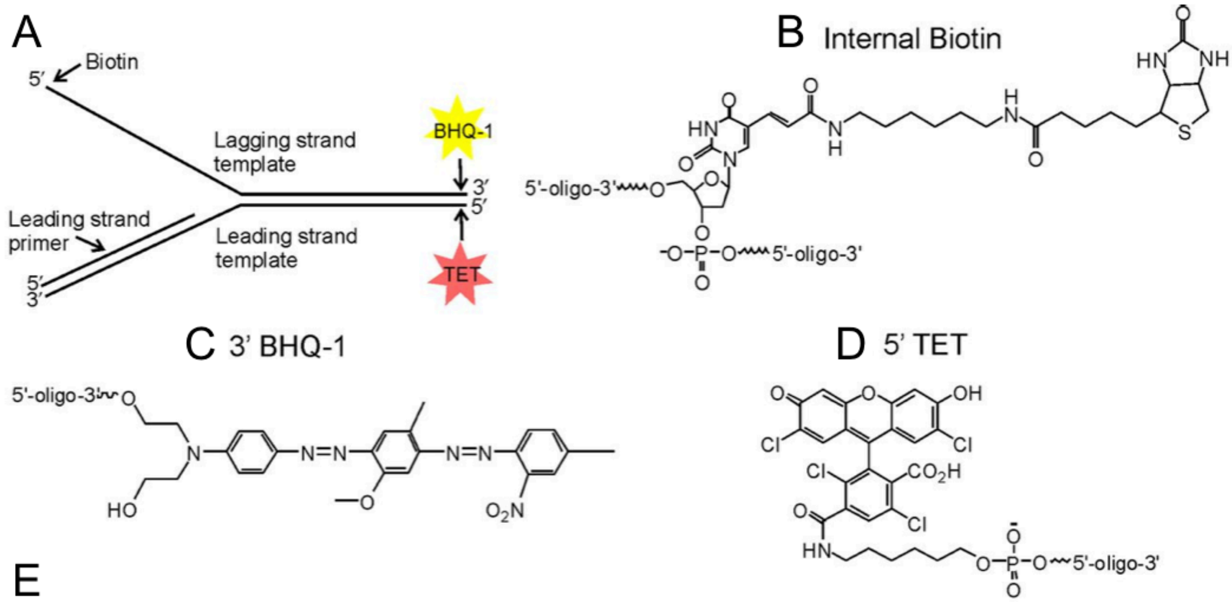

E

Fluorescent Leading Strand Template 90-mer (FT90)
5'-TET-CGCGTATAGATCATTACTATAACATGTTAGATTCATGATAATATACGAGATGACGAATATGATTTTGTCGGCTAATGTAAGAATCTTCAA-3'

Quenching Lagging Strand Template 90-mer (QT90)
5'-TT(biotin)TTTTTTTTTTTTTTTTTTTTTTTTTTTTTTTTTTTTTTTTTTTTTATATTATCATGAATCTAACATGTTATAGTAATGATCTATACGCG-BHQ-1-3'

Fluorescent Leading Strand Template 100-mer (FT100)
5'-TET-CGCGTATAGATCATTACTATAACATGTTAGATTCATGATAATATACGAGATGACGAATATGATTTTGTCGGCTAATGTAAGAATCTTCAAATGATCGTAG-3'

0 Nucleotide Gap Leading Strand Primer (P0g)
5'-TTGAAGATTCTTACATTAGCCGACAAAATCATATTCGTCATCTCG-3'

2 Nucleotide Gap Leading Strand Primer (P2g)
5'-TTGAAGATTCTTACATTAGCCGACAAAATCATATTCGTCATCT-3'

5 Nucleotide Gap Leading Strand Primer (P5g)
5'-TTGAAGATTCTTACATTAGCCGACAAAATCATATTCGTCA-3'

10 Nucleotide Gap Leading Strand Primer (P10g)
5'-TTGAAGATTCTTACATTAGCCGACAAAATCATATT-3'

20 Nucleotide Gap Leading Strand Primer (P20g)
5'-CTACGATCATTTGAAGATTCTTACATTAGCCGACA-3'

Trap Oligonucleotide
5'-TATATTATCATGAATCTAACATGTTATAGTAATGATCTATACGCG-3'

FIGURE 3.1
Model replication fork and oligonucleotides used in FRET helicase assays. (A) DNA substrate used in FRET unwinding reactions. Fluorescence of tetrachlorofluorescein (TET) on the 5'-terminus of the leading strand increases when separated from blackhole quencher 1 (BHQ-1) on the lagging strand. (B) internal biotin conjugated to modified thymidine. (C) black hole quencher 1 conjugated to 3'-end of the lagging strand. (D) tetrachlorofluorescein conjugated to 5'-end of the leading strand. (E) sequences of oligonucleotides (oligo) used to build substrates depicted in A for FRET assays. T(biotin) indicates the internal biotin modification in B.

50 mM NaCl, and 1 mM EDTA. Samples were heated to 95 °C for 5 min and cooled to 25 °C, decreasing the temperature by 1 °C/min. Unprimed forked template was constructed from FT90 and QT90; 0-nucleotide (nt) gap forked template from FT90, QT90, and P0g; 2 nt gap forked template from FT90, QT90, and P2g; 5 nt gap forked template from FT90, QT90, and P5g; 10 nt gap forked template from FT90, QT90, and P10g; and 20 nt gap forked template from FT100, QT90, and P20g.

For experiments on streptavidin beads, a biotinylated 10 nt gap forked template was constructed from biotinylated primer 35-mer, 5'-TT(biotin)GAAGATTCTTACATTAGCCGACAAAATCATATT-3' (biotin is conjugated to preceding modified thymidine); leading strand template 90-mer, 5'- CGC-GTATAGATCATTACTATAACATGTTAGATTCATGATAATATACGAGATGACGAATAT GATTTTGTCGGCTAATGTAAGAATCTTCAA-3'; and lagging strand template 90-mer, 5'-TTTTTTTTTTTTTTTTTTTTTTTTTTTTTTTTTTTTTTTTTTTTTTTATATTATCATGAATCT AACATGTTATAGTAATGATCTATACGCG-3'. Forked template was annealed identically to those for FRET experiments.

3.3.2 Proteins

E. coli Pol III HE and primosomal proteins were purified as described previously: Pol III [24], ε [25], τ [26], δ, δ' [27], χ, ψ [28], β [29], single-stranded DNA binding protein (SSB) [30], and wild-type PriA, PriB, DnaT, DnaB, and DnaC [31]. PriA K230R was a gift from Ken Marians [31]. The ε subunit used in our experiments was mutated at D12A

and E14A to eliminate endogenous 3'-5'-exonuclease activity, which degrades the primer [32]. *B. subtilis* protein components were purified as described for PolC, SSB, β, τ, δ, and δ' [33] and DnaE, PriA, DnaD, DnaB, DnaC, and DnaI [21].

Streptavidin was obtained from New England BioLabs. In experiments using T7 polymerase, USB Sequenase (version 2.0) DNA Polymerase (Affymetrix) was used. This is a genetically modified variant consisting of two subunits: *E. coli* protein thioredoxin and genetically engineered bacteriophage T7 gene 5 protein where amino acids 118 –145 are deleted to eliminate exonuclease activity. Polymerase activity is unaffected.

3.3.3 FRET Helicase Assays

Fluorescence helicase assays were carried out in a final volume of 50 μl with 20 nM substrate and 100 nM trap oligonucleotide in a black, round-bottomed 96-well plate (from Greiner Bio-One, catalog no. 650209) in a buffer containing 50 mM HEPES (pH 7.5), 20% (v/v) glycerol, 0.02% (v/v) Nonidet P40 detergent, 200 μg/ml BSA, 100 mM potassium glutamate, 10 mM DTT, 10 mM magnesium acetate, and 2 mM ATP. Unless otherwise noted, all substrates were preincubated for 5 min at room temperature with 200 nM streptavidin prior to the addition of other protein components. Helicase reactions were incubated at 30 °C for 15 min, which was within the linear time range of the assay under the conditions reported. Fluorescence emission was read at 535 nm using an EnVision plate reader (PerkinElmer Life Sciences) with an excitation at 485 nm. The fluorescent plate reader was equipped with excitation filter FITC 485 and emission

filter FITC 535. Unwound DNA concentration was related to fluorescence units using a linear calibration curve determined by fitting the fluorescence measurements of standard solutions with varying concentrations of unwound DNA. The standard solutions had concentrations ranging from 0 to 20 nM of unwound DNA in the reaction buffer with 100 nM trap oligonucleotide. The 0 nM point was taken to be when all of the fluorescent leading strand template was bound to the non-fluorescent quenching lagging strand template. The 20 nM standard was measured in the absence of quenching lagging strand template.

3.3.4 PriA Blocking Strand Displacement Reactions

The leading strand primer was labeled with ^{32}P on the 5'-end using T4 polynucleotide kinase according to the manufacturer's instructions (Invitrogen) prior to annealing. Unincorporated [γ-^{32}P]ATP was removed using a Microspin-G25 spin column (GE Healthcare). Experiments were carried out in the same reaction buffer as FRET experiments.

For reactions carried out in solution, 20 nM substrate was added to protein components from the indicated source organism: 500 nM PriA, 500 nM SSB_4, 500 nM β_2, 80 nM τ_3 complex, and 80 nM Pol III core (exo-) (or indicated *B. subtilis* polymerase) in a final reaction volume of 30 μl. The samples were incubated for 5 min at room temperature. dNTPs were added to 100 μM (final concentration) and incubated with the reaction for 5 min. The reactions were quenched in a sample of equal volume containing 96% formamide, 20 mM EDTA, and 1 mg/ml bromphenol blue, then heated

to 95 °C for 4 min. The samples were resolved by denaturing electrophoresis at 10 watts for 2 h in a 12% polyacrylamide gel (19:1 acrylamide:bisacrylamide) containing 8 M urea using 100 mM Tris borate and 2 mM EDTA as electrophoresis running buffer. Gels were dried onto DEAE paper and scanned by a phosphorimaging device.

For reactions carried out on streptavidin beads, 600 fmol of radiolabeled, biotinylated primer/10 nt gap forked template were bound to 25 μl of streptavidin beads (Promega Tetralink Tetrameric Avidin) pre-equilibrated in the reaction buffer. The forked template was incubated with the beads for 10 min at room temperature. The beads were then washed three times with 200 μl of reaction buffer to remove any unbound substrate. The bead-bound substrate was then incubated with 500 nM PriA, 500 nM SSB4, 500 nM β_2, 80 nM τ_3 complex, and 80 nM Pol III core (exo-) at room temperature for 15 min. The beads were then washed five times with 200 μl of the reaction buffer to remove free protein. dNTPs and/or primosomal proteins (PriB, DnaT, DnaB, and DnaC) were added to the reaction and incubated at room temperature for 15 min. The helicase loading conditions were independently optimized for this assay: 50 nM $PriB_2$, 500 nM $DnaT_3$, 12 nM $DnaB_6$, and 25 nM DnaC (Fig. A2.4). The reaction was quenched with 100 mM EDTA and 2% SDS. The product was removed from the bead by incubating with 20 μg of proteinase K at 37 °C for 1 h. A portion of the supernatant was then added to an equal volume of buffer containing 100 mM Tris borate, 2 mM EDTA, 20% (v/v) glycerol, 1 mg/ml bromphenol blue, and 1 mg/ml xylene cyanol FF prior to resolving in a native gel to assay helicase activity. These samples were resolved by electrophoresis at 75 V for 18 h in a 12% polyacrylamide gel (37.5:1 acrylamide:bisacrylamide) using the same electrophoresis buffer as denaturing gels. The gel was dried and scanned by a

PhosphorImager. A separate portion of the supernatant was analyzed by denaturing PAGE.

3.4 RESULTS

3.4.1 Development of a FRET Assay for Primosome Function

I adapted a FRET-based assay for helicase function [22] and optimized it for studying the helicase loading apparatus from two representative Gram-negative and Gram-positive organisms, *E. coli* and *B. subtilis*. The system employed model replication forks constructed from synthetic oligonucleotides with a fluorophore opposed by a quencher in the opposing strand (Fig. 3.1). Splitting the two strands apart results in an increase in fluorescence. I used an excess of a trapping oligonucleotide that was complementary to the duplex region of the leading strand template to sequester strands split apart by helicase so that they do not re-anneal. The leading strand template contained an annealed primer that modeled the leading strand replication product. Primers were synthesized with a variable sized gap between their 3'-ends and the fork. The 5'-end of the lagging strand also contained a biotin to which streptavidin could be bound, providing a steric block.

Titrating high concentrations of either the *E. coli* DnaB helicase or the *B. subtilis* DnaC replicative helicase onto templates in the absence of other proteins allowed helicase self-loading and function leading to extensive unwinding (Fig. 3.2A). To determine whether the hexameric helicase self-assembles on DNA by a mechanism

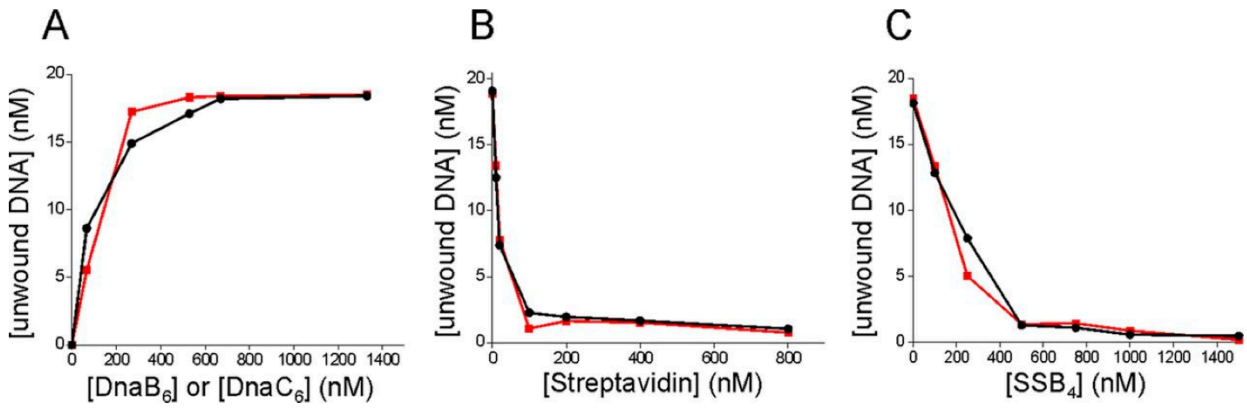

FIGURE 3.2
E. coli and *B. subtilis* helicases self-load onto replication forks by threading onto a free 5'-end on the lagging strand. Titrations performed against 20 nM unprimed forked template in the absence of streptavidin unless stated otherwise. (A) 550 nM *E. coli* $DnaB_6$ (red) and *B. subtilis* $DnaC_6$ (black). (B) streptavidin inhibits helicases from self-loading onto replication forks by binding to a biotin near the 5'-end of the lagging strand. Streptavidin was titrated using *E. coli* $DnaB_6$ (red) or *B. subtilis* $DnaC_6$ (black). (C) SSB can block the 5'-end of the lagging strand and prevent helicases from self-loading. *E. coli* or *B. subtilis* SSB was titrated in the presence of *E. coli* $DnaB_6$ (red) or *B. subtilis* $DnaC_6$ (black), respectively.

where it threads over a free 5'-end, I blocked the 5'-end of model substrates with streptavidin (Fig. 3.1). When the 5'-end of the lagging strand template at the fork was blocked, neither *E. coli* nor *B. subtilis* helicases were able to self-assemble (Fig. 3.2B). In the absence of streptavidin, the cognate SSB also prevents helicase self-loading in both systems (Fig. 3.2C).

To establish an optimal system for helicase loading that is dependent upon *E. coli* and *B. subtilis* primosomal proteins, I blocked the single-stranded 5'-end of forked templates with streptavidin to eliminate the helicase self-loading background and titrated each component to determine its optimum concentration (Fig. 3.3 and 3.4). The optimal level was selected for subsequent experiments except for SSB. I selected an excess, slightly inhibitory level, which proved effective in blocking helicase self-loading (Fig. 3.2C).

The preceding experiment was conducted under conditions using a forked substrate containing a 10 nt gap between the leading strand 3'-primer terminus and the fork. Similar experiments were conducted with a substrate that contained no gap (Figs. A2.1 and A2.2). Similar results were obtained, except higher concentrations of PriA, PriB, DnaT, and DnaC were required in the *E. coli* system and higher levels of PriA, DnaB, DnaD, and DnaI were required in the *B. subtilis* system. Thus, both systems required higher levels of all proteins that act prior to helicase loading, suggesting a lower functional affinity for templates that do not contain a gap in the leading strand.

Our initial forked substrate contained 90 nt leading and lagging strand templates with a 45 nt duplex ahead of the fork. This represented close to the longest practical length considering economic factors and current commercial capabilities for producing

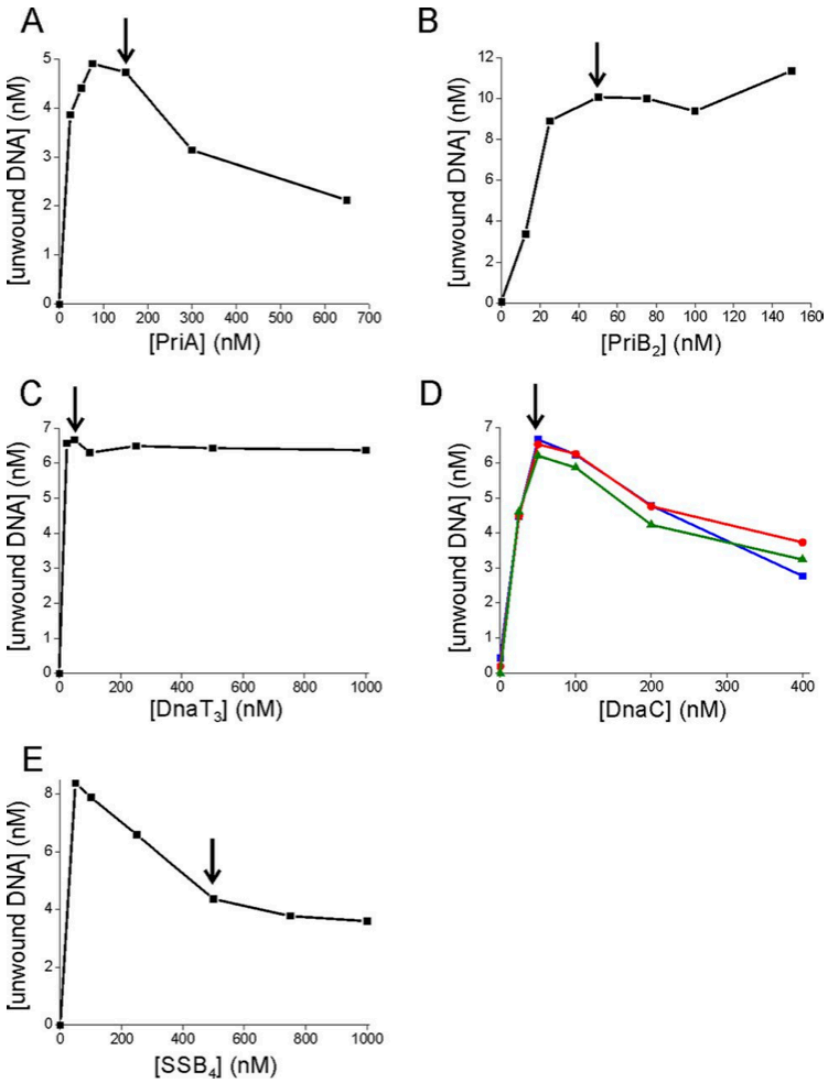

FIGURE 3.3
Optimizing *E. coli* protein concentrations using the 10 nt gap forked template. Helicase loading proteins and helicase were titrated sequentially (in the order they appear here) in the presence of all other primosomal proteins; the arrow indicates the chosen optimum for each. In subsequent experiments, that optimal level was used. The starting conditions used were as follows: 75 nM $PriB_2$, 250 nM $DnaT_3$, 12 nM $DnaB_6$, 100 nM DnaC, and 500 nM SSB_4. The final optimized conditions from this series of experiments were as follows: 150 nM PriA, 50 nM $PriB_2$, 50 nM $DnaT_3$, 12 nM $DnaB_6$, 50 nM DnaC, and 500 nM SSB_4. (A) PriA titration; (B) $PriB_2$ titration; (C) $DnaT_3$ titration; (D) DnaC helicase loader titrated at three different $DnaB_6$ concentrations (6 nM (green), 12 nM (red), and 24 nM (blue)); (E) SSB_4 titration. To prevent the helicase self-loading reaction, 500 nM SSB_4 was used for further experiments.

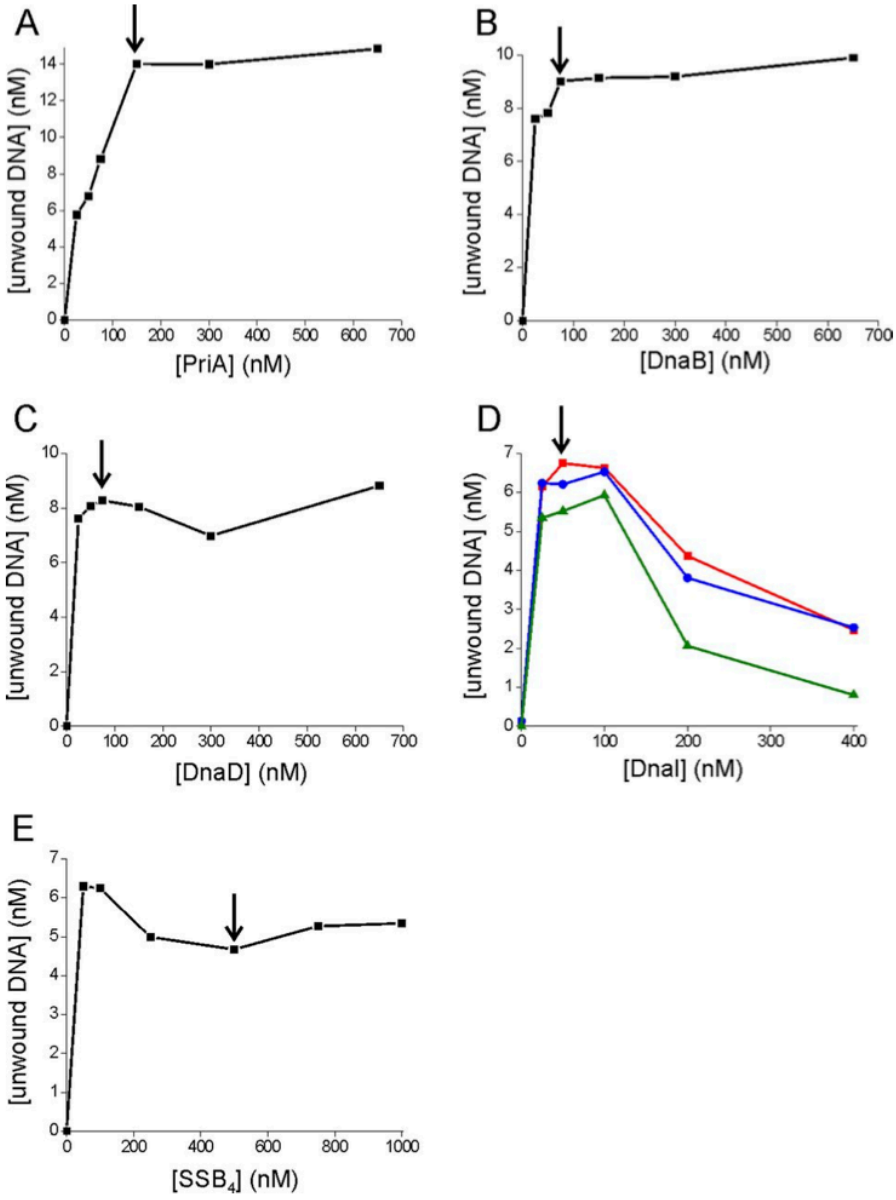

FIGURE 3.4
Optimizing *B. subtilis* protein concentrations on 10 nt gap forked template. The experiment was carried out as described in the legend to Fig. 3.3. The starting conditions used were as follows: 300 nM DnaB, 300 nM DnaD, 12 nM $DnaC_6$, 200 nM DnaI, and 500 nM SSB_4. The final optimized conditions from this series of experiments were as follows: 150 nM PriA, 75 nM DnaB, 75 nM DnaD, 12 nM $DnaC_6$, 50 nM DnaI, and 500 nM SSB_4. (A) PriA titration; (B) DnaB titration; (C) DnaD titration; (D) DnaI helicase loader titrated at three different $DnaC_6$ helicase concentrations (6 nM (green), 12 nM (red), and 24 nM (blue)); (E) SSB_4 titration. To prevent the helicase self-loading reaction, 500 nM SSB_4 was chosen for further experiments.

substituted oligonucleotides. Systematic efforts to decrease the size resulted in decreased activities (Table A2.1). Thus, I retained the use of forks composed of annealed 90-mers for most experiments.

3.4.2 The Intrinsic PriA ATPase Is Required for Primosome Assembly on Forks Containing Leading Strand Gaps

The preference for forked templates with variable gap length was determined. I observed significantly higher function with templates with the largest (10 nt) gap size in both the *E. coli* and *B. subtilis* primosomal systems (Fig. 3.5, A and D). In an earlier study, the opposite result was observed using a PriA derivative in which the intrinsic ATPase required to drive a 3' to 5' helicase activity was inactivated [11,34]. To permit a direct comparison, Ken Marians kindly provided some of the PriA K230R used in that study. Using our FRET assay, I reproduced their results (Fig. 3.5B). Thus, the reversal in gap size preference and the ability to efficiently use templates with gaps requires the activity of the PriA ATP-dependent helicase (Fig. 3.5C). The results reported in Fig. 3.5 were obtained under conditions optimized for forked templates containing a 10 nt gap. To ensure that the result was not condition-specific, I repeated the experiment using conditions that had been optimized for templates lacking a gap between the fork and the leading strand and obtained the same result (Fig. A2.3).

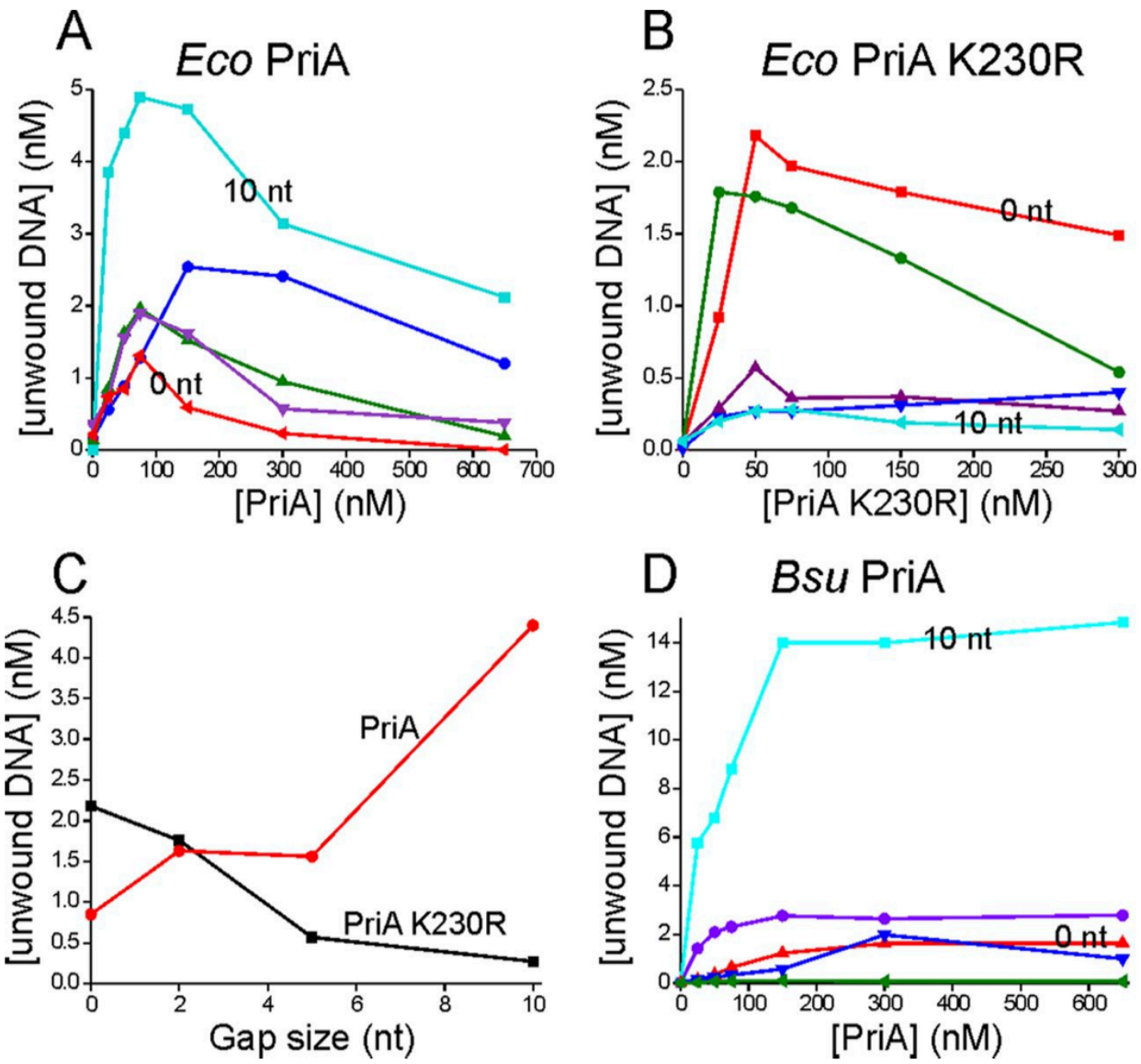

FIGURE 3.5
Wild-type PriA containing a functional ATPase prefers forked substrates with large leading strand gaps. For A, B, and D, five substrates were used: unprimed forked template (blue), 0 nt gap forked template (red), 2 nt gap forked template (green), 5 nt gap forked template (purple), or 10 nt gap forked template (cyan). Optimal *E. coli* protein concentrations listed in the legend of Fig. 3.3 were used. (A) wild-type PriA (*E. coli*) titration; (B) PriA K230R (*E. coli*) titration; (C) amount of DNA unwound plotted against gap size at 50 nM wild-type PriA (red) and 50 nM PriA K230R (black) for *E. coli*; (D) *B. subtilis* PriA titration. Optimal *B. subtilis* protein concentrations listed in the legend of Fig. 3.4.

3.4.3 PriA Functions as a Checkpoint Protein by Binding to Forks and Blocking Pol III HE Binding to the 3' Terminus of the Leading Strand

In addition to PriA serving as the lead protein in directing primosomal assembly and replicative helicase loading, it functions as a checkpoint protein, at least in *E. coli*, blocking the intrinsic strand displacement activity of the Pol III HE on forks lacking the replicative helicase [12,13]. I confirmed this result, using our FRET assay template with radiolabeled primers, permitting assay for primer extension, on templates containing 2 and 20 nt gaps (Fig. 3.6A, lanes 3 and 6). I observed, however, that I needed to add PriA before I added SSB. If I added SSB first, the checkpoint activity of PriA was not observed (compare Fig. 3.6A, lanes 2 with 3 and lanes 5 with 6). I also observed that the action of PriA in blocking the progression of Pol III is dependent upon a forked structure. Omitting the lagging strand template from the reaction does not support PriA functioning as a checkpoint protein (Fig. 3.6A, lanes 9 and 11). A control used to validate the assay (lane 8) shows that SSB is required to support strand displacement [13].

Next, I sought to determine whether *B.subtilis* PriA blocked the *B. subtilis* polymerases PolC HE and DnaE HE. As in the *E. coli* system, *B. subtilis* PriA served as a checkpoint protein that blocked the forward progression of both polymerases, but only if added before SSB (Fig. 3.6, B and C).

I next sought to determine whether the reaction was specific for cognate polymerases. I observed that both the PriAs could block *E. coli* Pol III HE and *B. subtilis*Pol C and DnaE HEs with equal efficiency. Furthermore, *B. subtilis* PriA blocked

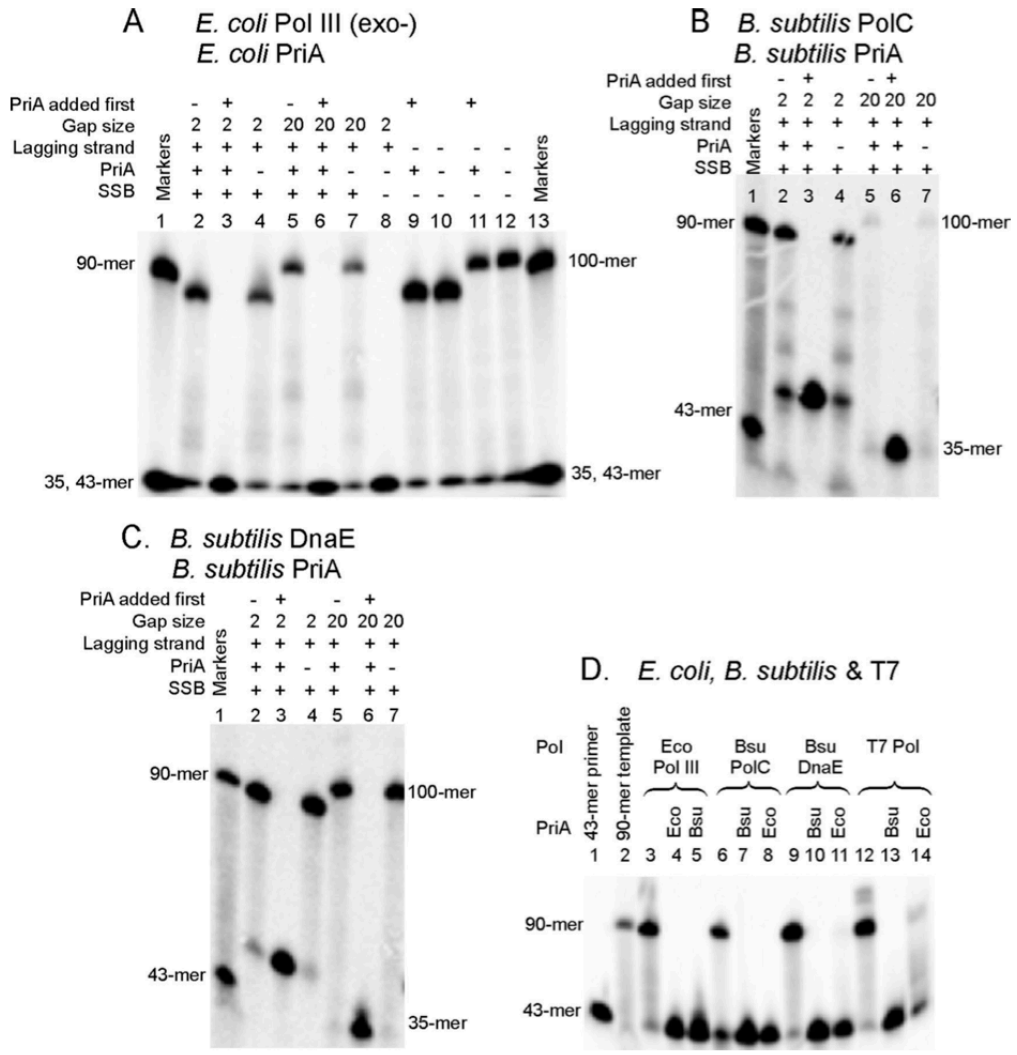

FIGURE 3.6
PriA blocks the strand displacement reaction by Pol III HE in *E. coli* and by both *B. subtilis* Pol IIIs. ^{32}P-Labeled products of strand displacement were resolved in 12% polyacrylamide with 8 M urea. Substrates are either a 2 nt gap forked template (giving a 90-mer product) or a 20 nt gap forked template (giving a 100-mer product). Substrates without a lagging strand consist of just primer bound to leading strand template. In reactions where PriA was not added first (lanes 2 and 5 in A–C) but is present in the reaction, PriA was added immediately after SSB, but before HE. (A) *E. coli* Pol III (exo-) HE and *E. coli* PriA. Lanes 9 –12 contain a substrate composed of only primed template. Substrates in lanes 9 and 10 are constructed from FT90 and P2g and lanes 11 and 12 from FT100 and P20g. (B) *B. subtilis* PolC HE and *B. subtilis* PriA. (C) *B. subtilis* DnaE HE and *B. subtilis* PriA. (D) PriA blocks the strand displacement reaction across species. All reactions were carried out on 20 nM 2 nt gap forked template. Reactions with *E. coli* Pol III HE and with T7 polymerase were performed with exonuclease-deficient polymerase. Lanes 1 and 2 contain markers to indicate the migration of the primer (43-mer) and the expected product (90-mer).

a polymerase that is not homologous to Pol IIIs, T7 DNA polymerase, completely. The *E. coli* PriA inhibited T7 significantly with only a small portion of the product reaching full length (Fig. 3.6D). The experiment shown was conducted with a template containing a 2 nt leading strand gap. Essentially, the same result was obtained on templates containing a 20 nt gap (data not shown).

Two models exist for PriA function. When the checkpoint action of the PriA protein was initially discovered, it was suggested that PriA may just act as a steric block, denying access of the Pol III HE to the primer terminus [12]. Later, a multifunction protein from bacteriophage T4, gp59, that is not homologous to PriA but exhibits similar checkpoint activity, was shown to function by binding to the blocked T4 polymerase at forks, forming an inactive ternary complex [35] until the helicase is loaded, which releases the inhibition. I chose to distinguish these two models, using *E. coli* PriA and Pol III HE. A system was developed where the forked template was immobilized on streptavidin beads, allowing rapid washing and determination of the proteins bound functionally (Fig. 3.7A). The Pol III HE once bound to DNA in an initiation complex requires bumpers to prevent it from sliding off. Thus, I moved the biotin from the lagging strand template to the 5'-end of the leading strand primer. The fork functioned as a bumper on the other end of the primer. The presence of SSB served to prevent self-assembly of helicase.

In the absence of primosomal proteins, the Pol III HE could efficiently form initiation complexes on primed bead-bound replication forks that survived washing and extensively elongated the leading strand primer in a strand displacement reaction upon addition of dNTPs (Fig. 3.7B, lane 3). The observed reaction was dependent upon the

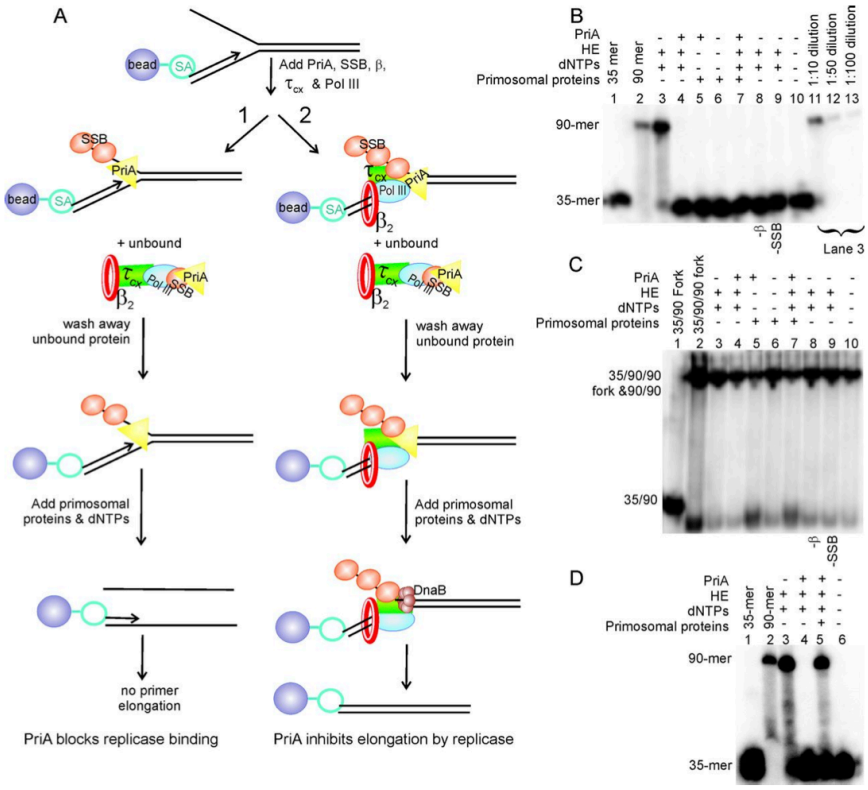

FIGURE 3.7

PriA and holoenzyme do not coexist on PriA-inhibited replication forks. (A) diagram depicting two possible models of PriA inhibiting the strand displacement reaction and the expected result of each for reactions on streptavidin (SA) beads. The primer is labeled on the 5'-end with ^{32}P so that primer extension and helicase activity can be monitored. The primer contains a biotin near the 5'-end so that substrates can be conjugated to streptavidin-linked beads. Scheme 1 depicts PriA blocking the 3'-OH of the primer, physically preventing Pol III HE from binding. Scheme 2 portrays an inhibition model where both PriA and Pol III HE bind to the substrate. Primosomal proteins (PriB, DnaT, DnaB, and DnaC) were added as described under 3.3 Materials and Methods. (B) denaturing gel analysis to monitor primer extension by *E. coli* Pol III (exo-). Lanes 11–13 are dilutions of the positive control lane 3 to establish detection limits. For both B and C, lanes 8 and 9 contain the full Pol III HE but in lane 8, the β-subunit was omitted, and in lane 9, SSB was omitted. (C) native gel analysis to monitor substrate unwinding by *E. coli* DnaB helicase. The upper band is the replication fork, and the 90/90 duplex product in those cases is where replication occurs. The lower band is the displaced leading strand primer template. In lane 5, ~45% of the substrate was unwound by the helicase. In lane 7, ~40% of the substrate was unwound by the helicase. In all other lanes, the amount of substrate unwound is not significantly above background. (D) denaturing gel analysis to monitor primer extension by *E. coli* Pol III (exo-) on immobilized substrate without a washing step. Experiment carried out as described under 3.3 Materials and Methods, except after incubation with Pol III HE components, the washing steps were omitted. In lane 5, ~45% of the primer is elongated.

presence of β_2, indicating it proceeds from authentic initiation complexes rather than residual polymerase not removed by the washing step (Fig. 3.7B, lane 8). Elongation did not occur in the absence of SSB, a required cofactor for the strand displacement activity of Pol III HE (Fig. 3.7B, lane 9) [13].

Addition of PriA to the reaction in the absence of other primosomal proteins prevented extension of primers, either by blocking Pol III HE binding or arresting the polymerase in an inactive state (Fig. 3.7B, lane 4). The remaining primosomal proteins were added to permit PriA-directed helicase assembly, yielding an active helicase. Control reactions run on native gels detect a labeled primed leading strand (35/90) split from the lagging strand template permitting an independent assessment of helicase function (Fig. 3.7C). These control experiments indicated that 40% of the bead-bound forks contained an active helicase (Fig. 3.7C, lane 7). Yet, no elongation product was observed in the corresponding lane 7 in Fig. 3.7B. If Pol III HE was present, sequestered in an inactive complex with PriA, elongation would have been expected at 40% of the level I observed in lane 3 once helicase was loaded, relieving inhibition by PriA. I could have detected elongation at a level of 1%, judging by the control shown in Fig. 3.7B, lane 13. Another control reaction where the washing step was omitted confirmed that PriA inhibition of the Pol III HE is relieved on the bead-bound substrate upon helicase assembly (Fig. 3.7D).

To check whether the result observed was caused by the 10 nt gap being too small to accommodate both Pol III HE and PriA at a fork, I repeated the experiment reported in Fig. 3.7 using a substrate containing a 20 nt gap and observed the same

result (Fig. A2.5). I conclude that PriA acts as a checkpoint protein by blocking Pol III HE binding.

3.5 DISCUSSION

In this work, I have used synthetic model replication forks to study aspects of the replication restart reaction in divergent Gram-negative and Gram-positive model organisms. It has been estimated that *E. coli* and *B. subtilis* diverged approximately two billion years ago, a greater evolutionary distance than yeast and humans [36 and references therein]. Important differences have been observed in the replication systems of *E. coli* and *B. subtilis* that suggest that the extensive replication studies conducted with *E. coli* do not always present an accurate model for replication in all bacteria [37]. For example, *B. subtilis* requires two DNA polymerase IIIs for replication, whereas *E. coli* requires only one [38]. It has been demonstrated that the second Pol III (DnaE) has a specialized role in lagging strand primer processing analogous to the role of DNA polymerase α in eukaryotes [21]. Additional proteins participate in initiation reactions, both at the origin and at the restart replication fork, that have no homologs in *E. coli* [39]. Thus, having a Gram-positive system to compare with *E. coli* will permit further understanding of the mechanistic basis for their functional divergence.

I adapted a simple FRET assay that has been used in the study of other helicases [22]. By blocking the 5'-end of the lagging strand, I was able to make both the *E. coli* and *B. subtilis* systems dependent on PriA and the remaining primosomal proteins. This indicates that the replicative helicase self-assembly reactions proceed by

threading of pre-assembled hexamers over free 5'-ends of model forks. An example of the alternative model, where a hexameric helicase could transiently open and close, sequestering a single- stranded template, has been provided by the double- stranded RNA virus Φ12 helicase [40]. This latter type of assembly should not be inhibited by a steric block on the 5'-end of the lagging strand template. The helicase self-assembly reaction only takes place at very high, non-physiological concentrations of helicase. I can conclude that this does not represent a common pathway *in vitro* consistent with genetic evidence that it does not take place *in vivo* [41,42].

Our initial forked substrate contained 90 nt single-stranded leading and lagging strand templates with a 45 nt duplex ahead of the fork. Systematic efforts to decrease their size resulted in significantly decreased activity. This result contrasts markedly from the requirements of model forks for reactions that only contain replicative helicase in self-assembly reactions [43]. There, a 15 nt lagging strand arm is sufficient to support an efficient reaction and a 10 nt arm is adequate for the reaction, although a 5 nt arm is not. In our system, a 15 nt lagging strand arm is inert (Table A2.1). Because it is thought that only the first 6–10 nts of the lagging strand tail productively interact with the helicase, the remaining length requirement must be for additional protein factors to bind. At least part of the binding site for PriA, PriB and DnaT is near the fork [14], but these factors productively interact with SSB [44,45], and additional lagging strand length is likely required to accommodate that interaction. The requirement for a long duplex ahead of the fork and within the leading strand arm is less explicable. Future studies, perhaps led by DNA site-specific cross-linking will likely provide insight into which factors interact within these regions.

I also examined the effect of the size of the gap between the 3'-end of the leading strand and the fork. I found differences depending on whether the ATPase within the PriA protein was active. PriA K230R with an inactive ATPase exhibits a strong preference for substrates with small or no gaps. Templates with gaps of 10 nt are inactive, consistent with published observations [34]. However, with ATPase-proficient wild-type PriA, the result is just the opposite, with discrimination against substrates with short gaps and the highest activity on substrates with 10 nt gaps. To our knowledge, this observation is without precedent. Although a large number of nucleic acid transactions are driven by ATPases and a large number of reactions are activated or dissociated by ATPase activity, our group knows of none where specificity in two robust reactions is reversed by the presence of an ancillary ATPase.

In addition to its key role in initiating primosome assembly, PriA serves as a checkpoint protein that prevents Pol III HE from catalyzing a strand displacement reaction in the absence of a replicative helicase at the fork [12]. One model initially proposed was that PriA merely blocked access of the Pol III HE to replication forks. Another model was provided by the established mechanism of phage T4 gp59. Gp59 serves as a helicase loader and also as a checkpoint protein. Although not homologous, its function is analogous to PriA. Gp59 binds to forks and the T4 DNA polymerase, locking it into an inactive conformation in a stable ternary complex [35]. Using forked templates bound to beads allowed rapid washing after complex formation so that bound components could be determined. I showed that PriA excluded Pol III HE, as initially hypothesized. Control experiments showed that in the absence of PriA, Pol III HE could form initiation complexes on primed forked templates.

Further supporting a nonspecific steric role for PriA in blocking strand displacement is our observation that PriA can block non-cognate polymerases. *E. coli* PriA can block strand dis-placement catalyzed by the *B. subtilis* Pol C and DnaE HEs, and *B. subtilis* PriA blocks strand displacement by the *E. coli* Pol III HE. It is conceivable that conserved protein interaction sites could enable the inhibition observed. But, I also demonstrated that both the *B. subtilis* and *E. coli* PriA proteins could block T7 DNA polymerase, which is not homologous to DNA Pol IIIs. These experiments also establish a checkpoint role for *B. subtilis* PriA, showing the original *E. coli* observation [12] is general.

In all assays conducted for this study, I observed that PriA had to be added before SSB for it to display function. Presumably, if added first, SSB covers the PriA binding site and prevents its interaction with the fork. However, in dynamic reactions where Pol III HE is catalyzing a strand displacement reaction that is dependent upon its interaction with SSB on the lagging strand, addition of PriA immediately stops the reaction [13]. This could be explained if PriA can bind to an initial segment of single-stranded DNA exposed on the lagging strand of the fork that is too small to stably or rapidly bind SSB. In this reaction, there could be transient interactions with Pol III HE, facilitating its displacement, but our results show a stable complex is not formed.

The substrates, assays, and basic principles established by this study provide a foundation for further pursuit of the mechanistic basis of differences between the replication restart reaction in Gram-negative and low GC Gram-positive bacteria. The simple oligonucleotide substrates should be amenable to cross-linking studies, using

nucleotide position-specific modifications, kinetic studies, screens for small molecule inhibitors, and structural studies.

3.6 REFERENCES

1 Kaguni, J. M. (2006) DnaA: controlling the initiation of bacterial DNA replication and more. Annual Review of Microbiology **60**, 351–75.

2 Mott, M. L. and Berger, J. M. (2007) DNA replication initiation: mechanisms and regulation in bacteria. Nature Reviews. Microbiology **5**, 343–54.

3 Cox, M. M., Goodman, M. F., Kreuzer, K. N., Sherratt, D. J., Sandler, S. J. and Marians, K. J. (2000) The importance of repairing stalled replication forks. Nature **404**, 37–41.

4 Marians, K. J. (2000) PriA-directed replication fork restart in *Escherichia coli*. Trends in Biochemical Sciences **25**, 185–9.

5 Polard, P., Marsin, S., McGovern, S., Velten, M., Wigley, D. B., Ehrlich, S. D. and Bruand, C. (2002) Restart of DNA replication in Gram-positive bacteria: functional characterisation of the *Bacillus subtilis* PriA initiator. Nucleic Acids Research **30**, 1593–605.

6 Ng, J. Y. and Marians, K. J. (1996) The ordered assembly of the ΦX174-type primosome. I. Isolation and identification of intermediate protein-DNA complexes. The Journal of Biological Chemistry **271**, 15642–8.

7 McGlynn, P., Al-Deib, A. A., Liu, J., Marians, K. J. and Lloyd, R. G. (1997) The DNA replication protein PriA and the recombination protein RecG bind D-loops. Journal of Molecular Biology **270**, 212–21.

8 Nurse, P., Liu, J. and Marians, K. J. (1999) Two modes of PriA binding to DNA. The Journal of Biological Chemistry **274**, 25026–32.

9 Lee, M. S. and Marians, K. J. (1987) *Escherichia coli* replication factor Y, a component of the primosome, can act as a DNA helicase. Proceedings of the National Academy of Sciences of the United States of America **84**, 8345–9.

10 Jones, J. M. and Nakai, H. (1999) Duplex opening by primosome protein PriA for replisome assembly on a recombination intermediate. Journal of Molecular Biology **289**, 503–16.

11 Zavitz, K. H. and Marians, K. J. (1992) ATPase-deficient mutants of the *Escherichia coli* DNA replication protein PriA are capable of catalyzing the assembly of active primosomes. The Journal of Biological Chemistry **267**, 6933–40.

12 Xu, L. and Marians, K. J. (2003) PriA mediates DNA replication pathway choice at recombination intermediates. Molecular Cell **11**, 817–26.

13 Yuan, Q. and McHenry, C. S. (2009) Strand displacement by DNA polymerase III occurs through a τ-ψ-χ link to single-stranded DNA-binding protein coating the lagging strand template. The Journal of Biological Chemistry **284**, 31672–9.

14 Lopper, M., Boonsombat, R., Sandler, S. J. and Keck, J. L. (2007) A hand-off mechanism for primosome assembly in replication restart. Molecular Cell **26**, 781–93.

15 Mok, M. and Marians, K. J. (1987) The *Escherichia coli* preprimosome and DNA B helicase can form replication forks that move at the same rate. The Journal of Biological Chemistry **262**, 16644–54.

16 Wu, C. A., Zechner, E. L., Reems, J. A., McHenry, C. S. and Marians, K. J. (1992) Coordinated leading- and lagging-strand synthesis at the *Escherichia coli* DNA replication fork. V. Primase action regulates the cycle of Okazaki fragment synthesis. The Journal of Biological Chemistry **267**, 4074–83.

17 Zechner, E. L., Wu, C. A. and Marians, K. J. (1992) Coordinated leading- and lagging-strand synthesis at the *Escherichia coli* DNA replication fork. II. Frequency of primer synthesis and efficiency of primer utilization control Okazaki fragment size. The Journal of Biological Chemistry **267**, 4045–53.

18 Kim, S., Dallmann, H. G., McHenry, C. S. and Marians, K. J. (1996) Coupling of a replicative polymerase and helicase: a τ-DnaB interaction mediates rapid replication fork movement. Cell **84**, 643–50.

19 Marsin, S., McGovern, S., Ehrlich, S. D., Bruand, C. and Polard, P. (2001) Early steps of *Bacillus subtilis* primosome assembly. The Journal of Biological Chemistry **276**, 45818–25.

20 Smits, W. K., Goranov, A. I. and Grossman, A. D. (2010) Ordered association of helicase loader proteins with the *Bacillus subtilis* origin of replication *in vivo*. Molecular Microbiology **75**, 452–61.

21 Sanders, G. M., Dallmann, H. G. and McHenry, C. S. (2010) Reconstitution of the *B. subtilis* replisome with 13 proteins including two distinct replicases. Molecular Cell, Elsevier Ltd **37**, 273–81.

22 Bjornson, K. P., Amaratunga, M., Moore, K. J. and Lohman, T. M. (1994) Single-turnover kinetics of helicase-catalyzed DNA unwinding monitored continuously by fluorescence energy transfer. Biochemistry **33**, 14306–16.

23 Houston, P. and Kodadek, T. (1994) Spectrophotometric assay for enzyme-mediated unwinding of double-stranded DNA. Proceedings of the National Academy of Sciences of the United States of America **91**, 5471–4.

24 Kim, D. R. and McHenry, C. S. (1996) *In vivo* assembly of overproduced DNA polymerase III. Overproduction, purification, and characterization of the α, α-ε, and α-ε-θ subunits. The Journal of Biological Chemistry **271**, 20681–9.

25 Wieczorek, A. and McHenry, C. S. (2006) The NH_2-terminal php domain of the alpha subunit of the *Escherichia coli* replicase binds the ε proofreading subunit. The Journal of Biological Chemistry **281**, 12561–7.

26 Dallmann, H. G., Thimmig, R. L. and McHenry, C. S. (1995) DnaX complex of *Escherichia coli* DNA polymerase III holoenzyme. Central role of τ in initiation complex assembly and in determining the functional asymmetry of holoenzyme. The Journal of Biological Chemistry **270**, 29555–62.

27 Song, M. S., Pham, P. T., Olson, M., Carter, J. R., Franden, M. A., Schaaper, R. M. and McHenry, C. S. (2001) The δ and δ' subunits of the DNA polymerase III holoenzyme are essential for initiation complex formation and processive elongation. The Journal of Biological Chemistry **276**, 35165–75.

28 Olson, M. W., Dallmann, H. G. and McHenry, C. S. (1995) DnaX complex of *Escherichia coli* DNA polymerase III holoenzyme. The χψ complex functions by increasing the affinity of τ and γ for δδ' to a physiologically relevant range. The Journal of Biological Chemistry **270**, 29570–7.

29 Johanson, K. O., Haynes, T. E. and McHenry, C. S. (1986) Chemical characterization and purification of the β subunit of the DNA polymerase III holoenzyme from an overproducing strain. The Journal of Biological Chemistry **261**, 11460–5.

30 Griep, M. A. and McHenry, C. S. (1989) Glutamate overcomes the salt inhibition of DNA polymerase III holoenzyme. The Journal of Biological Chemistry **264**, 11294–301.

31 Marians, K. J. (1995) ϕX174-type primosomal proteins: purification and assay. Methods in Enzymology **262**, 507–21.

32 Fijalkowska, I. J. and Schaaper, R. M. (1996) Mutants in the Exo I motif of *Escherichia coli* dnaQ: defective proofreading and inviability due to error catastrophe. Proceedings of the National Academy of Sciences of the United States of America **93**, 2856–61.

33 Dallmann, H. G., Fackelmayer, O. J., Tomer, G., Chen, J., Wiktor-Becker, A., Ferrara, T., Pope, C., Oliveira, M. T., Burgers, P. M. J., Kaguni, L. S., *et al.* (2010)

Parallel multiplicative target screening against divergent bacterial replicases: identification of specific inhibitors with broad spectrum potential. Biochemistry **49**, 2551–62.

34 Heller, R. C. and Marians, K. J. (2005) The disposition of nascent strands at stalled replication forks dictates the pathway of replisome loading during restart. Molecular Cell **17**, 733–43.

35 Xi, J., Zhang, Z., Zhuang, Z., Yang, J., Spiering, M. M., Hammes, G. G. and Benkovic, S. J. (2005) Interaction between the T4 helicase loading protein (gp59) and the DNA polymerase (gp43): unlocking of the gp59-gp43-DNA complex to initiate assembly of a fully functional replisome. Biochemistry **44**, 7747–56.

36 Condon, C. (2003) RNA processing and degradation in *Bacillus subtilis*. Microbiology and Molecular Biology Reviews.

37 McHenry, C. S. (2011) Breaking the rules: bacteria that use several DNA polymerase IIIs. EMBO Reports **12**, 408–14.

38 Dervyn, E., Suski, C., Daniel, R., Bruand, C., Chapuis, J., Errington, J., Jannière, L. and Ehrlich, S. D. (2001) Two essential DNA polymerases at the bacterial replication fork. Science (New York, N.Y.) **294**, 1716–9.

39 Bruand, C., Farache, M., McGovern, S., Ehrlich, S. D. and Polard, P. (2001) DnaB, DnaD and DnaI proteins are components of the *Bacillus subtilis* replication restart primosome. Molecular Microbiology **42**, 245–55.

40 Lísal, J., Lam, T. T., Kainov, D. E., Emmett, M. R., Marshall, A. G. and Tuma, R. (2005) Functional visualization of viral molecular motor by hydrogen-deuterium exchange reveals transient states. Nature Structural & Molecular Biology **12**, 460–6.

41 Sandler, S. J., Marians, K. J., Zavitz, K. H., Coutu, J., Parent, M. A. and Clark, A. J. (1999) dnaC mutations suppress defects in DNA replication- and recombination-associated functions in priB and priC double mutants in *Escherichia coli* K-12. Molecular Microbiology **34**, 91–101.

42 Bruand, C., Velten, M., McGovern, S., Marsin, S., Sérèna, C., Ehrlich, S. D. and Polard, P. (2005) Functional interplay between the *Bacillus subtilis* DnaD and DnaB proteins essential for initiation and re-initiation of DNA replication. Molecular Microbiology **55**, 1138–50.

43 Kaplan, D. L. and Steitz, T. A. (1999) DnaB from *Thermus aquaticus* unwinds forked duplex DNA with an asymmetric tail length dependence. The Journal of Biological Chemistry **274**, 6889–97.

44 Cadman, C. J. and McGlynn, P. (2004) PriA helicase and SSB interact physically and functionally. Nucleic Acids Research **32**, 6378–87.

45 Costes, A., Lecointe, F., McGovern, S., Quevillon-Cheruel, S. and Polard, P. (2010) The C-terminal domain of the bacterial SSB protein acts as a DNA maintenance hub at active chromosome replication forks. PLoS Genetics **6**, e1001238.

46 Manhart, C. M. and McHenry, C. S. (2013) The PriA Replication Restart Protein Blocks Replicase Access Prior to Helicase Assembly and Directs Template Specificity through Its ATPase Activity. The Journal of Biological Chemistry **288**, 3989–99.

CHAPTER 4[*]

Bacteriophage SPP1 DNA replication strategies promote viral and disable host replication *in vitro*[†]

4.1 ABSTRACT

Complex viruses that encode their own initiation proteins and subvert the host's elongation apparatus have provided valuable insights into DNA replication. Using purified bacteriophage SPP1 and *Bacillus subtilis* proteins, we have reconstituted a rolling circle replication system that recapitulates genetically defined protein requirements. Eleven proteins are required: phage-encoded helicase (G*40*P), helicase loader (G*39*P), origin binding protein (G*38*P) and G*36*P single-stranded DNA-binding protein (SSB); and host-encoded PolC and DnaE polymerases, processivity factor (β_2), clamp loader (τ-δ-δ') and primase (DnaG). This study revealed a new role for the SPP1 origin binding protein. In the presence of SSB, it is required for initiation on replication forks that lack origin sequences, mimicking the activity of the PriA replication restart protein in bacteria. The SPP1 replisome is supported by both host and viral SSBs, but phage SSB is unable to support *B. subtilis* replication, likely owing to its inability to stimulate the PolC holoenzyme in the *B. subtilis* context. Moreover, phage SSB inhibits

[*] My experimental work is the FRET assay presented in Fig. 4.6 of this chapter and described in sections 4.3.3, 4.4.4, and 4.4.6. The remaining experimental work was performed by the co-authors of the corresponding publication [57].

[†] The contents of this chapter were published in [57] and are presented here with few modifications.

host replication, defining a new mechanism by which bacterial replication could be regulated by a viral factor.

4.2 INTRODUCTION

Double-stranded (ds) DNA viruses encode components capable of carrying out their own replication, as in the case of the T4, Φ29 or HSV-1 viruses [1–3], or may encode a subset of proteins, including an origin-specific initiation protein, and recruit the host DNA replication machinery to achieve efficient viral replication. The study of the replication mechanisms of the latter type of viruses has provided significant insight into cellular DNA replication processes. For example, SV40, a virus that encodes its own origin binding protein and helicase within the T antigen has provided a viral window into eukaryotic DNA replication [4,5]. Its use enabled the only full reconstitution of a eukaryotic DNA replication system with purified proteins and revealed the special roles of Pol α-primase and the Pol δ holoenzyme in the process [5,6]. Bacteriophage λ has provided similar insight into the replication of Gram-negative bacteria [7]. λ encodes its own origin binding protein and a helicase loader that subverts the host $DnaB_6$ replicative helicase, leading to the acquisition of the cell's elongation apparatus. Through this system, the role of heat shock proteins in freeing the DnaB helicase from tightly bound λ O and P proteins was discovered, providing one of the initial observations of chaperone function [7,8]. The mechanism used by these viruses to recruit host proteins could provide significant insight into viral and host processes.

Bacillus subtilis SPP1 is a virulent dsDNA phage whose mature genome is a linear 45.4-kb dsDNA. The ends of the packaged DNA are terminally redundant and are permuted to facilitate circularization after DNA injection into cells. SPP1 replication starts with the circle-to-circle replication mode (θ replication), but after one or a few rounds, it switches to concatemeric replication (termed s replication or rolling circle replication) by a process driven by homologous recombination [9,10]. This switch in the mode of replication is a strategy used by many viruses to produce linear head-to-tail concatemers that are used by the packaging machinery. This late-phase DNA replication, which is believed to be independent of an origin of replication, has been reconstituted *in vitro* for viruses that encode their own polymerase [e.g. HSV-1, T7, T4 and Φ29, [11–14] and for bacteriophage λ [15].

Genetic analyses showed that SPP1 DNA replication is independent of the host origin binding protein (DnaA), the replicative DNA helicase (DnaC), primosomal proteins DnaB and PriA and RNA polymerase. These studies also showed that SPP1 replication requires the host DnaG primase and PolC DNA polymerase [16–18].

The SPP1 phage possesses two origins of replication, *ori*L and *ori*R, which are 32.1kb apart in a linear map of the SPP1 genome. Replication proteins are encoded by two operons. The first one, which is under the control of the early promoter P_{E2}, codes for proteins that have been shown to be required for θ replication: the G*38*P origin binding protein, the G*39*P helicase loader and the G*40*P helicase. G*38*P, which does not belong to the AAA+ family, is widely conserved in phages [19,20]. G*38*P binds with high affinity to the two origins of replication [21] and forms a complex with G*39*P [17]. G*39*P does not share homology with other studied helicase loaders but performs a

similar role: it delivers G*40*P, on interacting with G*38*P, to the origin of replication [22,23]. G*40*P is a widely studied helicase that belongs to the DnaB family [24–26].

Genes required for the recombination-dependent s replication mode are under the control of the early promoter P_{E3}. These include a recombinase, G*35*P [18,27], and a 5'-3' exonuclease, G*34.1*P [28]. In this operon, there is also a gene (gene *36*) that encodes a single-stranded DNA-binding protein (SSB), G*36*P, whose role in replication has not yet been analyzed. G*36*P is 48% identical to the essential host SSB (*B. subtilis* SsbA, Fig. A3.1), and 38% identical to the competence-specific SSB [*B. subtilis* SsbB, [29].

We have exploited the apparatus required for the s mode of replication to establish a robust rolling circle replication system that requires four phage proteins and seven host elongation proteins. These studies revealed surprising new roles for the G*38*P origin binding protein in the initiation of DNA replication on forks that do not contain origin sequences. In addition, they show the versatility of the SPP1 replication fork, where both the viral and the host SSB may be used, in contrast to the *B. subtilis* replication fork, which uses only its own SSB (the SsbA protein). Moreover, *B. subtilis* replication is inhibited by the viral SSB (G*36*P), a mechanism that is likely exploited by the phage to shut down host DNA replication synthesis and foster its own replication.

4.3 MATERIALS AND METHODS

4.3.1 Rolling circle assays

Standard reactions consisted of 30 nM G*40*P_6, 300 nM G*39*P, 300 nM G*38*P, 8 nM DnaG, 15 nM DnaE, 20 nM PolC, 25 nM τ_4, 25 nM δ, 25 nM δ', 24 nM β_2, 30 nM G*36*P_4, 5 nM mini-circular DNA template, 350 μM ATP, 100 μM CTP, GTP and UTP, 48 μM dNTPs (except 18 μM dCTP or dGTP for the leading and lagging strand DNA synthesis, respectively) and 0.2 μCi/reaction [α-^{32}P]dCTP or [α-^{32}P]dGTP. The DNA template was a 409-nt circle containing a 396-nt tail described in [30], but prepared by an alternative procedure that included a polymerase chain reaction amplification step (Yuan and McHenry, in preparation). The reactions were carried out in 12.5 μl of buffer BsRC [40 mM Tris-acetate (pH 7.8), 12 mM magnesium acetate, 3 μM $ZnSO_4$, 1mM dithiothreitol, 0.02% (w/v) Pluronic F68, [30]] that contained 500 mM potassium glutamate and 1% (w/v) polyethylene glycol (PEG-8K). The buffer also contained 4% glycerol, 19 mM NaCl and 4 mM Tris-HCl that was contributed by the addition of protein solutions. Incubations were conducted for 10 min at 37 ºC. An enzyme mix containing all protein components except SSB (G*36*P, or SsbA, as indicated) was prepared in buffer BsRC. Two different substrate mixes containing template DNA, rNTPs, dNTPs, SSB (G*36*P or SsbA) and either [α-^{32}P]dCTP or [α-^{32}P]dGTP for measurement of leading and lagging strand synthesis, respectively, were prepared. Reactions were initiated by mixing the enzyme mix and a substrate mix. After incubation, reactions were stopped by addition of an equal volume of stop mix [40 mM Tris-HCl (pH 8.0), 0.2%

SDS, 100 mM EDTA, and 50 μg/ml proteinase K]. Samples were treated for 20 min at 37 ºC, then applied onto Sephadex G-50 columns to eliminate non-incorporated dNTPs. The extent of DNA synthesis in leading and lagging strands was quantified by scintillation counting.

For the analysis of the size of leading and lagging strand products, samples were brought to 50 mM NaOH, 5% (v/v) glycerol and 0.05% bromphenol blue and fractionated on alkaline 0.5% agarose gels for ~3 h at 80 V. Alkaline agarose gel buffer consisted of 30 mM NaOH and 0.5 mM EDTA. Gels were fixed in 7% (w/v) trichloroacetic acid, dried, autoradiographed on storage phosphor screens and analyzed with Quantity One (Bio-Rad) software.

For calculating the rate of SPP1 fork progression, aliquots were removed, quenched and processed as described earlier in the text. The molecular weight of the longest leading strand product at each time was extrapolated from labeled DNA size standards and plotted as a function of time. The elongation rate was determined by calculating the slope of this curve [31].

The protein concentrations in the *B. subtilis* replication system were as follows: 15 nM DnaE, 20 nM PolC, 8 nM DnaG, 25nM τ_4, 25nM δ, 25nM δ', 24nM β_2, 30nM $DnaC_6$, 15 nM PriA, 50 nM $DnaD_4$, 100 nM $DnaB_4$, 40 nM $DnaI_6$ and various amounts of $SsbA_4$ and $G36P_4$.

4.3.2 Extension of DNA primers annealed to M13

Templates were prepared by mixing 50 pmol single-stranded $M13_{Gori}$ DNA [32] with 60 pmol synthetic DNA primer (5'-AGGCTGGCTGACCTTCATCAAGAGTAATCT-3') in 70 ml of a buffer consisting of 40 mM Tris-HCl (pH 7.8), 150 mM NaCl and 1 mM EDTA, heating to 95 ºC, cooling to room temperature over 1 h and diluting the resulting mixture to 29 nM as circles. Holoenzyme reactions (25 μl each) contained 2.3 nM template; 2 nM PolC or 3 nM DnaE; 25 nM β_2, if present, 15 nM τ_4, 20 nM δ, 20 nM δ', and variable concentrations of *B. subtilis* $SsbA_4$ or SPP1 G*36*P_4; 48mM dATP, dGTP and dCTP; 18 μM [^{3}H]dTTP (specific activity 113 cpm/pmol); and 250 μM ATP in buffer BsM13 [40 mM Tris-acetate (pH 7.8), 340 mM potassium glutamate, 10 mM magnesium acetate, 4 mM $ZnSO_4$, 0.015% (w/v) Pluronic F68]. Reaction mixtures were prepared on ice, initiated by incubation at 30 ºC, stopped after 3 min (for PolC) or 5 min (for DnaE) with 2 drops of 0.2 M sodium pyrophosphate, and incorporated nucleotides were precipitated with 0.5 ml 10% (w/v) trichloroacetic acid. Unincorporated nucleotides were removed, and reaction products were quantified as described [33].

4.3.3 Helicase assays

Oligonucleotides were obtained from Biosearch Technologies. The substrate diagrammed in Fig. 4.6A was assembled from the following HPLC-purified oligonucleotides. Leading strand template 90-mer- 5'-tetrachloro- fluorescein (TET)-CGCGTATAGATCATTACTATAACATGTTAGATTCATGATAATATAAGAGATGACGA

ATATGATTTTGTCGGCTAATGTAAGAATCTTCAA-3' contained fluorescent TET at the 5' terminus. Lagging strand template 90-mer- 5'-TT(biotin)T_{44}ATATTATCATGAATCTAACATGTTATAGTAATGATCTATACGCG-BHQ-1-3' contained biotin conjugated to preceding thymidine and Black Hole Quencher-1 (BHQ-1) at 3' terminus that quenches fluorescent TET dye. Primer 35-mer- 5'-TTGAAGATTCTTACATTAGTTGACAAAATCATATT-3', when annealed to the leading strand template, created a 10 nt gap. Trap oligo 45-mer 5'-TATATTATCATGAATCTAACATGTTATAGTAATGATCTATACGCG-3' was used to capture helicase-displaced leading strand so that it did not re-anneal to the lagging strand template that contained the fluorescence quencher. The substrate was formed by annealing 1 μM leading strand template with 1 μM lagging strand template and 1 μM primer in a buffer containing 10 mM Tris (pH 7.75), 50 mM NaCl and 1mM EDTA in a final volume of 25 μl. The sample was heated to 95 ºC for 5 min and cooled to 25 ºC at 1 ºC /min.

For FRET experiments, 20 nM oligonucleotide substrate was combined with 100 nM trap oligo, 200 nM streptavidin and protein components in a buffer containing 50 mM Hepes (pH 7.5), 10 mM magnesium acetate, 10 mM dithiothreitol, 20% (v/v) glycerol, 0.02% (v/v) Nonidet P40 detergent, 200 μg/ml bovine serum albumin, 100 mM potassium glutamate and 10 mM ATP in a round-bottomed black 96-well plate in a final volume of 50 μl. Samples were incubated at 30 ºC for 15 min. Fluorescence emission was detected at 535 nm using an Envision plate reader with an excitation of 485 nm. Using concentrations of unannealed fluorescent leading strand template that are in the

linear range of the assay, fluorescence units were converted to molarity using a standard curve.

4.3.4 In vivo *replication of SPP1 in a* ssbΔ35 *background*

The *B. subtilis* FLB22 (*ssbΔ35*) and FLB23 (*ssb3*+) strains were a kind gift of P. Polard (CNRS, France). They were obtained by a single crossing-over integration procedure of pMUTIN-SPA derivatives; in those two strains, the essential *rpsR* gene, which is located immediately after *ssb*, is placed under the control of the IPTG-inducible Pspac promoter [34]. FLB22 is a mutant strain, which expresses from its natural promoter an SsbA truncated of its last 35 amino acids. *ssbΔ35* cells are temperature sensitive for growth above 47 ºC in LB medium. FLB23 is an isogenic strain encoding a wild-type SsbA protein. FLB22 and FLB23 cells were grown at 30 ºC in LB medium with 0.5 mM IPTG until OD_{560} = 0.2 and then shifted to 50 ºC. After 15 min incubation, the cells were infected with a multiplicity of infection of 10 with the SPP1 phage, and the cultures were incubated for 120 min at 50 ºC. Infection experiments at permissive temperature were performed in parallel. After centrifugation, the supernatant that contained free phage particles was filtered through 0.45 μm filters. Titrations were carried out using *B. subtilis* BG214 as the indicator strain.

4.4 RESULTS

4.4.1 Reconstitution of a SPP1 replication fork

We reconstituted replication on a synthetic 409-bp circle containing a long flap that mimics a replication fork (Fig. 4.1B). A 50:1 asymmetric G:C distribution in the synthetic template permits facile quantification of leading and lagging strand synthesis (Fig. 4.1C). The structure of this template may mimic the intermediate that is formed in SPP1 once the D-loop, formed by recombination, is resolved to initiate concatemeric (σ mode) replication [35]. SPP1 proteins were expressed and purified to homogeneity (Fig. A3.1, Fig. 4.1A) and added to various combinations of purified *B. subtilis* DNA replication proteins [30] to determine which combination was required for efficient replication. Consistent with genetic requirements, SPP1 G*39*P and G*40*P were required, as were host PolC and DnaG (Fig. 4.1D and E). Additional components of the host replicase including the clamp loader (τcomplex, which consists of the τ, δ and δ' subunits) and sliding clamp processivity factor (β_2) were also found to be required. As observed in *B. subtilis*, DnaE was also necessary, and like primase, it plays primarily a lagging strand role [30,36]. The decreased level of leading strand synthesis in the absence of DnaE and DnaG may be due to a decreased efficiency when the replisome is incomplete—lacking these factors. To our surprise, the G*38*P origin binding protein was also essential, even though the origin sequence was not contained within the DNA template. G*36*P was also required, but some synthesis was observed in the absence of G*36*P, owing to a non-physiological reaction where the helicase can 'self-load' by threading

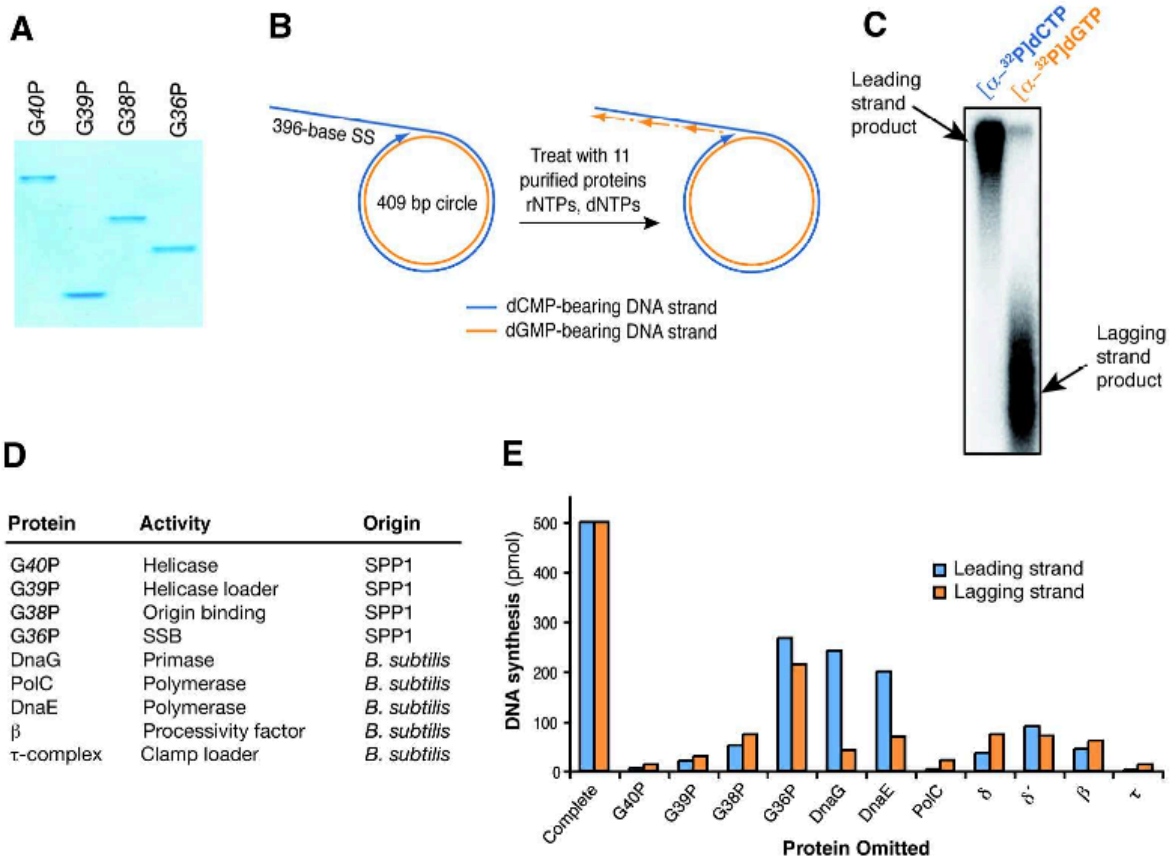

Protein	Activity	Origin
G*40*P	Helicase	SPP1
G*39*P	Helicase loader	SPP1
G*38*P	Origin binding	SPP1
G*36*P	SSB	SPP1
DnaG	Primase	*B. subtilis*
PolC	Polymerase	*B. subtilis*
DnaE	Polymerase	*B. subtilis*
β	Processivity factor	*B. subtilis*
τ-complex	Clamp loader	*B. subtilis*

FIGURE. 4.1
Reconstitution of SPP1 rolling circle DNA replication with *B. subtilis* and SPP1 purified proteins. (A) 15% SDS-PAGE gel of purified SPP1 bacteriophage proteins used to reconstitute rolling circle DNA replication: G*40*P (49.8kDa), G*39*P (14.6kDa), G*38*P (29.9kDa) and G*36*P (18 kDa). The purification of these proteins is described in section A3.1. (B) Diagram of the DNA template used. It has an asymmetric G:C ratio (50:1) between the two strands, permitting quantification of leading and lagging strand synthesis by measuring radioactive dCMP and dGMP incorporation. (C) Addition of [α-^{32}P]dCTP or [α-^{32}P]dGTP allows the detection of products corresponding to leading and lagging strands synthesis, respectively, resolved on an alkaline agarose gel. (D) Activity and source of proteins involved in SPP1 rolling circle replication. (E) Protein requirements for SPP1 rolling circle DNA replication. The values represented are the mean of three independent experiments.

over the 5'-end of the template flap (Chapter 3). The required proteins were individually titrated in the presence of optimal concentrations of the remaining proteins to optimize the replicative reaction (Fig. A3.2).

We examined the time course of DNA leading and lagging strand synthesis with the SPP1 replisome. Both leading and lagging strand synthesis exhibited a lag phase of 1 min, presumably the time required for loading of the helicase and assembly of the replication fork. After the lag, the synthesis rate remained linear for ~5min (Fig. 4.2A). We examined the elongation rate of reconstituted SPP1 replication forks by analyzing leading strand product formation after the first minute lag (Fig. 4.2B and C). From these data, a rate of progression of 224 ± 7 nt/s was obtained. We performed, as a control, the same assays with a reconstituted *B. subtilis* replication fork and obtained a value of 200 ± 6 nt/s. These results show that both replisomes progress at a similar rate under the experimental conditions used.

4.4.2 Primase, not DnaE, regulates the length of Okazaki fragments

B. subtilis DnaG primase cycles on and off the replication fork through association with the DnaC helicase. Thus, higher concentrations of primase lead to more frequent associations with helicase and more frequent priming, resulting in shorter Okazaki fragments [30]. We also observed a decrease in Okazaki fragment size with increasing DnaG primase concentration in our SPP1 system (Fig. 4.3A). Okazaki fragment length varied from ca. 4-kb at 1.5 nM primase down to ca. 400-bp at 100nM primase (Fig. 4.3A). *B. subtilis* DnaE functions like eukaryotic DNA polymerase α, adding a stretch of

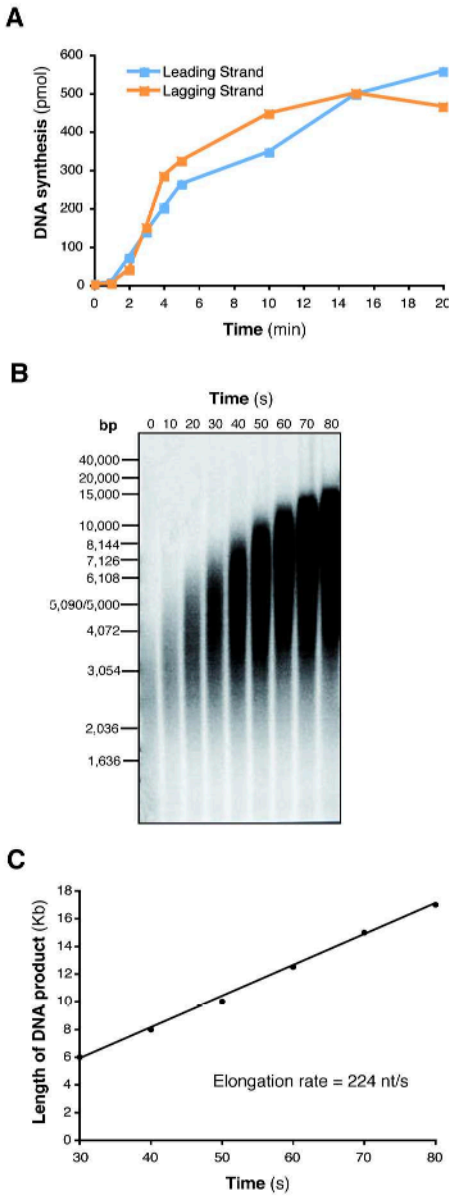

FIGURE 4.2
Progression of the reconstituted SPP1 replication fork. (A) Time course of the leading strand and lagging strand DNA synthesis. The values represented are the mean of three independent experiments. (B) Rate of SPP1 replication fork progression. Standard reactions were scaled up to a volume of 125 μl and incubated at 37 ºC with [α-^{32}P]dCTP to detect leading strand synthesis. After the first minute (indicated as time 0), aliquots of 12.5 μl were removed and quenched every 10 s. (C) Quantification of the rate of SPP1 fork movement. Plot of the largest DNA fragment present versus time to determine replication fork rate.

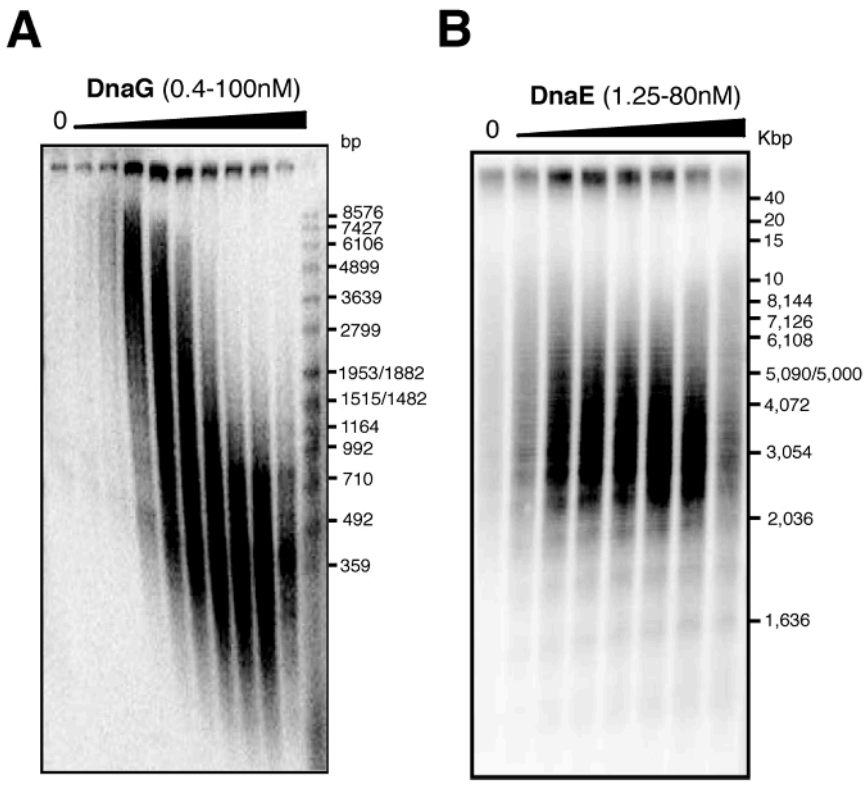

FIGURE 4.3
Effect of increasing DnaG and DnaE on the size of Okazaki fragments. (A) Size of Okazaki fragments varies inversely with primase concentration. Rolling circle reactions were performed in the presence of [α-^{32}P]dGTP and were stopped after 10min. The reactions were run on an alkaline agarose gel. Primase concentrations assayed varied in a 2-fold dilution series from 100 nM down to 0.4 nM. (B) Variations in DnaE concentrations do not alter the size of the Okazaki fragments. Reactions were performed changing the DnaE concentration in a 2-fold dilution series from 80 nM to 1.25 nM.

deoxynucleotides to the RNA primer before handoff to the major replicase [30]. We also investigated whether variations in DnaE concentration influence Okazaki fragment length. In the absence of DnaE, lagging strand synthesis was very low (Fig. 4.1E and Fig. 4.3B). Most of the synthesis observed in the absence of DnaE was owing to background incorporation of [α-^{32}P]dGTP into the leading strand product. The leading strand template contains 2% of the template C residues within our rolling circle template, and the resulting incorporation yields a significant background only in the absence of lagging strand synthesis. The size of Okazaki fragments was similar over a wide range of concentrations (1.25–80 nM DnaE, Fig. 4.3B).

4.4.3 SPP1 replication forks can be reconstituted with SsbA from B. subtilis*, but the helicase loaders are not interchangeable*

To see if some SPP1 components could be replaced by their *B. subtilis* counterparts, we first determined whether host SsbA could replace G*36*P. *B. subtilis* SsbA supports an efficient reaction at both 30 nM [the optimal G*36*P concentration, that is also the amount of SSB needed to cover the 396-nt tail present in the DNA template in the 65-nt DNA-binding mode [38]] and at higher concentrations (Fig. 4.4A, lanes 7 and 11). We observed a stronger dependence on G*38*P at 90 nM *B. subtilis* SsbA. The reactions were dependent on G*39*P under both conditions tested. In the absence of any SSB, efficient reactions are also observed, but dependence on G*38*P and G*39*P was lost. In the absence of SSB, helicases can self-assemble by threading over the exposed 5'-end of the flap of the forked substrates (Chapter 3). We found that G*40*P could not be

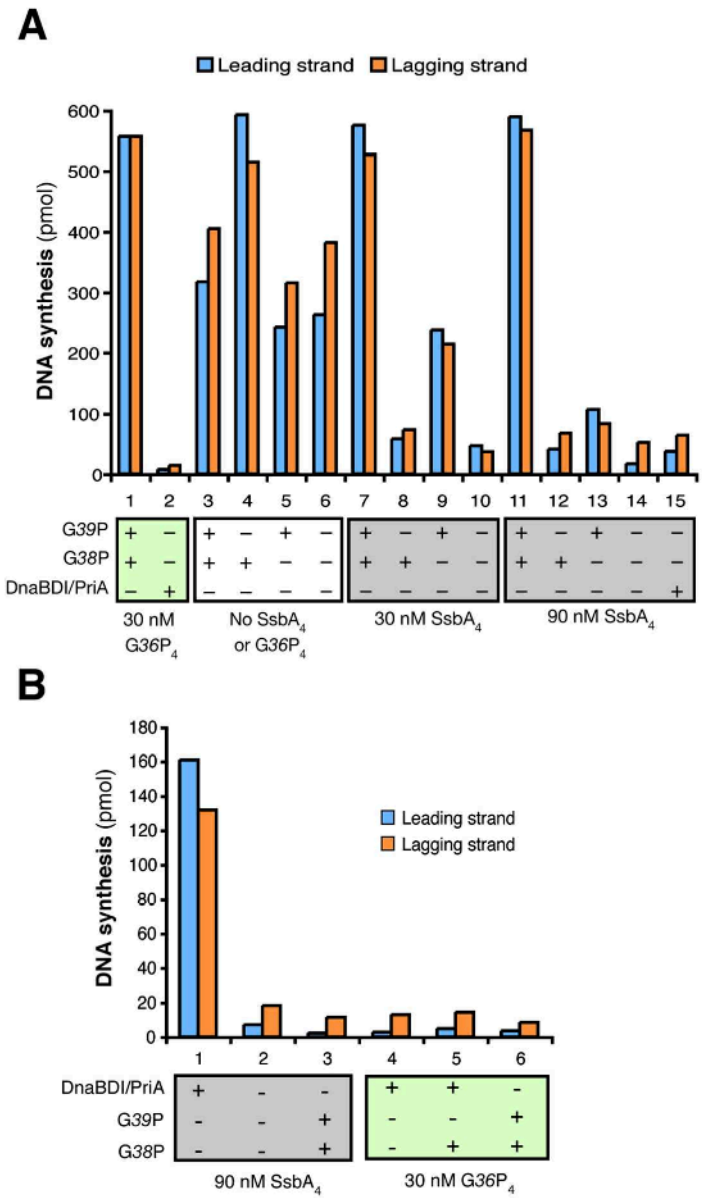

FIGURE 4.4
Interchangeable components of the replication machinery of *B. subtilis* and SPP1. (A) The SPP1 replication fork can use SsbA or G*36*P. In vitro replication of reconstituted SPP1 replication forks assembled in the presence of 30nM G*36*P_4 (lanes 1–2), in the absence of an SSB (lanes 3–6) or in the presence of 30nM or 90nM $SsbA_4$, (lanes 7–10 and 11–15, respectively). The presence of G*39*P (helicase loader) and G*38*P (origin binding) or the *B. subtilis* loading system (formed by DnaB-DnaD-DnaI-PriA) is indicated. (B) The *B. subtilis* replication fork strictly requires SsbA, and it owns helicase loading system. *In vitro* replication of reconstituted *B. subtilis* replication forks assembled in the presence of 90 nM $SsbA_4$ or 30 nM $G36P_4$ and the indicated components. The data shown are the mean of at least three independent experiments.

assembled onto the fork by the host loading system (DnaB/DnaD/DnaI/PriA) in the presence of either SsbA or G*36*P (Fig. 4.4A, lanes 2 and 15).

We then tested whether G*36*P can replace SsbA in support of the *B. subtilis* replisome. *B. subtilis* chromosomal replication does not occur in the presence of G*36*P either in the presence of the natural helicase loading system (PriA, DnaD, DnaB, DnaI) (Fig. 4.4B, lane 4) or in the presence of the phage G*38*P-G*39*P helicase loading system (Fig. 4.4B, lane 6). Increasing G*36*P concentrations to levels found to be optimal for SsbA also did not stimulate the *B. subtilis* reaction (Fig. A3.3). In the presence of SsbA, the bacterial helicase worked well with its own helicase loading proteins (Fig. 4.4B, lane 1), but they could not be substituted with the viral helicase loading proteins (Fig. 4.4B, lane 3).

4.4.4 Elevated levels of G38P are required to reverse inhibition of DNA replication by high concentrations of G36P

The above experiments showed that G*36*P and SsbA could work similarly on SPP1 replication forks. In titration experiments that we performed to optimize protein concentrations, we noted that increasing concentrations of G*36*P significantly reduced lagging strand DNA synthesis, whereas this effect was not observed with increasing SsbA (Fig. 4.5A and B). We were concerned that the leading strand synthesis observed at elevated G*36*P may have been an inauthentic reaction, resulting from helicase independent strand displacement by the PolC holoenzyme. Such a reaction is catalyzed by the *E. coli* Pol III holoenzyme at high SSB concentrations [31]. However, dropout

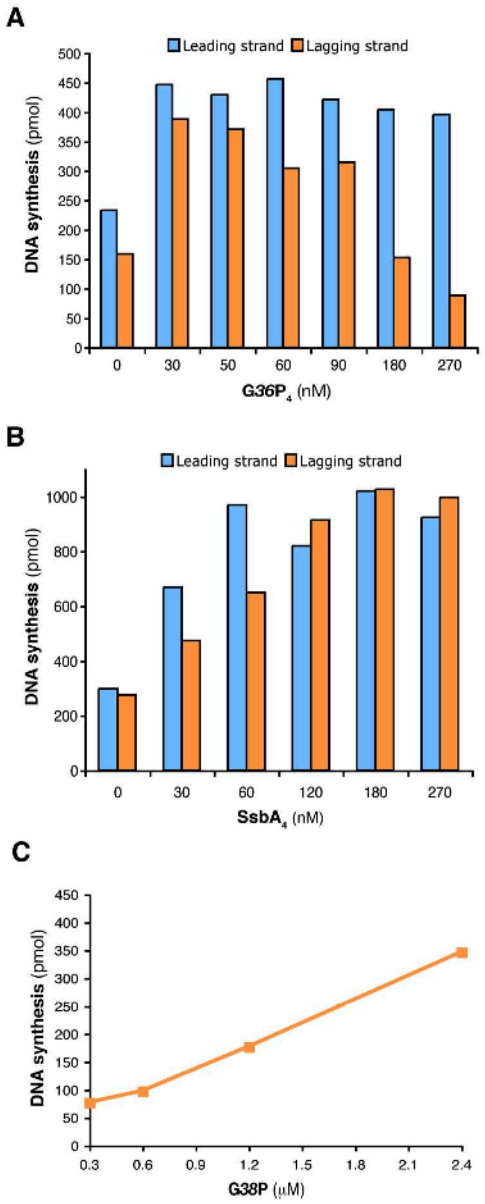

FIGURE 4.5
Increasing concentrations of G*36*P protein inhibit lagging strand DNA synthesis; synthesis can be restored by increasing G*38*P. (A) G*36*P_4 titration in SPP1 replication fork reconstitution. Standard reactions to measure DNA synthesis at leading and lagging strands were performed at the indicated G*36*P_4 concentrations. (B) High $SsbA_4$ concentrations do not inhibit lagging strand synthesis. (C) Effect on lagging strand synthesis of increasing G*38*P at high G*36*P_4 (180 nM). The values represented are the mean of three independent experiments.

experiments where one protein was deleted from the reaction at a time confirmed that leading strand synthesis in the presence of elevated G*36*P concentrations retained a dependency on all of the leading strand replication proteins, including helicase (Fig. A3.4).

We suspected the inhibition by high G*36*P may have been caused by sequestering a component in a binary complex in solution, preventing its participation in the replicative reaction. In a search for proteins that reversed the G*36*P inhibitory effect at high concentrations, we found that G*38*P elicited this effect (Fig. 4.5C). We also tested the other viral protein that participates in helicase loading, G*39*P, but observed no effect (data not shown).

I performed an independent fluorescence-based assay that detects helicase loading and ensuing strand separation (see Fig. 4.6A for a description of the substrate). This permits analysis of the SSB effect on helicase activity independent of its influence on priming and polymerase activity. The 5'-end of the lagging strand template was blocked by streptavidin attachment, preventing helicase self-assembly by threading over the 5'-flap in the absence of SSB (Chapter 3). With the G*40*P helicase, I also observed in these assays greater efficacy of G*36*P relative to SsbA at low concentrations (Fig. A3.5D). Furthermore, I observed an absolute requirement for G*38*P (Fig. A3.5A), consistent with a role for this protein at the helicase assembly step.

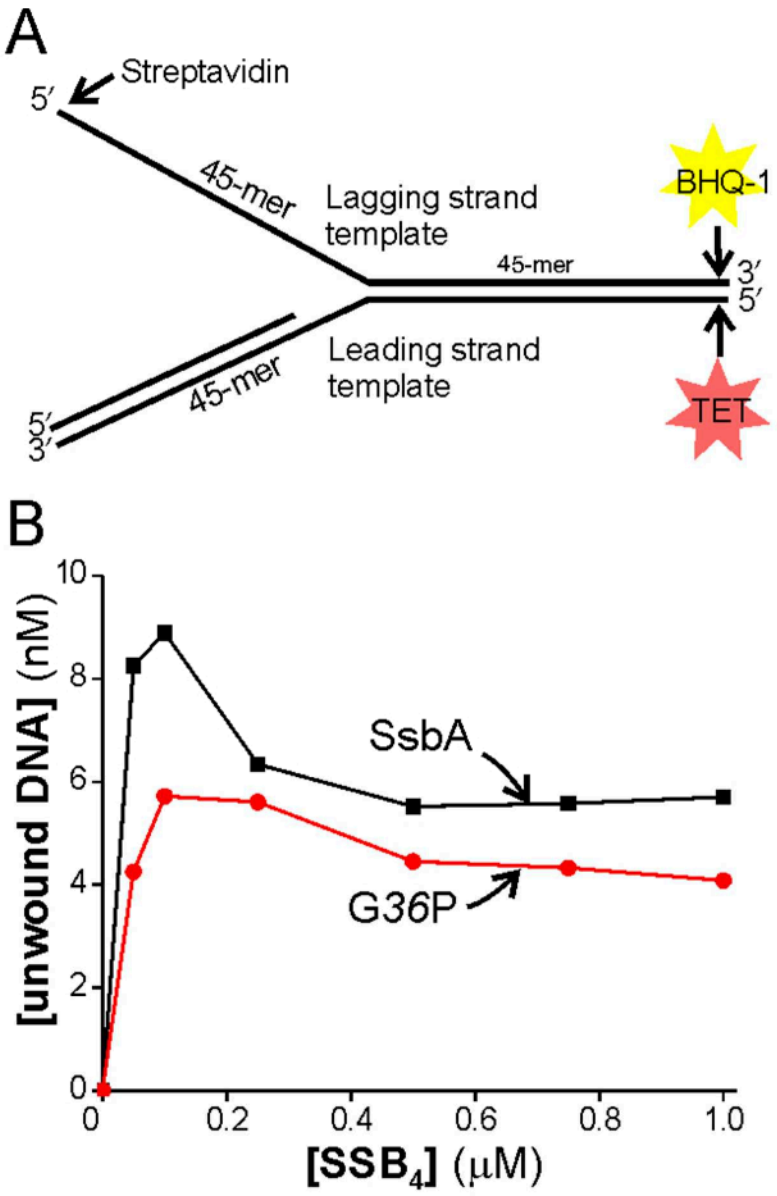

FIGURE 4.6
Either SsbA or G*36*P will support *B. subtilis* helicase loading and unwinding. (A) DNA substrate used in unwinding reactions. The fluorescence of TET on the 5'-terminus increases on being separated from a quencher (BHQ-1) on the opposing strand. The 5'-end of the lagging strand template is blocked by attachment of streptavidin to an incorporated biotinylated thymidine to inhibit helicase self-loading by threading over a free 5'-end. (B) *B. subtilis* helicase activity in the presence of SsbA or G*36*P. DNA substrate was combined with varying amounts of either SsbA or G*36*P, and 150 nM PriA, 75 nM DnaD, 75 nM DnaB, 12 nM $DnaC_6$, and 50 nM DnaI.
both viral G*36*P and host SsbA similarly. SPP1 rolling circle reaction requires an SSB

4.4.5 SPP1 does not require SsbA in vivo

The previous assays showed that the *in vitro* SPP1 replication system can use both viral G36P and host SsbA similarly. SPP1 rolling circle reaction requires an SSB with a C-terminal tail (Supplementary (Fig. A3.6) that is the site of interaction for almost all proteins that bind SSB [39]. To test whether the SPP1 phage requires the SsbA protein *in vivo*, we analyzed the levels of amplification of the SPP1 phage in a *B. subtilis* mutant strain, FLB22, which expresses from its natural promoter SsbA truncated of its last 35 amino acids. *ssbΔ35* cells and an isogenic control were infected at 30 ºC, and after 2 h of infection the phage titer was determined. *ssbΔ35* cells are temperature sensitive for growth above 47 ºC in LB medium [34]. Cultures were also grown at a permissive temperature until OD_{560nm} = 0.2 and then shifted to 50 ºC. After 15 min incubation, the cells were infected with SPP1, and the cultures were incubated for 2 h at 50 ºC. Titrations of three independent experiments yielded a mean of 3 x 10^9 phage/ml and 1 x 10^9 phage/ml for infections of *ssbΔ35* cells at permissive and non-permissive temperature, respectively. 3 x 10^9 and 4 x 10 phage/ml titers were obtained when the isogenic strain (*ssb3+*) was infected at the permissive and non-permissive temperature, respectively.

4.4.6 The DnaC helicase unwinds DNA in the presence of G36P

The preceding results show that G*36*P is not able to support replication in the full *B. subtilis* replication system. In an attempt to identify the defective step, I tested whether

the DnaC helicase can be assembled onto DNA and unwind DNA efficiently in the presence of G*36*P. I exploited the fluorescence-based assay (Fig. 4.6A). The results showed that SPP1 G*36*P and SsbA are interchangeable in the helicase assays (Fig. 4.6B). Thus, the defect in the *B. subtilis* assay in the presence of G*36*P occurs after helicase loading and DNA unwinding.

4.4.7 G36P stimulates synthesis by DnaE, but not by the PolC holoenzyme

Continuing our search for the defect in *B. subtilis* chromosomal replication in the presence of G*36*P, we tested for its ability to stimulate reactions catalyzed by the DnaE and PolC holoenzymes. We observed that SsbA and G*36*P stimulate the DnaE holoenzyme with similar efficiency (Fig. 4.7A). However, G*36*P failed to stimulate the PolC holoenzyme (Fig. 4.7B). The same defect was observed in RNA primer extension reactions conducted with DnaE in the presence of PolC, which mimicked the reactions occurring at the lagging strand of the replication fork (Fig. A3.7). This suggests that the defect in the G*36*P-supported *B. subtilis* reaction likely resides in its inability to stimulate the PolC holoenzyme.

4.4.8 G36P blocks host DNA replication

The observation that G*36*P does not support *B. subtilis* replication led us to investigate whether this could also occur in the physiological context, when both host and phage SSBs are present in the same reaction. *B. subtilis* replication forks were

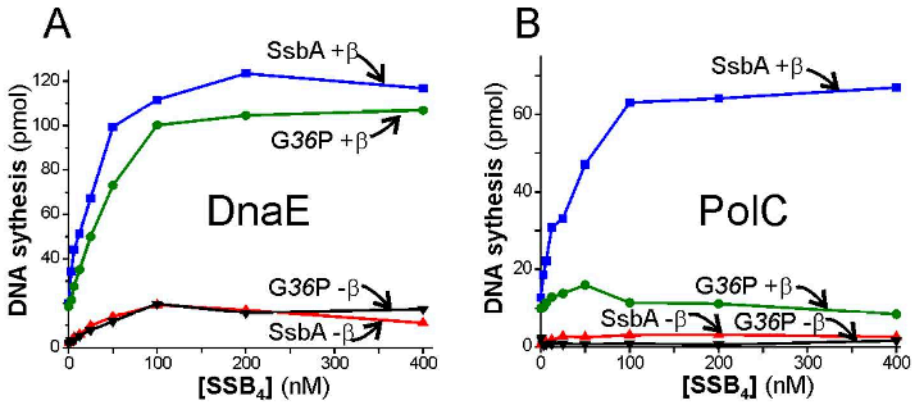

FIGURE 4.7
SPP1 G*36*P stimulates DnaE holoenzyme, but not PolC holoenzyme. (A) Extension of a DNA primer by the DnaE holoenzyme using either SsbA or G*36*P. SsbA or G*36*P were titrated in a DNA-primed $M13_{Gori}$ reaction containing 3 nM DnaE in the presence (+) or absence (-) of β_2 as indicated. (B) Extension of a DNA primer by the PolC holoenzyme (2 nM) using either SsbA or G*36*P. Total DNA synthesis was analyzed by quantification of incorporated [^{3}H]dTTP.

assembled in the presence of saturating concentrations of $SsbA_4$ and increasing concentrations of G*36*P_4. Both leading and lagging strand synthesis were significantly inhibited even at the lowest G*36*P concentration tested (30 nM) (Fig. 4.8).

4.5 DISCUSSION

We have reconstituted an efficient rolling circle SPP1 reaction that recapitulates the concatemeric phase of SPP1 DNA replication. The reaction requires all proteins defined by genetic studies including the phage helicase (G*40*P), its loading protein (G*39*P) and the host DnaG primase and PolC DNA polymerase. We also observed a requirement for the G*36*P protein. Neither the *B. subtilis* helicase loading proteins nor the helicase are required, but all of the polymerase elongation components are necessary, including β_2, the τ complex and a second DNA polymerase III, DnaE. The rate of elongation is similar to the rate of *B. subtilis* replication under the conditions used.

In the well-characterized *E. coli* system, DnaG primase binds to the $DnaB_6$ helicase before the synthesis of each primer and then dissociates [40]. Because of this equilibrium, high concentrations of primase lead to more frequent priming and shorter Okazaki fragments. A similar observation has been made in a reconstituted *B. subtilis* DNA replication system [30] and in the SPP1 system, presumably for the same reasons. DnaE has been previously shown to be required to extend RNA primers a short distance before handing them off to PolC, analogous to the process in eukaryotes where Pol α and the Pol δ holoenzyme are required [5,6,30]. Thus, it is possible that DnaE could also influence primer synthesis owing to an interaction with primase. We

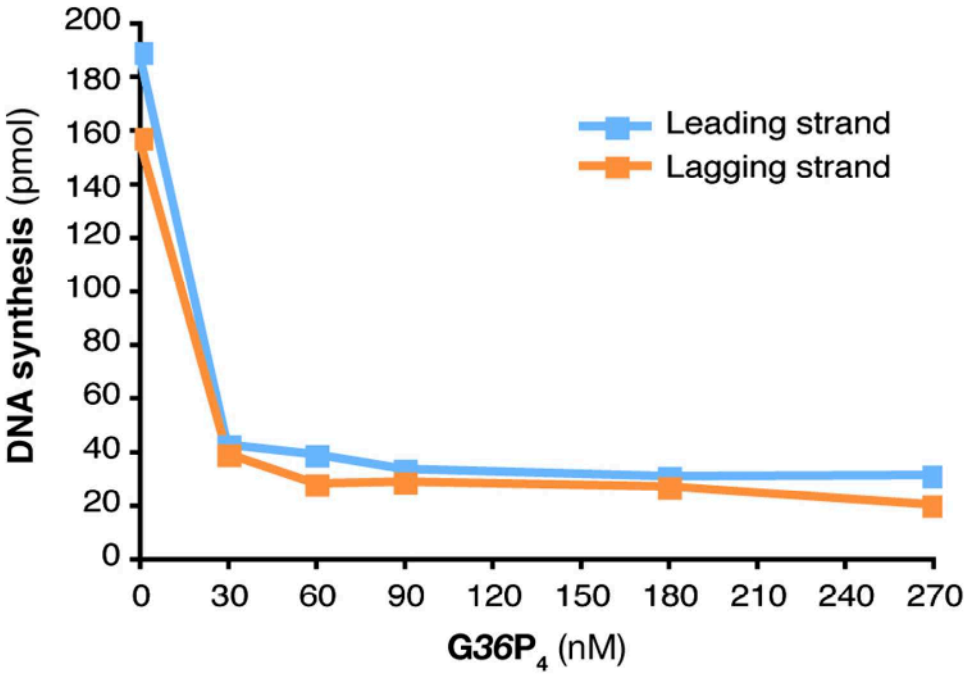

FIGUR 4.8
G*36*P inhibits *B. subtilis* rolling circle DNA replication even when SsbA is present at saturating concentrations. *In vitro* replication of reconstituted *B. subtilis* replication forks assembled in the presence of increasing concentrations of G*36*P_4 (30, 60, 90, 180 and 270 nM tetramer) and 90 nM $SsbA_4$. Both SSBs were added simultaneously to the substrate mix. The data shown are the mean of at least three independent experiments.

tested this possibility and found it not to be the case. Okazaki fragment length did not vary over a wide range of DnaE concentrations in the SPP1 system as may also occur in the bacterial systems.

These studies identified a requirement for the G*38*P origin binding protein for a replicative reaction initiating on forks that mimic the concatemeric stage of SPP1 replication. In SPP1, this type of replication initiates after recombinational events [after the processing of the D-loop formed by fork stalling, [10]. Therefore, such reactions might mimic the replication restart reactions that occur on stalled forks in chromosomal systems that require PriA for their initiation [41]. PriA was an essential component of the *in vitro* rolling circle replication with the *B. subtilis* system [30], but SPP1 replication does not require PriA, consistent with genetic data [18]. Thus, it appears that G*38*P plays a dual role as an origin-specific and forked structure-specific initiation protein. Future studies directed at common features of PriA- and G*38*P-supported replication initiation may provide insight regarding the mechanism used by these proteins to drive the replication restart reaction in cellular systems. In *B. subtilis*, the loading of the replicative helicase DnaC at *ori*C relies on the ordered associations of DnaA, DnaB, DnaD and DnaI proteins [42] and outside of the origin relies on the PriA, DnaB, DnaD and DnaI proteins, also through a cascade of protein interactions that are crucial for the loading of the replicative helicase on SSB-coated ssDNA [43]. The results of the current study show that in SPP1, this reaction is restricted to two proteins (G*38*P and G*39*P).

We found that both SPP1 G*36*P and *B. subtilis* SsbA supported the SPP1 replicative reaction, but with interesting differences. Under standard reaction conditions, ~180 nM $SsbA_4$ was required to achieve an optimal rate of leading and lagging strand

synthesis. However, with G*36*P$_4$, an optimum rate is achieved at a 6-fold lower concentration. Further increases of G*36*P concentration result in marked inhibition of lagging strand synthesis. The most straightforward explanation for this observation is that G*36*P makes specific protein–protein interactions that sequester some viral component in inactive binary complexes. As elevated levels of G*38*P reverse the lagging strand inhibition induced by elevated G*36*P, it is the most likely candidate as the sequestration target. Future work needs to be done to unravel the cause of these differences. It is interesting that G*38*P is involved in both loading the replicative helicase and reversing the inhibition by high G*36*P concentrations specifically for the lagging strand. This dual activity suggests an additional function that is required for ongoing lagging strand replication after helicase loading.

In contrast to the above observations, the phage-encoded SSB, G*36*P, will not support a full host replisome-dependent replicative reaction. Dissection of the individual reaction steps shows that G*36*P is fully competent to support PriA/DnaD/DnaB/DnaI-dependent helicase loading and ensuing advancement to separate DNA strands. G*36*P is also able to stimulate a DnaE holoenzyme activity as good as the host SSB. The only defect detected was a failure of G*36*P to stimulate the major Gram-positive replicase, the PolC holoenzyme. Yet, the PolC holoenzyme supports efficient replication in the fully reconstituted SPP1 protein-dependent reaction. This suggests the presence of additional or stronger PolC holoenzyme-phage protein interactions that either stimulate PolC, protect it from inhibition or bypass its requirement for lagging strand replication.

The lack of support by G*36*P of the *B. subtilis* replication fork and the efficient use in the SPP1 replication fork of the two SSBs (the viral G*36*P and the host SsbA) could

be used *in vivo* as a strategy of the phage to amplify its own DNA while inhibiting host chromosomal replication. This hypothesis is supported by our observation that even at saturating amounts of SsbA, the *B. subtilis* replication system was inhibited by low concentrations of G*36*P. Examples of viral inhibitors that block host proliferation by binding to host proteins have been reported [44–46]. But a strategy based on inhibition by a viral encoded SSB has not been reported to date. It is interesting to note that many viruses encode SSB proteins [47]. These include *Staphylococcus aureus* phage 80α, which transfers pathogenicity islands between staphylococci. This phage also encodes a G*38*P-like protein [48].

G*36*P is 48% identical to *B. subtilis* SsbA. Identity in the C-terminus, which is important for most SSB-protein interactions, is even higher (~75%). The most critical residues required for SSB-protein interactions are the Pro–Phe pair found at the extreme C-terminus [39]. The C-terminal Phe of the *E. coli* homolog fits into a hydrophobic pocket of the χ subunit of the *E. coli* DNA polymerase III holoenzyme, and the carboxyl group of this residue forms a salt bridge [49]. Slightly more internal within SSB are three conserved acidic residues that form ionic bonds with positively charged residues in SSB- binding sites [50]. The C-terminus of G*36*P contains two of these three acidic residues. In other systems, mutation of only one of the C-terminal three acidic residues of SSB results in only a modest decrease in binding to interacting proteins [39,50]. Thus, explanation of the differential effects observed between G*36*P and SsbA on PolC holoenzyme stimulation and the specific inhibition of SPP1 replication at high G*36*P levels may require additional interactions outside of the prototypical C-terminal SSB interaction sequences.

Viruses that encode their own initiation machinery but depend on the host for elongation functions have provided significant insight into cellular processes [4,5,7,51]. With the simple single-stranded DNA coli-phages, the only viral protein that is required for replication is a nicking/religation activity that functions after duplex formation to shift SS → RF to duplex DNA replication [52]. The bacteriophage λ encodes its own origin binding protein and helicase loader and subverts the host helicase [7]. Thus, it differs from SPP1 in that it does not encode a helicase or an SSB. However, important similarities are also noted. λ, like SPP1, encodes an origin-specific initiation protein (O protein) that is not a DnaA homolog. The O protein, like SPP1 G*38*P, can serve to initiate DNA synthesis on artificial replication forks that lack origin sequences [15]. SV40, like SPP1, encodes its own origin binding protein and helicase, both contained within the same polypeptide chain as the T-antigen [53]. This system has been invaluable in revealing the mechanisms of eukaryotic DNA replication [4,5].

The best biochemically defined Gram-positive bacteriophage is Φ29 [54]. It encodes its own replication machinery and has provided a wealth of tools and insight, varying from basic models for viral replication that extend to eukaryotic adenoviruses [55] to tools for biotechnology [56]. Before this work, an *in vitro* replication system for a Gram-positive phage that is dependent on host proteins had not been established.

Thus, the present study provides a new viral window into Gram-positive replication processes. The availability of a hybrid assay that exploits the efficiency and simplicity of initiation by phage-encoded proteins and a requirement for host proteins for elongation provides a powerful tool to support studies of fork dynamics, macromolecular interactions and regulation of replicative processes in Gram-positive organisms. Having

two SSBs that can be used interchangeably with differential effects should help unravel the importance of SSB interactions in replication fork processes. And, having the G*38*P protein that supports initiation on both defined duplex origins and replication forks may provide an opportunity to learn more about the mechanistic features common to these two important processes.

4.6 REFERENCES

1 Miller, E. S., Kutter, E., Mosig, G., Arisaka, F., Kunisawa, T. and Rüger, W. (2003) Bacteriophage T4 genome. Microbiology and Molecular Biology reviews : MMBR **67**, 86–156, table of contents.

2 Salas, M. (1991) Protein-priming of DNA replication. Annual Review of Biochemistry **60**, 39–71.

3 Boehmer, P. E. and Lehman, I. R. (1997) Herpes simplex virus DNA replication. Annual Review of Biochemistry **66**, 347–84.

4 Li, J. J. and Kelly, T. J. (1985) Simian virus 40 DNA replication *in vitro*: specificity of initiation and evidence for bidirectional replication. Molecular and Cellular Biology **5**, 1238–46.

5 Tsurimoto, T. and Stillman, B. (1991) Replication factors required for SV40 DNA replication *in vitro*. II. Switching of DNA polymerase α and δ during initiation of leading and lagging strand synthesis. The Journal of Biological Chemistry **266**, 1961–8.

6 Nethanel, T. and Kaufmann, G. (1990) Two DNA polymerases may be required for synthesis of the lagging DNA strand of simian virus 40. Journal of Virology **64**, 5912–8.

7 Mensa-Wilmot, K., Seaby, R., Alfano, C., Wold, M. C., Gomes, B. and McMacken, R. (1989) Reconstitution of a nine-protein system that initiates bacteriophage λ DNA replication. The Journal of Biological Chemistry **264**, 2853–61.

8 Alfano, C. and McMacken, R. (1989) Heat shock protein-mediated disassembly of nucleoprotein structures is required for the initiation of bacteriophage λ DNA replication. The Journal of Biological Chemistry **264**, 10709–18.

9 Alonso, J.C., Tavares, P., Lurz, R. and Trautner, T. A. (2006) Bacteriophage SPP1. Calendar,R. (ed.), The Bacteriophages, 2nd edn., Oxford University Press, Oxford, New York.

10 Lo Piano, A., Martínez-Jiménez, M. I., Zecchi, L. and Ayora, S. (2011) Recombination-dependent concatemeric viral DNA replication. Virus Research **160**, 1–14.

11 Stengel, G. and Kuchta, R. D. (2011) Coordinated leading and lagging strand DNA synthesis by using the herpes simplex virus 1 replication complex and minicircle DNA templates. Journal of Virology **85**, 957–67.

12 Lee, J., Chastain, P. D., Kusakabe, T., Griffith, J. D. and Richardson, C. C. (1998) Coordinated leading and lagging strand DNA synthesis on a minicircular template. Molecular Cell **1**, 1001–10.

13 Nelson, S. W., Kumar, R. and Benkovic, S. J. (2008) RNA primer handoff in bacteriophage T4 DNA replication: the role of single-stranded DNA-binding protein and polymerase accessory proteins. The Journal of Biological Chemistry **283**, 22838–46.

14 Salas, M. (2006) Phage Φ29 and its relatives. Calendar,R. (ed.), The Bacteriophages, 2nd edn, Oxford University Press, Oxford, New York.

15 Stephens, K. M. and McMacken, R. (1997) Functional properties of replication fork assemblies established by the bacteriophage λO and P replication proteins. The Journal of Biological Chemistry **272**, 28800–13.

16 Viret, J. F., Bravo, A. and Alonso, J. C. (1991) Recombination-dependent concatemeric plasmid replication. Microbiological Reviews **55**, 675–83.

17 Pedré, X., Weise, F., Chai, S., Lüder, G. and Alonso, J. C. (1994) Analysis of *cis* and *trans* acting elements required for the initiation of DNA replication in the *Bacillus subtilis* bacteriophage SPP1. Journal of Molecular Biology **236**, 1324–40.

18 Ayora, S., Missich, R., Mesa, P., Lurz, R., Yang, S., Egelman, E. H. and Alonso, J. C. (2002) Homologous-pairing activity of the *Bacillus subtilis* bacteriophage SPP1 replication protein G*35*P. The Journal of Biological Chemistry **277**, 35969–79.

19 Kaguni, J. M. (2006) DnaA: controlling the initiation of bacterial DNA replication and more. Annual Review of Microbiology **60**, 351–75.

20 Mott, M. L. and Berger, J. M. (2007) DNA replication initiation: mechanisms and regulation in bacteria. Nature Reviews. Microbiology **5**, 343–54.

21 Missich, R., Weise, F., Chai, S., Lurz, R., Pedré, X. and Alonso, J. C. (1997) The replisome organizer (G*38*P) of *Bacillus subtilis* bacteriophage SPP1 forms specialized nucleoprotein complexes with two discrete distant regions of the SPP1 genome. Journal of Molecular Biology **270**, 50–64.

22 Ayora, S., Stasiak, A. and Alonso, J. C. (1999) The *Bacillus subtilis* bacteriophage SPP1 G*39*P delivers and activates the G*40*P DNA helicase upon interacting with the G*38*P-bound replication origin. Journal of Molecular Biology **288**, 71–85.

23 Bailey, S., Sedelnikova, S. E., Mesa, P., Ayora, S., Waltho, J. P., Ashcroft, A. E., Baron, A. J., Alonso, J. C. and Rafferty, J. B. (2003) Structural analysis of *Bacillus*

subtilis SPP1 phage helicase loader protein G*39*P. The Journal of Biological Chemistry **278**, 15304–12.

24 Ayora, S., Weise, F., Mesa, P., Stasiak, A. and Alonso, J. C. (2002) *Bacillus subtilis* bacteriophage SPP1 hexameric DNA helicase, G*40*P, interacts with forked DNA. Nucleic Acids Research **30**, 2280–9.

25 Mesa, P., Alonso, J. C. and Ayora, S. (2006) *Bacillus subtilis* bacteriophage SPP1 G*40*P helicase lacking the n-terminal domain unwinds DNA bidirectionally. Journal of Molecular Biology **357**, 1077–88.

26 Wang, G., Klein, M. G., Tokonzaba, E., Zhang, Y., Holden, L. G. and Chen, X. S. (2008) The structure of a DnaB-family replicative helicase and its interactions with primase. Nature Structural & Molecular Biology **15**, 94–100.

27 Iyer, L. M., Koonin, E. V and Aravind, L. (2002) Classification and evolutionary history of the single-strand annealing proteins, RecT, Redbeta, ERF and RAD52. BMC Genomics **3**, 8.

28 Martínez-Jiménez, M. I., Alonso, J. C. and Ayora, S. (2005) *Bacillus subtilis* bacteriophage SPP1-encoded gene 34.1 product is a recombination-dependent DNA replication protein. Journal of Molecular Biology **351**, 1007–19.

29 Kidane, D., Ayora, S., Sweasy, J. B., Graumann, P. L. and Alonso, J. C. The cell pole: the site of cross talk between the DNA uptake and genetic recombination machinery. Critical Reviews in Biochemistry and Molecular Biology **47**, 531–55.

30 Sanders, G. M., Dallmann, H. G. and McHenry, C. S. (2010) Reconstitution of the *B. subtilis* replisome with 13 proteins including two distinct replicases. Molecular Cell, Elsevier Ltd **37**, 273–81.

31 Yuan, Q. and McHenry, C. S. (2009) Strand displacement by DNA polymerase III occurs through a τ–ψ–χ link to single-stranded DNA-binding protein coating the lagging strand template. The Journal of Biological Chemistry **284**, 31672–9.

32 Kaguni, J. and Ray, D. S. (1979) Cloning of a functional replication origin of phage G4 into the genome of phage M13. Journal of Molecular Biology **135**, 863–78.

33 McHenry, C. S. and Crow, W. (1979) DNA polymerase III of *Escherichia coli*. Purification and identification of subunits. The Journal of Biological Chemistry **254**, 1748–53.

34 Lecointe, F., Sérèna, C., Velten, M., Costes, A., McGovern, S., Meile, J.-C., Errington, J., Ehrlich, S. D., Noirot, P. and Polard, P. (2007) Anticipating chromosomal replication fork arrest: SSB targets repair DNA helicases to active forks. The EMBO Journal **26**, 4239–51.

35 Zecchi, L., Lo Piano, A., Suzuki, Y., Cañas, C., Takeyasu, K. and Ayora, S. (2012) Characterization of the Holliday junction resolving enzyme encoded by the *Bacillus subtilis* bacteriophage SPP1. PloS One **7**, e48440.

36 Dervyn, E., Suski, C., Daniel, R., Bruand, C., Chapuis, J., Errington, J., Jannière, L. and Ehrlich, S. D. (2001) Two essential DNA polymerases at the bacterial replication fork. Science (New York, N.Y.) **294**, 1716–9.

37 Manhart, C. M. and McHenry, C. S. (2013) The PriA Replication Restart Protein Blocks Replicase Access Prior to Helicase Assembly and Directs Template Specificity through Its ATPase Activity. The Journal of Biological Chemistry **288**, 3989–99.

38 Lohman, T. M. and Ferrari, M. E. (1994) *Escherichia coli* single-stranded DNA-binding protein: multiple DNA-binding modes and cooperativities. Annual Review of Biochemistry **63**, 527–70.

39 Shereda, R. D., Kozlov, A. G., Lohman, T. M., Cox, M. M. and Keck, J. L. SSB as an organizer/mobilizer of genome maintenance complexes. Critical Reviews in Biochemistry and Molecular Biology **43**, 289–318.

40 Tougu, K., Peng, H. and Marians, K. J. (1994) Identification of a domain of *Escherichia coli* primase required for functional interaction with the DnaB helicase at the replication fork. The Journal of Biological Chemistry **269**, 4675–82.

41 Liu, J. and Marians, K. J. (1999) PriA-directed assembly of a primosome on D loop DNA. The Journal of Biological Chemistry **274**, 25033–41.

42 Smits, W. K., Goranov, A. I. and Grossman, A. D. (2010) Ordered association of helicase loader proteins with the *Bacillus subtilis* origin of replication *in vivo*. Molecular Microbiology **75**, 452–61.

43 Bruand, C., Velten, M., McGovern, S., Marsin, S., Sérèna, C., Ehrlich, S. D. and Polard, P. (2005) Functional interplay between the *Bacillus subtilis* DnaD and DnaB proteins essential for initiation and re-initiation of DNA replication. Molecular Microbiology **55**, 1138–50.

44 Liu, J., Dehbi, M., Moeck, G., Arhin, F., Bauda, P., Bergeron, D., Callejo, M., Ferretti, V., Ha, N., Kwan, T., *et al.* (2004) Antimicrobial drug discovery through bacteriophage genomics. Nature Biotechnology **22**, 185–91.

45 Cámara, B., Liu, M., Reynolds, J., Shadrin, A., Liu, B., Kwok, K., Simpson, P., Weinzierl, R., Severinov, K., Cota, E., et al. (2010) T7 phage protein Gp2 inhibits the *Escherichia coli* RNA polymerase by antagonizing stable DNA strand separation near the transcription start site. Proceedings of the National Academy of Sciences of the United States of America **107**, 2247–52.

46 Yano, S. T. and Rothman-Denes, L. B. (2011) A phage-encoded inhibitor of *Escherichia coli* DNA replication targets the DNA polymerase clamp loader. Molecular Microbiology **79**, 1325–38.

47 Lopes, A., Amarir-Bouhram, J., Faure, G., Petit, M.-A. and Guerois, R. (2010) Detection of novel recombinases in bacteriophage genomes unveils Rad52, Rad51 and Gp2.5 remote homologs. Nucleic Acids Research **38**, 3952–62.

48 Christie, G. E., Matthews, A. M., King, D. G., Lane, K. D., Olivarez, N. P., Tallent, S. M., Gill, S. R. and Novick, R. P. (2010) The complete genomes of Staphylococcus aureus bacteriophages 80 and 80α--implications for the specificity of SaPI mobilization. Virology **407**, 381–90.

49 Marceau, A. H., Bahng, S., Massoni, S. C., George, N. P., Sandler, S. J., Marians, K. J. and Keck, J. L. (2011) Structure of the SSB-DNA polymerase III interface and its role in DNA replication. The EMBO Journal **30**, 4236–47.

50 Lu, D. and Keck, J. L. (2008) Structural basis of *Escherichia coli* single-stranded DNA-binding protein stimulation of exonuclease I. Proceedings of the National Academy of Sciences of the United States of America **105**, 9169–74.

51 Schekman, R., Weiner, J. H., Weiner, A. and Kornberg, A. (1975) Ten proteins required for conversion of ΦX174 single-stranded DNA to duplex form *in vitro*. Resolution and reconstitution. The Journal of Biological Chemistry **250**, 5859–65.

52 Eisenberg, S., Griffith, J. and Kornberg, A. (1977) ΦX174 cistron A protein is a multifunctional enzyme in DNA replication. Proceedings of the National Academy of Sciences of the United States of America **74**, 3198–202.

53 Dean, F. B., Bullock, P., Murakami, Y., Wobbe, C. R., Weissbach, L. and Hurwitz, J. (1987) Simian virus 40 (SV40) DNA replication: SV40 large T antigen unwinds DNA containing the SV40 origin of replication. Proceedings of the National Academy of Sciences of the United States of America **84**, 16–20.

54 Blanco, L. and Salas, M. (1985) Replication of phage Φ29 DNA with purified terminal protein and DNA polymerase: synthesis of full-length Φ29 DNA. Proceedings of the National Academy of Sciences of the United States of America **82**, 6404–8.

55 Salas, M. (1984) A new mechanism for the initiation of replication of Φ29 and adenovirus DNA: priming by the terminal protein. Current Topics in Microbiology and Immunology **109**, 89–106.

56 Dean, F. B., Nelson, J. R., Giesler, T. L. and Lasken, R. S. (2001) Rapid amplification of plasmid and phage DNA using Φ29 DNA polymerase and multiply-primed rolling circle amplification. Genome Research **11**, 1095–9.

57 Seco, E. M., Zinder, J. C., Manhart, C. M., Lo Piano, A., McHenry, C. S. and Ayora, S. (2013) Bacteriophage SPP1 DNA replication strategies promote viral and disable host replication *in vitro*. Nucleic Acids Research **41**, 1711–21.

CHAPTER 5[*]

Multiple C-terminal tails within a single *E. coli* SSB homotetramer coordinate DNA replication and repair[†]

5.1 ABSTRACT

E. coli single strand DNA binding protein (SSB) plays essential roles in DNA replication, recombination and repair. SSB functions as a homotetramer with each subunit possessing a DNA binding domain (OB-fold) and an intrinsically disordered C-terminus, the last nine amino acids of which provides the site for interaction with at least a dozen other proteins that function in DNA metabolism. To examine how many C-termini are needed for SSB function we engineered covalently linked forms of SSB that possess only one or two C-termini within a four OB-fold "tetramer". Whereas *E. coli* expressing SSB with only two tails can survive, expression of a single tailed SSB is dominant negative. *E. coli* expressing only the two-tailed SSB recovers faster from exposure to DNA damaging agents, but accumulate more mutations. A single tailed SSB shows defects in coupled leading and lagging strand DNA replication and is

[*] My experimental work is the FRET assay presented in Fig. 5.5 of this chapter and described in sections 5.3.10 and in 5.4.6. The remaining experimental work was performed by the co-authors of the corresponding publication that is in preparation (Antony, E., Weiland, E., Yuan, Q., Manhart, C. M., Nguyen, B., McHenry, C. S., and Lohman, T. M. *Multiple C-terminal tails within a single* E. coli *SSB homotetramer coordinate DNA replication and repair*).

[†] The contents of this chapter are in preparation for publication in collaboration with Tim Lohman's lab at Washington University and are presented here with few modifications.

inactive in supporting replication restart *in vitro*. This provides a plausible explanation for the lethality observed *in vivo*.

5.2 INTRODUCTION

Single strand DNA binding (SSB) proteins are essential in all kingdoms of life and function in part by binding to the single stranded (ss) DNA intermediates that form transiently during genome maintenance [1]. SSB proteins both protect the ssDNA and remove secondary structures, such as hairpins, that can inhibit replication, recombination and repair of DNA [2]. In most bacteria, including *E. coli*, SSB protein functions as a homotetramer with each subunit (176 amino acids) possessing two domains: a DNA binding domain containing an oligonucleotide/oligosaccharide binding (OB)-fold (residues 1-112) and an intrinsically disordered C-terminal tail (64 residues) [2–5]. The last nine amino acids of the C-terminal tail (MDFDDDIPF in *E. coli*) contains the site of direct interaction between SSB and more than a dozen other proteins that SSB recruits to their sites of function in DNA replication, repair and recombination [6].

Due in part to its homo-tetrameric nature, *E. coli (Ec)* SSB can bind to long ssDNA in several DNA binding modes. The dominant binding modes observed *in vitro* are referred to as $(SSB)_{65}$, $(SSB)_{55}$ and $(SSB)_{35}$, where the subscript denotes the average number of nucleotides occluded by each SSB tetramer [7–10]. In the $(SSB)_{65}$ mode, favored at high monovalent salt and divalent cation concentrations, ssDNA wraps around all four subunits of the tetramer with a topology resembling that of the seams of a baseball [4,10]. In contrast, in the $(SSB)_{35}$ binding mode, ssDNA is only partially

wrapped around the tetramer, interacting with an average of only two subunits [4,7,10]. The ssDNA binding properties of these two major binding modes differ significantly. In the $(SSB)_{65}$ mode, an SSB tetramer binds with high affinity, but with little cooperativity [11], yet can undergo a random diffusion along ssDNA, a feature that is important for its ability to transiently destabilize DNA hairpins and facilitate RecA filament formation on natural ssDNA [12,13]. The $(SSB)_{35}$ mode, favored at low salt and high protein to DNA ratios, displays extensive positive inter-tetramer cooperativity and thus can form protein clusters or filaments on ssDNA [9,11,14]. Based on these differences, it has been suggested that the $(SSB)_{35}$ binding mode may function in DNA replication, whereas the $(SSB)_{65}$ binding mode might mediate DNA repair and/or recombination [1,3,15].

In eukaryotes, the hetero-trimeric Replication Protein A (RPA) is the SSB analog that functions in genomic DNA replication [16]. However, eukaryotes also encode a homo-tetrameric mitochondrial SSB protein with a DNA binding core that is structurally similar to *E. coli* SSB, but does not possess the unstructured C-termini of bacterial SSB [17–19]. Organelle-specific homotetrameric SSB proteins are also found in eukaryotic parasites such as *Plasmodium falciparum* (*Pf*) and *Toxoplasma gondii (Tg)* and localize to the apicoplast where they presumably function in apicoplast DNA maintenance [20–22]. Although both *Pf*-SSB and *Tg*-SSB proteins also possess C-terminal tails, the sequences of these tails differ considerably from those of bacterial SSB proteins.

DNA replication is a complex process mediated by a replisome containing multiple proteins and enzymes [23] and SSB is a central component of these complexes. The DNA polymerase III holoenzyme (Pol III HE) consists of a DNA Pol III core (α-ε-θ), the multi-subunit DnaX complex clamp loader (τ, γ, δ, δ', χ and ψ subunits) and the β

clamp, a processivity factor. SSB binds to the $\chi\psi$ complex within the clamp loader [24,25] and has been shown to contribute to processive replication [26,27]. A second interaction with an unknown Pol III HE target, other than χ, contributes to rapid initiation complex formation in a process where DnaX complex chaperones Pol III onto β_2 loaded in the same reaction cycle [28]. Recent studies also show that leading and lagging strand DNA replication is uncoupled when the SSB-χ interaction is lost [29]. The interaction between SSB and χ is critical as mutations in the protein-protein interaction domain in SSB (*ssb-113*) are conditionally lethal [30,31]. Furthermore, stand displacement synthesis catalyzed by the Pol III HE in the absence of helicase is dependent on SSB [32]. SSB may play a role in primer hand-off and the detachment of primase from RNA primers formed on the lagging strand, although aspects of this model have been brought into question [29]. SSB directly interacts with primase (DnaG) [33]. SSB also interacts directly with the PriA protein [24,34] and this interaction is critical to restart of DNA replication at stalled forks and this activity is further enhanced by recruitment of PriB onto DNA [34,35].

*Ec*SSB also binds a variety of DNA repair proteins including RecQ (a DNA helicase) [36,37], RecJ [38] and ExoI nucleases [39], and the recombination mediator RecO [40]. These proteins are involved at various stages in DNA recombination and perturbation of the interaction between SSB and these proteins leads to severe DNA repair defects [6,41]. SSB also interacts with Uracil DNA glycosylase [42], a key component of the base excision repair pathway. Interactions between SSB and two repair specific polymerases, DNA Pol II and Pol V, have also been identified highlighting a role for SSB in translesion DNA synthesis [43,44].

Extremophilic bacteria such as *Thermus aquaticus* and *Deinococcus radiodurans (Dr)* have a dimeric version of SSB [45,46] in which each subunit contains two OB-folds, hence the DNA binding core still possesses four OB-folds and thus is structurally similar to the homotetrameric SSB. In fact, comparisons of the crystal structures and DNA binding properties of the *Dr*-SSB and *Ec*-SSB suggest that they share similar mechanisms of DNA binding and wrapping [45,47–49]. However, one consequence of the dimeric nature of *Dr*-SSB is that it possesses only two C-terminal tails that can mediate protein-protein interactions.

Whether *E. coli* SSB requires all four C-terminal tails for its functions *in vivo* is not known. To investigate this we examined the functional consequences of having an SSB with less than four C-terminal tails. We engineered and characterized SSB variants in which either two or all four OB-folds were covalently linked, thus forming a four OB-fold "tetramer" possessing either only two C-terminal tails (linked SSB dimers (SSB-LD)) or only one C-terminal tail (linked SSB tetramer (SSB-LT)). We find that a single tailed SSB "tetramer" (SSB-LT) is unable to complement wild type SSB and thus cannot carry out one or more essential functions *in vivo*. This single-tailed SSB also shows defects in coupling leading and lagging strand DNA replication and in replication restart *in vitro*. However, a two-tailed SSB "tetramer" (SSB-LD-Drl) is functional *in vivo* and is competent for DNA replication *in vitro*, but it shows defects in DNA repair and consequently *E. coli* accumulates significantly more mutations.

5.3 MATERIALS AND METHODS

5.3.1 Cloning of linked SSBs

The *WT-SSB* gene was cloned into a pET-21a protein expression vector (EMD, Germany) with NdeI and BamHI restriction sites flanking its coding region. Using site-directed mutagenesis (Quikchange kit, Agilent Technologies, CA) we inserted three additional restriction sites before the stop codon of the gene (AgeI, NheI and KpnI). This version of the protein called SSB-S_1 has an additional 6 amino acids (TGASGT) coded by the nucleic acid sequence of the three restriction sites. We then cloned three separate copies of the SSB genes (called SSB-S_2, SSB-S_3 and SSB-S_4) with unique pairs of restriction sites flanking the 5' and 3' regions into a Topo TA vector (Invitrogen, CA). In each of these SSB clones, we removed the stop codons and also included an AgeI restriction site at the 3' end of the coding sequence to be able change the length of the individual linkers if required. SSB_2 has a 5' KpnI site and 3' AgeI, NcoI and ClaI sites. This step added an additional 6 amino acids (TGPWID) before the stop codon. SSB_3 has a 5' ClaI and 3' AgeI, AatII and AvrII restriction sites and results in the addition of 6 amino acids (TGRPVD) after the third SSB subunit. SSB_4 was amplified using 5' AvrII and 3' BamHI sites. To generate the SSB-LD construct, we cut the SSB_2-Topo plasmid with KpnI and BamHI and inserted it into the SSB_1-pET21a vector followed by insertion of a stop codon at the end of the C-terminus using site-directed mutagenesis. Hence the C-terminus of the corresponding SSB-LD protein has the correct sequence at its C-terminus (MDFDDDIPF) required for binding of the SSB interacting proteins (SIPs).

Similarly, the SSB-LT construct was generated by splicing together the SSB-S_1, SSB-S_2, SSB-S_3 and SSB-S_4 fragments. To generate the SSB-LD-DrI construct, we designed a linker based on the sequence of *Deinococcus radiodurans* SSB protein (QLGTQPELIQDAGGGVRMSGA). Using a primer that carried the coding sequence for these residues, we PCR amplified the SSB-S_1 clone to end at position 112 followed by this linker sequence. The resulting product was pasted before the SSB-S_2 gene yielding the SSB-LD-DrI construct. To Generate the SSB-LT-DrI construct, we PCR amplified the SSB-LD-DrI sequence with flanking BamHI sites and pasted it onto to the end of the SSB-LD-DrI gene, followed by removal of the internal STOP codon. The individual deletion constructs were generated using site-directed mutagenesis. For the deletions in the linked dimers, we first generated the deletions in the appropriate individual Topo-vector clones and inserted the resulting deletions into the appropriate sections of the SSB-LD-pET21a plasmid. Plasmids for the *in vivo* bumping experiments were generated by cloning the entire *E. coli* SOS promoter region that controls the expression of the *SSB* and *UvrA* genes [50] and in front of the 5' ATG of the appropriate SSB coding sequence using flanking NdeI restriction sites. All the clones were confirmed by sequencing.

5.3.2 Protein purification

The SSB-WT, SSB-S1 and deletion constructs were purified using a protocol previously described for WT-SSB (Bujalowski and Lohman, 1991; Lohman, 1986) and all the buffers included a 1x final concentration of the protease inhibitor cocktail (Sigma,

MO). The linked SSBs were purified using a slightly modified procedure as described in the supplemental materials. DNA replication β_2 [51], $DnaB_6$ [52], and DnaG [53] were purified as described. DNA Polymerase III* (Pol $III_3\tau_2\gamma\delta\delta'\chi\psi$) was purified as described [54] from overexpressing cells that contained a plasmid bearing an artificial operon containing all of the Pol III* subunit genes. Primosomal proteins PriA, $PriB_2$, $DnaT_3$, and DnaC were obtained using a published strategy [52] with modifications (Yuan and McHenry; in preparation for publication).

5.3.3 DNA

The oligodeoxynucleotides, $(dT)_{35}$ and $(dT)_{70}$, were synthesized and purified as described [14]. Poly(dT) was purchased from Midland Certified Reagent Co, (Midland, TX) and dialyzed extensively against buffer using a 3500 Da molecular weight cut-off dialysis membrane (Spectrum Inc., Houston, TX). All ssDNA concentrations were determined spectrophotometrically using the extinction coefficient ε_{260} = 8.1 x 10^3 M^{-1} (nucleotide) cm^{-1} for oligo(dT) and poly(dT) (Kowalczykowski et al., 1981). Mini-circle DNA templates were 409-nucleotide duplex circles with a 396-nucleotide single-stranded tail that served as the initial lagging strand template [55]. The leading and lagging strands had a 50:1 asymmetric G:C distribution, allowing quantification of leading and lagging strand synthesis by ^{32}P-dCTP and dGTP incorporation, respectively. DNA was prepared as described [55] with modifications (Yuan and McHenry; unpublished).

5.3.4 Analytical Sedimentation

Sedimentation velocity and equilibrium experiments were performed using an Optima XL-A analytical ultracentrifuge equipped with an An50Ti rotor (Beckman Coulter, Fullerton, CA) at 25 ˚C. For sedimentation velocity experiments, we measured the sedimentation properties of 1 μM SSB (4-OB folds) in 30 mM Tris-Cl, pH 8.0, 10 % glycerol, 0.2 M NaCl and 1 mM EDTA. 380 μl of the sample and 392 μl of the buffer were loaded into their appropriate sectors of an Epon charcoal-filled two-sector centerpiece and centrifuged at 42000 rpm (25 °C) while the absorbance was monitored at 280 nm. The continuous sedimentation coefficient *c(s)* was calculated using the program SEDFIT [56,57]. For sedimentation equilibrium experiments, 120 μL of protein solution was loaded into each of the three channels of an Epon charcoal-filled six-channel centerpiece with 130 μl of buffer in each reference channels. Protein concentration was monitored by absorbance at 280 nm (SSB-LD-Drl) and 230 nm (SSB-LT-Drl) at three different protein concentrations ([SSB-LD-Drl] = 3.6 μM, 2.3 μM and 1 μM; [SSB-LT-Drl] = 2.2 μM, 1.2 μM and 0.6 μM). Data were collected with a spacing of 0.001 cm with an average of ten scans per step at three rotor speeds: 9500, 11500, 14000 and 17000 rpm. At each speed sedimentation equilibrium was determined when successive scans measured over a 2 hour time window were superimposable. Data sets were edited and extracted using SEDFIT [56,57] followed by analysis by nonlinear least squares (NLLS) using the program SEDPHAT [58]. Apparent molecular weights were obtained by fitting the data to eq 1:

$$A_T = \sum_{i=1}^{n} \exp(\ln A_{0,i} + \sigma_i (r^2 - r_{ref}^2)/2) + b \qquad (1)$$

where A_T is the total absorbance at radial position r, $A_{0,i}$ is the absorbance of component i at the reference radial position (r_{ref}), b is the baseline offset, $\sigma_i = [M_i(1-\bar{\vartheta}_i\rho)\omega^2]/RT$, M_i and $\bar{\vartheta}_i$ are the molecular mass and partial specific volume of component i, respectively (calculated using SEDENTREP). For *Pf*-SSB the $\bar{\vartheta}_i$ value (0.7191 mL g^{-1} at 25 ºC) was calculated based on its amino acid composition (residues 77-284). The solution density ρ for buffer $H^{0.1M}$ was 1.0026 (calculated using SEDENTREP). ω is the angular velocity, R is the ideal gas constant and T is the absolute temperature. A global NLLS fit to eq 1 of the nine absorbance files was used to calculate the molecular weight.

5.3.5 Fluorescence titrations

Equilibrium binding of SSB to oligodeoxynucleotides Poly (dT) and $(dT)_L$, was performed by monitoring the quenching of intrinsic SSB tryptophan fluorescence upon addition of DNA (PTI-QM-2000 spectrofluorimeter, PTI Inc., Lawrenceville, NJ) [λ_{ex} = 296 nm (2 nm band-pass), and λ_{em} = 345 nm (2-5 nm band-pass)] with corrections applied as described [14,59]. Experiments were carried out at 25 ˚C in Buffer T: 10 mM Tris-Cl, pH 8.1, 0.1 mM EDTA and [NaCl] varied as noted in the text.

5.3.6 Wrapping Experiment

Wrapping of ssDNA around the SSB tetramer was measured on a deoxyoligonucleotide 65 nt in length with a Cy5.5 fluorophore at the 5´ end and a Cy3 fluorophore at the 3'-end. 50 nM of the DNA was incubated with increasing [SSB] and the enhancement of Cy5.5 fluorescence was monitored at 700 nm by exciting the Cy3 probe at 515 nm. These experiments were perfomred at 25 ˚C.

5.3.7 In Vivo *Bumping Experiments*

Bumping experiments were performed as described previously [60]. *RPD317* is a strain where the chromosomal *SSB* gene has been deleted, but the strains survive using a copy of the *SSB* gene on a helper plasmid with a Tet^r cassette. We transformed these cells with our test-SSB containing plasmid carrying the Amp^r cassette. We selected transformants that grew on the LB agar plates with ampicillin (Amp, 100 µg/ml) and kanamycin (Kan, 50 µg/ml) and passaged them six times in 5 ml LB media containing Amp+Kan. For each passage the cells were grown overnight for 16 hours at 37 ˚C with shaking at 250 rpm. After the final passage, the cells were diluted 1:1000 and plated onto LB agar containing either Kan+Amp or Kan+Tet (34 g/ml tetracycline). Strains that can complement loss of *SSB-WT* grew only on the plates with Amp+Kan whereas those that did not complement grew on plates with either Kan+Amp or Kan+Tet because they could not bump the functional version of the SSB-WT protein.

5.3.8 In Vitro *Single-stranded Replication Assays*

0.8 μM SSB_4 was incubated with 2.3 nM M13Gori ssDNA annealed with a 30 nt primer, 15 nM β_2, and 2 nM Pol III* in the presence of 0.1 mM ATP, 18 μM [^{3}H] dTTP (100 cpm/pmol total nucleotide), 48 μM dATP, 48 μM dGTP, and 48 μM dCTP at 30 °C for indicated time periods . The single-stranded DNA replication buffer contains 10 mM magnesium acetate, 200 mM NaCl, 50 mM Hepes (pH 7.5), 100 mM potassium glutamate, 20 % glycerol, 200 μg/ml bovine serum albumin, 0.02% Nonidet P-40, and 10 mM dithiothreitol. Reactions were quenched, and products were quantified by scintillation counting as previously described [32].

5.3.9 In Vitro *Rolling Circle Replication Assays*

20 nM mini-circle DNA template, the designated level of SSB_4, 100 nM β_2, 12 nM $DnaB_6$, 100 nM DnaG, 2.5 nM Pol III*, 160 nM PriA, 50 nM $PriB_2$, 333 nM $DnaT_3$, and 108 nM DnaC were incubated with 5 μM ATPγS, 200 μM CTP, 200 μM UTP, and 200 μM GTP for 5 min at 30 °C. The reaction buffer was the same as in the single-stranded replication assay except 50 or 25 mM NaCl (contributed by 0.8 μM or 0.4 μM SSB_4, respectively) was used instead of 200 mM. 1 mM ATP and 100 μM dNTPs were added to start the reaction. After 3 min, [α-^{32}P] dCTP or dGTP were added to allow quantification of leading and lagging strand synthesis, respectively. The reaction was quenched with an equal volume of stop mix (40 mM Tris-HCl (pH 8.0), 0.2% SDS, 100 mM EDTA, and 50 μg/ml proteinase K) after 5 min. DNA product was quantified as in

the single-stranded replication assays [32]. For the analysis of the size of lagging strand products, samples were mixed with 30 mM NaOH, 2 mM EDTA, 2% glycerol, and 0.02% bromophenol blue and fractionated on 0.6% alkaline agarose gels for approximately 18 h at 24 V in a running buffer of 30 mM NaOH and 2 mM EDTA. Gels were fixed in 8% (w/v) trichloroacetic acid, dried onto DEAE paper, autoradiographed on storage phosphor screens, and scanned with a PhosphorImager. The lengths of Okazaki fragment (L) were determined by a method that removed the bias of more radioactivity being incorporated into longer products using $L = \sum(L_i \bullet n_i) / \sum n_i$. n_i is the relative molar amount of the Okazaki fragments with a certain length L_i. $n_i = density_i / L_i$, where $density_i$ is the pixel density at L_i in a lane determined using ImageQuant. Thus, $L = \sum density_i / \sum(density_i / length_i)$.

5.3.10 FRET Replication Restart Assay

This assay was conducted as previously described (Chapter 3): 20 nM substrate constructed from FT_{90}, QT_{90}, and P_{10g} (defined in Chapter 3) was combined with 100 nM trap oligo (45-mer complimentary to duplex region of FT_{90}), 200 nM streptavidin, and protein components in a buffer containing 50 mM Hepes (pH 7.5), 10 mM magnesium acetate, 10 mM dithiothreitol, 20% (v/v) glycerol, 0.02% (v/v) Nonidet-P40 detergent, 200 μg/mL bovine serum albumin, 100 mM potassium glutamate, and 10 mM ATP in a round-bottomed black 96-well plate in a final volume of 50 μL. Samples were incubated at 30 °C for 15 min. Fluorescence emission was detected at 535 nm using an Envision plate reader with an excitation of 485 nm. Using concentrations of un-annealed

fluorescent leading strand template that are in the linear range of the assay, fluorescent units were converted to molarity using a standard curve.

5.3.11 DNA damage experiments

Effect of HU and HN2: A 5 ml culture of *RDP317* cells with either *SSB-WT* or *SSB-LD-Drl* under the control of the native SSB promoter was grown to an OD_{600} of 0.2 in the presence of 50 µg/ml kanamycin and 100 µg/ml ampicillin. HU was added to the cultures (final concentration 100 mM) and grown for an additional 5 hours at 37 ˚C. The cells were harvested and washed five times with 5 ml of ice-cold PBS. After the final wash, the cells were resuspended in 10 ml of 1X PBS and five serial dilutions were generated. 4 µl from each dilution in the series were plated onto LB and grown overnight at 37 ˚C. To quantitate the effect of nitrogen mustard (HN2), cells carrying either the wt-SSB or SSB-LD-Drl genes were grown as for the HU experiment and 2 mM HN2 (final concentration) was added to the cells when the OD_{600} reached 0.5. The cells were grown for another hour at 37 ˚C and 1 ml of this culture was directly diluted into 10 ml of M9 media. Serial dilutions were generated and immediately plated onto LB agar media containing 100 µg/ml of ampicillin and 50 µg/ml of kanamycin.

UV Sensitivity: *RDP317* cells with either *SSB-WT* or *SSB-LD-Drl* under the control of native SSB promoter were grown overnight and 5 serially dilutions of these cells were made and 4 µl of the dilutions were spotted on a LB plate carrying 50 µg/ml Kanamycin. The plates were dried for 30 min at 37 ˚C and exposed to UV.

5.3.12 RecA Western Blot

RDP317 cells with either *SSB-WT* or *SSB-LD-Drl* under the control of native SSB promoter were grown to an OD_{600} of 0.5 in the presence of both 100 µg/ml ampicillin and 50 µg/ml kanamycin. Nalidixic acid was added to the cultures (final concentration was 100 µg/ml) followed by growth at 37 ˚C. 1 ml of the sample was removed at the appropriate time intervals (30, 60, 90 and 120 min), spun down using a table top centrifuge and the cells were washed three times with 1.5 ml of ice cold phosphate buffered saline. 50 µg of the total cell lysate collected at each time point were resolved on a 10% SDS-PAGE gel followed by western blotting. We used an 1:15000 ration of the anti-RecA antibody (MD-03-3; MBL Corp. MA, USA) and detected the levels of RecA using chemiluminiscence.

5.3.13 Rifampicin resistance

To measure the rate of spontaneous mutagenesis of the RDP317 cells carrying either the wt-SSB or the SSB-LD-Drl genes, overnight cultures of these cells were grown in the presence of 100 µg/ml ampicillin and 50 µg/ml kanamycin. The cultures were then plated onto LB agar media and 20 colonies were picked for each strain and 5 ml cultures for each colony were grown overnight at 37 ˚C. The cultures were then plated onto LB agar media containing 10 µg/ml rifampicin (Sigma, MO, USA). The plates were incubated overnight at 37˚C and the numbers of colonies were counted.

Thee experiment was repeated three times and the mutagenesis of 20 individual colonies were screened during each trial.

5.3.14 Growth Curves

To measure the growth kinetics of RDP317 cells carrying either the wt-SSB or SSB-LD-Drl genes, we selected 8 colonies for each plate and either grew and overnight culture or to an OD_{600} of 0.6. We diluted 1 µl from each of these starting conditions to 1 ml of fresh LB with 100 µg/ml ampicillin and 50 µg/ml of kanamycin. 200 µl of this diluted culture was added into a 96-well Greiner cell culture plate (USA Scientific, Cat # 655180) and the cells grown in a Tecan infinite M200 pro plate reader (Tecan Systems, CA, USA) with constant shaking at 250 rpm. The OD_{600} was measured every 10 minutes and plotted versus time to generate the growth curves.

5.4 RESULTS

5.4.1 Design of covalently linked SSB subunits with two or one C-termini per four OB-folds

A wild type *Ec*-SSB tetramer contains four-OB folds and four C-termini. To probe the functionality of the four C-terminal tails we engineered a set of covalently-linked-SSB proteins that maintain the four OB-folds, but possess either only one or two C-termini. Our first attempt was to clone two or four *ssb* genes in tandem and remove the

appropriate stop codons, generating SSB-Linked-Dimers (SSB-LD) and SSB-Linked-Tetramers (SSB-LT), respectively (Fig. A4.1). In these constructs, the amino acid linker between two covalently linked OB-folds consisted of the full length wild type C-terminal tail linked directly to the N-terminus of the next OB-fold. We were able to express and purify these recombinant proteins. However, unlike the WT SSB protein that is a monodisperse homo-tetramer in solution [3] both the SSB-LD and SSB-LT proteins formed a mixture of higher order oligomers in solution (Fig. A4.2A). Sedimentation velocity analysis of the purified proteins showed multiple broad peaks whose apparent molecular weights corresponded to complexes containing 4-OB folds, 8-OB folds, 12-OB folds and higher (Fig. A4.2A) suggesting the formation of species in which two or more OB-folds that are covalently linked could be shared to form higher order non-covalent complexes. Even though both the SSB-LD and SSB-LT proteins can bind tightly to ssDNA (Fig. A4.2B), we modified the length and composition of the amino acid linkers between the subunits in an attempt to prevent the formation of these higher order oligomers.

The SSB protein encoded by *D. radiodurans* (*Dr*) is a homodimer with each subunit containing two-OB-folds connected by a 23 amino acid linker with the sequence: QLGTQPELIQDAGGGVRMSGAGT [45]. Since this is a naturally occurring linker, and because the DNA binding domains of *Ec*-SSB and *Dr*-SSB are structurally similar, we used this linker to connect the *Ec-SSB* subunits and generated linked dimer (SSB-LD-Drl) and linked tetramer (SSB-LT-Drl) constructs (Fig. 5.1). Upon expression and purification (Fig. 5.2A), we found that more than 70-80% of these proteins were single tetramers and after fractionation over a S200 size exclusion column, we were able to

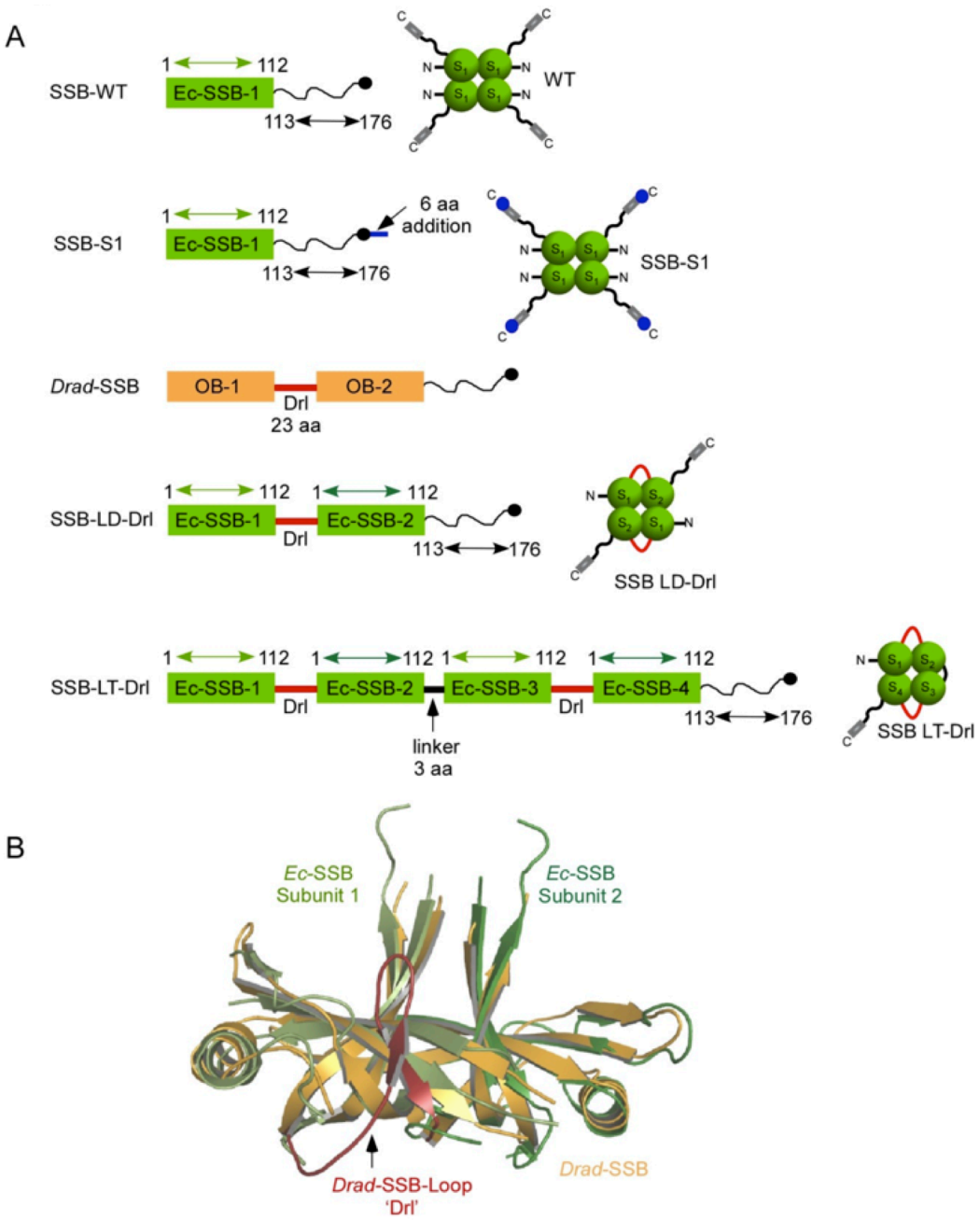

FIGURE 5.1
Design of linked SSB tetramers. (A) Schematic of the linker design used to generate the linked SSB dimer (SSB-LD-Drl) and the linked SSB tetramer (SSB-LT-Drl) resulting in two and one C-terminal tail per 4-OB folds respectively. (B) Superimposition of the Dr-SSB protein with two OB-folds in a single subunit and two subunits of the Ec-SSB protein with one OB-fold per subunit. The linker observed between the two OB-folds in the Dr-SSB protein is shown in red and is the linker used to design the SSB-LD –Drl and SSB-LT-Drl proteins.

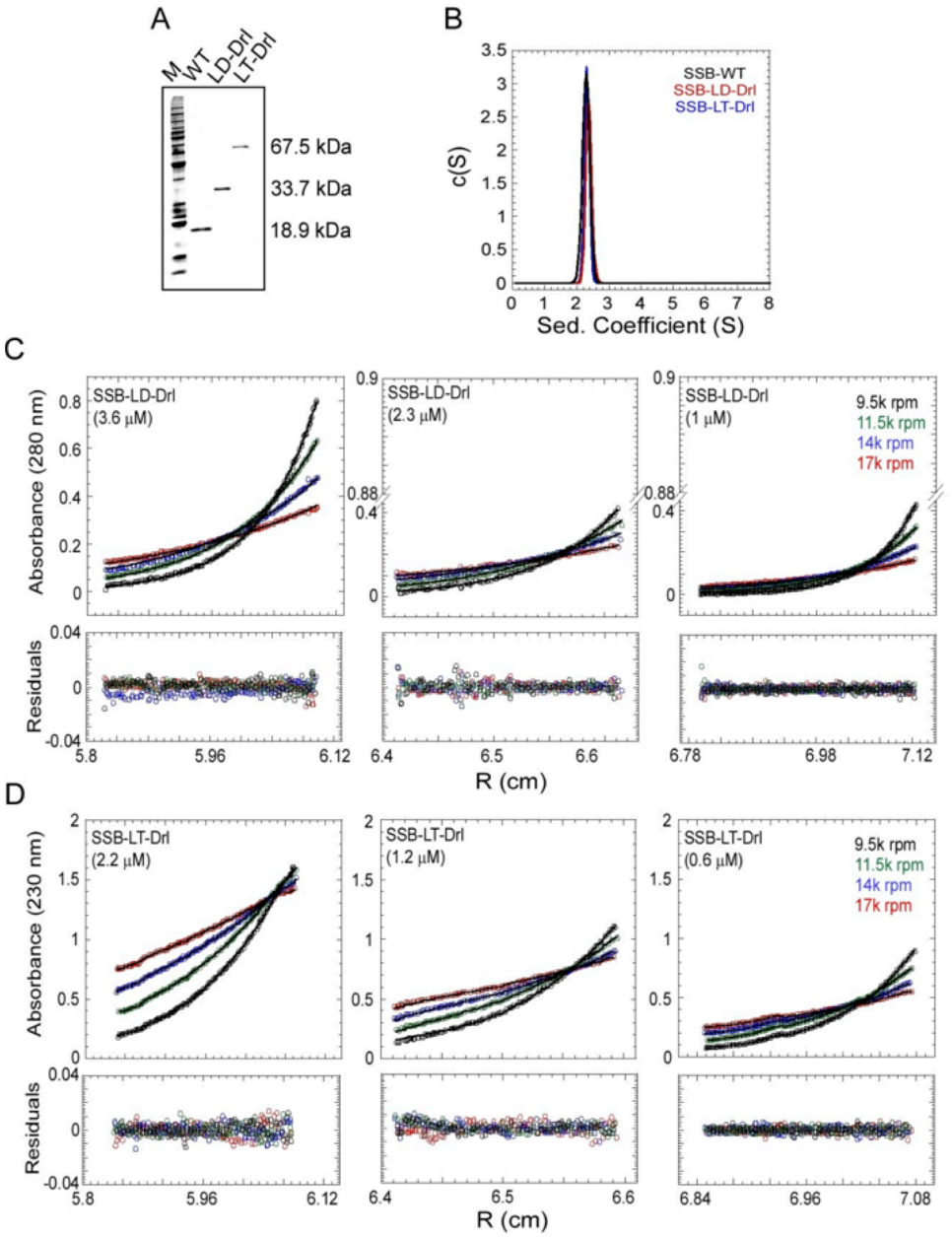

FIGURE 5.2
(A) SDS-PAGE analysis of recombinantly purified WT, SSB-LD-DrI and SSB-LT-DrI proteins. (B) Sedimentation velocity analysis of SSB-WT, SSB-LD-DrI andSSB-LT-DrI proteins at 42000 rpm show the presence of a single species in solution for all three proteins. The SSB-LD-DrI (C) and SSB-LT-DrI (D) proteins sediment as tetramers in equilirium centrifugation experiments with molecular weights corresponding to a single tetramer with 4-OB folds (LD-DrI: 65380 Da and LT-DrI: 61629 Da). The experiments were done using three different protein concentrations (as noted) and at four rotor speeds (9500, 11500, 14000 and 17000 rpm). These experiments were perfomred at 25 ˚C in buffer containing 30 mM Tris-Cl, pH 8.0, 10 % glycerol, 0.2 M NaCl and 1 mM EDTA.

obtain stable tetrameric versions of both the SSB-LD-Drl and SSB-LT-Drl proteins. This is further supported by sedimentation velocity experiments where both the SSB-LD-Drl and SSB-LT-Drl proteins form single species with apparent molecular weights consistent with the presence of four-OB folds in each construct (Fig. 5.2B). This was confirmed using sedimentation equilibrium analysis revealing a single oligomeric species for both proteins with average molecular masses of M_r = 65070 ± 612 Da and M_r = 61626 ± 112 Da for SSB-LD-Drl and SSB-LT-Drl, respectively (Figs. 5.2C & 5.2D). These values agree with the predicted molecular masses of 67343 Da for the SSB-LD-Drl (4-OB folds + 2 C-tails) and 61266 Da for the SSB-LT-Drl (4-OB folds + 1 C-tail) based on their amino acid sequences.

5.4.2 DNA binding properties of covalently linked SSB proteins

We next examined the ssDNA binding properties of the linked SSB proteins. WT SSB binds tightly to ssDNA and can bind in a number of distinct DNA binding modes *in vitro*, depending on solution conditions, especially salt concentration and type [3]. On poly(dT), three major ssDNA binding modes can form, denoted $(SSB)_{35}$, $(SSB)_{55}$ and $(SSB)_{65}$ modes, where the subscript denotes the average number of nucleotides occluded per tetramer [3,7,10]. We measured the average occluded site sizes for the SSB-LD-Drl and SSB-LT-Drl proteins in Buffer T (10 mM Tris-HCl, pH 8.1 and 0.1 mM EDTA) at 25˚C by monitoring the quenching of the intrinsic SSB tryptophan fluorescence upon binding poly(dT) as a function of [NaCl]. Both SSB-LD-Drl and SSB-LT-Drl can form the same three distinct DNA binding modes, $(SSB)_{35}$, $(SSB)_{55}$ and

$(SSB)_{65}$, that are observed for WT SSB (Fig. 5.3A). However, the transitions between the binding modes shift to higher [NaCl] as the number of C-terminal tails decreases from four to two to one. This effect is consistent with previous observations that showed a shift in the $(SSB)_{35}$ to $(SSB)_{65}$ transition to higher [NaCl] when all four C-terminal tails were removed [62]. These results indicate that the covalently linked SSB proteins are able to bind and wrap ssDNA to form the same complexes as the WT SSB protein, although the relative stabilities of the different modes are slightly affected.

We also compared the ssDNA binding properties of WT SSB, SSB-LD-Drl and SSB-LT-Drl in the same buffer that we used in the DNA replication assays discussed below [50 mM Hepes, pH 7.5, 100 mM NaCl, 10 mM $Mg(CH_3CO_2)_2$, 100 mM potassium glutamate and 20 % (w/v) glycerol] at 25˚C. Under these conditions we measure similar occluded site sizes of 64 ± 3, 59 ± 4 and 58 ± 3 nucleotides on poly(dT) for the WT SSB, SSB-LD-Drl and SSB-LT-Drl proteins (per 4 OB-folds), respectively (Fig. 5.3B). All three proteins also show the same maximum Trp fluorescence quenching. We also examined binding of these proteins to $(dT)_{70}$ by monitoring the quenching of SSB Trp fluorescence. WT SSB, SSB-LD-Drl and SSB-LT-Drl all bind tightly to $(dT)_{70}$ with a stoichiometry of one $(dT)_{70}$ molecule per 4-OB folds with the same Trp fluorescence quenching consistent with DNA interacting with all four OB-folds with similar wrapping (Fig. 5.3C). These results indicate that the number of C-terminal tails does not affect the ability of these SSB proteins to form a fully wrapped ssDNA complex.

To directly measure the extent of ssDNA wrapping around the 4-OB folds, we also examined protein binding to a $(dT)_{65}$ labeled with a fluorescence donor (3´-Cy3) and acceptor (5´-Cy5.5) at either end. As shown previously [62,63] when this ssDNA

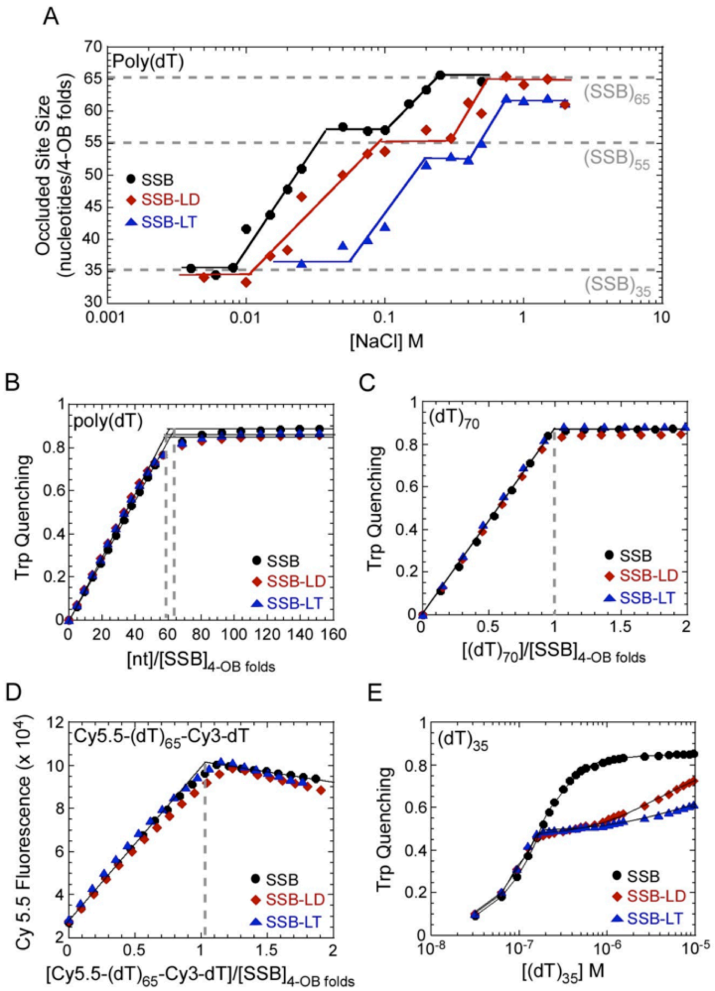

FIGURE 5.3
ssDNA binding properties of linked SSB tetramers. (A) Occluded site-size measurements as a function of increasing [NaCl] for the WT and linked SSB proteins on poly(dT) ssDNA show the presence of three distinct DNA binding modes $(SSB)_{35}$, $(SSB)_{55}$, and $(SSB)_{65}$ for all three proteins. (B) Measurement of occluded site size in replication buffer show that all three proteins bind to ssDNA in the $(SSB)_{65}$ binding mode. (C) Quenching of intrinsic SSB Trp fluorescecene upon binding to a $(dT)_{70}$ oligonucleotide shows that all three proteins bind stoichiometrically. (D) Wrapping of ssDNA around WT and linked SSB proteins measured using a oligonucleotide with Cy5.5 and Cy3 fluorophores positioned at the 5' and 3' ends respectively, and monitoring enhancement of Cy5.5 fluorescence at 700 nm by exciting the Cy3 probe at 515 nm. (E) Binding of $(dT)_{35}$ to WT and linked SSB tetramers show binding of two $(dT)_{35}$ molecules to SSB-WT ($K_1 > 10^{15}$ M^{-1} and $K_2 = 1.60 \pm 0.16 \times 10^7$ M^{-1}) whereas both the LD-Drl and LT-Drl tetramers bind to one $(dT)_{35}$ with high affinity ($K_1 > 10^{15}$ M^{-1} for both LD-Drl and LT-Drl) whereas the second $(dT)_{35}$ binding is weaker ($K_2 = 1.66 \pm 0.71 \times 10^5$ M^{-1} and $2.34 \pm 0.29 \times 10^5$ M^{-1} for LD-Drl and LT-Drl respectively). These experiments were done at 25 ˚C in buffer containing 50 mM Hepes pH 7.5, 10 mM $Mg(OAc)_2$, 100 mM NaCl, 100 mM $KC_5H_8NO_4$, and 20 % glycerol.

forms a fully wrapped 1:1 molar complex with an SSB tetramer to form an $(SSB)_{65}$ complex, the two fluorophores are brought into close proximity yielding a large Fluorescence Resonance Energy Transfer (FRET) signal (monitored as a Cy5.5 fluorescence increase). At higher SSB concentrations, two SSB tetramers can bind per DNA, each in the $(SSB)_{35}$ binding mode, resulting in an increase in the distance between the Cy3 and Cy5.5 fluorophores and thus a decrease in FRET. Fig. 5.3D shows that we observe the highest FRET signal at a stoichiometry of one $(dT)_{65}$ per "tetramer" (4 OB-folds) for all three proteins. Furthermore, upon further titration a decrease in FRET is observed consistent with binding of a second "tetramer" of both the SSB-LD-Drl and SSB-LT-Drl proteins.

Ec-SSB is also able to bind two molecules of $(dT)_{35}$ per tetramer, but with negative cooperativity such that the second molecule of $(dT)_{35}$ binds with lower affinity [64,65]. Fig. 5.3E shows that we observe the same behavior for both the SSB-LD-Drl and SSB-LT-Drl proteins in our DNA replication buffer (50 mM Hepes, pH 7.5, 100 mM NaCl, 10 mM $Mg(OAc)_2$, 20% glycerol and 100 mM $KC_5H_8NO_4$). Since the first $(dT)_{35}$ binds with such high affinity (stoichiometrically), an accurate estimate of the binding constant cannot be obtained, but the second $(dT)_{35}$, binds with lower affinity allowing estimates of the binding constants as $1.66 \pm 0.71 \times 10^5\ M^{-1}$ and $2.34 \pm 0.29 \times 10^5\ M^{-1}$ for the SSB-LD-Drl and SSB-LT-Drl proteins, respectively compared to $1.60 \pm 0.16 \times 10^7\ M^{-1}$ for WT SSB (Fig. 5.3E). The lower affinities for the binding of the second $(dT)_{35}$ for the linked proteins is consistent with the higher stability of the $(SSB)_{35}$ binding mode at higher [NaCl] for these proteins on poly(dT) (Fig. 5.3A). However, all three proteins are able to bind two molecules of $(dT)_{35}$ per 4 OB-folds.

Recent single molecule Forster Resonance Energy Transfer (smFRET) studies have shown that an *Ec*- SSB tetramer is able to diffuse along ssDNA [62] and uses this ability to transiently melt a double stranded DNA hairpin and this activity explains how SSB facilitates formation of a RecA filament on natural ssDNA [12]. The mechanism of hairpin melting appears to be that the SSB can diffuse into and stabilize the transiently formed ssDNA when the hairpin undergoes a transient partial melting due to thermal fluctuations ("breathing") [12]. Using these same approaches we tested whether the covalently linked SSB proteins are also able to diffuse along ssDNA. Cy5.5 and Cy3 fluorophores were incorporated into the base of a hairpin DNA substrate positioned at the end of a $(dT)_{65}$ ssDNA (Fig. A4.3). We excite the Cy3 fluorophore and monitor the change in Cy5.5 fluorescence. As SSB diffuses onto the ssDNA formed by transiently fluctuations (breathing) of the base pairs at the base of the hairpin, a decrease in FRET signal is observed due to an increase in the distance between the fluorophores. Three FRET states are observed for the DNA when bound to WT SSB, SSB-LD-Drl and SSB-LT-Drl proteins. Previous studies [12,13,62] suggest that each FRET state corresponds to roughly 2-3 bp melted in a two-step three-state pathway for SSB diffusion and hairpin melting. We designate the three states as A, B and C; where A and C are the end states depicting low FRET (fully melted) and high FRET (fully base paired) states, respectively, and B denotes the partially melted intermediate state (Fig. A4.3). A schematic of the probable states during the hairpin melting reaction is shown in Fig. A4.3. These data indicate that the reduced number of C-terminal tails does not affect the ability of SSB to diffuse along ssDNA.

5.4.3 An SSB with at least two C-terminal tails is required for E. coli *survival*

We next examined the ability of the covalently linked SSB proteins to function in *E. coli*. We tested whether the SSB-LDI or SSB-LT proteins can functionally complement the loss of WT SSB protein *in vivo* using the "bumping" assay developed by Porter [66]. *E. coli* strain RDP317 lacks a chromosomal copy of the wild type *ssb* gene and thus can survive only if it also carries a plasmid expressing a version of an *ssb* gene that can functionally complement the *wt ssb* gene. We first grew RDP317 cells containing a plasmid expressing the wt *ssb* gene (pEW-WT-*t*) that also contains a tetracycline resistance cassette (tet^R). The *ssb* mutant gene to be tested for functional complementation was then cloned into a second compatible plasmid containing ampicillin resistance (amp^R) (pEW-X-*a*; where 'X' denotes the SSB variant to be tested and '*a*' denotes the resistance to ampicillin; Table A4.1). We cloned each *ssb* gene under control of the natural *ssb* promoter to regulate expression levels of all SSB constructs [67–69]. RDP317 cells containing the pEW-WT-*t* (ssb^+, tet^+) were then co-transformed with the test plasmid (pEW-X-*a*). The transformed cells were then passaged five to six times, screening for cells possessing ampicillin resistance (100 µg/ml Ampicillin). If the test *ssb-x* gene is able to complement wt *ssb*, the plasmid containing the wt *ssb* gene along with its tet^R cassette can be lost (bumped) from RDP317. However, if the test gene is unable to complement wt *ssb*, then the original (ssb^+, tet^+) plasmid will be retained in RDP317. Consequently, if a test *ssb-x* gene complements the wt *ssb* gene, then cells containing the test *ssb-x* gene will possess

only ampicillin resistance, whereas if the test *ssb-x* gene does not complement the wt *ssb* gene, then cells containing the *test ssb-x* gene will be resistant to both ampicillin and tetracycline. Our results indicate that the *ssb-LD-Drl* gene expressing SSB with only two C-tails was able to functionally complement the loss of wt *ssb* gene *in vivo*; however, the *ssb-LT-Drl* showed a dominant negative phenotype (Table 5.1; discussed below).

The last 9 amino acids of the SSB C-tail contains the site of interaction with the more than one dozen SSB interacting proteins (SIPs) and are critical for SSB function as *ssb* genes with deletions of the last 8 amino acids (*ssb-ΔC8*) [70] or that contain an additional 6 amino acid extension (*ssb-S1*) do not complement loss of the wt *ssb* gene (Table 5.1). The genes encoding for covalently linked SSB proteins possessing only two C-tails (*ssb-LD* and *ssb-LD-Drl*) were able to complement the wt *ssb* gene (Table 5.1). To check the integrity of the genes encoding the linked SSB proteins, we amplified the test *ssb-x* gene of interest by PCR after the final passage. Sequencing of the gene showed the expected sequence with no evidence for any recombination. Hence two functional C-terminal tails within an SSB construct containing 4-OB folds are sufficient to support growth. However, both the single C-terminal tailed genes encoding *ssb-LT* and *ssb-LT-Drl* were dominant negative (Table 5.1). We were able to successfully clone these constructs into plasmids in the absence of the native *ssb* promoter (which drives SSB production in *E. coli* cells) but in the presence of a T7 promoter, but multiple parallel attempts to clone them under control of the native SOS promoter were unsuccessful. For both the *ssb-LT* and *ssb-LT-Drl* constructs, only a few colonies appeared after transformation, but in every case (total of 9 colonies from 8 attempts) the genes contained mutations that introduced premature stop codons within the open

Construct	Phenotype
Un-Linked monomers	
WT	Complements
ssb-ΔC8	No Complementation
ssb-S1	No Complementation
SSB-Δ121-167	Complements
SSB-Δ131-167	Complements
SSB-Δ146-167	Complements
SSB-Δ163-167	Complements
Linked Dimers	
SSB-LD	Complements
SSB-LD-Drl	Complements
Linked Tetramers	
SSB-LT	Dominant Negative
SSB-LT-Drl	Dominant Negative

TABLE 5.1

reading frame. These results suggest that an SSB tetramer with one free tail is toxic to *E. coli* when under the control of the SOS promoter and constitutively expressed.

Since the *ssb-LD-drl* gene was able to functionally complement *wt* ssb, we also tested whether the *Dr ssb* gene (which encodes a naturally occurring two C-tail protein in *Deinococcus radiodurans*) can functionally complement *wt SSB*. The C-terminal 9 amino acids of the *Dr*-SSB protein are PPEEDDLPF which is similar to the MDFDDDIPF sequence found in the *Ec*-SSB protein. In fact, we find that *Dr* SSB is able to functionally complement *wt* SSB protein *in vivo*, providing additional evidence that an SSB with only two C-terminal tails is sufficient to allow *E. coli* survival and growth.

5.4.4 SSBs containing fewer than four C-terminal tails exhibit decreased stimulation of the DNA polymerase III holoenzyme on single-stranded templates

SSB supports multiple important functions in *E. coli* DNA replication. We initially examined a simple reaction–the conversion of primed single-stranded DNA to a duplex (Fig. 5.4A). This reaction requires the ability of the Pol III HE to form an ATP-dependent initiation complex on a primer and to processively elongate it approximately 8000 nucleotides. The reaction is independent of SSB under low salt conditions, but becomes partially (~3-4-fold) dependent upon SSB at elevated salt concentrations (200 mM NaCl). We observe full stimulation of the reaction by wild-type SSB and incrementally decreased stimulation by SSB-LD-Drl and SSB-LT-Drl respectively (Fig.

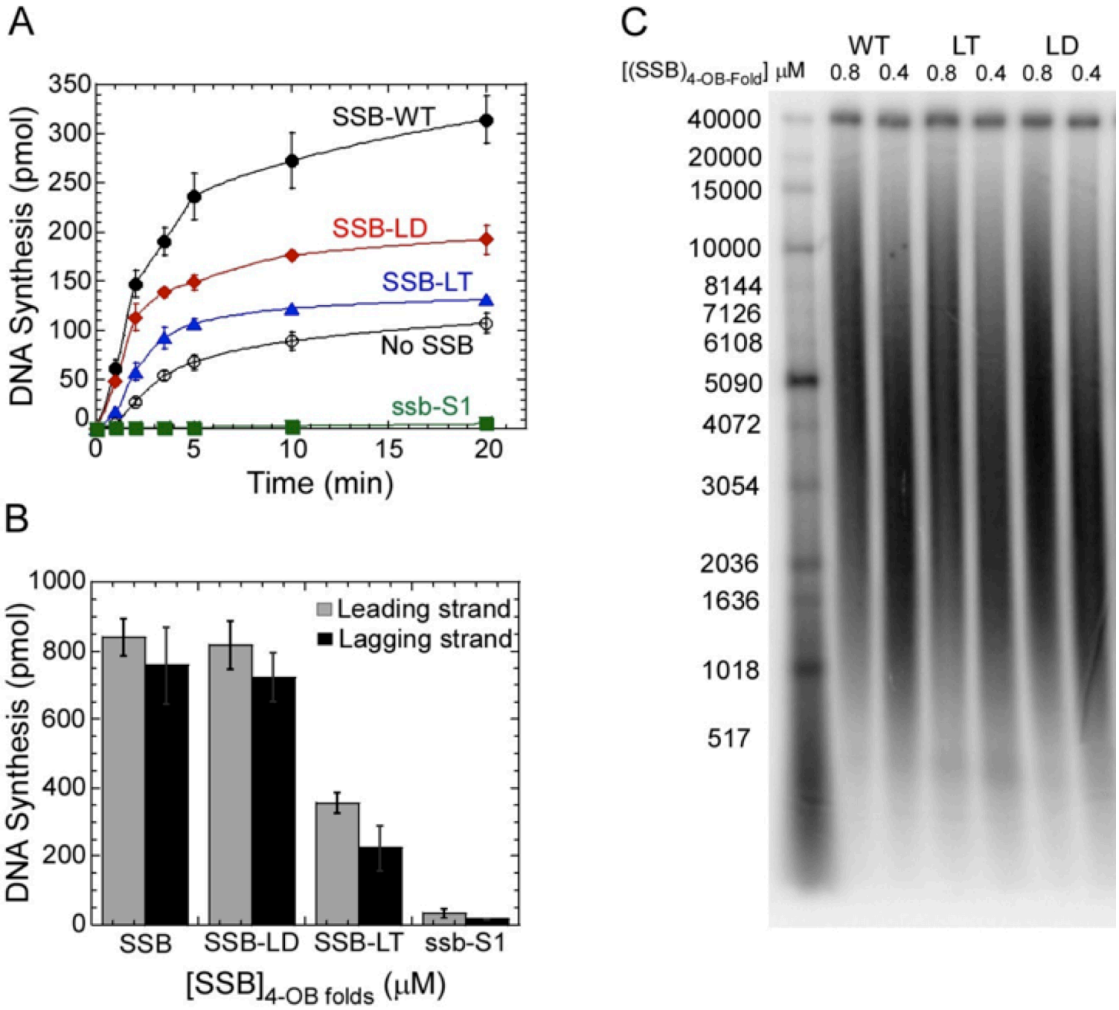

FIGURE 5.4
SSB tetramers with only one C-terminal tail inhibits DNA replication. (A) *In-vitro* single-stranded DNA replication assays were carried out in the presence of indicated SSB derivative. (B) *In-vitro* rolling circle DNA replication assays were carried out in the presence of indicated SSB. (C) The products from the rolling circle replication reactions were fractionated on an alkaline agarose gel and the length of Okazaki fragments were determined. (From left to right: 2775, 2260, 2630, 2145, 2615, and 2145 nt.)

5.4A). The level of DNA synthesis observed in reactions containing one-tailed SSB-LT-Drl is only slightly above that observed in the absence of SSB. SSB-S1 severely inhibits the reaction to baseline values (Fig. 5.4A).

SSB-S1 is a tetramer that possesses four C-terminal tails but contains a 6 amino acid extension after the 9 amino acid SIP interaction motif. Extensions beyond the C-terminal phenylalanine has been shown to block SIP interaction [24]. We have previously observed inhibition of other SSB derivatives that lack portions of the C-terminal tail [32].

5.4.5 SSB containing only one C-terminal tail is defective in supporting rolling circle replicative reactions that mimic chromosomal replication forks

Duplex circles containing a 5'-flap on one strand provide a substrate for reconstitution of replication forks that exhibit the same characteristics of replication forks *in vivo* [71]. Replication is dependent upon restart primosomal proteins (PriA, PriB, DnaT) that direct the assembly of the DnaB helicase in the presence of the DnaC helicase loader and SSB. Once the helicase is loaded on the lagging strand template, it uses its ATP-dependent DNA helicase activity to unwind the duplex DNA at the replication fork, permitting the dimeric Pol III HE (associated with DnaB through an interaction with the τ subunit of Pol III HE [71,72] to follow. Primers are provided on the lagging strand by a reversible interaction between the DnaG primase and DnaB [73].

The lagging strand primers are extended by the lagging strand half of the dimeric Pol III HE in a coupled reaction [74].

We find that SSB-LD-DrI functions equivalently to wt SSB in this system. However, SSB-LT-DrI, containing only one C-terminal tail, exhibits a defect with the level of leading strand synthesis diminished approximately two-fold (Fig. 5.4B). The levels of lagging strand synthesis are decreased further, indicating that the leading and lagging strand reactions frequently become uncoupled.

To determine whether the decrease in lagging strand synthesis relative to leading strand was due to a defect in primer formation, we examined Okazaki fragment length by electrophoresis of labeled lagging strand products in alkaline agarose gels (Fig. 5.4C). We observe the same product length with all three proteins (wt SSB, SSB-LD-DrI and SSB-LT-DrI) suggesting that the replication defect is not associated with formation of primers. Uniform Okazaki fragment length is an indication that primers are synthesized with the same frequency and spacing in the presence of all three SSBs tested [75].

5.4.6 A one-tailed SSB tetramer does not support replication restart

In the rolling circle replication reactions described in the preceding section, the initial PriA-dependent helicase assembly occurred during a five minute pre-incubation of components in the presence of ATPγS. This precluded use of the rolling circle reactions to examine the effect of SSBs with variable numbers of tails on the kinetics of the replication restart reaction. To enable this determination, I used a FRET assay that

monitors PriA- and SSB-dependent helicase assembly on model forks (Chapter 3). Using this assay under conditions where the signal observed is proportional to the length of time the reaction is conducted, I observe a modest decrease when SSB-LD-DrI is substituted for SSB. However, substitution by one-tailed SSB-LT-DrI results in a signal near the baseline determined by use of the inert SSB-S1 derivative (Fig. 5.5B).

5.4.7 **E. coli** *cells harboring the two-tailed SSB tetramer are more resistant to the effects of DNA damage, but accumulate more mutations.*

Since *Ec-SSB* interacts with several SIPs that are involved in DNA repair [36,76,77], we tested whether the number of C-tails associated with a single SSB tetramer has an effect on the ability of cells to recover from DNA damage. *E. coli* cells expressing either SSB-WT or SSB-LD-DrI were grown in the presence of the DNA damaging agents, hydroxyurea (HU), nitrogen mustard ($N(CH_2CH_2Cl)_3$ or HN3), or exposed to UV irradiation. HU is an inhibitor of ribonucleotide reductase and treatment of *E. coli* results in depletion of dNTP pools leading to DNA double strand breaks near replication forks [78,79], whereas HN3 inhibits DNA replication by covalently crosslinking the two DNA strands [80]. Exposure of cells to UV irradiation leads to formation of DNA breaks and UV-sensitivity [81]. To assess the ability of a four tailed versus two-tailed SSB to respond to DNA damage, we grew cells carrying these genes in the presence of either HU (100 mM) or HN3 (2 mM). We then compared the relative ability of the wt SSB or SSB-LD-DrI cells to grow after exposure to these DNA damaging

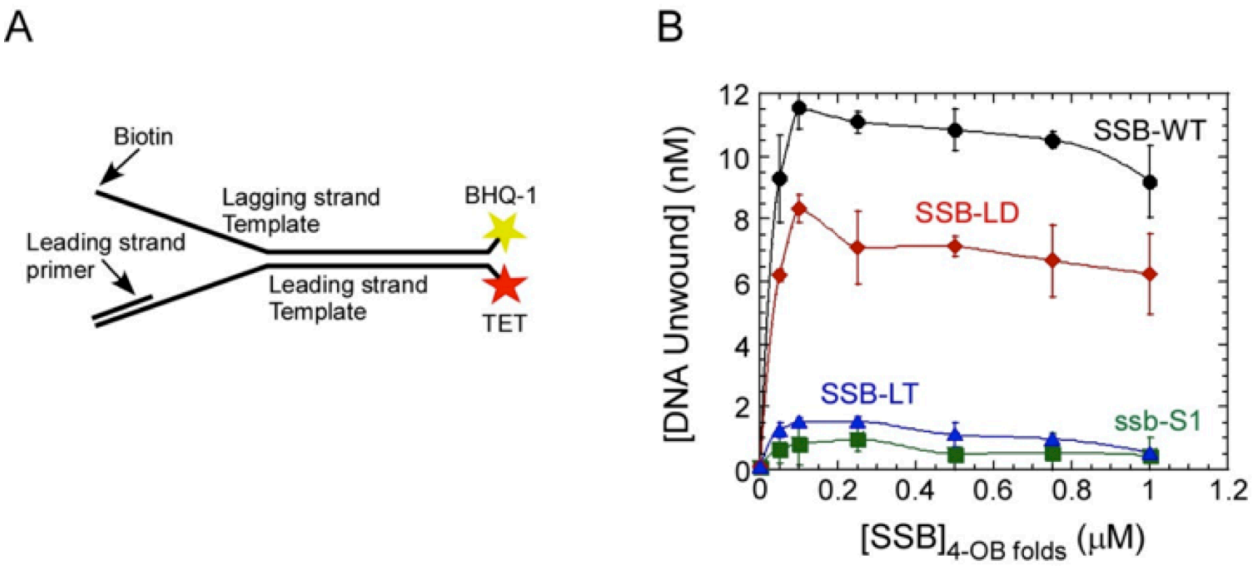

FIGURE 5.5
SSB-LT-DrI does not support PriA-dependent replication restart pathway. (A) DNA substrate used in unwinding reactions. The fluorescence of TET on the 5' terminus increases when separated by helicase action from a quencher (BHQ-1) on the lagging strand template. Streptavidin binding to biotinylated thymidine on the 5'-end of the lagging strand template blocks helicase self-loading by threading over a free 5'-end. There is a 10 nt gap between the 3'-OH of the leading strand primer and the duplex region of the fork. (B) DrI SSB forms titrated individually in triplicate in the presence of 150 nM PriA, 50 nM $PriB_2$, 50 nM $DnaT_3$, 12 nM $DnaB_6$, 50 nM DnaC.

agents. Surprisingly, cells expressing the two-tailed SSB-LD-DrI recover faster from exposure to both DNA damaging agents as indicated by better cell growth observed across the serial dilutions (Fig. 5.6A & B).

To test the ability of the RDP317 cells carrying either the wt *ssb* or *ssb-LD-DrI* genes to recover from UV induced damage, we grew overnight cultures, plated serial dilutions of these cells and exposed them to varying levels of UV irradiation. *E. coli* cells expressing either WT-SSB or SSB-LD-DrI display comparable sensitivities to low levels of UV irradiation (0 – 25 J/m^2) as indicated by the growth of the colonies across the serial dilutions (Fig. 5.6C). However, after exposure to higher UV levels (150 J/m^2), the cells expressing SSB-LD-DrI show a slight recovery, compared to the failure of cells expressing wt SSB to recover from these high UV doses (Fig. 5.6D). Since one of the major proteins expressed in response to DNA damage is RecA, we hypothesized that the ability of the cells expressing SSB-LD-DrI to better recover from the effects of DNA damage might be due to expression of higher levels of RecA. To test this, we treated cells with the DNA damaging agent Nalidixic acid and quantified the expression levels of RecA using an anti-RecA antibody. However, Western blots (Fig. 5.6E) show a similar level of induction of RecA protein in the presence of nalidixic acid for cells expressing either wt SSB or SSB-LD-DrI.

Another possible explanation for the faster recovery of the SSB-LD-DrI cells after DNA damage is that the DNA lesions are not repaired but bypassed. If this were the case, then an elevated rate of mutagenesis should occur in these cells. We thus compared the rate of mutagenesis in *E. coli* expressing wt SSB or SSB-LD-DrI using the

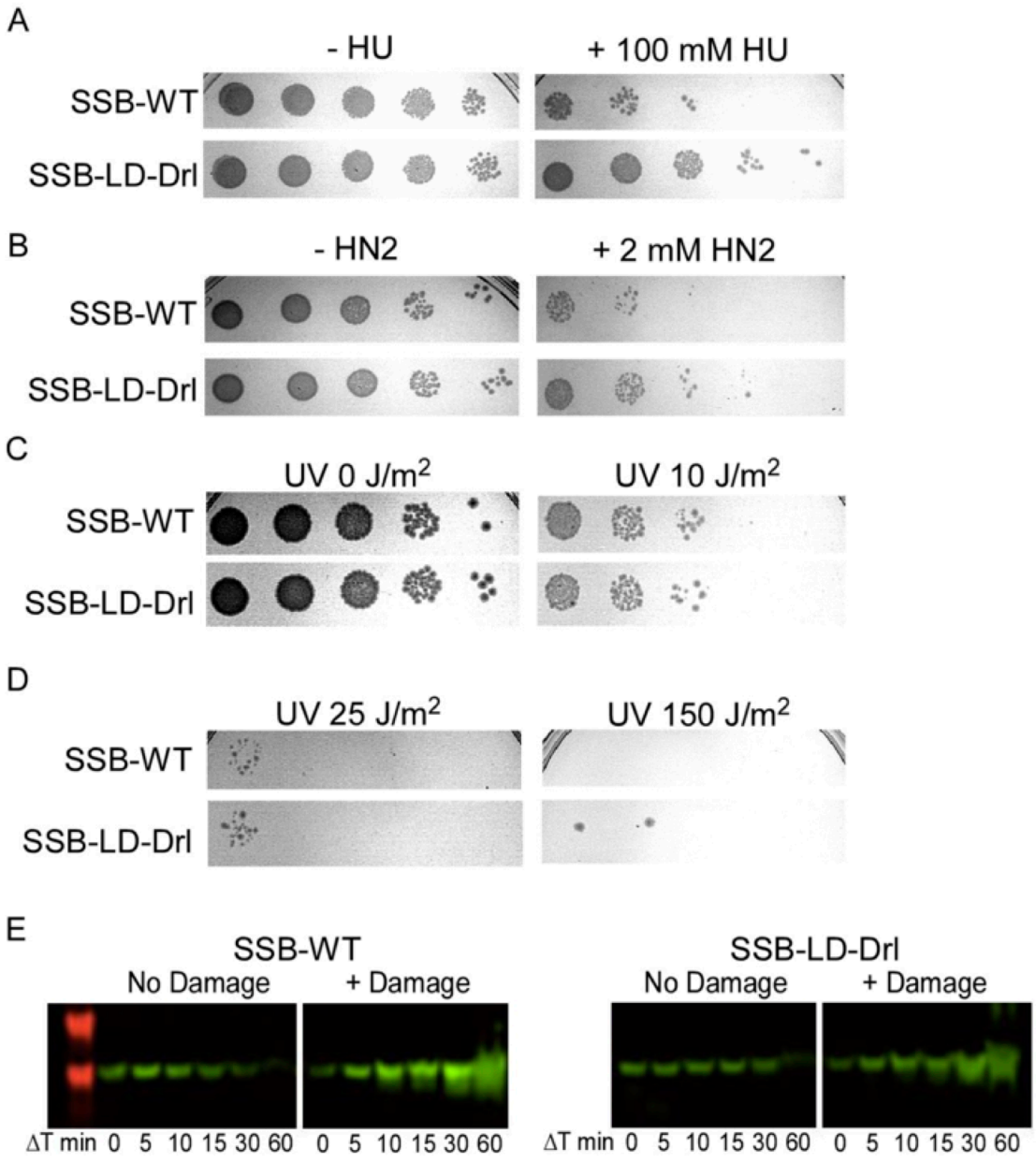

FIGURE 5.6
In vivo repair capabilities of *E.coli* strains carrying *SSB-WT* or *SSB-LD-Drl* genes. Serial dilututions of cells in the absence or presence of 100 mM hydroxyurea (A) or 2 mM nitrogen mustard (B). Cells harboring the SSB-LD-Drl gene recover better compared to the WT cells in the presence of the either DNA damaging agent. Both strains are resistant to DNA damage by 0.02 % MMS (C) and tolerate lower levels of UV to similar extents (D). However at a higher dose of UV (E), only the cells carrying the SSB-LD-Drl gene is able to grow. F) Western blot detection of RecA levels in the absence or presence of 100 mM Nalidixic acid. Both strains are capable of inducing RecA expression in the presence of DNA damage.

Rifampicin resistance assay [82]. *E. coli* grown in the presence of Rifampicin can survive through spontaneous mutations in the rifampicin binding site on the β subunit of RNA polymerase. We observe a 30-fold increase in the number of *Rif*^{r} colonies in the SSB-LD-DrI cells compared to the wt SSB cells (Fig. 5.7A). These results suggest that the better recovery from the effects of the DNA damaging agents are due to a lower level of DNA repair of mutations in cells expressing SSB-LD-DrI. Repair of mutations after DNA damage results in slower cell growth [83]. Since cells expressing SSB-LD-DrI are deficient in repairing mutations, we would expect these cells to display faster growth kinetics. The data in Fig. 5.7 (panels B and C) show this to be the case as cells expressing SSB-LD-DrI enter the exponential growth phase significantly faster than cells expressing wt SSB. When cell growth is initiated from overnight cultures, cells expressing SSB-LD-DrI reach mid-log stage about 70 min faster than cells expressing wt SSB (Fig. 5.7B). When cell growth is initiated from cells in log-phase, the SSB-LD-DrI cells reach mid-log about 120 min faster than the wt SSB cells (Fig. 5.7C). These results support the conclusion that the SSB-LD-DrI protein with two C-tails per tetramer shows defects in DNA repair, but is able to support DNA replication.

5.5 DISCUSSION

The ability of *Ec-SSB* to bind more than a dozen proteins (SIPs) via its unstructured C-terminal tails indicates the importance of SSB as a recruitment platform during DNA replication, repair and recombination. Each SSB homotetramer has four

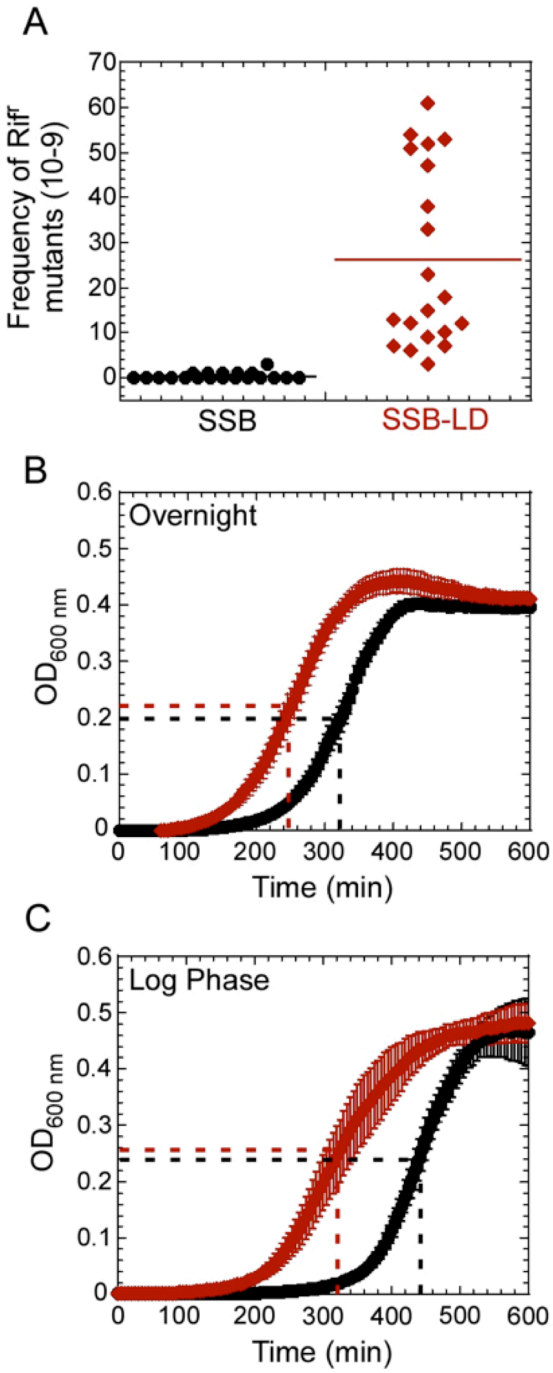

FIGURE 5.7
Growth characteristics of *E.coli* cells carrying either four or two tailed SSB tetramers. A) Rifampicin resistance assay showing the frequency of mutations in strains carrying the SSB-WT or the SSB-LD-Drl genes. Growth analysis of *E.coli* cells with the SSB-WT gene or SSB-LD-Drl gene shows faster recovery of the two tailed SSB strain when the cultures are started from a overnight passage (B) or from a log phase starter culture (C).

potential SIP binding sites. Reducing the number of C-terminal tails associated with each tetramer has deleterious effects on many of SSB's biological functions.

E. coli cells that express SSB containing four OB-folds but two C-terminal tails (SSB-LD-Drl or *Drad* SSB) are viable. *E. coli* is unable to survive when only one C-terminal tail (SSB-LT-Drl) is present. In an attempt to reconcile the lethal dominant negative phenotype of *ssb*-LT-*Drl* with *in vitro* biochemical observations, we examined the consequence of substituting SSB with the SSB-LD-Drl and SSB-LT-Drl derivatives in DNA replication assays. In a relatively simple assay where the processive activity of Pol III HE is required for efficient conversion of an 8000 nt single-stranded circle to a duplex, we observed a decrease in the ability of the SSB derivatives with one or two tails to stimulate this reaction. The defect with the one-tailed SSB-LT-Drl was most severe, giving little stimulation above the level observed in the absence of SSB. In these reactions, the extent of the reaction was most severely reduced. The reduced velocities can be explained by fewer DNA molecules participating in the reaction. Thus, at least part of the defect appears to be in the initiation phase of the reaction. The χ subunit of the Pol III HE interacts with the C-terminal tail of SSB and facilitates binding to and elongating templates that are coated with SSB [24–27]. We have observed that an interaction between Pol III HE component other than χ and the C-terminal tail of SSB is required for the optimal efficiency of initiation complex formation under conditions where Pol III associated with τ-containing DnaX complexes is chaperoned onto newly assembled β_2 [28]. It is possible that during initiation complex formation in the presence of single-tailed SSB-LT-Drl that a portion of the Pol III HE interacts through χ precluding

stimulation by the second interaction site or even trapping the enzyme in a non-productive complex.

In a more complex rolling circle replication reaction, we observe an *ca.* two-fold decrease in leading strand synthesis and a further decrease in lagging strand synthesis. In this assay, a dimeric Pol III HE simultaneously replicates the leading and lagging strand in a reaction that is coupled, in part, through an interaction with the DnaB helicase [71,72,74]. The decrease in leading strand synthesis could be explained by a defect in interaction of the Pol III HE through χ to SSB coating the lagging strand. This interaction has been shown to be important for stabilizing leading strand replication during the extensive elongation that takes place on rolling circle templates [29] and in stabilizing leading strand Pol III HE in strand displacement reactions [32].

To determine whether the additional lagging strand defect was due to slower lagging strand specific elongation or a defect in priming, we examined the length of Okazaki fragments produced. The length of Okazaki fragments is very sensitive to Pol III HE elongation rates and the frequency of primer synthesis and utilization [75]. We see the same average lengths in the presence of all SSB forms, eliminating these possibilities.

The additional decrease in lagging strand synthesis may be due to an occasional defect in DNA replication initiation on RNA primers. This defect is not absolute. Approximately 60 Okazaki fragments are made in the reaction with wt SSB during the five minute reaction (~ 2500 nt Okazaki fragments synthesized at ~ 500 nt/s). Thus, repeated cycles of initiation, elongation and recycling to new primers occurs, even in the

presence of SSB-LT-DrI. But, failure to reinitiate lagging strand synthesis likely leads to uncoupling of the reaction and possible replication fork collapse.

Intuitively, the replication defects observed do not appear to be sufficiently severe to result in the dominant lethal phenotype observed for *ssb-LT-DrI*. Mechanisms exist in *E. coli* for reinitiation at collapsed initiation forks. The principal pathway proceeds through a PriA-dependent reaction. PriA recognizes collapsed forks and through a reaction dependent on sequential interactions with PriB, DnaT, and DnaC, leads to the reassembly of the DnaB helicase at forks and the ensuing re-entry of Pol III HE, re-establishing replication forks [84]. The PriA-dependent reaction is absolutely dependent upon SSB (Chapter 3). Thus, we sought to determine whether this replication restart reaction is impaired in the presence of SSB with less than the full complement of C-terminal tails.

We employed a FRET assay that monitors the separation of two strands by helicase on artificial replication forks. Sterically blocking the 5'-end of the lagging strand template precludes helicase self-assembly by a threading reaction, making helicase PriA-, PriB-, DnaT-, DnaC- and SSB-dependent (Chapter 3). In the presence of SSB-LD-DrI the reaction decreases approximately 30%. However, in the presence of SSB-LT-DrI, the reaction is nearly completely inactive, falling to the baseline determined by addition of SSB-S1 lacking any functional tails.

An interaction between SSB and PriA is important to support PriA function [24,34]. SPR studies of PriA binding to synthetic replication forks suggest multiple copies of PriA interact (Yuan and McHenry, unpublished result). It is possible that multiple PriA monomers must interact with multiple C-terminal tails in a single SSB

tetramer. The replication restart primosomal reaction involves sequential interactions of the PriA, PriB, DnaT and DnaC/DnaB proteins in a possible handoff reaction [85,86]. Thus, an SSB with multiple C-terminal tails could be required to bind to a partner downstream of PriA facilitating complex stability or requisite handoffs.

E. coli priA mutants yield very small slow growing colonies and exhibit a low viability upon dilution and re-plating [84]. Viability could be due to a percentage of cells that do not experience replication fork collapse in sequential divisions. SSB-LT-Drl supports decreased levels of replication at reconstituted replication forks in reactions that likely lead to uncoupling and increased frequencies of replication fork collapse. That defect superimposed on the inability of cells to reinitiate by the PriA-dependent replication restart pathway provides a plausible explanation for the lethality observed from *ssb-LT-Drl*.

5.6 REFERENCES

1 Lohman, T. M., Bujalowski, W. and Overman, L. B. (1988) *E. coli* single strand binding protein: a new look at helix-destabilizing proteins. Trends in Biochemical Sciences **13**, 250–5.

2 Williams, K. R., Spicer, E. K., LoPresti, M. B., Guggenheimer, R. A. and Chase, J. W. (1983) Limited proteolysis studies on the *Escherichia coli* single-stranded DNA binding protein. Evidence for a functionally homologous domain in both the Escherichia coli and T4 DNA binding proteins. The Journal of Biological Chemistry **258**, 3346–55.

3 Lohman, T. M. and Ferrari, M. E. (1994) *Escherichia coli* single-stranded DNA-binding protein: multiple DNA-binding modes and cooperativities. Annual Review of Biochemistry **63**, 527–70.

4 Raghunathan, S. and Kozlov, A. G., Lohman, T.M., and Waksman, G. (2000) Structure of the DNA binding domain of *E . coli* SSB bound to ssDNA. Nature Structural Biology **7**, 648–652.

5 Raghunathan, S., Ricard, C. S., Lohman, T. M. and Waksman, G. (1997) Crystal structure of the homo-tetrameric DNA binding domain of *Escherichia coli* single-stranded DNA-binding protein determined by multiwavelength x-ray diffraction on the selenomethionyl protein at 2.9-A resolution. Proceedings of the National Academy of Sciences of the United States of America **94**, 6652–7.

6 Shereda, R. D., Reiter, N. J., Butcher, S. E. and Keck, J. L. (2009) Identification of the SSB binding site on *E. coli* RecQ reveals a conserved surface for binding SSB's C terminus. Journal of Molecular Biology **386**, 612–25.

7 Bujalowski, W. and Lohman, T. M. (1986) *Escherichia coli* single-strand binding protein forms multiple, distinct complexes with single-stranded DNA. Biochemistry **25**, 7799–802.

8 Chrysogelos, S. and Griffith, J. (1982) *Escherichia coli* single-strand binding protein organizes single-stranded DNA in nucleosome-like units. Proceedings of the National Academy of Sciences of the United States of America **79**, 5803–7.

9 Griffith, J. D., Harris, L. D. and Register, J. (1984) Visualization of SSB-ssDNA complexes active in the assembly of stable RecA-DNA filaments. Cold Spring Harbor Symposia on Quantitative Biology **49**, 553–9.

10 Lohman, T. M. and Overman, L. B. (1985) Two binding modes in *Escherichia coli* single strand binding protein-single stranded DNA complexes. Modulation by NaCl concentration. The Journal of Biological Chemistry **260**, 3594–603.

11 Lohman, T. M., Overman, L. B. and Datta, S. (1986) Salt-dependent changes in the DNA binding co-operativity of *Escherichia coli* single strand binding protein. Journal of Molecular Biology **187**, 603–15.

12 Roy, R., Kozlov, A. G., Lohman, T. M. and Ha, T. (2009) SSB protein diffusion on single-stranded DNA stimulates RecA filament formation. Nature **461**, 1092–7.

13 Zhou, R., Kozlov, A. G., Roy, R., Zhang, J., Korolev, S., Lohman, T. M. and Ha, T. (2011) SSB functions as a sliding platform that migrates on DNA via reptation. Cell **146**, 222–32.

14 Ferrari, M. E., Bujalowski, W. and Lohman, T. M. (1994) Co-operative binding of *Escherichia coli* SSB tetramers to single-stranded DNA in the $(SSB)_{35}$ binding mode. Journal of Molecular Biology **236**, 106–23.

15 Bujalowski, W., Overman, L. B. and Lohman, T. M. (1988) Binding mode transitions of *Escherichia coli* single strand binding protein-single-stranded DNA complexes. Cation, anion, pH, and binding density effects. The Journal of Biological Chemistry **263**, 4629–40.

16 Braun, K. A., Lao, Y., He, Z., Ingles, C. J. and Wold, M. S. (1997) Role of protein-protein interactions in the function of replication protein A (RPA): RPA modulates the activity of DNA polymerase α by multiple mechanisms. Biochemistry **36**, 8443–54.

17 Li, K. and Williams, R. S. (1997) Tetramerization and single-stranded DNA binding properties of native and mutated forms of murine mitochondrial single-stranded DNA-binding proteins. The Journal of Biological Chemistry **272**, 8686–94.

18 Tiranti, V., Rocchi, M., DiDonato, S. and Zeviani, M. (1993) Cloning of human and rat cDNAs encoding the mitochondrial single-stranded DNA-binding protein (SSB). Gene **126**, 219–25.

19 Yang, C., Curth, U., Urbanke, C. and Kang, C. (1997) Crystal structure of human mitochondrial single-stranded DNA binding protein at 2.4 A resolution. Nature Structural Biology **4**, 153–7.

20 Antony, E., Weiland, E. A., Korolev, S. and Lohman, T. M. (2012) Plasmodium falciparum SSB tetramer wraps single-stranded DNA with similar topology but opposite polarity to *E. coli* SSB. Journal of Molecular Biology **420**, 269–83.

21 Antony, E., Kozlov, A. G., Nguyen, B. and Lohman, T. M. (2012) Plasmodium falciparum SSB tetramer binds single-stranded DNA only in a fully wrapped mode. Journal of Molecular Biology **420**, 284–95.

22 Prusty, D., Dar, A., Priya, R., Sharma, A., Dana, S., Choudhury, N. R., Rao, N. S. and Dhar, S. K. (2010) Single-stranded DNA binding protein from human malarial parasite Plasmodium falciparum is encoded in the nucleus and targeted to the apicoplast. Nucleic Acids Research **38**, 7037–53.

23 McHenry, C. S. (2011) DNA replicases from a bacterial perspective. Annual Review of Biochemistry **80**, 403–36.

24 Kozlov, A. G., Cox, M. M. and Lohman, T. M. (2010) Regulation of single-stranded DNA binding by the C termini of *Escherichia coli* single-stranded DNA-binding (SSB) protein. The Journal of Biological Chemistry **285**, 17246–52.

25 Naue, N. and Curth, U. (2012) Investigation of protein-protein interactions of single-stranded DNA-binding proteins by analytical ultracentrifugation. Methods in Molecular Biology (Clifton, N.J.) **922**, 133–49.

26 Glover, B. P. and McHenry, C. S. (1998) The $\chi\psi$ subunits of DNA polymerase III holoenzyme bind to single-stranded DNA-binding protein (SSB) and facilitate replication of an SSB-coated template. The Journal of Biological Chemistry **273**, 23476–84.

27 Kelman, Z., Yuzhakov, A., Andjelkovic, J. and O'Donnell, M. (1998) Devoted to the lagging strand-the subunit of DNA polymerase III holoenzyme contacts SSB to promote processive elongation and sliding clamp assembly. The EMBO Journal **17**, 2436–49.

28 Downey, C. D. and McHenry, C. S. (2010) Chaperoning of a replicative polymerase onto a newly assembled DNA-bound sliding clamp by the clamp loader. Molecular Cell **37**, 481–91.

29 Marceau, A. H., Bahng, S., Massoni, S. C., George, N. P., Sandler, S. J., Marians, K. J. and Keck, J. L. (2011) Structure of the SSB-DNA polymerase III interface and its role in DNA replication. The EMBO Journal **30**, 4236–47.

30 Kelman, Z. and Hurwitz, J. (1998) Protein-PCNA interactions: a DNA-scanning mechanism? Trends in Biochemical Sciences **23**, 236–8.

31 Quiñones, A. and Neumann, S. (1997) The ssb-113 allele suppresses the dnaQ49 mutator and alters DNA supercoiling in *Escherichia coli*. Molecular Microbiology **25**, 237–46.

32 Yuan, Q. and McHenry, C. S. (2009) Strand displacement by DNA polymerase III occurs through a τ-ψ-χ link to single-stranded DNA-binding protein coating the lagging strand template. The Journal of Biological Chemistry **284**, 31672–9.

33 Yuzhakov, A., Kelman, Z. and O'Donnell, M. (1999) Trading places on DNA--a three-point switch underlies primer handoff from primase to the replicative DNA polymerase. Cell **96**, 153–63.

34 Cadman, C. J. and McGlynn, P. (2004) PriA helicase and SSB interact physically and functionally. Nucleic Acids Research **32**, 6378–87.

35 Cadman, C. J., Lopper, M., Moon, P. B., Keck, J. L. and McGlynn, P. (2005) PriB stimulates PriA helicase via an interaction with single-stranded DNA. The Journal of Biological Chemistry **280**, 39693–700.

36 Lecointe, F., Sérèna, C., Velten, M., Costes, A., McGovern, S., Meile, J.-C., Errington, J., Ehrlich, S. D., Noirot, P. and Polard, P. (2007) Anticipating chromosomal replication fork arrest: SSB targets repair DNA helicases to active forks. The EMBO Journal **26**, 4239–51.

37 Shereda, R. D., Bernstein, D. A. and Keck, J. L. (2007) A central role for SSB in *Escherichia coli* RecQ DNA helicase function. The Journal of Biological Chemistry **282**, 19247–58.

38 Han, E. S., Cooper, D. L., Persky, N. S., Sutera, V. A., Whitaker, R. D., Montello, M. L. and Lovett, S. T. (2006) RecJ exonuclease: substrates, products and interaction with SSB. Nucleic Acids Research **34**, 1084–91.

39 Lu, D., Myers, A. R., George, N. P. and Keck, J. L. (2011) Mechanism of Exonuclease I stimulation by the single-stranded DNA-binding protein. Nucleic Acids Research **39**, 6536–45.

40 Umezu, K. and Kolodner, R. D. (1994) Protein interactions in genetic recombination in *Escherichia coli*. Interactions involving RecO and RecR overcome the inhibition of RecA by single-stranded DNA-binding protein. The Journal of Biological Chemistry **269**, 30005–13.

41 Kowalczykowski, S. C., Dixon, D. A., Eggleston, A. K., Lauder, S. D. and Rehrauer, W. M. (1994) Biochemistry of homologous recombination in *Escherichia coli*. Microbiological Reviews **58**, 401–65.

42 Handa, P., Acharya, N. and Varshney, U. (2001) Chimeras between single-stranded DNA-binding proteins from *Escherichia coli* and Mycobacterium tuberculosis reveal that their C-terminal domains interact with uracil DNA glycosylases. The Journal of Biological Chemistry **276**, 16992–7.

43 Arad, G., Hendel, A., Urbanke, C., Curth, U. and Livneh, Z. (2008) Single-stranded DNA-binding protein recruits DNA polymerase V to primer termini on RecA-coated DNA. The Journal of Biological Chemistry **283**, 8274–82.

44 Molineux, I. J. and Gefter, M. L. (1974) Properties of the *Escherichia coli* in DNA binding (unwinding) protein: interaction with DNA polymerase and DNA. Proceedings of the National Academy of Sciences of the United States of America **71**, 3858–62.

45 Bernstein, D. A., Eggington, J. M., Killoran, M. P., Misic, A. M., Cox, M. M. and Keck, J. L. (2004) Crystal structure of the *Deinococcus radiodurans* single-stranded DNA-binding protein suggests a mechanism for coping with DNA damage. Proceedings of the National Academy of Sciences of the United States of America **101**, 8575–80.

46 Fedorov, R., Witte, G., Urbanke, C., Manstein, D. J. and Curth, U. (2006) 3D structure of *Thermus aquaticus* single-stranded DNA-binding protein gives insight into the functioning of SSB proteins. Nucleic Acids Research **34**, 6708–17.

47 George, N. P., Ngo, K. V, Chitteni-Pattu, S., Norais, C. A., Battista, J. R., Cox, M. M. and Keck, J. L. (2012) Structure and cellular dynamics of *Deinococcus radiodurans* single-stranded DNA (ssDNA)-binding protein (SSB)-DNA complexes. The Journal of Biological Chemistry **287**, 22123–32.

48 Kozlov, A. G., Jezewska, M. J., Bujalowski, W. and Lohman, T. M. (2010) Binding specificity of *Escherichia coli* single-stranded DNA binding protein for the χ subunit of DNA pol III holoenzyme and PriA helicase. Biochemistry **49**, 3555–66.

49 Witte, G., Urbanke, C. and Curth, U. (2005) Single-stranded DNA-binding protein of *Deinococcus radiodurans*: a biophysical characterization. Nucleic Acids Research **33**, 1662–70.

50 Brandsma, J. A., Bosch, D., De Ruÿter, M. and Van de Putte, P. (1985) Analysis of the regulatory region of the ssb gene of *Escherichia coli*. Nucleic Acids Research **13**, 5095–109.

51 LaDuca, R. J., Crute, J. J., McHenry, C. S. and Bambara, R. A. (1986) The β subunit of the *Escherichia coli* DNA polymerase III holoenzyme interacts functionally with the catalytic core in the absence of other subunits. The Journal of Biological Chemistry **261**, 7550–7.

52 Marians, K. J. (1995) ΦX174-type primosomal proteins: purification and assay. Methods in Enzymology **262**, 507–21.

53 Griep, M. A. and McHenry, C. S. (1989) Glutamate overcomes the salt inhibition of DNA polymerase III holoenzyme. The Journal of Biological Chemistry **264**, 11294–301.

54 Fay, P. J., Johanson, K. O., McHenry, C. S. and Bambara, R. A. (1982) Size classes of products synthesized processively by two subassemblies of *Escherichia coli* DNA polymerase III holoenzyme. The Journal of Biological Chemistry **257**, 5692–9.

55 Sanders, G. M., Dallmann, H. G. and McHenry, C. S. (2010) Reconstitution of the *B. subtilis* replisome with 13 proteins including two distinct replicases. Molecular Cell, Elsevier Ltd **37**, 273–81.

56 Dam, J. and Schuck, P. (2004) Calculating sedimentation coefficient distributions by direct modeling of sedimentation velocity concentration profiles. Methods in Enzymology **384**, 185–212.

57 Schuck, P. (1998) Sedimentation analysis of noninteracting and self-associating solutes using numerical solutions to the Lamm equation. Biophysical Journal **75**, 1503–12.

58 Vistica, J., Dam, J., Balbo, A., Yikilmaz, E., Mariuzza, R. A., Rouault, T. A. and Schuck, P. (2004) Sedimentation equilibrium analysis of protein interactions with global implicit mass conservation constraints and systematic noise decomposition. Analytical Biochemistry **326**, 234–56.

59 Lohman, T. M. (1992) *Escherichia coli* DNA helicases: mechanisms of DNA unwinding. Molecular Microbiology **6**, 5–14.

60 Porter, R. D., Black, S., Pannuri, S. and Carlson, A. (1990) Use of the *Escherichia coli* SSB gene to prevent bioreactor takeover by plasmidless cells. Bio/technology (Nature Publishing Company) **8**, 47–51.

61 Manhart, C. M. and McHenry, C. S. (2013) The PriA Replication Restart Protein Blocks Replicase Access Prior to Helicase Assembly and Directs Template Specificity through Its ATPase Activity. The Journal of Biological Chemistry **288**, 3989–99.

62 Roy, R., Kozlov, A. G., Lohman, T. M. and Ha, T. (2007) Dynamic structural rearrangements between DNA binding modes of *E. coli* SSB protein. Journal of Molecular Biology **369**, 1244–57.

63 Kozlov, A. G. and Lohman, T. M. (2002) Stopped-flow studies of the kinetics of single-stranded DNA binding and wrapping around the *Escherichia coli* SSB tetramer. Biochemistry **41**, 6032–44.

64 Bujalowski, W. and Lohman, T. M. (1989) Negative co-operativity in *Escherichia coli* single strand binding protein-oligonucleotide interactions. II. Salt, temperature and oligonucleotide length effects. Journal of Molecular Biology **207**, 269–88.

65 Lohman, T. M. and Bujalowski, W. (1988) Negative cooperativity within individual tetramers of *Escherichia coli* single strand binding protein is responsible for the transition between the $(SSB)_{35}$ and $(SSB)_{56}$ DNA binding modes. Biochemistry **27**, 2260–5.

66 Porter, R. D. and Black, S. (1991) The single-stranded-DNA-binding protein encoded by the *Escherichia coli* F factor can complement a deletion of the chromosomal ssb gene. Journal of Bacteriology **173**, 2720–3.

67 Sugiura, S., Ohkubo, S. and Yamaguchi, K. (1993) Minimal essential origin of plasmid pSC101 replication: requirement of a region downstream of iterons. Journal of Bacteriology **175**, 5993–6001.

68 Wadood, A., Dohmoto, M., Sugiura, S. and Yamaguchi, K. (1997) Characterization of copy number mutants of plasmid pSC101. The Journal of General and Applied Microbiology **43**, 309–316.

69 Yamaguchi, K. and Yamaguchi, M. The replication origin of pSC101: the nucleotide sequence and replication functions of the ori region. Gene **29**, 211–9.

70 Curth, U., Genschel, J., Urbanke, C. and Greipel, J. (1996) *In vitro* and *in vivo* function of the C-terminus of *Escherichia coli* single-stranded DNA binding protein. Nucleic Acids Research **24**, 2706–11.

71 Kim, S., Dallmann, H. G., McHenry, C. S. and Marians, K. J. (1996) Coupling of a replicative polymerase and helicase: a τ-DnaB interaction mediates rapid replication fork movement. Cell **84**, 643–50.

72 Gao, D. and McHenry, C. S. (2001) τ binds and organizes *Escherichia coli* replication proteins through distinct domains. Domain III, shared by γ and τ, binds $\delta\delta'$ and $\chi\psi$. The Journal of Biological Chemistry **276**, 4447–53.

73 Tougu, K. and Marians, K. J. (1996) The extreme C terminus of primase is required for interaction with DnaB at the replication fork. The Journal of Biological Chemistry **271**, 21391–7.

74 Kim, S., Dallmann, H. G., McHenry, C. S. and Marians, K. J. (1996) τ couples the leading- and lagging-strand polymerases at the *Escherichia coli* DNA replication fork. The Journal of Biological Chemistry **271**, 21406–12.

75 Zechner, E. L., Wu, C. A. and Marians, K. J. (1992) Coordinated leading- and lagging-strand synthesis at the *Escherichia coli* DNA replication fork. II.

Frequency of primer synthesis and efficiency of primer utilization control Okazaki fragment size. The Journal of Biological Chemistry **267**, 4045–53.

76 Costes, A., Lecointe, F., McGovern, S., Quevillon-Cheruel, S. and Polard, P. (2010) The C-terminal domain of the bacterial SSB protein acts as a DNA maintenance hub at active chromosome replication forks. PLoS Genetics **6**, e1001238.

77 Shereda, R. D., Kozlov, A. G., Lohman, T. M., Cox, M. M. and Keck, J. L. SSB as an organizer/mobilizer of genome maintenance complexes. Critical Reviews in Biochemistry and Molecular Biology **43**, 289–318.

78 Rosenkranz, H. S., Garro, A. J., Levy, J. A. and Carr, H. S. (1966) Studies with hydroxyurea. I. The reversible inhibition of bacterial DNA synthesis and the effect of hydroxyurea on the bactericidal action of streptomycin. Biochimica et Biophysica Acta **114**, 501–15.

79 Rosenkranz, H. S. And Levy, J. A. (1965) Hydroxyurea: A Specific Inhibitor Of Deoxyribonucleic Acid Synthesis. Biochimica Et Biophysica Acta **95**, 181–3.

80 Biesele, J. J., Philips, F. S., Thiersch, J. B., Burchenal, J. H., Buckley, S. M., Stock, C. C., Loveless, A. And Ross, W. C. J. (1950) Chromosome Alteration And Tumour Inhibition By Nitrogen Mustards; The Hypothesis Of Crosslinking Alkylation. Nature **166**, 1112–4.

81 Bonura, T. and Smith, K. C. (1975) Quantitative evidence for enzymatically-indeced DNA double-strand breaks as lethal lesions in UV irradiated pol+ and polA1 strains of E. coli K-12. Photochemistry and Photobiology **22**, 243–8.

82 Ezekiel, D. H. and Hutchins, J. E. (1968) Mutations affecting RNA polymerase associated with rifampicin resistance in *Escherichia coli*. Nature **220**, 276–7.

83 Rosenberg, S. M. (2001) Evolving responsively: adaptive mutation. Nature reviews. Genetics **2**, 504–15.

84 Marians, K. J. (2000) PriA-directed replication fork restart in *Escherichia coli*. Trends in Biochemical Sciences **25**, 185–9.

85 Liu, J., Nurse, P. and Marians, K. J. (1996) The ordered assembly of the ΦX174-type primosome. III. PriB facilitates complex formation between PriA and DnaT. The Journal of Biological Chemistry **271**, 15656–61.

86 Lopper, M., Boonsombat, R., Sandler, S. J. and Keck, J. L. (2007) A hand-off mechanism for primosome assembly in replication restart. Molecular Cell **26**, 781–93.

CHAPTER 6*

Identifying the protein-DNA contacts between the *E. coli* replication restart machinery and a model replication fork using photo-crosslinking

6.1 ABSTRACT

In *E. coli*, a pathway dependent on the PriA protein has been established for helicase-reloading after replication fork collapse. PriA functions in concert with SSB, PriB, and DnaT to recruit DnaC helicase loader and DnaB helicase to be reloaded onto the lagging strand prior to restarting replication. I used a phenyldiazirine photo-crosslinker to probe the arrangement and rearrangement of the primosomal proteins involved in replication restart on model replication forks. Here I show that SSB binds to forked structures in a different manner than it binds to ssDNA. A DNA-DNA photo-crosslink occurs only when DNA-binding proteins bind at the replication fork. I observe that PriA prevents SSB from binding near the fork juncture. When DnaB is loaded it contacts the displaced strand upstream of the fork juncture and diffuses at least three nucleotides into the duplex in the presence of ATPγS.

* I performed the entirety of the experimental work presented in this chapter.

6.2 INTRODUCTION

Replication begins at a unique chromosomal origin. A replication fork will often encounter unrepaired DNA damage, causing dissociation of the replisome. Such damage may need to be resolved by recombination. Following repair, the helicase must be reloaded before replication can resume.

There is a network of proteins in *E. coli* that attract and facilitate loading of the helicase by the helicase loader [1]. PriA, PriB, and DnaT have been genetically and biochemically defined to act sequentially for reloading the DnaB helicase on collapsed forks [2–4]. Based on a study examining protein-protein and protein-DNA interactions among the *E. coli* primosomal proteins and single-stranded DNA (ssDNA) substrate, it has been suggested that there may be a handoff of ssDNA from PriA to PriB in the early stage of primosome assembly [5]. This model proposes that the PriA-PriB complex then recruits DnaT which displaces PriB from ssDNA [5]. The evidence for this model is largely based on weak affinities between PriA and PriB and between PriB and DnaT that are strengthened in the presence of ssDNA and evidence suggesting that the binding site on PriB for ssDNA overlaps with its binding sites for PriA and DnaT [5].

PriA binds to the C-terminal tail of SSB [6,7]. This interaction stimulates the 3' to 5' helicase activity of PriA through a specific protein-protein interaction between SSB and PriA [6]. PriB is a homolog of SSB [8–10] that stabilizes PriA on DNA [1]. Structurally, PriB is very similar to SSB [9]. Each PriB monomer contains a single OB fold motif structurally identical to the N-terminal ssDNA binding domain of SSB [9], and like SSB, PriB has been shown to stimulate PriA's helicase activity [11]. A major

distinction between the two proteins is that in solution SSB forms a tetramer, while PriB forms a dimer. It is not clear exactly what role PriB plays in assembly of the primosome. It is suggested that the tetrameric state of SSB allows it to bind tightly to ssDNA, while the dimeric PriB binds ssDNA more weakly so that PriB can more readily dissociate upon primosomal assembly [9].

DnaT's involvement at a replication fork is even less clear. DnaT does not have intrinsic activity, yet it is a required component in primosomal assembly in the replication restart process [2]. A PriA-DnaT interaction is stimulated in the presence of PriB [12], and a PriA-DnaT complex on DNA is thought to exist throughout the course of the helicase loading reaction [13].

In this study, I employed a photo-crosslinking technique to identify contacts between the *E. coli* replication restart proteins and a model replication fork. For this, I used a phenyldiazirine attached at the 5-position of thymidylate incorporated at unique locations within a substrate modeling a replication fork. A diazirine was chosen because when irradiated it can efficiently insert itself into a C-H bond in any adjacent amino acid [14,15].

A substrate and protein system were optimized to support photo-crosslinking studies to probe the sequential assembly of the primosomal proteins in Chapter 3. Here, I used a photo-crosslinking method established in Chapter 2 to identify contacts between DNA and SSB, PriA, PriB, DnaT, DnaB, and DnaC as the assembly necessary to reload the DnaB helicase on a collapsed fork is constructed.

6.3 MATERIALS AND METHODS

6.3.1 Oligonucleotides

All oligonucleotides were obtained from Biosearch Technologies. Oligonucleotides containing amino-modified C2 dT from Glen Research were derivatized with the phenyldiazirine photo-crosslinker and HPLC-purified as described in Chapter 2. Substrates used in all photo-crosslinking reactions were assembled from HPLC-purified oligonucleotides listed in Fig. 6.1A.

Prior to annealing, the phenyldiazirine-labeled oligonucleotide was labeled with ^{32}P on the 5'-end using T4 polynucleotide kinase according to the manufacturer's instructions (Invitrogen). Unincorporated [γ-^{32}P]ATP was removed by a Microspin-G25 column purchased from GE Healthcare.

Substrates were assembled by combining 1 μM phenyldiazirine-labeled oligonucleotide with 2 μM of the appropriate unlabeled oligonucleotides in a final volume of 50 μL in a buffer containing 10 mM Tris-HCl (pH 7.75), 50 mM NaCl, and 1 mM EDTA. Samples were heated to 95 ºC for 5 min and cooled to 25 ºC, decreasing the temperature by 1 ºC/10 min. Forked substrates were prepared from oligonucleotides in Fig. 6.1A: photocrosslinking substrate -35 was constructed from T-35, uLeT, and uLeP; substrate -3 from T-3, uLeT, and uLeP; substrate +3 from T+3, uLeT, and uLeP; substrate 3'-end from T3'end, uLeT, and uLeP; substrate -6 from T-6, uLaT, and uLeP; substrate -12 from P-12, uLeT, and uLaT; substrate -6 with no flap on the lagging strand was constructed from: T-6, uLeP, and unlabeled 45-mer, 5'-

A

T-35
5’-T-T(Biotin)-TTTTTTTTtTTTTTTTTTTTTTTTTTTTTTTTTTTATATTATCATGAATCTAACATGTTATAGTAATGATCTATACGCG-3’

T-3
5’-T-T(Biotin)-TTTTTTTTTTTTTTTTTTTTTTTTTTTTTTTTTTTTTTTTtTTTATATTATCATGAATCTAACATGTTATAGTAATGATCTATACGCG-3’

T+3
5’-T-T(Biotin)-TTTTTTTTTTTTTTTTTTTTTTTTTTTTTTTTTTTTTTTTTTTTAtATTATCATGAATCTAACATGTTATAGTAATGATCTATACGCG-3’

T3’end
5’-T-T(Biotin)-TTTTTTTTTTTTTTTTTTTTTTTTTTTTTTTTTTTTTTTTTTTTATATTATCATGAATCTAACATGTTATAGTAATGATCtATACGCG-3’

T-6
5’-CGCGTATAGATCATTACTATAACATGTTAGATTCATGATAATATAGGAGAtGACGAATATGATTTTGTCGGCTAATGTAAGAATCTTCAA-3’

P-12
5’-TTGAAGATTCTTACATTAGTTGACAAAATCATAtT-3’

Unlabeled Leading Strand Template (uLeT)
5’-CGCGTATAGATCATTACTATAACATGTTAGATTCATGATAATATAGGAGATGACGAATATGATTTTGTCGGCTAATGTAAGAATCTTCAA-3’

Unlabeled Lagging Strand Template (uLaT)
5’-T-T(Biotin)-TTTTTTTTTTTTTTTTTTTTTTTTTTTTTTTTTTTTTTTTTTTTATATTATCATGAATCTAACATGTTATAGTAATGATCTATACGCG-3’

Unlabeled Leading Strand Primer (uLeP)
5’-TTGAAGATTCTTACATTAGTTGACAAAATCATATT-3’

B

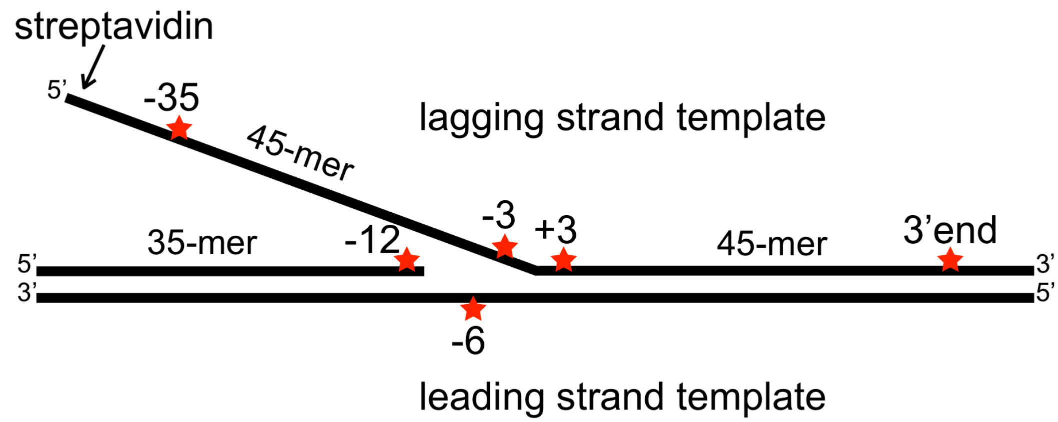

C

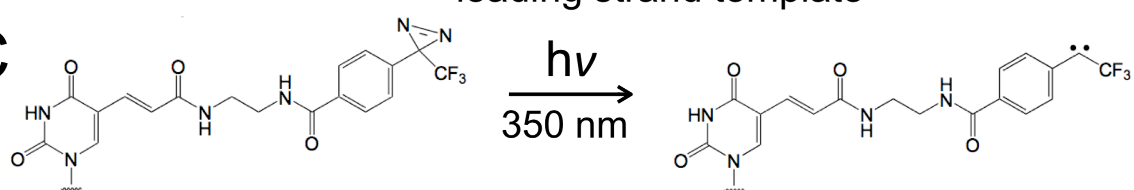

FIGURE 6.1
(A) Oligonucleotide sequences used in photo-crosslinking experiments. The position of the phenyldiazirine photo-crosslinker is indicated by red lowercase t. (B) Diagram of forked substrate used in photo-crosslinking studies. The starred positions indicate placement of the phenyldiazirine photo-crosslinker. The position number is given as the number of nucleotides away from the fork juncture with the exception of the 3’ end. (C) Structure of thymine-linked phenyldiazirine photo-crosslinker inserted at positions in A and B and formation of carbene upon irradiation.

TATATTATCATGAATCTAACATGTTATAGTAATGATCTATACGCG-3'. Annealed products were desalted by Microspin-G25 column (GE Healthcare) according to the manufacturer's protocol.

6.3.2 Proteins

E. coli primosomal proteins were purified as described previously: SSB [16], PriA [17], PriB [17], DnaT [17], DnaB [17], and DnaC [17].

6.3.3 Photo-crosslinking

Photo-crosslinking reactions were carried out in a final volume of 50 μL containing 20 nM radiolabeled phenyldiazirine-containing substrate in a buffer containing 50 mM Hepes (pH 7.5), 10 mM magnesium acetate, 10 mM dithiothreitol, 20% (v/v) glycerol, 0.02% (v/v) Nonidet P40 detergent, 100 mM potassium glutamate, and 100 μM ATPγS. Reactions were irradiated at room temperature in siliconized Pyrex test tubes covered in Parafilm at 350 nm in a Rayonet Photochemical Reactor-200 outputting ~1.65 x 10 photons/s/cm^3 at 350 nm (Southern New England Ultra Violet Company) for 1 h.

For reactions that were blocked by streptavidin, 200 nM streptavidin was incubated at room temperature with the substrate for 5 min prior to the addition of other protein components.

Where proteolysis is indicated, 30 μg of Proteinase K was added to the reaction after irradiation. Reactions were incubated at 37 ºC for 1 h in the dark prior to quenching.

Samples were quenched in 2x SDS-PAGE sample buffer: 0.25 M Tris-HCl (pH 6.8), 5% (w/v) SDS, 0.1 mM β-mercaptoethanol, 10% (v/v) glycerol, 0.005% (w/v) bromphenol blue, and 0.005% (w/v) xylene cyanol FF. Reactions were boiled at 95 ºC for 10 min prior to gel loading.

6.3.4 Gel Electrophoresis

Reactions were resolved by 4-20% SDS-PAGE containing 4 M urea. Gels were run at 15 W for 4 h using 25 mM Tris base, 190 mM glycine, 0.1% (w/v) SDS for electrophoresis buffer.

Gels were exposed to a Storage Phosphor Screen (GE) overnight prior to being scanned by a PhosphorImager.

6.4 RESULTS

6.4.1 SSB participates in a unique interaction with the replication fork

I placed photo-crosslinkers at positions surrounding a fork juncture, at a position 35 nucleotides away from the juncture in the lagging strand arm, and at a position 37 nucleotides away from the juncture near the 3'-end of the lagging strand in the duplex.

At photo-crosslinking positions near the fork juncture (Fig. 6.2A), there are multiple SSB-containing crosslinks (identified by comparing lanes ± protease treatment). By comparing photo-crosslinking positions, there are two primary crosslinked products on the denaturing gel, a faster mobility band (SSB-90mer (A) or the SSB-35mer (A)—the equivalent on the 35-mer primer) and a slower migrating band (SSB-90mer (B)). At the -35 position on the lagging strand arm and at the 3' end of the lagging strand, SSB photo-crosslinks shift to a single band, SSB-90mer (A) (lanes 1-4 Fig. 6.2A). At the -3 and +3 positions, the SSB-90mer (A) photo-crosslink occurs in addition to the slower migrating SSB-90mer (B) crosslink (lanes 5-8). A DNA-DNA crosslink is identified at the +3 position by comparing equivalent lanes ± protease treatment. At the -6 position, a region in the ssDNA gap on the leading strand arm, the SSB-90mer (A) crosslinked product is no longer observed. SSB-90mer (B) is the primary SSB-containing photo-crosslink (lanes 9-10). At the -12 position (the penultimate nucleotide of the primer terminus) on a 35-mer primer, there is only photo-crosslinked product, SSB-35mer (A) (lanes 11-12).

I examined the phenyldiazirine-labeled oligonucleotides in their single strand form to determine which bands require the forked structure (Fig. 6.2B). Comparing the forked substrates with ssDNA, I observed only the high mobility product (the A crosslink) on simple single-stranded templates. Thus, the SSB-90mer (B) product requires the forked structure.

Substrate identical to that in Fig. 6.1B but lacking the 45-mer single strand portion of the lagging strand template was examined at the -6 crosslinking position (data

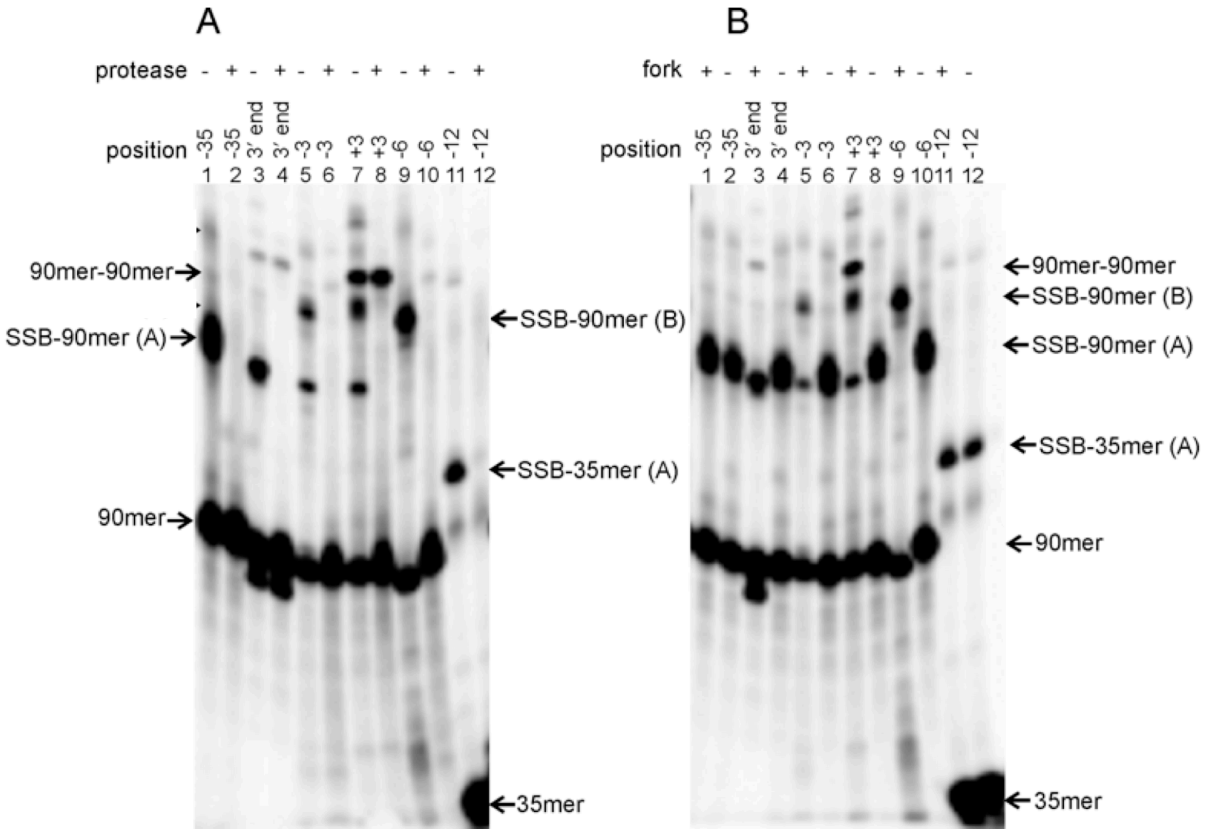

FIGURE 6.2
A novel interaction occurs between SSB and the replication fork juncture. (A) An SSB crosslink migrates slower at probe sites near the fork juncture. 500 nM SSB_4 was combined with 20 nM forked substrate. Lanes that indicate + protease were subjected to treatment with Proteinase K post-irradiation to identify protein-containing bands. (B) Multiple SSB-containing bands do not occur on ssDNA. 500 nM SSB_4 was reacted with 20 nM un-annealed template.

not shown). The SSB-90mer (B) crosslink is not observed with this substrate, further indicating the requirement of the fork structure to cause the slower migrating band.

To determine if the SSB-90mer (B) band is caused by incomplete denaturation, I subjected reactions to autoclaving prior to gel loading. Presumably an autoclaving step would denature any protein or nucleic acid. In this case, the slower migrating bands failed to reduce to a single band (data not shown).

6.4.2 PriA selectively binds near the replication fork juncture

To identify locations on the replication fork where PriA binds, an experiment identical to that presented with SSB was performed (Fig. 6.3). PriA does not bind at the -35 position on the lagging strand arm (lanes 1-2 Fig. 6.3A) or in the duplex on the end opposing the fork (land 3-4). PriA binds at the -3 position and the +3 position (lanes 5-8). An efficient photo-crosslink occurs at the -6 position in the single-stranded gap on the leading strand. At the -3, +3, and -6 positions, PriA facilitates a 90mer-90mer photo-crosslink identified by proteolysis treatment. PriA also binds at the -12 position, the penultimate nucleotide of the leading strand primer.

The photo-reactive single-strand forms of each position were photo-crosslinked to PriA (Fig. 6.3B). PriA binds to the single-strand equivalent of all probe positions even when it does not bind to that position when annealed in the model replication fork. A DNA-DNA crosslink forms on these single-stranded substrates between non-complementary strands.

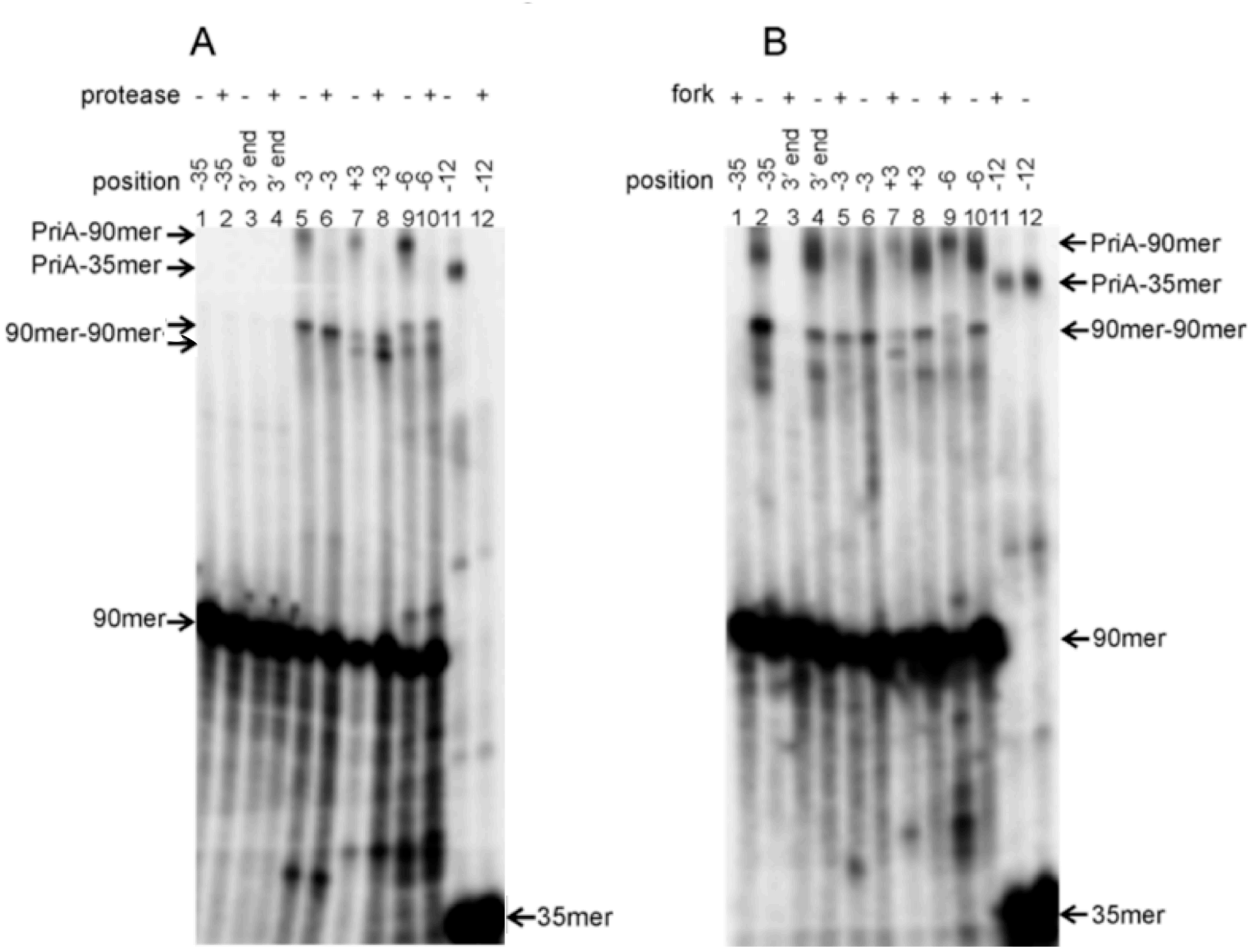

FIGURE 6.3
PriA selectively binds near the replication fork juncture. (A) 500 nM PriA was combined with 20 nM forked substrate. Lanes that indicate + protease were subjected to treatment with Proteinase K post-irradiation to identify protein-containing bands. (B) PriA binds to ssDNA and facilitates a DNA-DNA crosslink between non-complementary strands.

6.4.3 PriA can prevent SSB from binding at the replication fork juncture

SSB and PriA both crosslink at probe positions near the fork juncture (Figs. 6.2 and 6.3). An experiment including both proteins where PriA binds to the substrate prior to the addition of SSB was performed (Fig. 6.4). The only probe positions where SSB was observed to crosslink with approximately equal efficiency to that in Fig. 6.2 are probe positions were PriA does not crosslink (-35 position in lanes 1-2 Fig. 6.4 and 3' end position in lanes 3-4). At probe positions closest to the fork juncture, crosslinking to PriA dominates over crosslinking to SSB.

SSB crosslinks at all probe positions on the model replication fork (Fig. 6.2). When PriA binds to the substrate prior to the addition of SSB, very little SSB crosslinking occurs at positions that PriA occupied in Fig. 6.3, indicating that PriA prevents SSB from binding near the replication fork juncture.

6.4.4 DnaB helicase contacts the displaced strand and diffuses several nucleotides into the duplex

On substrate identical to that in Fig. 6.1B, the DnaB helicase has been shown to self-load by threading itself onto the 5'-end of the lagging strand arm in the absence of a steric block (Chapter 3). This self-loading reaction was performed here in the presence of ATPγS to identify helicase-DNA interactions.

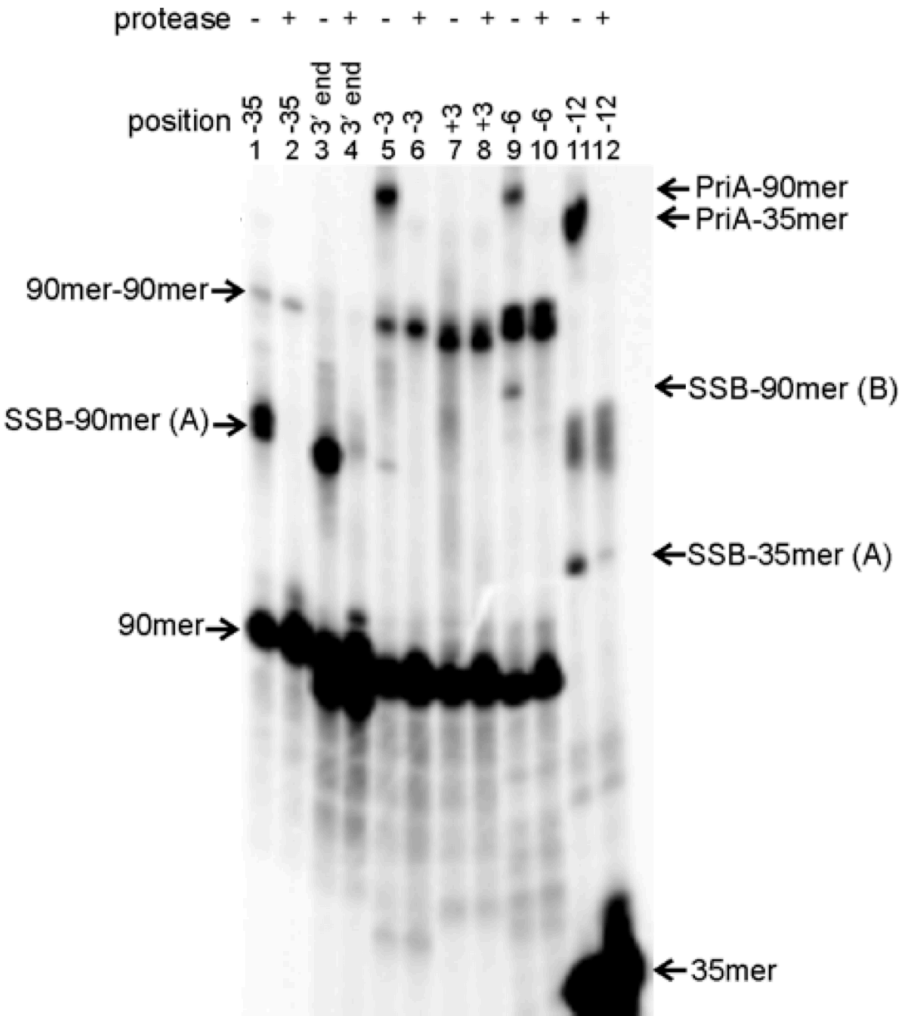

FIGURE 6.4
PriA can prevent SSB from binding at the replication fork juncture. 20 nM forked substrate was combined with 500 nM PriA followed by 500 nM SSB_4. Lanes that indicate + protease were subjected to treatment with Proteinase K post-irradiation to identify protein-containing bands.

Helicase does not crosslink at the -35 position in the lagging strand arm or in the duplex region distal to the fork at the 3' end position (lanes 1-4 Fig. 6.5). DnaB binds 3 nucleotides upstream of the fork on the lagging strand arm (along with a DNA-DNA crosslink) (lanes 5-6). DnaB binds at the probe position 3 nucleotides into the duplex (lanes 7-8) and efficiently crosslinks at the position 6 nucleotides upstream of the fork in the leading strand (lanes 9-10). DnaB does not crosslink at the -12 position near the terminus of the leading strand primer (lanes 11-12).

The DNA substrates used in this study contain a biotin near the 5'-terminus of the lagging strand arm (Fig. 6.1). Binding streptavidin to the substrate prior to the addition of DnaB blocks photo-crosslinking to helicase (and the formation of a 90mer-90mer crosslink) at the +3 position and the -6 position (lanes 13-14 Fig. 6.5). Streptavidin does not photo-crosslink at the probe positions as indicated by control experiments in lanes 15-17.

Previous work to optimize a PriA-dependent helicase loading reaction was performed in the presence of ATP (Chapter 3). Those experiments yielded an optimum concentration of 12 nM $DnaB_6$ loaded onto substrate identical to that used here by 50 nM DnaC with 150 nM PriA, 50 nM $PriB_2$, 50 nM $DnaT_3$, and 500 nM SSB_4 (Chapter 3). A titration was performed to optimize the helicase/helicase loader concentrations in the presence of ATPγS with the same PriA-dependent system (Fig. 6.6). Here, 60 nM $DnaB_6$ is loaded efficiently by 50 nM DnaC with ATPγS.

Using these newly optimized DnaB/DnaC concentrations, the helicase was loaded by the PriA-pathway in the presence of ATPγS on streptavidin blocked substrate

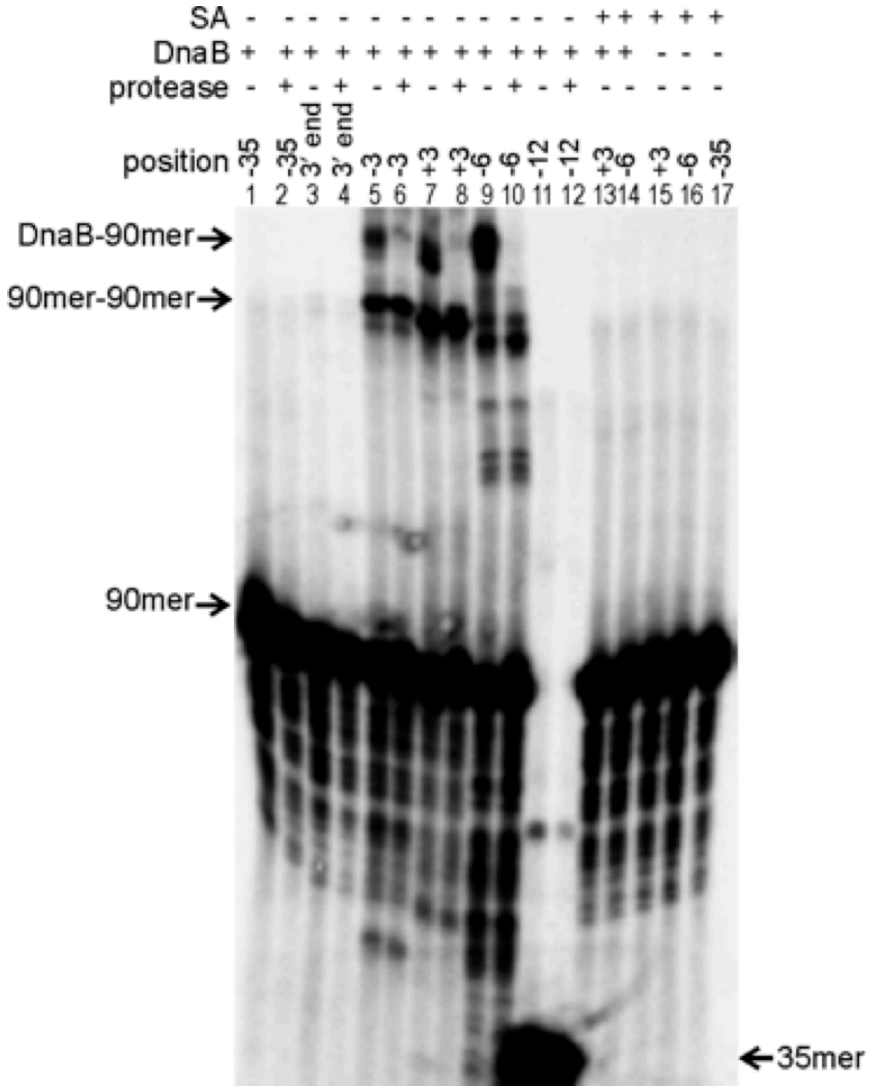

FIGURE 6.5
DnaB self-loads at high concentrations by threading itself onto a non-sterically blocked lagging strand arm in the presence of ATPγS. DnaB makes contact with the displaced strand at the -6 position and 3 nucleotides into the duplex when loaded. 20 nM forked substrate was combined with 550 nM $DnaB_6$ (where + DnaB is indicated). Lanes that indicate + protease were subjected to treatment with Proteinase K post-irradiation to identify protein-containing bands. Lanes 13-17 contain 200 nM streptavidin pre-bound to the biotin-containing substrate prior to addition of DnaB.

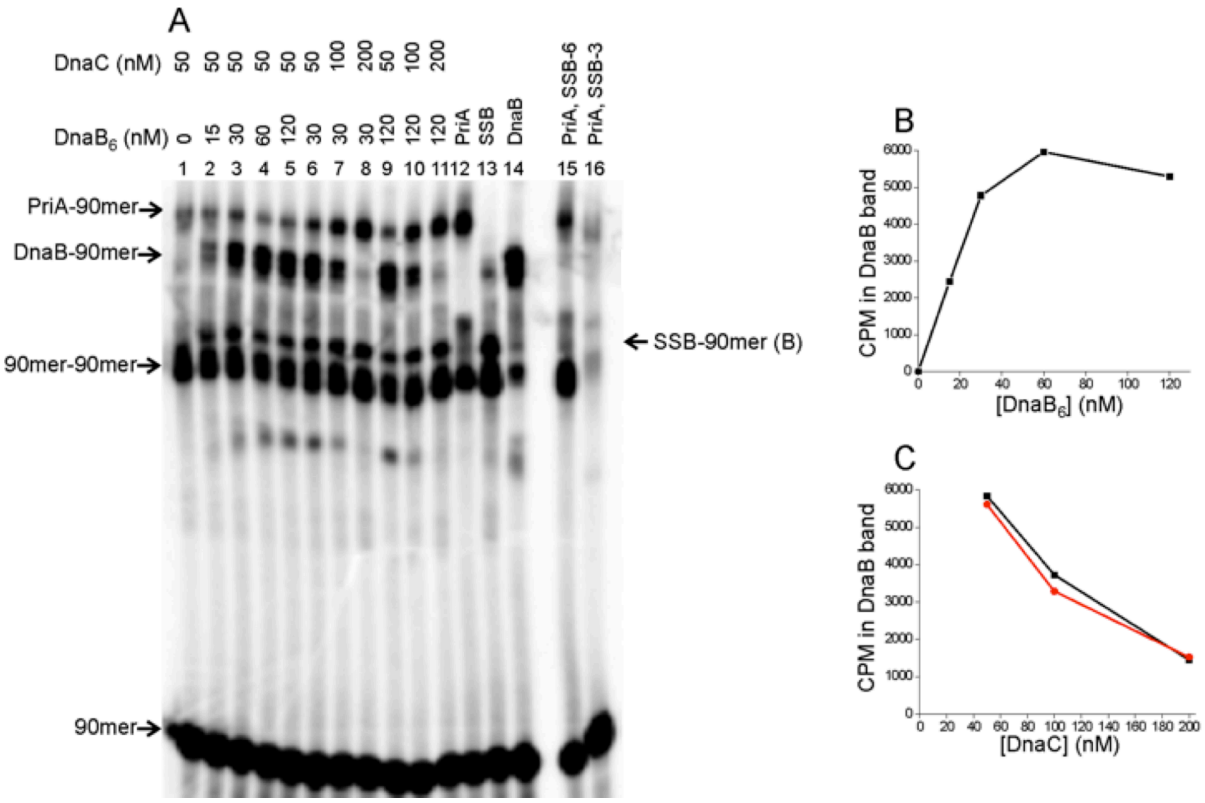

FIGURE 6.6
Titration of DnaB helicase and DnaC helicase loader in the presence of ATPγS at the -6 photo-crosslinking position with 150 nM PriA, 50 nM $PriB_2$, 50 nM $DnaT_3$, and 500 nM SSB_4. (A) Various concentrations of DnaB/DnaC were loaded by the PriA-pathway onto substrate blocked with 200 nM streptavidin and analyzed by SDS-PAGE. Markers for PriA, SSB, and DnaB were included in lanes 12-16 (each containing 500 nM protein in its oligomeric state). (B) The CPM values in the DnaB-containing bands were plotted at each $DnaB_6$ concentration. (C) The CPM values in the DnaB-containing bands were plotted against DnaC concentration. The experiment was performed at 30 nM $DnaB_6$ (black) and 120 nM $DnaB_6$ (red).

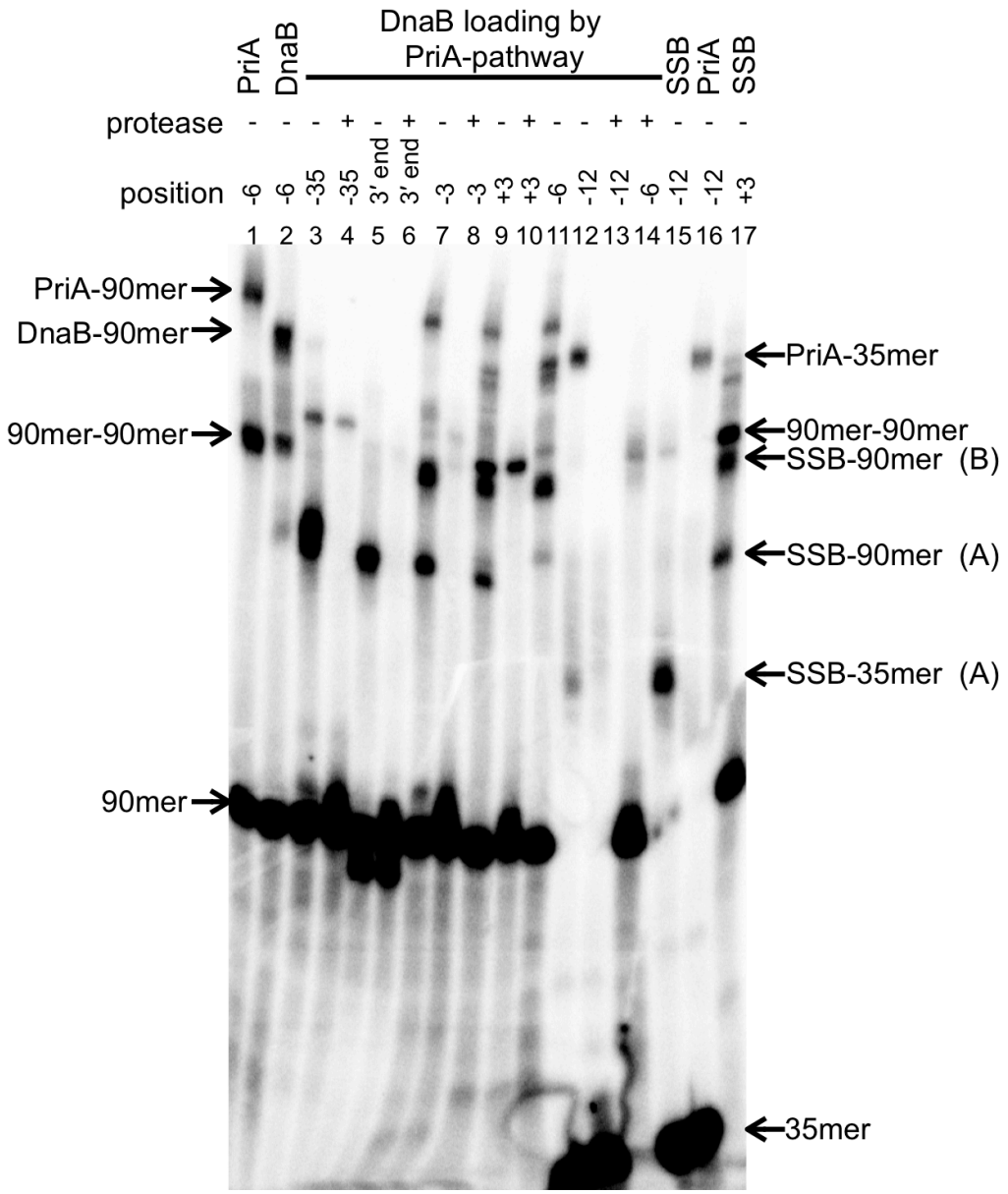

FIGURE 6.7
PriA and SSB remain bound to the replication fork upon DnaB helicase loading. On substrates blocked with 200 nM streptavidin, 60 nM $DnaB_6$ was loaded onto substrate by 150 nM PriA, 50 nM $PriB_2$, 50 nM $DnaT_3$, 50 nM DnaC, and 500 nM SSB_4 in the presence of ATPγS (lanes 3-14). Markers in lanes 1-2 and 15-17 contain 500 nM of the indicated protein in its oligomeric state.

(Fig. 6.7). At the -35 and 3' end positions (lanes 3-6 Fig. 6.7), SSB is the only protein bound. At the -3 position, PriA and SSB remain bound after helicase loading (lanes 7-8). DnaB does not crosslink. At the +3 and -6 positions, PriA, SSB, and DnaB all form crosslinks (lanes 9-11 and lane 14 for proteolysis of the material in lane 11). At the -12 position at the primer terminus (lanes 12-13), only PriA and SSB bind. Like in Fig. 6.6, DnaB crosslinks 6 nucleotides upstream of the fork in the displaced strand and at a position at least three nucleotides into the duplex.

6.5 DISCUSSION

Using a non-specific photo-crosslinker, interactions between the proteins involved in the replication restart process and a model replication fork were identified. This method allows for localization of proteins on regions of DNA.

SSB appears to make unique contacts with the forked structure that it does not make to ssDNA or duplex DNA. I observed a slower migrating band at probe positions closest to the replication fork juncture that I did not observe in other regions of the substrate. The slower resolving band may be caused by SSB binding in a different mode causing a unique crosslinking product not seen with ssDNA. In SSB, the residues that are key interactors with ssDNA are interior in SSB's primary sequence (Trp40, Trp54, Phe60, Trp88, and all lysine residues) [18–23]. Studies into how SSB is interacting with forked structures have not been performed, so the residues in SSB that make contact with fork junctions are unknown. If residues at the N- or C-terminus of SSB make contact with the fork juncture, the resulting denatured crosslinked product

would have a larger effective radius than the product resulting from an interior residue crosslinked to the template (Fig. 6.8). Since increasing the radius of a species slows mobility of that species in a gel, this provides a possible explanation for the SSB-90mer (B) crosslink.

SSB is known to play an important role at replication forks and is a requirement of the PriA-directed replication restart pathway (Chapters 3 and 5). The C-terminal tail of SSB interacts with and stimulates the activity of at least 14 different proteins [24], including PriA [6,7]. Accordingly, if SSB is not bound to a collapsed replication fork, this critical PriA-SSB interaction will not occur, and the helicase will not be reloaded to reestablish a replication fork. At a collapsed fork, residues interior in SSB's primary sequence are likely making contact with exposed ssDNA on the lagging strand arm. Residues near the termini, likely the intrinsically disordered C-terminus, are available and conceivably in position to make contact with the fork juncture. A single SSB tetramer may be making simultaneous contact with ssDNA on the lagging strand and the fork juncture. Such an interaction would have a multiplicative effect on the K_d between SSB and DNA. A strengthened interaction between SSB and a replication fork could be beneficial to a cell. It would ensure SSB's presence at a replication fork and localize/stabilize the protein so it can interact with other necessary protein components. This work provides a basis for further exploration into SSB's unique interactions with forked DNA substrates.

PriA preferentially photo-crosslinks to probe sites near the fork juncture. It has been shown previously that PriA recognizes forked structures [25], and a structural

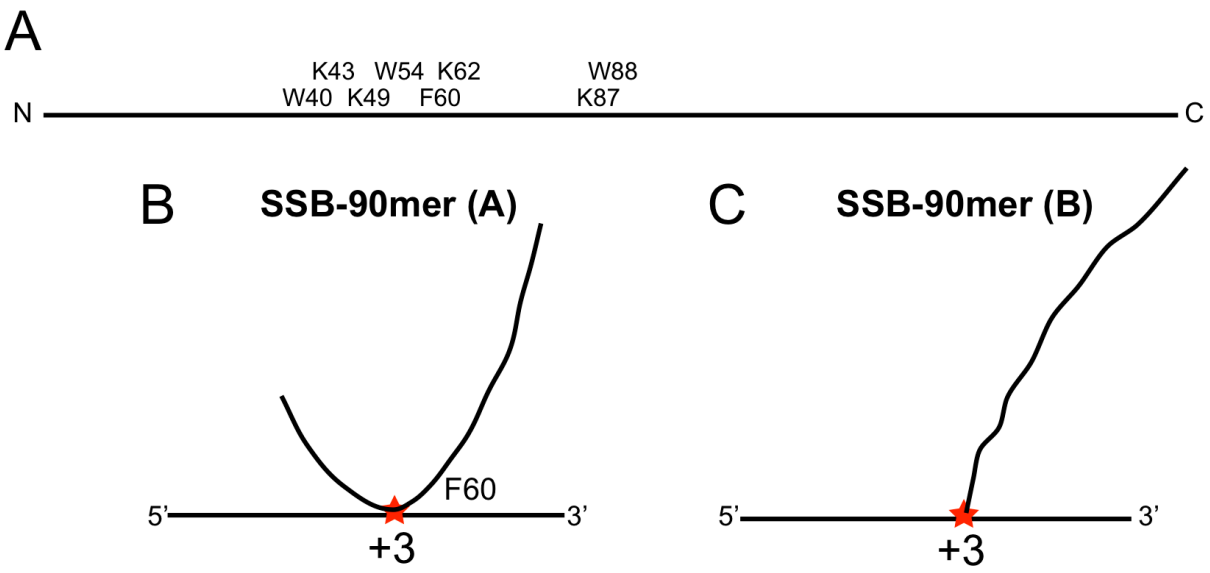

FIGURE 6.8
(A) Schematic of SSB's primary sequence (178 amino acids). Residues known to make direct contact with ssDNA are indicated. (B) Proposed crosslinking product SSB-90mer (A). F60 is shown as an example. (C) Proposed crosslinking product SSB-90mer (B).

study has shown PriA binding specifically to the terminus of the leading strand primer [26]. These data are congruent with the observations presented here.

More than one PriA molecule is likely binding to the model replication fork restricting the length of available ssDNA on the lagging strand arm. An SPR study using a model replication fork with a 24 nt duplex region, a 26 nt single-stranded lagging strand arm, and a 67-mer primer on the leading strand with no gap between the 3'-end of the primer and the duplex, suggested that multiple PriA monomers can interact on a model replication fork (Yuan and McHenry, unpublished result). The binding stoichiometry between PriA and the model fork was found to be 3.5:1 (Yuan and McHenry, unpublished result). Also using SPR, on a 32-mer primer bound to a 91-mer template, PriA was observed to bind with a 3:1 stoichiometry to the primer-template (Yuan and McHenry, unpublished result). A fluorescence-based study has shown that multiple PriA molecules can also bind to ssDNA [27]. A binding stoichiometry of 2:1 between PriA and ssDNA at least 30 nt in length was observed [27]. These observations indicate that multiple copies of PriA can interact on long stretches of ssDNA and at replication forks. It has been shown that PriA occludes 20 nt when complexed to ssDNA or duplex DNA [27,28]. On the model fork in this work, if multiple PriA molecules are binding near the fork juncture, there may not be enough ssDNA exposed for PriA to bind the lagging strand arm away from the fork juncture. This could account for why PriA crosslinks to un-annealed template both 90 and 35 nts in length, but not at the -35 position in the model replication fork.

When PriA binds ssDNA, a DNA-DNA crosslink occurs. Presumably, PriA is binding the single-stranded oligonucleotides and multiple PriAs are binding one another bringing the non-complementary strands together.

DNA-DNA crosslinks form at several probe positions, but only in the presence of a bound protein. Photolysis of diazirines generate highly reactive carbenes which efficiently insert themselves into available C-H or O-H bonds [14,15]. The lifetime of a carbene produced from a phenyldiazirine is very short (nanoseconds) and if a protein is not making close contact at a probe position, the reactive diazirine will be quenched by surrounding water [15,29]. I do not observe DNA-DNA crosslinks in the absence of a bound protein. When no protein is present at a given site, the larger proximal concentration of solvating water molecules likely react with the carbene with much greater probability. Therefore, the carbene is quenched by the dominating carbene-water reaction. When a protein is bound, the DNA is at least partially dehydrated causing a slower quenching of the carbene and facilitating the DNA-DNA crosslink.

I show here that photo-crosslinking can be used to show one protein blocking another from binding. In Chapter 3, I observe that PriA needs to be added to a reaction before SSB for PriA to inhibit the strand displacement reaction by Pol III. There, I hypothesize that SSB can block the PriA binding site and prevent interaction between the fork and PriA if SSB is added to the reaction first, allowing the necessary contact between SSB and Pol III for the strand displacement reaction to occur. It follows that in a dynamic system PriA may bind to an initial single-stranded portion of the lagging strand near the fork juncture that is too small to stably bind SSB. SSB binding is blocked thereby preventing contact with Pol III, stopping the strand displacement

reaction. In this study, I show that SSB photo-crosslinks with little efficiency where PriA binds when PriA is added to the reaction first. This validates the claim that PriA is can bind to initial single-stranded regions of DNA near the fork juncture, and physically block these regions from SSB.

It has previously been established that using high non-physiological concentrations, DnaB can self-load onto the lagging strand arm of a model replication fork (Chapter 3). There, I observe that in the presence of ATP nearly all of the DNA substrate was unwound by the self-loading helicase (Chapter 3). The self-loading reaction was blocked by the presence of either streptavidin on the 5'-end of the lagging strand or SSB (Chapter 3). Similar conditions were examined here in Fig. 6.5 in the presence of non-hydrolyzable ATPγS to stabilize the helicase on the DNA. Here, DnaB contacts ssDNA in the displaced strand 6 nucleotides upstream of the fork juncture. DnaB also makes contact with the lagging strand at least 3 nucleotides into the duplex. Ostensibly, DnaB is loaded onto the lagging strand and diffuses partially into the duplex in the presence of non-hydrolyzable ATPγS, allowing the photo-crosslink.

To date, this study contains the only observation of a direct contact between DnaB helicase and the single-strand portion of the leading strand. Such an interaction has previously been proposed to take place in both *E. coli* [30] and in *Thermus aquaticus* [31], but never directly observed. In *E. coli*, kinetic and equilibrium data suggest that the leading strand arm may act as a type of fulcrum for the advancing helicase [30]. In that study, there was an optimal length for the leading strand arm (as opposed to a minimum length) to give a high unwinding rate and processivity along with the lowest dissociation rate [30]. It was suggested based on equilibrium experiments

that this interaction is transient and completely non-specific—that a large structure in the spatial location of the leading strand arm will give the same results [30]. In *T. aquaticus*, a stimulation of the helicase is observed on substrate with a leading strand arm [31].

A physical contact between the leading strand and the helicase might provide stabilization for the helicase as it advances on the lagging strand during unwinding. The portions of the protein that are known to interact with the lagging strand are in the center of the hexameric helicase [32,33]. As the helicase progresses along the lagging strand, amino acids on the exterior portion of the ring make contact with the displaced leading strand resulting in interactions between the exterior of the helicase and the leading strand that mutually stabilize both the unwound strand and the protein. Preliminary tests to identify residues within a protein that photo-crosslink to model substrates are discussed in Appendix 5 and references therein. A similar experiment could be performed using DnaB helicase and a model replication fork with the photo-crosslinker placed at the -6 position to initially identify the residues within DnaB that make contact with the displaced strand. The importance of this interaction can be tested by making point mutations at these residues.

DnaB also photo-crosslinks at the -6 and +3 positions when the helicase is loaded by the PriA-pathway. At these probe positions, crosslinks to DnaB, PriA, and SSB are observed. A competition experiment will need to be performed to conclusively determine whether or not PriA and SSB can be excluded upon DnaB loading. Likely multiple populations are being observed in the experiments reported here. I none

population, the helicase is loaded. Another population consists of incomplete, uninitiated complexes.

The photo-crosslinking method presented here shows that placement of a non-specific photo-crosslinker in a model substrate can be used to identify contacts between DNA and protein subunits. This method is extremely valuable in detecting and identifying protein-DNA contacts on model substrates.

6.6 REFERENCES

1 Ng, J. Y. and Marians, K. J. (1996) The ordered assembly of the ΦX174-type primosome. I. Isolation and identification of intermediate protein-DNA complexes. The Journal of Biological Chemistry **271**, 15642–8.

2 McCool, J. D., Ford, C. C. and Sandler, S. J. (2004) A dnaT mutant with phenotypes similar to those of a priA2::kan mutant in *Escherichia coli* K-12. Genetics **167**, 569–78.

3 Sandler, S. J., Marians, K. J., Zavitz, K. H., Coutu, J., Parent, M. A. and Clark, A. J. (1999) dnaC mutations suppress defects in DNA replication- and recombination-associated functions in priB and priC double mutants in *Escherichia coli* K-12. Molecular Microbiology **34**, 91–101.

4 Heller, R. C. and Marians, K. J. (2005) The disposition of nascent strands at stalled replication forks dictates the pathway of replisome loading during restart. Molecular Cell **17**, 733–43.

5 Lopper, M., Boonsombat, R., Sandler, S. J. and Keck, J. L. (2007) A hand-off mechanism for primosome assembly in replication restart. Molecular Cell **26**, 781–93.

6 Cadman, C. J. and McGlynn, P. (2004) PriA helicase and SSB interact physically and functionally. Nucleic Acids Research **32**, 6378–87.

7 Costes, A., Lecointe, F., McGovern, S., Quevillon-Cheruel, S. and Polard, P. (2010) The C-terminal domain of the bacterial SSB protein acts as a DNA maintenance hub at active chromosome replication forks. PLoS Genetics **6**, e1001238.

8 Liu, J.-H., Chang, T.-W., Huang, C.-Y., Chen, S.-U., Wu, H.-N., Chang, M.-C. and Hsiao, C.-D. (2004) Crystal structure of PriB, a primosomal DNA replication protein of *Escherichia coli*. The Journal of Biological Chemistry **279**, 50465–71.

9 Shioi, S., Ose, T., Maenaka, K., Shiroishi, M., Abe, Y., Kohda, D., Katayama, T. and Ueda, T. (2005) Crystal structure of a biologically functional form of PriB from Escherichia coli reveals a potential single-stranded DNA-binding site. Biochemical and Biophysical Research Communications **326**, 766–76.

10 Lopper, M., Holton, J. M. and Keck, J. L. (2004) Crystal structure of PriB, a component of the *Escherichia coli* replication restart primosome. Structure (London, England : 1993) **12**, 1967–75.

11 Cadman, C. J., Lopper, M., Moon, P. B., Keck, J. L. and McGlynn, P. (2005) PriB stimulates PriA helicase via an interaction with single-stranded DNA. The Journal of Biological Chemistry **280**, 39693–700.

12 Liu, J., Nurse, P. and Marians, K. J. (1996) The ordered assembly of the ΦX174-type primosome. III. PriB facilitates complex formation between PriA and DnaT. The Journal of Biological Chemistry **271**, 15656–61.

13 Ng, J. Y. and Marians, K. J. (1996) The ordered assembly of the ΦX174-type primosome. II. Preservation of primosome composition from assembly through replication. The Journal of Biological Chemistry **271**, 15649–55.

14 Bayley, H. (1983) Laboratory techniques in biochemistry and molecular biology: Photogenerated reagents in biochemistry and molecular biology / Hagan Bayley, Volume 12, p 187, Elsevier.

15 Tate, J. J., Persinger, J. and Bartholomew, B. (1998) Survey of four different photoreactive moieties for DNA photoaffinity labeling of yeast RNA polymerase III transcription complexes. Nucleic Acids Research **26**, 1421–6.

16 Griep, M. A. and McHenry, C. S. (1989) Glutamate overcomes the salt inhibition of DNA polymerase III holoenzyme. The Journal of Biological Chemistry **264**, 11294–301.

17 Marians, K. J. (1995) ΦX174-type primosomal proteins: purification and assay. Methods in Enzymology **262**, 507–21.

18 Curth, U., Greipel, J., Urbanke, C. and Maass, G. (1993) Multiple binding modes of the single-stranded DNA binding protein from *Escherichia coli* as detected by tryptophan fluorescence and site-directed mutagenesis. Biochemistry **32**, 2585–91.

19 Casas-Finet, J. R., Jhon, N. I., Khamis, M. I., Maki, A. H., Ruvolo, P. P. and Chase, J. W. (1988) An IncY plasmid-encoded single-stranded DNA-binding protein from *Escherichia coli* shows the identical pattern of stacked tryptophan residues as the chromosomal ssb gene product. European Journal of Biochemistry / FEBS **178**, 101–7.

20 Casas-Finet, J. R., Khamis, M. I., Maki, A. H. and Chase, J. W. (1987) Tryptophan 54 and phenylalanine 60 are involved synergistically in the binding of *E. coli* SSB protein to single-stranded polynucleotides. FEBS Letters **220**, 347–52.

21 Raghunathan, S., Ricard, C. S., Lohman, T. M. and Waksman, G. (1997) Crystal structure of the homo-tetrameric DNA binding domain of *Escherichia coli* single-stranded DNA-binding protein determined by multiwavelength x-ray diffraction on

the selenomethionyl protein at 2.9-A resolution. Proceedings of the National Academy of Sciences of the United States of America **94**, 6652–7.

22 Anderson, R. A. and Coleman, J. E. (1975) Physiochemical properties of DNA binding proteins: gene 32 protein of T4 and *Escherichia coli* unwinding protein. Biochemistry **14**, 5485–91.

23 Overman, L. B., Bujalowski, W. and Lohman, T. M. (1988) Equilibrium binding of Escherichia coli single-strand binding protein to single-stranded nucleic acids in the $(SSB)_{65}$ binding mode. Cation and anion effects and polynucleotide specificity. Biochemistry **27**, 456–71.

24 Shereda, R. D., Kozlov, A. G., Lohman, T. M., Cox, M. M. and Keck, J. L. SSB as an organizer/mobilizer of genome maintenance complexes. Critical Reviews in Biochemistry and Molecular Biology **43**, 289–318.

25 Jones, J. M. and Nakai, H. (2000) PriA and phage T4 gp59: factors that promote DNA replication on forked DNA substrates microreview. Molecular Microbiology **36**, 519–27.

26 Sasaki, K., Ose, T., Okamoto, N., Maenaka, K., Tanaka, T., Masai, H., Saito, M., Shirai, T. and Kohda, D. (2007) Structural basis of the 3'-end recognition of a leading strand in stalled replication forks by PriA. The EMBO Journal **26**, 2584–93.

27 Jezewska, M. J., Rajendran, S. and Bujalowski, W. (2000) *Escherichia coli* replicative helicase PriA protein-single-stranded DNA complex. Stoichiometries, free energy of binding, and cooperativities. The Journal of Biological Chemistry **275**, 27865–73.

28 Tanaka, T., Mizukoshi, T., Sasaki, K., Kohda, D. and Masai, H. (2007) Escherichia coli PriA protein, two modes of DNA binding and activation of ATP hydrolysis. The Journal of Biological Chemistry **282**, 19917–27.

29 Wang, T., Toscano, J. P. and Celius, T. C. (2010) CRC Handbookof Organic Photochemistry and Photobiology, Volumes 1 & 2, Second Edition 2nd ed., p 2904, CRC Press.

30 Galletto, R., Jezewska, M. J. and Bujalowski, W. (2004) Unzipping mechanism of the double-stranded DNA unwinding by a hexameric helicase: the effect of the 3' arm and the stability of the dsDNA on the unwinding activity of the *Escherichia coli* DnaB helicase. Journal of Molecular Biology **343**, 101–14.

31 Kaplan, D. L. and Steitz, T. A. (1999) DnaB from *Thermus aquaticus* unwinds forked duplex DNA with an asymmetric tail length dependence. The Journal of Biological Chemistry **274**, 6889–97.

32 Singleton, M. R., Sawaya, M. R., Ellenberger, T. and Wigley, D. B. (2000) Crystal structure of T7 gene 4 ring helicase indicates a mechanism for sequential hydrolysis of nucleotides. Cell **101**, 589–600.

33 Bailey, S., Eliason, W. K. and Steitz, T. A. (2007) Structure of hexameric DnaB helicase and its complex with a domain of DnaG primase. Science (New York, N.Y.) **318**, 459–63.

COMPLETE BIBLIOGRAPHY*

1 Alberts, B. M., Barry, J., Bedinger, P., Formosa, T., Jongeneel, C. V and Kreuzer, K. N. (1983) Studies on DNA replication in the bacteriophage T4 *in vitro* system. Cold Spring Harbor Symposia on Quantitative Biology **47 Pt 2**, 655–68.

2 Alfano, C. and McMacken, R. (1989) Heat shock protein-mediated disassembly of nucleoprotein structures is required for the initiation of bacteriophage λ DNA replication. The Journal of Biological Chemistry **264**, 10709–18.

3 Allen, G. C. and Kornberg, A. (1993) Assembly of the primosome of DNA replication in *Escherichia coli*. The Journal of Biological Chemistry **268**, 19204–9.

4 Alonso, J.C., Tavares, P., Lurz, R. and Trautner, T. A. (2006) Bacteriophage SPP1. Calendar, R. (ed.), The Bacteriophages, 2nd edn., Oxford University Press, Oxford, New York.

5 Anderson, R. A. and Coleman, J. E. (1975) Physiochemical properties of DNA binding proteins: gene 32 protein of T4 and *Escherichia coli* unwinding protein. Biochemistry **14**, 5485–91.

6 Antony, E., Kozlov, A. G., Nguyen, B. and Lohman, T. M. (2012) Plasmodium falciparum SSB tetramer binds single-stranded DNA only in a fully wrapped mode. Journal of Molecular Ciology **420**, 284–95.

7 Antony, E., Weiland, E. A., Korolev, S. and Lohman, T. M. (2012) Plasmodium falciparum SSB tetramer wraps single-stranded DNA with similar topology but opposite polarity to *E. coli* SSB. Journal of Molecular Biology **420**, 269–83.

8 Arad, G., Hendel, A., Urbanke, C., Curth, U. and Livneh, Z. (2008) Single-stranded DNA-binding protein recruits DNA polymerase V to primer termini on RecA-coated DNA. The Journal of Biological Chemistry **283**, 8274–82.

9 Arai, K., Low, R., Kobori, J., Shlomai, J. and Kornberg, A. (1981) Mechanism of dnaB protein action. V. Association of dnaB protein, protein n', and other repriming proteins in the primosome of DNA replication. The Journal of Biological Chemistry **256**, 5273–80.

10 Ayora, S., Missich, R., Mesa, P., Lurz, R., Yang, S., Egelman, E. H. and Alonso, J. C. (2002) Homologous-pairing activity of the *Bacillus subtilis* bacteriophage

* The references included at the end of each chapter are compiled here in alphabetical order.

SPP1 replication protein G35P. The Journal of Biological Chemistry **277**, 35969–79.

11 Ayora, S., Stasiak, A. and Alonso, J. C. (1999) The *Bacillus subtilis* bacteriophage SPP1 G39P delivers and activates the G40P DNA helicase upon interacting with the G38P-bound replication origin. Journal of Molecular Biology **288**, 71–85.

12 Ayora, S., Weise, F., Mesa, P., Stasiak, A. and Alonso, J. C. (2002) *Bacillus subtilis* bacteriophage SPP1 hexameric DNA helicase, G40P, interacts with forked DNA. Nucleic Acids Research **30**, 2280–9.

13 Bailey, S., Eliason, W. K. and Steitz, T. A. (2007) Structure of hexameric DnaB helicase and its complex with a domain of DnaG primase. Science (New York, N.Y.) **318**, 459–63.

14 Bailey, S., Sedelnikova, S. E., Mesa, P., Ayora, S., Waltho, J. P., Ashcroft, A. E., Baron, A. J., Alonso, J. C. and Rafferty, J. B. (2003) Structural analysis of *Bacillus subtilis* SPP1 phage helicase loader protein G39P. The Journal of Biological Chemistry **278**, 15304–12.

15 Bayley, H. (1983) Laboratory techniques in biochemistry and molecular biology: Photogenerated reagents in biochemistry and molecular biology / Hagan Bayley, Volume 12, p 187, Elsevier.

16 Bernstein, D. A., Eggington, J. M., Killoran, M. P., Misic, A. M., Cox, M. M. and Keck, J. L. (2004) Crystal structure of the *Deinococcus radiodurans* single-stranded DNA-binding protein suggests a mechanism for coping with DNA damage. Proceedings of the National Academy of Sciences of the United States of America **101**, 8575–80.

17 Biesele, J. J., Philips, F. S., Thiersch, J. B., Burchenal, J. H., Buckley, S. M., Stock, C. C., Loveless, A. And Ross, W. C. J. (1950) Chromosome alteration and tumour inhibition by nitrogen mustards; the hypothesis of crosslinking alkylation. Nature **166**, 1112–4.

18 Bjornson, K. P., Amaratunga, M., Moore, K. J. and Lohman, T. M. (1994) Single-turnover kinetics of helicase-catalyzed DNA unwinding monitored continuously by fluorescence energy transfer. Biochemistry **33**, 14306–16.

19 Blanco, L. and Salas, M. (1985) Replication of phage Φ29 DNA with purified terminal protein and DNA polymerase: synthesis of full-length Φ29 DNA. Proceedings of the National Academy of Sciences of the United States of America **82**, 6404–8.

20 Boehmer, P. E. and Lehman, I. R. (1997) Herpes simplex virus DNA replication. Annual Review of Biochemistry **66**, 347–84.

21 Bonura, T. and Smith, K. C. (1975) Quantitative evidence for enzymatically-indeced DNA double-strand breaks as lethal lesions in UV irradiated pol+ and polA1 strains of *E. coli* K-12. Photochemistry and photobiology **22**, 243–8.

22 Brandsma, J. A., Bosch, D., De Ruÿter, M. and Van de Putte, P. (1985) Analysis of the regulatory region of the ssb gene of *Escherichia coli*. Nucleic Acids Research **13**, 5095–109.

23 Braun, K. A., Lao, Y., He, Z., Ingles, C. J. and Wold, M. S. (1997) Role of protein-protein interactions in the function of replication protein A (RPA): RPA modulates the activity of DNA polymerase α by multiple mechanisms. Biochemistry **36**, 8443–54.

24 Breier, A. M., Weier, H.-U. G. and Cozzarelli, N. R. (2005) Independence of replisomes in *Escherichia coli* chromosomal replication. Proceedings of the National Academy of Sciences of the United States of America **102**, 3942–7.

25 Bruand, C., Ehrlich, S. D. and Jannière, L. (1995) Primosome assembly site in *Bacillus subtilis*. The EMBO Journal **14**, 2642–50.

26 Bruand, C., Farache, M., McGovern, S., Ehrlich, S. D. and Polard, P. (2001) DnaB, DnaD and DnaI proteins are components of the *Bacillus subtilis* replication restart primosome. Molecular Microbiology **42**, 245–55.

27 Bruand, C., Velten, M., McGovern, S., Marsin, S., Sérèna, C., Ehrlich, S. D. and Polard, P. (2005) Functional interplay between the *Bacillus subtilis* DnaD and DnaB proteins essential for initiation and re-initiation of DNA replication. Molecular Microbiology **55**, 1138–50.

28 Bruck, I. and O'Donnell, M. (2000) The DNA replication machine of a gram-positive organism. The Journal of Biological Chemistry **275**, 28971–83.

29 Bujalowski, W. and Lohman, T. M. (1986) *Escherichia coli* single-strand binding protein forms multiple, distinct complexes with single-stranded DNA. Biochemistry **25**, 7799–802.

30 Bujalowski, W. and Lohman, T. M. (1991) Monomers of the *Escherichia coli* SSB-1 mutant protein bind single-stranded DNA. Journal of Molecular Biology **217**, 63–74.

31 Bujalowski, W. and Lohman, T. M. (1989) Negative co-operativity in *Escherichia coli* single strand binding protein-oligonucleotide interactions. I. Evidence and a quantitative model. Journal of Molecular Biology **207**, 249–68.

32 Bujalowski, W. and Lohman, T. M. (1989) Negative co-operativity in *Escherichia coli* single strand binding protein-oligonucleotide interactions. II. Salt, temperature and oligonucleotide length effects. Journal of Molecular Biology **207**, 269–88.

33 Bujalowski, W., Overman, L. B. and Lohman, T. M. (1988) Binding mode transitions of *Escherichia coli* single strand binding protein-single-stranded DNA complexes. Cation, anion, pH, and binding density effects. The Journal of Biological Chemistry **263**, 4629–40.

34 Cadman, C. J., Lopper, M., Moon, P. B., Keck, J. L. and McGlynn, P. (2005) PriB stimulates PriA helicase via an interaction with single-stranded DNA. The Journal of Biological Chemistry **280**, 39693–700.

35 Cadman, C. J. and McGlynn, P. (2004) PriA helicase and SSB interact physically and functionally. Nucleic Acids Research **32**, 6378–87.

36 Carter, J. R., Franden, M. A., Aebersold, R., Kim, D. R. and McHenry, C. S. (1993) Isolation, sequencing and overexpression of the gene encoding the θ subunit of DNA polymerase III holoenzyme. Nucleic Acids Research **21**, 3281–6.

37 Casas-Finet, J. R., Jhon, N. I., Khamis, M. I., Maki, A. H., Ruvolo, P. P. and Chase, J. W. (1988) An IncY plasmid-encoded single-stranded DNA-binding protein from *Escherichia coli* shows the identical pattern of stacked tryptophan residues as the chromosomal ssb gene product. European Journal of Biochemistry / FEBS **178**, 101–7.

38 Casas-Finet, J. R., Khamis, M. I., Maki, A. H. and Chase, J. W. (1987) Tryptophan 54 and phenylalanine 60 are involved synergistically in the binding of *E. coli* SSB protein to single-stranded polynucleotides. FEBS Letters **220**, 347–52.

39 Christie, G. E., Matthews, A. M., King, D. G., Lane, K. D., Olivarez, N. P., Tallent, S. M., Gill, S. R. and Novick, R. P. (2010) The complete genomes of *Staphylococcus aureus* bacteriophages 80 and 80α--implications for the specificity of SaPI mobilization. Virology **407**, 381–90.

40 Chrysogelos, S. and Griffith, J. (1982) *Escherichia coli* single-strand binding protein organizes single-stranded DNA in nucleosome-like units. Proceedings of the National Academy of Sciences of the United States of America **79**, 5803–7.

41 Condon, C. (2003) RNA processing and degradation in *Bacillus subtilis*. Microbiology and Molecular Biology Reviews.

42 Costes, A., Lecointe, F., McGovern, S., Quevillon-Cheruel, S. and Polard, P. (2010) The C-terminal domain of the bacterial SSB protein acts as a DNA maintenance hub at active chromosome replication forks. PLoS Genetics **6**, e1001238.

43 Cox, M. M. (2001) Recombinational DNA repair of damaged replication forks in *Escherichia coli*: questions. Annual Review of Genetics **35**, 53–82.

44 Cox, M. M., Goodman, M. F., Kreuzer, K. N., Sherratt, D. J., Sandler, S. J. and Marians, K. J. (2000) The importance of repairing stalled replication forks. Nature **404**, 37–41.

45 Curth, U., Genschel, J., Urbanke, C. and Greipel, J. (1996) *In vitro* and *in vivo* function of the C-terminus of *Escherichia coli* single-stranded DNA binding protein. Nucleic Acids Research **24**, 2706–11.

46 Curth, U., Greipel, J., Urbanke, C. and Maass, G. (1993) Multiple binding modes of the single-stranded DNA binding protein from *Escherichia coli* as detected by tryptophan fluorescence and site-directed mutagenesis. Biochemistry **32**, 2585–91.

47 Cámara, B., Liu, M., Reynolds, J., Shadrin, A., Liu, B., Kwok, K., Simpson, P., Weinzierl, R., Severinov, K., Cota, E., *et al*. (2010) T7 phage protein Gp2 inhibits the *Escherichia coli* RNA polymerase by antagonizing stable DNA strand separation near the transcription start site. Proceedings of the National Academy of Sciences of the United States of America **107**, 2247–52.

48 Dallmann, H. G., Fackelmayer, O. J., Tomer, G., Chen, J., Wiktor-Becker, A., Ferrara, T., Pope, C., Oliveira, M. T., Burgers, P. M. J., Kaguni, L. S., *et al*. (2010) Parallel multiplicative target screening against divergent bacterial replicases: identification of specific inhibitors with broad spectrum potential. Biochemistry **49**, 2551–62.

49 Dallmann, H. G., Thimmig, R. L. and McHenry, C. S. (1995) DnaX complex of Escherichia coli DNA polymerase III holoenzyme. Central role of τ in initiation complex assembly and in determining the functional asymmetry of holoenzyme. The Journal of Biological Chemistry **270**, 29555–62.

50 Dalrymple, B. P., Kongsuwan, K., Wijffels, G., Dixon, N. E. and Jennings, P. A. (2001) A universal protein-protein interaction motif in the eubacterial DNA replication and repair systems. Proceedings of the National Academy of Sciences of the United States of America **98**, 11627–32.

51 Dam, J. and Schuck, P. (2004) Calculating sedimentation coefficient distributions by direct modeling of sedimentation velocity concentration profiles. Methods in Enzymology **384**, 185–212.

52 Dean, F. B., Bullock, P., Murakami, Y., Wobbe, C. R., Weissbach, L. and Hurwitz, J. (1987) Simian virus 40 (SV40) DNA replication: SV40 large T antigen unwinds DNA containing the SV40 origin of replication. Proceedings of the National Academy of Sciences of the United States of America **84**, 16–20.

53 Dean, F. B., Nelson, J. R., Giesler, T. L. and Lasken, R. S. (2001) Rapid amplification of plasmid and phage DNA using Φ29 DNA polymerase and multiply-primed rolling circle amplification. Genome Research **11**, 1095–9.

54 Dervyn, E., Suski, C., Daniel, R., Bruand, C., Chapuis, J., Errington, J., Jannière, L. and Ehrlich, S. D. (2001) Two essential DNA polymerases at the bacterial replication fork. Science (New York, N.Y.) **294**, 1716–9.

55 Dohrmann, P. R., Manhart, C. M., Downey, C. D. and McHenry, C. S. (2011) The Rate of Polymerase Release upon Filling the Gap between Okazaki Fragments Is Inadequate to Support Cycling during Lagging Strand Synthesis. Journal of Molecular Biology, Elsevier Ltd **414**, 15–27.

56 Dohrmann, P. R. and McHenry, C. S. (2005) A bipartite polymerase-processivity factor interaction: only the internal β binding site of the alpha subunit is required for processive replication by the DNA polymerase III holoenzyme. Journal of Molecular Biology **350**, 228–39.

57 Downey, C. D., Crooke, E. and McHenry, C. S. (2011) Polymerase chaperoning and multiple ATPase sites enable the *E. coli* DNA polymerase III holoenzyme to rapidly form initiation complexes. Journal of Molecular Biology **412**, 340–53.

58 Downey, C. D. and McHenry, C. S. (2010) Chaperoning of a replicative polymerase onto a newly assembled DNA-bound sliding clamp by the clamp loader. Molecular Cell **37**, 481–91.

59 Eisenberg, S., Griffith, J. and Kornberg, A. (1977) ΦX174 cistron A protein is a multifunctional enzyme in DNA replication. Proceedings of the National Academy of Sciences of the United States of America **74**, 3198–202.

60 Evans, R. J., Davies, D. R., Bullard, J. M., Christensen, J., Green, L. S., Guiles, J. W., Pata, J. D., Ribble, W. K., Janjic, N. and Jarvis, T. C. (2008) Structure of PolC reveals unique DNA binding and fidelity determinants. Proceedings of the National Academy of Sciences of the United States of America **105**, 20695–700.

61 Ezekiel, D. H. and Hutchins, J. E. (1968) Mutations affecting RNA polymerase associated with rifampicin resistance in *Escherichia coli*. Nature **220**, 276–7.

62 Fay, P. J., Johanson, K. O., McHenry, C. S. and Bambara, R. A. (1982) Size classes of products synthesized processively by two subassemblies of *Escherichia coli* DNA polymerase III holoenzyme. The Journal of Biological Chemistry **257**, 5692–9.

63 Fedorov, R., Witte, G., Urbanke, C., Manstein, D. J. and Curth, U. (2006) 3D structure of *Thermus aquaticus* single-stranded DNA-binding protein gives insight into the functioning of SSB proteins. Nucleic Acids Research **34**, 6708–17.

64 Ferrari, M. E., Bujalowski, W. and Lohman, T. M. (1994) Co-operative binding of *Escherichia coli* SSB tetramers to single-stranded DNA in the $(SSB)_{35}$ binding mode. Journal of Molecular Biology **236**, 106–23.

65 Fijalkowska, I. J. and Schaaper, R. M. (1996) Mutants in the Exo I motif of *Escherichia coli* dnaQ: defective proofreading and inviability due to error catastrophe. Proceedings of the National Academy of Sciences of the United States of America **93**, 2856–61.

66 Fleming, S. A. (1995) Chemical Reagents in Photoaffinity Labeling. Tetrahedron **51**, 12479–12520.

67 Galletto, R., Jezewska, M. J. and Bujalowski, W. (2004) Unzipping mechanism of the double-stranded DNA unwinding by a hexameric helicase: the effect of the 3' arm and the stability of the dsDNA on the unwinding activity of the *Escherichia coli* DnaB helicase. Journal of Molecular Biology **343**, 101–14.

68 Gao, D. and McHenry, C. S. (2001) τ binds and organizes *Escherichia coli* replication proteins through distinct domains. Domain III, shared by γ and τ, binds δδ' and χψ. The Journal of Biological Chemistry **276**, 4447–53.

69 George, N. P., Ngo, K. V, Chitteni-Pattu, S., Norais, C. A., Battista, J. R., Cox, M. M. and Keck, J. L. (2012) Structure and cellular dynamics of *Deinococcus radiodurans* single-stranded DNA (ssDNA)-binding protein (SSB)-DNA complexes. The Journal of Biological Chemistry **287**, 22123–32.

70 Georgescu, R. E., Kurth, I., Yao, N. Y., Stewart, J., Yurieva, O. and O'Donnell, M. (2009) Mechanism of polymerase collision release from sliding clamps on the lagging strand. The EMBO Journal **28**, 2981–91.

71 Glover, B. P. and McHenry, C. S. (1998) The χ ψ subunits of DNA polymerase III holoenzyme bind to single-stranded DNA-binding protein (SSB) and facilitate replication of an SSB-coated template. The Journal of Biological Chemistry **273**, 23476–84.

72 Glover, B. P. and McHenry, C. S. (2000) The DnaX-binding subunits δ' and ψ are bound to γ and not τ in the DNA polymerase III holoenzyme. The Journal of Biological Chemistry **275**, 3017–20.

73 Golden, M. C., Resing, K. A., Collins, B. D., Willis, M. C. and Koch, T. H. (1999) Mass spectral characterization of a protein-nucleic acid photocrosslink. Protein science : a publication of the Protein Society **8**, 2806–12.

74 Gomes, A. F. and Gozzo, F. C. (2010) Chemical cross-linking with a diazirine photoactivatable cross-linker investigated by MALDI- and ESI-MS/MS. Journal of Mass Spectrometry : JMS **45**, 892–9.

75 Griep, M. A. and McHenry, C. S. (1989) Glutamate overcomes the salt inhibition of DNA polymerase III holoenzyme. The Journal of Biological Chemistry **264**, 11294–301.

76 Griffith, J. D., Harris, L. D. and Register, J. (1984) Visualization of SSB-ssDNA complexes active in the assembly of stable RecA-DNA filaments. Cold Spring Harbor Symposia on Quantitative Biology **49**, 553–9.

77 Hamdan, S. M., Loparo, J. J., Takahashi, M., Richardson, C. C. and Van Oijen, A. M. (2009) Dynamics of DNA replication loops reveal temporal control of lagging-strand synthesis. Nature **457**, 336–9.

78 Han, E. S., Cooper, D. L., Persky, N. S., Sutera, V. A., Whitaker, R. D., Montello, M. L. and Lovett, S. T. (2006) RecJ exonuclease: substrates, products and interaction with SSB. Nucleic Acids Research **34**, 1084–91.

79 Handa, P., Acharya, N. and Varshney, U. (2001) Chimeras between single-stranded DNA-binding proteins from *Escherichia coli* and *Mycobacterium tuberculosis* reveal that their C-terminal domains interact with uracil DNA glycosylases. The Journal of Biological Chemistry **276**, 16992–7.

80 Heller, R. C. and Marians, K. J. (2005) The disposition of nascent strands at stalled replication forks dictates the pathway of replisome loading during restart. Molecular Cell **17**, 733–43.

81 Houston, P. and Kodadek, T. (1994) Spectrophotometric assay for enzyme-mediated unwinding of double-stranded DNA. Proceedings of the National Academy of Sciences of the United States of America **91**, 5471–4.

82 Huynh, M.-L., Russell, P. and Walsh, B. (2009) Tryptic digestion of in-gel proteins for mass spectrometry analysis. Methods in Molecular Biology (Clifton, N.J.) **519**, 507–13.

83 Iyer, L. M., Koonin, E. V and Aravind, L. (2002) Classification and evolutionary history of the single-strand annealing proteins, RecT, Redbeta, ERF and RAD52. BMC Genomics **3**, 8.

84 Jezewska, M. J., Rajendran, S. and Bujalowski, W. (2000) *Escherichia coli* replicative helicase PriA protein-single-stranded DNA complex. Stoichiometries, free energy of binding, and cooperativities. The Journal of Biological Chemistry **275**, 27865–73.

85 Johanson, K. O., Haynes, T. E. and McHenry, C. S. (1986) Chemical characterization and purification of the β subunit of the DNA polymerase III holoenzyme from an overproducing strain. The Journal of Biological Chemistry **261**, 11460–5.

86 Johanson, K. O. and McHenry, C. S. (1982) The β subunit of the DNA polymerase III holoenzyme becomes inaccessible to antibody after formation of an initiation complex with primed DNA. The Journal of Biological Chemistry **257**, 12310–5.

87 Jonczyk, P., Nowicka, A., Fijałkowska, I. J., Schaaper, R. M. and Cieśla, Z. (1998) *In vivo* protein interactions within the *Escherichia coli* DNA polymerase III core. Journal of Bacteriology **180**, 1563–6.

88 Jones, J. M. and Nakai, H. (1999) Duplex opening by primosome protein PriA for replisome assembly on a recombination intermediate. Journal of Molecular Biology **289**, 503–16.

89 Jones, J. M. and Nakai, H. (2000) PriA and phage T4 gp59: factors that promote DNA replication on forked DNA substrates microreview. Molecular Microbiology **36**, 519–27.

90 Jongsma, M. A. and Litjens, R. H. G. M. (2006) Self-assembling protein arrays on DNA chips by auto-labeling fusion proteins with a single DNA address. Proteomics **6**, 2650–5.

91 Kaboord, B. F. and Benkovic, S. J. (1993) Rapid assembly of the bacteriophage T4 core replication complex on a linear primer/template construct. Proceedings of the National Academy of Sciences of the United States of America **90**, 10881–5.

92 Kaguni, J. M. (2006) DnaA: controlling the initiation of bacterial DNA replication and more. Annual Review of Microbiology **60**, 351–75.

93 Kaguni, J. and Ray, D. S. (1979) Cloning of a functional replication origin of phage G4 into the genome of phage M13. Journal of Molecular Biology **135**, 863–78.

94 Kaplan, D. L. and Steitz, T. A. (1999) DnaB from *Thermus aquaticus* unwinds forked duplex DNA with an asymmetric tail length dependence. The Journal of Biological Chemistry **274**, 6889–97.

95 Kelman, Z. and Hurwitz, J. (1998) Protein-PCNA interactions: a DNA-scanning mechanism? Trends in Biochemical Sciences **23**, 236–8.

96 Kelman, Z., Yuzhakov, A., Andjelkovic, J. and O'Donnell, M. (1998) Devoted to the lagging strand-the subunit of DNA polymerase III holoenzyme contacts SSB to promote processive elongation and sliding clamp assembly. The EMBO Journal **17**, 2436–49.

97 Kidane, D., Ayora, S., Sweasy, J. B., Graumann, P. L. and Alonso, J. C. The cell pole: the site of cross talk between the DNA uptake and genetic recombination machinery. Critical Reviews in Biochemistry and Molecular Biology **47**, 531–55.

98 Kim, D. R. and McHenry, C. S. (1996) Identification of the β-binding domain of the α subunit of *Escherichia coli* polymerase III holoenzyme. The Journal of Biological Chemistry **271**, 20699–704.

99 Kim, D. R. and McHenry, C. S. (1996) *In vivo* assembly of overproduced DNA polymerase III. Overproduction, purification, and characterization of the α, α-ε, and α-ε-θ subunits. The Journal of Biological Chemistry **271**, 20681–9.

100 Kim, S., Dallmann, H. G., McHenry, C. S. and Marians, K. J. (1996) Coupling of a replicative polymerase and helicase: a τ-DnaB interaction mediates rapid replication fork movement. Cell **84**, 643–50.

101 Kim, S., Dallmann, H. G., McHenry, C. S. and Marians, K. J. (1996) τcouples the leading- and lagging-strand polymerases at the *Escherichia coli* DNA replication fork. The Journal of Biological Chemistry **271**, 21406–12.

102 Kogoma, T., Cadwell, G. W., Barnard, K. G. and Asai, T. (1996) The DNA replication priming protein, PriA, is required for homologous recombination and double-strand break repair. Journal of Bacteriology **178**, 1258–64.

103 Kong, X. P., Onrust, R., O'Donnell, M. and Kuriyan, J. (1992) Three-dimensional structure of the β subunit of *E. coli* DNA polymerase III holoenzyme: a sliding DNA clamp. Cell **69**, 425–37.

104 Konrad, E. B. and Lehman, I. R. (1974) A conditional lethal mutant of *Escherichia coli* K12 defective in the 5' leads to 3' exonuclease associated with DNA polymerase I. Proceedings of the National Academy of Sciences of the United States of America **71**, 2048–51.

105 Koonin, E. V and Bork, P. (1996) Ancient duplication of DNA polymerase inferred from analysis of complete bacterial genomes. Trends in Biochemical Sciences **21**, 128–9.

106 Kornberg, A. (1992) DNA Polymerase II of E. coli. In DNA Replication, p 167, W.H. Freeman and Company New York, NY.

107 Kowalczykowski, S. C., Dixon, D. A., Eggleston, A. K., Lauder, S. D. and Rehrauer, W. M. (1994) Biochemistry of homologous recombination in *Escherichia coli*. Microbiological reviews **58**, 401–65.

108 Kozlov, A. G., Cox, M. M. and Lohman, T. M. (2010) Regulation of single-stranded DNA binding by the C termini of *Escherichia coli* single-stranded DNA-binding (SSB) protein. The Journal of Biological Chemistry **285**, 17246–52.

109 Kozlov, A. G., Jezewska, M. J., Bujalowski, W. and Lohman, T. M. (2010) Binding specificity of *Escherichia coli* single-stranded DNA binding protein for the χ subunit of DNA pol III holoenzyme and PriA helicase. Biochemistry **49**, 3555–66.

110 Kozlov, A. G. and Lohman, T. M. (2002) Stopped-flow studies of the kinetics of single-stranded DNA binding and wrapping around the *Escherichia coli* SSB tetramer. Biochemistry **41**, 6032–44.

111 Krivos, K. L. and Limbach, P. A. (2010) Sequence analysis of peptide:oligonucleotide heteroconjugates by electron capture dissociation and electron transfer dissociation. Journal of the American Society for Mass Spectrometry **21**, 1387–97.

112 LaDuca, R. J., Crute, J. J., McHenry, C. S. and Bambara, R. A. (1986) The beta subunit of the *Escherichia coli* DNA polymerase III holoenzyme interacts functionally with the catalytic core in the absence of other subunits. The Journal of Biological Chemistry **261**, 7550–7.

113 Lamers, M. H., Georgescu, R. E., Lee, S.-G., O'Donnell, M. and Kuriyan, J. (2006) Crystal structure of the catalytic α subunit of *E. coli* replicative DNA polymerase III. Cell **126**, 881–92.

114 Lark, C. A., Riazi, J. and Lark, K. G. (1978) dnaT, dominant conditional-lethal mutation affecting DNA replication in *Escherichia coli*. Journal of Bacteriology **136**, 1008–17.

115 Lecointe, F., Sérèna, C., Velten, M., Costes, A., McGovern, S., Meile, J.-C., Errington, J., Ehrlich, S. D., Noirot, P. and Polard, P. (2007) Anticipating chromosomal replication fork arrest: SSB targets repair DNA helicases to active forks. The EMBO Journal **26**, 4239–51.

116 Lee, E. H. and Kornberg, A. (1991) Replication deficiencies in priA mutants of *Escherichia coli* lacking the primosomal replication n' protein. Proceedings of the National Academy of Sciences of the United States of America **88**, 3029–32.

117 Lee, J., Chastain, P. D., Kusakabe, T., Griffith, J. D. and Richardson, C. C. (1998) Coordinated leading and lagging strand DNA synthesis on a minicircular template. Molecular Cell **1**, 1001–10.

118 Lee, J.-B., Hite, R. K., Hamdan, S. M., Xie, X. S., Richardson, C. C. and Van Oijen, A. M. (2006) DNA primase acts as a molecular brake in DNA replication. Nature **439**, 621–4.

119 Lee, M. S. and Marians, K. J. (1987) *Escherichia coli* replication factor Y, a component of the primosome, can act as a DNA helicase. Proceedings of the National Academy of Sciences of the United States of America **84**, 8345–9.

120 Lee, M. S. and Marians, K. J. (1989) The *Escherichia coli* primosome can translocate actively in either direction along a DNA strand. The Journal of Biological Chemistry **264**, 14531–42.

121 Lee, S. H. and Walker, J. R. (1987) *Escherichia coli* DnaX product, the τ subunit of DNA polymerase III, is a multifunctional protein with single-stranded DNA-dependent ATPase activity. Proceedings of the National Academy of Sciences of the United States of America **84**, 2713–7.

122 Leu, F. P., Georgescu, R. and O'Donnell, M. (2003) Mechanism of the *E. coli* τ processivity switch during lagging-strand synthesis. Molecular Cell **11**, 315–27.

123 Leu, F. P., Hingorani, M. M., Turner, J. and O'Donnell, M. (2000) The δ subunit of DNA polymerase III holoenzyme serves as a sliding clamp unloader in *Escherichia coli*. The Journal of Biological Chemistry **275**, 34609–18.

124 Li, J. J. and Kelly, T. J. (1985) Simian virus 40 DNA replication *in vitro*: specificity of initiation and evidence for bidirectional replication. Molecular and Cellular Biology **5**, 1238–46.

125 Li, K. and Williams, R. S. (1997) Tetramerization and single-stranded DNA binding properties of native and mutated forms of murine mitochondrial single-stranded DNA-binding proteins. The Journal of Biological Chemistry **272**, 8686–94.

126 Li, X. and Marians, K. J. (2000) Two distinct triggers for cycling of the lagging strand polymerase at the replication fork. The Journal of Biological Chemistry **275**, 34757–65.

127 Liu, B., Lin, J. and Steitz, T. A. (2013) Structure of the PolIIIα-τ_C-DNA Complex Suggests an Atomic Model of the Replisome. Structure (London, England : 1993).

128 Liu, J., Dehbi, M., Moeck, G., Arhin, F., Bauda, P., Bergeron, D., Callejo, M., Ferretti, V., Ha, N., Kwan, T., *et al*. (2004) Antimicrobial drug discovery through bacteriophage genomics. Nature Biotechnology **22**, 185–91.

129 Liu, J. and Marians, K. J. (1999) PriA-directed assembly of a primosome on D loop DNA. The Journal of Biological Chemistry **274**, 25033–41.

130 Liu, J., Nurse, P. and Marians, K. J. (1996) The ordered assembly of the ΦX174-type primosome. III. PriB facilitates complex formation between PriA and DnaT. The Journal of Biological Chemistry **271**, 15656–61.

131 Liu, J.-H., Chang, T.-W., Huang, C.-Y., Chen, S.-U., Wu, H.-N., Chang, M.-C. and Hsiao, C.-D. (2004) Crystal structure of PriB, a primosomal DNA replication protein of *Escherichia coli*. The Journal of Biological Chemistry **279**, 50465–71.

132 Liu, Y., Kao, H.-I. and Bambara, R. A. (2004) Flap endonuclease 1: a central component of DNA metabolism. Annual Review of Biochemistry **73**, 589–615.

133 Lohman, T. M. (1992) *Escherichia coli* DNA helicases: mechanisms of DNA unwinding. Molecular Microbiology **6**, 5–14.

134 Lohman, T. M. (1986) Kinetics of protein-nucleic acid interactions: use of salt effects to probe mechanisms of interaction. CRC Critical Reviews in Biochemistry **19**, 191–245.

135 Lohman, T. M. and Bujalowski, W. (1988) Negative cooperativity within individual tetramers of *Escherichia coli* single strand binding protein is responsible for the transition between the $(SSB)_{35}$ and $(SSB)_{56}$ DNA binding modes. Biochemistry **27**, 2260–5.

136 Lohman, T. M., Bujalowski, W. and Overman, L. B. (1988) *E. coli* single strand binding protein: a new look at helix-destabilizing proteins. Trends in Biochemical Sciences **13**, 250–5.

137 Lohman, T. M. and Ferrari, M. E. (1994) *Escherichia coli* single-stranded DNA-binding protein: multiple DNA-binding modes and cooperativities. Annual Review of Biochemistry **63**, 527–70.

138 Lohman, T. M. and Overman, L. B. (1985) Two binding modes in *Escherichia coli* single strand binding protein-single stranded DNA complexes. Modulation by NaCl concentration. The Journal of Biological Chemistry **260**, 3594–603.

139 Lohman, T. M., Overman, L. B. and Datta, S. (1986) Salt-dependent changes in the DNA binding co-operativity of *Escherichia coli* single strand binding protein. Journal of Molecular Biology **187**, 603–15.

140 Lopes, A., Amarir-Bouhram, J., Faure, G., Petit, M.-A. and Guerois, R. (2010) Detection of novel recombinases in bacteriophage genomes unveils Rad52, Rad51 and Gp2.5 remote homologs. Nucleic Acids Research **38**, 3952–62.

141 Lopper, M., Boonsombat, R., Sandler, S. J. and Keck, J. L. (2007) A hand-off mechanism for primosome assembly in replication restart. Molecular Cell **26**, 781–93.

142 Lopper, M., Holton, J. M. and Keck, J. L. (2004) Crystal structure of PriB, a component of the *Escherichia coli* replication restart primosome. Structure (London, England : 1993) **12**, 1967–75.

143 Lu, D. and Keck, J. L. (2008) Structural basis of *Escherichia coli* single-stranded DNA-binding protein stimulation of exonuclease I. Proceedings of the National Academy of Sciences of the United States of America **105**, 9169–74.

144 Lu, D., Myers, A. R., George, N. P. and Keck, J. L. (2011) Mechanism of Exonuclease I stimulation by the single-stranded DNA-binding protein. Nucleic Acids Research **39**, 6536–45.

145 Lísal, J., Lam, T. T., Kainov, D. E., Emmett, M. R., Marshall, A. G. and Tuma, R. (2005) Functional visualization of viral molecular motor by hydrogen-deuterium exchange reveals transient states. Nature Structural & Molecular Biology **12**, 460–6.

146 López de Saro, F. J., Georgescu, R. E., Goodman, M. F. and O'Donnell, M. (2003) Competitive processivity-clamp usage by DNA polymerases during DNA replication and repair. The EMBO Journal **22**, 6408–18.

147 López de Saro, F. J., Georgescu, R. E. and O'Donnell, M. (2003) A peptide switch regulates DNA polymerase processivity. Proceedings of the National Academy of Sciences of the United States of America **100**, 14689–94.

148 Maki, H. and Kornberg, A. (1985) The polymerase subunit of DNA polymerase III of *Escherichia coli*. II. Purification of the α subunit, devoid of nuclease activities. The Journal of Biological Chemistry **260**, 12987–92.

149 Maki, S. and Kornberg, A. (1988) DNA polymerase III holoenzyme of *Escherichia coli*. II. A novel complex including the gamma subunit essential for processive synthesis. The Journal of Biological Chemistry **263**, 6555–60.

150 Maki, S. and Kornberg, A. (1988) DNA polymerase III holoenzyme of *Escherichia coli*. III. Distinctive processive polymerases reconstituted from purified subunits. The Journal of Biological Chemistry **263**, 6561–9.

151 Manhart, C. M. and McHenry, C. S. (2013) The PriA Replication Restart Protein Blocks Replicase Access Prior to Helicase Assembly and Directs Template Specificity through Its ATPase Activity. The Journal of Biological Chemistry **288**, 3989–99.

152 Manosas, M., Spiering, M. M., Zhuang, Z., Benkovic, S. J. and Croquette, V. (2009) Coupling DNA unwinding activity with primer synthesis in the bacteriophage T4 primosome. Nature Chemical Biology **5**, 904–12.

153 Marceau, A. H., Bahng, S., Massoni, S. C., George, N. P., Sandler, S. J., Marians, K. J. and Keck, J. L. (2011) Structure of the SSB-DNA polymerase III interface and its role in DNA replication. The EMBO Journal **30**, 4236–47.

154 Marians, K. J. (1995) ΦX174-type primosomal proteins: purification and assay. Methods in Enzymology **262**, 507–21.

155 Marians, K. J. (2000) PriA-directed replication fork restart in *Escherichia coli*. Trends in Biochemical Sciences **25**, 185–9.

156 Marsin, S., McGovern, S., Ehrlich, S. D., Bruand, C. and Polard, P. (2001) Early steps of *Bacillus subtilis* primosome assembly. The Journal of Biological Chemistry **276**, 45818–25.

157 Martínez-Jiménez, M. I., Alonso, J. C. and Ayora, S. (2005) *Bacillus subtilis* bacteriophage SPP1-encoded gene 34.1 product is a recombination-dependent DNA replication protein. Journal of Molecular Biology **351**, 1007–19.

158 Masai, H. and Arai, K. (1988) Operon structure of dnaT and dnaC genes essential for normal and stable DNA replication of *Escherichia coli* chromosome. The Journal of Biological Chemistry **263**, 15083–93.

159 Masai, H., Asai, T., Kubota, Y., Arai, K. and Kogoma, T. (1994) *Escherichia coli* PriA protein is essential for inducible and constitutive stable DNA replication. The EMBO Journal **13**, 5338–45.

160 Masai, H., Bond, M. W. and Arai, K. (1986) Cloning of the *Escherichia coli* gene for primosomal protein i: the relationship to dnaT, essential for chromosomal DNA replication. Proceedings of the National Academy of Sciences of the United States of America **83**, 1256–60.

161 Masai, H., Matsumoto, S., You, Z., Yoshizawa-Sugata, N. and Oda, M. (2010) Eukaryotic chromosome DNA replication: where, when, and how? Annual Review of Biochemistry **79**, 89–130.

162 McCauley, M. J., Shokri, L., Sefcikova, J., Venclovas, C., Beuning, P. J. and Williams, M. C. (2008) Distinct double- and single-stranded DNA binding of *E. coli* replicative DNA polymerase III alpha subunit. ACS Chemical Biology **3**, 577–87.

163 McCool, J. D., Ford, C. C. and Sandler, S. J. (2004) A dnaT mutant with phenotypes similar to those of a priA2::kan mutant in *Escherichia coli* K-12. Genetics **167**, 569–78.

164 McGlynn, P., Al-Deib, A. A., Liu, J., Marians, K. J. and Lloyd, R. G. (1997) The DNA replication protein PriA and the recombination protein RecG bind D-loops. Journal of Molecular Biology **270**, 212–21.

165 McHenry, C. and Kornberg, A. (1977) DNA polymerase III holoenzyme of *Escherichia coli*. Purification and resolution into subunits. The Journal of Biological Chemistry **252**, 6478–84.

166 McHenry, C. S. (2011) Breaking the rules: bacteria that use several DNA polymerase IIIs. EMBO Reports **12**, 408–14.

167 McHenry, C. S. (2011) DNA replicases from a bacterial perspective. Annual Review of Biochemistry **80**, 403–36.

168 McHenry, C. S. (1982) Purification and characterization of DNA polymerase III'. Identification of τ as a subunit of the DNA polymerase III holoenzyme. The Journal of Biological Chemistry **257**, 2657–63.

169 McHenry, C. S. and Crow, W. (1979) DNA polymerase III of *Escherichia coli*. Purification and identification of subunits. The Journal of Biological Chemistry **254**, 1748–53.

170 Mensa-Wilmot, K., Seaby, R., Alfano, C., Wold, M. C., Gomes, B. and McMacken, R. (1989) Reconstitution of a nine-protein system that initiates bacteriophage lambda DNA replication. The Journal of Biological Chemistry **264**, 2853–61.

171 Mesa, P., Alonso, J. C. and Ayora, S. (2006) *Bacillus subtilis* bacteriophage SPP1 G40P helicase lacking the N-terminal domain unwinds DNA bidirectionally. Journal of Molecular Biology **357**, 1077–88.

172 Miller, E. S., Kutter, E., Mosig, G., Arisaka, F., Kunisawa, T. and Rüger, W. (2003) Bacteriophage T4 genome. Microbiology and Molecular Biology Reviews : MMBR **67**, 86–156, table of contents.

173 Missich, R., Weise, F., Chai, S., Lurz, R., Pedré, X. and Alonso, J. C. (1997) The replisome organizer (G38P) of *Bacillus subtilis* bacteriophage SPP1 forms specialized nucleoprotein complexes with two discrete distant regions of the SPP1 genome. Journal of Molecular Biology **270**, 50–64.

174 Modrich, P. (1989) Methyl-directed DNA mismatch correction. The Journal of Biological Chemistry **264**, 6597–600.

175 Mok, M. and Marians, K. J. (1987) Formation of rolling-circle molecules during ΦX174 complementary strand DNA replication. The Journal of Biological Chemistry **262**, 2304–9.

176 Mok, M. and Marians, K. J. (1987) The *Escherichia coli* preprimosome and DNA B helicase can form replication forks that move at the same rate. The Journal of Biological Chemistry **262**, 16644–54.

177 Molineux, I. J. and Gefter, M. L. (1974) Properties of the *Escherichia coli* in DNA binding (unwinding) protein: interaction with DNA polymerase and DNA. Proceedings of the National Academy of Sciences of the United States of America **71**, 3858–62.

178 Mott, M. L. and Berger, J. M. (2007) DNA replication initiation: mechanisms and regulation in bacteria. Nature Reviews. Microbiology **5**, 343–54.

179 Naue, N. and Curth, U. (2012) Investigation of protein-protein interactions of single-stranded DNA-binding proteins by analytical ultracentrifugation. Methods in Molecular Biology (Clifton, N.J.) **922**, 133–49.

180 Nelson, S. W., Kumar, R. and Benkovic, S. J. (2008) RNA primer handoff in bacteriophage T4 DNA replication: the role of single-stranded DNA-binding protein and polymerase accessory proteins. The Journal of Biological Chemistry **283**, 22838–46.

181 Nethanel, T. and Kaufmann, G. (1990) Two DNA polymerases may be required for synthesis of the lagging DNA strand of simian virus 40. Journal of Virology **64**, 5912–8.

182 Ng, J. Y. and Marians, K. J. (1996) The ordered assembly of the ΦX174-type primosome. I. Isolation and identification of intermediate protein-DNA complexes. The Journal of Biological Chemistry **271**, 15642–8.

183 Ng, J. Y. and Marians, K. J. (1996) The ordered assembly of the ΦX174-type primosome. II. Preservation of primosome composition from assembly through replication. The Journal of Biological Chemistry **271**, 15649–55.

184 Nurse, P., Liu, J. and Marians, K. J. (1999) Two modes of PriA binding to DNA. The Journal of Biological Chemistry **274**, 25026–32.

185 Nurse, P., Zavitz, K. H. and Marians, K. J. (1991) Inactivation of the *Escherichia coli* priA DNA replication protein induces the SOS response. Journal of Bacteriology **173**, 6686–93.

186 Olson, M. W., Dallmann, H. G. and McHenry, C. S. (1995) DnaX complex of *Escherichia coli* DNA polymerase III holoenzyme. The $\chi\psi$ complex functions by increasing the affinity of τ and γ for $\delta.\delta'$ to a physiologically relevant range. The Journal of Biological Chemistry **270**, 29570–7.

187 Overman, L. B., Bujalowski, W. and Lohman, T. M. (1988) Equilibrium binding of *Escherichia coli* single-strand binding protein to single-stranded nucleic acids in the $(SSB)_{65}$ binding mode. Cation and anion effects and polynucleotide specificity. Biochemistry **27**, 456–71.

188 O'Donnell, M. E. (1987) Accessory proteins bind a primed template and mediate rapid cycling of DNA polymerase III holoenzyme from *Escherichia coli*. The Journal of Biological Chemistry **262**, 16558–65.

189 O'Donnell, M. and Studwell, P. S. (1990) Total reconstitution of DNA polymerase III holoenzyme reveals dual accessory protein clamps. The Journal of Biological Chemistry **265**, 1179–87.

190 Pandey, M., Syed, S., Donmez, I., Patel, G., Ha, T. and Patel, S. S. (2009) Coordinating DNA replication by means of priming loop and differential synthesis rate. Nature **462**, 940–3.

191 Pedré, X., Weise, F., Chai, S., Lüder, G. and Alonso, J. C. (1994) Analysis of *cis* and *trans* acting elements required for the initiation of DNA replication in the Bacillus subtilis bacteriophage SPP1. Journal of Molecular Biology **236**, 1324–40.

192 Lo Piano, A., Martínez-Jiménez, M. I., Zecchi, L. and Ayora, S. (2011) Recombination-dependent concatemeric viral DNA replication. Virus Research **160**, 1–14.

193 Polard, P., Marsin, S., McGovern, S., Velten, M., Wigley, D. B., Ehrlich, S. D. and Bruand, C. (2002) Restart of DNA replication in Gram-positive bacteria: functional characterisation of the *Bacillus subtilis* PriA initiator. Nucleic Acids Research **30**, 1593–605.

194 Porter, R. D. and Black, S. (1991) The single-stranded-DNA-binding protein encoded by the *Escherichia coli* F factor can complement a deletion of the chromosomal ssb gene. Journal of Bacteriology **173**, 2720–3.

195 Porter, R. D., Black, S., Pannuri, S. and Carlson, A. (1990) Use of the *Escherichia coli* SSB gene to prevent bioreactor takeover by plasmidless cells. Bio/technology (Nature Publishing Company) **8**, 47–51.

196 Pritchard, A. E., Dallmann, H. G., Glover, B. P. and McHenry, C. S. (2000) A novel assembly mechanism for the DNA polymerase III holoenzyme DnaX complex: association of δδ’ with DnaX(4) forms DnaX(3)δδ'. The EMBO Journal **19**, 6536–45.

197 Pritchard, A. E., Dallmann, H. G. and McHenry, C. S. (1996) *In vivo* assembly of the τ-complex of the DNA polymerase III holoenzyme expressed from a five-gene artificial operon. Cleavage of the τ-complex to form a mixed γ-τ-complex by the OmpT protease. The Journal of Biological Chemistry **271**, 10291–8.

198 Prusty, D., Dar, A., Priya, R., Sharma, A., Dana, S., Choudhury, N. R., Rao, N. S. and Dhar, S. K. (2010) Single-stranded DNA binding protein from human malarial parasite Plasmodium falciparum is encoded in the nucleus and targeted to the apicoplast. Nucleic Acids Research **38**, 7037–53.

199 Quiñones, A. and Neumann, S. (1997) The ssb-113 allele suppresses the dnaQ49 mutator and alters DNA supercoiling in *Escherichia coli*. Molecular Microbiology **25**, 237–46.

200 Raghunathan, S., Kozlov, A. G., Lohman, T. M. and Waksman, G. (2000) Structure of the DNA binding domain of *E. coli* SSB bound to ssDNA. Nature Structural Biology **7**, 648–52.

201 Raghunathan, S., Ricard, C. S., Lohman, T. M. and Waksman, G. (1997) Crystal structure of the homo-tetrameric DNA binding domain of *Escherichia coli* single-stranded DNA-binding protein determined by multiwavelength x-ray diffraction on the selenomethionyl protein at 2.9-A resolution. Proceedings of the National Academy of Sciences of the United States of America **94**, 6652–7.

202 Reems, J. A., Wood, S. and McHenry, C. S. (1995) *Escherichia coli* DNA polymerase III holoenzyme subunits α, β, and γ directly contact the primer-template. The Journal of Biological Chemistry **270**, 5606–13.

203 Richter, F. M., Hsiao, H.-H., Plessmann, U. and Urlaub, H. (2009) Enrichment of protein-RNA crosslinks from crude UV-irradiated mixtures for MS analysis by on-line chromatography using titanium dioxide columns. Biopolymers **91**, 297–309.

204 Rosenberg, S. M. (2001) Evolving responsively: adaptive mutation. Nature reviews. Genetics **2**, 504–15.

205 Rosenkranz, H. S., Garro, A. J., Levy, J. A. and Carr, H. S. (1966) Studies with hydroxyurea. I. The reversible inhibition of bacterial DNA synthesis and the effect of hydroxyurea on the bactericidal action of streptomycin. Biochimica et Biophysica Acta **114**, 501–15.

206 Rosenkranz, H. S. And Levy, J. A. (1965) Hydroxyurea: A Specific Inhibitor Of Deoxyribonucleic Acid Synthesis. Biochimica Et Biophysica Acta **95**, 181–3.

207 Roy, R., Kozlov, A. G., Lohman, T. M. and Ha, T. (2007) Dynamic structural rearrangements between DNA binding modes of *E. coli* SSB protein. Journal of Molecular Biology **369**, 1244–57.

208 Roy, R., Kozlov, A. G., Lohman, T. M. and Ha, T. (2009) SSB protein diffusion on single-stranded DNA stimulates RecA filament formation. Nature **461**, 1092–7.

209 Salas, M. (1984) A new mechanism for the initiation of replication of Φ29 and adenovirus DNA: priming by the terminal protein. Current Topics in Microbiology and Immunology **109**, 89–106.

210 Salas, M. (2006) Phage Φ29 and its relatives. Calendar, R. (ed.), The Bacteriophages, 2nd edn, Oxford University Press, Oxford, New York.

211 Salas, M. (1991) Protein-priming of DNA replication. Annual Review of Biochemistry **60**, 39–71.

212 Sanders, G. M., Dallmann, H. G. and McHenry, C. S. (2010) Reconstitution of the *B. subtilis* replisome with 13 proteins including two distinct replicases. Molecular Cell, Elsevier Ltd **37**, 273–81.

213 Sandler, S. J. (2000) Multiple genetic pathways for restarting DNA replication forks in *Escherichia coli* K-12. Genetics **155**, 487–97.

214 Sandler, S. J. (1996) Overlapping functions for recF and priA in cell viability and UV-inducible SOS expression are distinguished by dnaC809 in *Escherichia coli* K-12. Molecular Microbiology **19**, 871–80.

215 Sandler, S. J., Marians, K. J., Zavitz, K. H., Coutu, J., Parent, M. A. and Clark, A. J. (1999) dnaC mutations suppress defects in DNA replication- and recombination-associated functions in priB and priC double mutants in *Escherichia coli* K-12. Molecular Microbiology **34**, 91–101.

216 Sandler, S. J., Samra, H. S. and Clark, A. J. (1996) Differential suppression of priA2::kan phenotypes in *Escherichia coli* K-12 by mutations in priA, lexA, and dnaC. Genetics **143**, 5–13.

217 Sasaki, K., Ose, T., Okamoto, N., Maenaka, K., Tanaka, T., Masai, H., Saito, M., Shirai, T. and Kohda, D. (2007) Structural basis of the 3'-end recognition of a leading strand in stalled replication forks by PriA. The EMBO Journal **26**, 2584–93.

218 Schekman, R., Weiner, J. H., Weiner, A. and Kornberg, A. (1975) Ten proteins required for conversion of ΦX174 single-stranded DNA to duplex form *in vitro*. Resolution and reconstitution. The Journal of Biological Chemistry **250**, 5859–65.

219 Scheuermann, R. H. and Echols, H. (1984) A separate editing exonuclease for DNA replication: the ε subunit of *Escherichia coli* DNA polymerase III holoenzyme. Proceedings of the National Academy of Sciences of the United States of America **81**, 7747–51.

220 Schuck, P. (1998) Sedimentation analysis of noninteracting and self-associating solutes using numerical solutions to the Lamm equation. Biophysical Journal **75**, 1503–12.

221 Seco, E. M., Zinder, J. C., Manhart, C. M., Lo Piano, A., McHenry, C. S. and Ayora, S. (2013) Bacteriophage SPP1 DNA replication strategies promote viral and disable host replication *in vitro*. Nucleic Acids Research **41**, 1711–21.

222 Shereda, R. D., Bernstein, D. A. and Keck, J. L. (2007) A central role for SSB in *Escherichia coli* RecQ DNA helicase function. The Journal of Biological Chemistry **282**, 19247–58.

223 Shereda, R. D., Kozlov, A. G., Lohman, T. M., Cox, M. M. and Keck, J. L. SSB as an organizer/mobilizer of genome maintenance complexes. Critical Reviews in Biochemistry and Molecular Biology **43**, 289–318.

224 Shereda, R. D., Reiter, N. J., Butcher, S. E. and Keck, J. L. (2009) Identification of the SSB binding site on *E. coli* RecQ reveals a conserved surface for binding SSB's C terminus. Journal of Molecular Biology **386**, 612–25.

225 Shioi, S., Ose, T., Maenaka, K., Shiroishi, M., Abe, Y., Kohda, D., Katayama, T. and Ueda, T. (2005) Crystal structure of a biologically functional form of PriB from *Escherichia coli* reveals a potential single-stranded DNA-binding site. Biochemical and Biophysical Research Communications **326**, 766–76.

226 Singleton, M. R., Sawaya, M. R., Ellenberger, T. and Wigley, D. B. (2000) Crystal structure of T7 gene 4 ring helicase indicates a mechanism for sequential hydrolysis of nucleotides. Cell **101**, 589–600.

227 Smits, W. K., Goranov, A. I. and Grossman, A. D. (2010) Ordered association of helicase loader proteins with the *Bacillus subtilis* origin of replication *in vivo*. Molecular Microbiology **75**, 452–61.

228 Song, M. S., Pham, P. T., Olson, M., Carter, J. R., Franden, M. A., Schaaper, R. M. and McHenry, C. S. (2001) The δ and δ' subunits of the DNA polymerase III holoenzyme are essential for initiation complex formation and processive elongation. The Journal of Biological Chemistry **276**, 35165–75.

229 Steen, H., Petersen, J., Mann, M. and Jensen, O. N. (2001) Mass spectrometric analysis of a UV-cross-linked protein-DNA complex: tryptophans 54 and 88 of *E. coli* SSB cross-link to DNA. Protein Science : a publication of the Protein Society **10**, 1989–2001.

230 Stengel, G. and Kuchta, R. D. (2011) Coordinated leading and lagging strand DNA synthesis by using the herpes simplex virus 1 replication complex and minicircle DNA templates. Journal of Virology **85**, 957–67.

231 Stephens, K. M. and McMacken, R. (1997) Functional properties of replication fork assemblies established by the bacteriophage λ O and P replication proteins. The Journal of Biological Chemistry **272**, 28800–13.

232 Stewart, J., Hingorani, M. M., Kelman, Z. and O'Donnell, M. (2001) Mechanism of β clamp opening by the δ subunit of *Escherichia coli* DNA polymerase III holoenzyme. The Journal of Biological Chemistry **276**, 19182–9.

233 Studwell-Vaughan, P. S. and O'Donnell, M. (1991) Constitution of the twin polymerase of DNA polymerase III holoenzyme. The Journal of Biological Chemistry **266**, 19833–41.

234 Studwell-Vaughan, P. S. and O'Donnell, M. (1993) DNA polymerase III accessory proteins. V. θ encoded by holE. The Journal of Biological Chemistry **268**, 11785–91.

235 Stukenberg, P. T., Turner, J. and O'Donnell, M. (1994) An explanation for lagging strand replication: polymerase hopping among DNA sliding clamps. Cell **78**, 877–87.

236 Sugiura, S., Ohkubo, S. and Yamaguchi, K. (1993) Minimal essential origin of plasmid pSC101 replication: requirement of a region downstream of iterons. Journal of Bacteriology **175**, 5993–6001.

237 Tanaka, T., Mizukoshi, T., Sasaki, K., Kohda, D. and Masai, H. (2007) *Escherichia coli* PriA protein, two modes of DNA binding and activation of ATP hydrolysis. The Journal of Biological Chemistry **282**, 19917–27.

238 Tate, J. J., Persinger, J. and Bartholomew, B. (1998) Survey of four different photoreactive moieties for DNA photoaffinity labeling of yeast RNA polymerase III transcription complexes. Nucleic Acids Research **26**, 1421–6.

239 Theobald, D. L., Mitton-Fry, R. M. and Wuttke, D. S. (2003) Nucleic acid recognition by OB-fold proteins. Annual Review of Biophysics and Biomolecular Structure **32**, 115–33.

240 Tiranti, V., Rocchi, M., DiDonato, S. and Zeviani, M. (1993) Cloning of human and rat cDNAs encoding the mitochondrial single-stranded DNA-binding protein (SSB). Gene **126**, 219–25.

241 Tougu, K. and Marians, K. J. (1996) The extreme C terminus of primase is required for interaction with DnaB at the replication fork. The Journal of Biological Chemistry **271**, 21391–7.

242 Tougu, K., Peng, H. and Marians, K. J. (1994) Identification of a domain of *Escherichia coli* primase required for functional interaction with the DnaB helicase at the replication fork. The Journal of Biological Chemistry **269**, 4675–82.

243 Tsur, D., Tanner, S., Zandi, E., Bafna, V. and Pevzner, P. A. (2005) Identification of post-translational modifications by blind search of mass spectra. Nature Biotechnology **23**, 1562–7.

244 Tsurimoto, T. and Stillman, B. (1991) Replication factors required for SV40 DNA replication *in vitro*. II. Switching of DNA polymerase α and δ during initiation of leading and lagging strand synthesis. The Journal of Biological Chemistry **266**, 1961–8.

245 Umezu, K. and Kolodner, R. D. (1994) Protein interactions in genetic recombination in *Escherichia coli*. Interactions involving RecO and RecR overcome the inhibition of RecA by single-stranded DNA-binding protein. The Journal of Biological Chemistry **269**, 30005–13.

246 Velten, M., McGovern, S., Marsin, S., Ehrlich, S. D., Noirot, P. and Polard, P. (2003) A two-protein strategy for the functional loading of a cellular replicative DNA helicase. Molecular Cell **11**, 1009–20.

247 Viret, J. F., Bravo, A. and Alonso, J. C. (1991) Recombination-dependent concatemeric plasmid replication. Microbiological Reviews **55**, 675–83.

248 Vistica, J., Dam, J., Balbo, A., Yikilmaz, E., Mariuzza, R. A., Rouault, T. A. and Schuck, P. (2004) Sedimentation equilibrium analysis of protein interactions with global implicit mass conservation constraints and systematic noise decomposition. Analytical Biochemistry **326**, 234–56.

249 Wadood, A., Dohmoto, M., Sugiura, S. and Yamaguchi, K. (1997) Characterization of copy number mutants of plasmid pSC101. The Journal of General and Applied Microbiology **43**, 309–316.

250 Wang, G., Klein, M. G., Tokonzaba, E., Zhang, Y., Holden, L. G. and Chen, X. S. (2008) The structure of a DnaB-family replicative helicase and its interactions with primase. Nature Structural & Molecular Biology **15**, 94–100.

251 Wang, T., Toscano, J. P. and Celius, T. C. (2010) CRC Handbookof Organic Photochemistry and Photobiology, Volumes 1 & 2, Second Edition 2nd ed., p 2904, CRC Press.

252 Weiner, J. H., McMacken, R. and Kornberg, A. (1976) Isolation of an intermediate which precedes dnaG RNA polymerase participation in enzymatic replication of bacteriophage ΦX174 DNA. Proceedings of the National Academy of Sciences of the United States of America **73**, 752–6.

253 Wickner, S. (1976) Mechanism of DNA elongation catalyzed by *Escherichia coli* DNA polymerase III, dnaZ protein, and DNA elongation factors I and III. Proceedings of the National Academy of Sciences of the United States of America **73**, 3511–5.

254 Wickner, S. and Hurwitz, J. (1974) Conversion of ΦX174 viral DNA to double-stranded form by purified *Escherichia coli* proteins. Proceedings of the National Academy of Sciences of the United States of America **71**, 4120–4.

255 Wickner, S. and Hurwitz, J. (1975) Interaction of *Escherichia coli* dnaB and dnaC(D) gene products *in vitro*. Proceedings of the National Academy of Sciences of the United States of America **72**, 921–5.

256 Wieczorek, A. and McHenry, C. S. (2006) The NH_2-terminal php domain of the α subunit of the *Escherichia coli* replicase binds the ε proofreading subunit. The Journal of Biological Chemistry **281**, 12561–7.

257 Williams, K. R., Spicer, E. K., LoPresti, M. B., Guggenheimer, R. A. and Chase, J. W. (1983) Limited proteolysis studies on the *Escherichia coli* single-stranded DNA binding protein. Evidence for a functionally homologous domain in both the *Escherichia coli* and T4 DNA binding proteins. The Journal of Biological Chemistry **258**, 3346–55.

258 Wing, R. A, Bailey, S. and Steitz, T. A. (2008) Insights into the replisome from the structure of a ternary complex of the DNA polymerase III α-subunit. Journal of Molecular Biology **382**, 859–69.

259 Wing, R. A. (2010) Structural studies of the prokaryotic replisome, Yale University.

260 Witte, G., Urbanke, C. and Curth, U. (2005) Single-stranded DNA-binding protein of *Deinococcus radiodurans*: a biophysical characterization. Nucleic Acids Research **33**, 1662–70.

261 Wolf, P. (1983) A critical reappraisal of Waddell's technique for ultraviolet spectrophotometric protein estimation. Analytical Biochemistry **129**, 145–55.

262 Wu, C. A., Zechner, E. L. and Marians, K. J. (1992) Coordinated leading- and lagging-strand synthesis at the *Escherichia coli* DNA replication fork. I. Multiple effectors act to modulate Okazaki fragment size. The Journal of Biological Chemistry **267**, 4030–44.

263 Wu, C. A., Zechner, E. L., Reems, J. A., McHenry, C. S. and Marians, K. J. (1992) Coordinated leading- and lagging-strand synthesis at the *Escherichia coli* DNA replication fork. V. Primase action regulates the cycle of Okazaki fragment synthesis. The Journal of Biological Chemistry **267**, 4074–83.

264 Xi, J., Zhang, Z., Zhuang, Z., Yang, J., Spiering, M. M., Hammes, G. G. and Benkovic, S. J. (2005) Interaction between the T4 helicase loading protein (gp59) and the DNA polymerase (gp43): unlocking of the gp59-gp43-DNA complex to initiate assembly of a fully functional replisome. Biochemistry **44**, 7747–56.

265 Xu, L. and Marians, K. J. (2003) PriA mediates DNA replication pathway choice at recombination intermediates. Molecular Cell **11**, 817–26.

266 Yamaguchi, K. and Yamaguchi, M. The replication origin of pSC101: the nucleotide sequence and replication functions of the ori region. Gene **29**, 211–9.

267 Yang, C., Curth, U., Urbanke, C. and Kang, C. (1997) Crystal structure of human mitochondrial single-stranded DNA binding protein at 2.4 A resolution. Nature Structural Biology **4**, 153–7.

268 Yang, J., Nelson, S. W. and Benkovic, S. J. (2006) The control mechanism for lagging strand polymerase recycling during bacteriophage T4 DNA replication. Molecular Cell **21**, 153–64.

269 Yano, S. T. and Rothman-Denes, L. B. (2011) A phage-encoded inhibitor of *Escherichia coli* DNA replication targets the DNA polymerase clamp loader. Molecular Microbiology **79**, 1325–38.

270 Yuan, Q. and McHenry, C. S. (2009) Strand displacement by DNA polymerase III occurs through a τ-ψ-χ link to single-stranded DNA-binding protein coating the lagging strand template. The Journal of Biological Chemistry **284**, 31672–9.

271 Yuzhakov, A., Kelman, Z. and O'Donnell, M. (1999) Trading places on DNA--a three-point switch underlies primer handoff from primase to the replicative DNA polymerase. Cell **96**, 153–63.

272 Zavitz, K. H. and Marians, K. J. (1992) ATPase-deficient mutants of the *Escherichia coli* DNA replication protein PriA are capable of catalyzing the assembly of active primosomes. The Journal of Biological Chemistry **267**, 6933–40.

273 Zecchi, L., Lo Piano, A., Suzuki, Y., Cañas, C., Takeyasu, K. and Ayora, S. (2012) Characterization of the Holliday junction resolving enzyme encoded by the *Bacillus subtilis* bacteriophage SPP1. PloS One **7**, e48440.

274 Zechner, E. L., Wu, C. A. and Marians, K. J. (1992) Coordinated leading- and lagging-strand synthesis at the *Escherichia coli* DNA replication fork. II. Frequency of primer synthesis and efficiency of primer utilization control Okazaki fragment size. The Journal of Biological Chemistry **267**, 4045–53.

275 Zhou, R., Kozlov, A. G., Roy, R., Zhang, J., Korolev, S., Lohman, T. M. and Ha, T. (2011) SSB functions as a sliding platform that migrates on DNA via reptation. Cell **146**, 222–32.

APPENDIX 1*

Supplementary material for

Chapter 2

The rate of polymerase release upon filling the gap between Okazaki fragments is inadequate to support cycling during lagging strand synthesis†

A1.1 SUPPLEMENTARY FIGURES

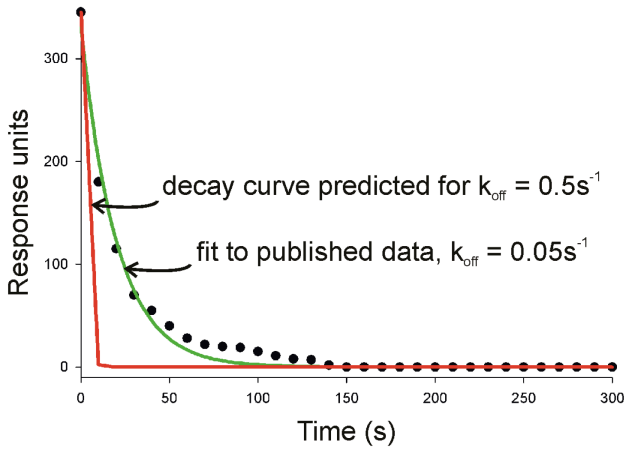

FIGURE A1.1
Re-analysis of published data for the dissociation of Pol III* from a primed template in the presence of dNTPs. The coordinates for the raw data points were taken at 10 s intervals from Fig. 2.4B of from reference 10 in the main paper. The dNTPs injection point was set as time zero. Since the dissociation curve approached baseline at 80 RU, an offset value of 80 RU was subtracted from the Y-value data so that the baseline would reach zero. Regression analysis of the raw data using a single exponential decay model generated a k_{off} = 0.05 s^{-1} (green). A curve representing the exponential decay with k_{off} = 0.5 s^{-1} (red), as reported in Fig 2.4B is shown for comparison.

* My experimental work is the photo-crosslinking experiment presented in Fig. A1.4 of this appendix. The remaining experimental work was performed by the co-authors of the corresponding publication [1].
† The contents of this appendix are the supplementary material for [1] and are presented here with few modifications.

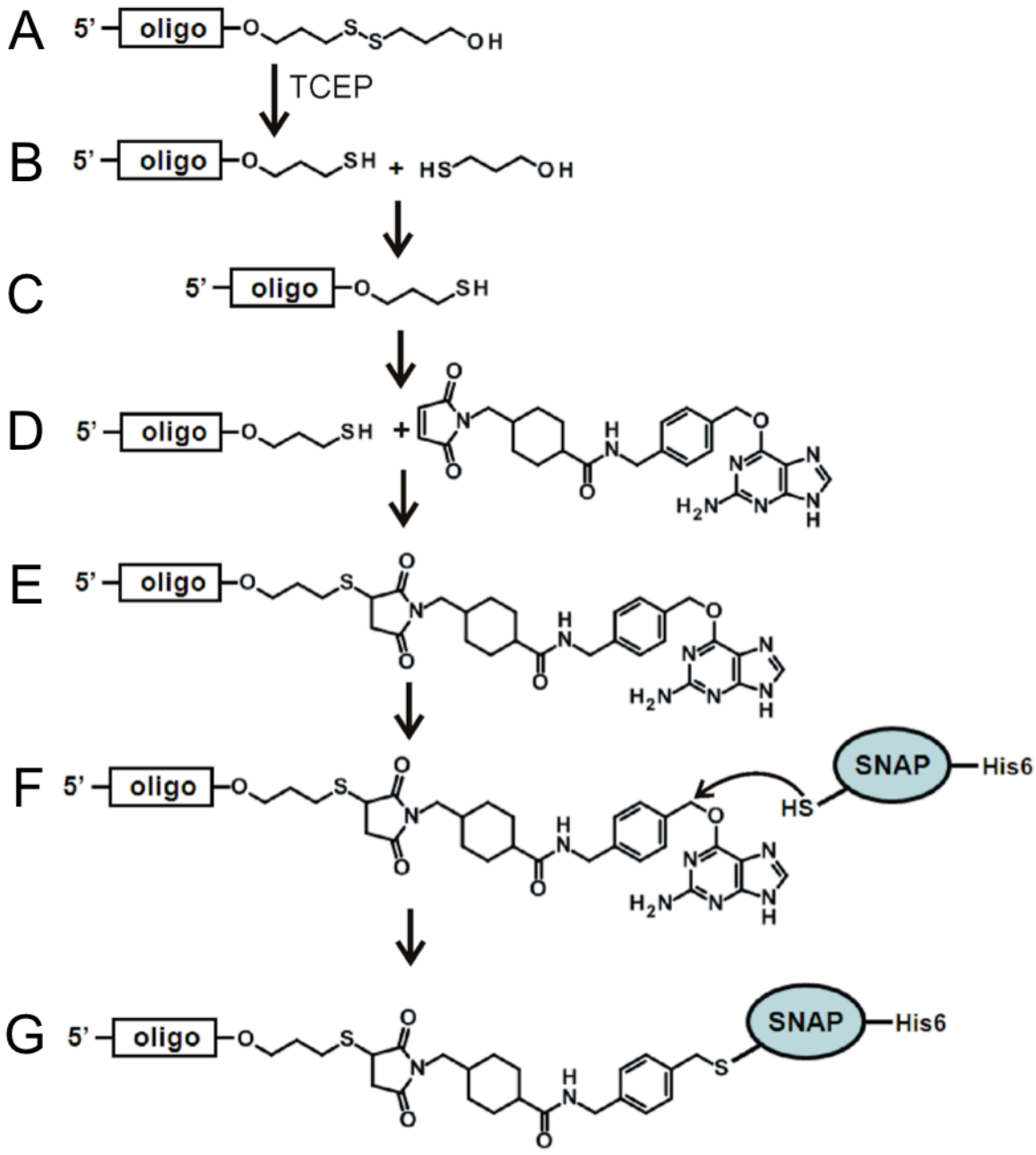

FIGURE A1.2
Preparation of the SNAP-Protein Conjugated blocking oligonucleotide. (A) The disulfide-blocked oligonucleotide was reduced with TCEP. (B) Gel filtration was used to purify reduced thio-39-mer (C) away from 3-carbon blocking agent. (D) Thio 39-mer was reacted with benzylguanine-maleimide and the benzylguanine 39-mer product (E) purified by gel filtration. (F) Benzylguanine 39-mer was reacted with His_6-SNAP protein (O^6-alkylguanine-DNA-alkyltransferase) which becomes covalently bound to the oligomer via an active site Cys residue. (G) The product was purified by Ni^{2+}NTA chromatography.

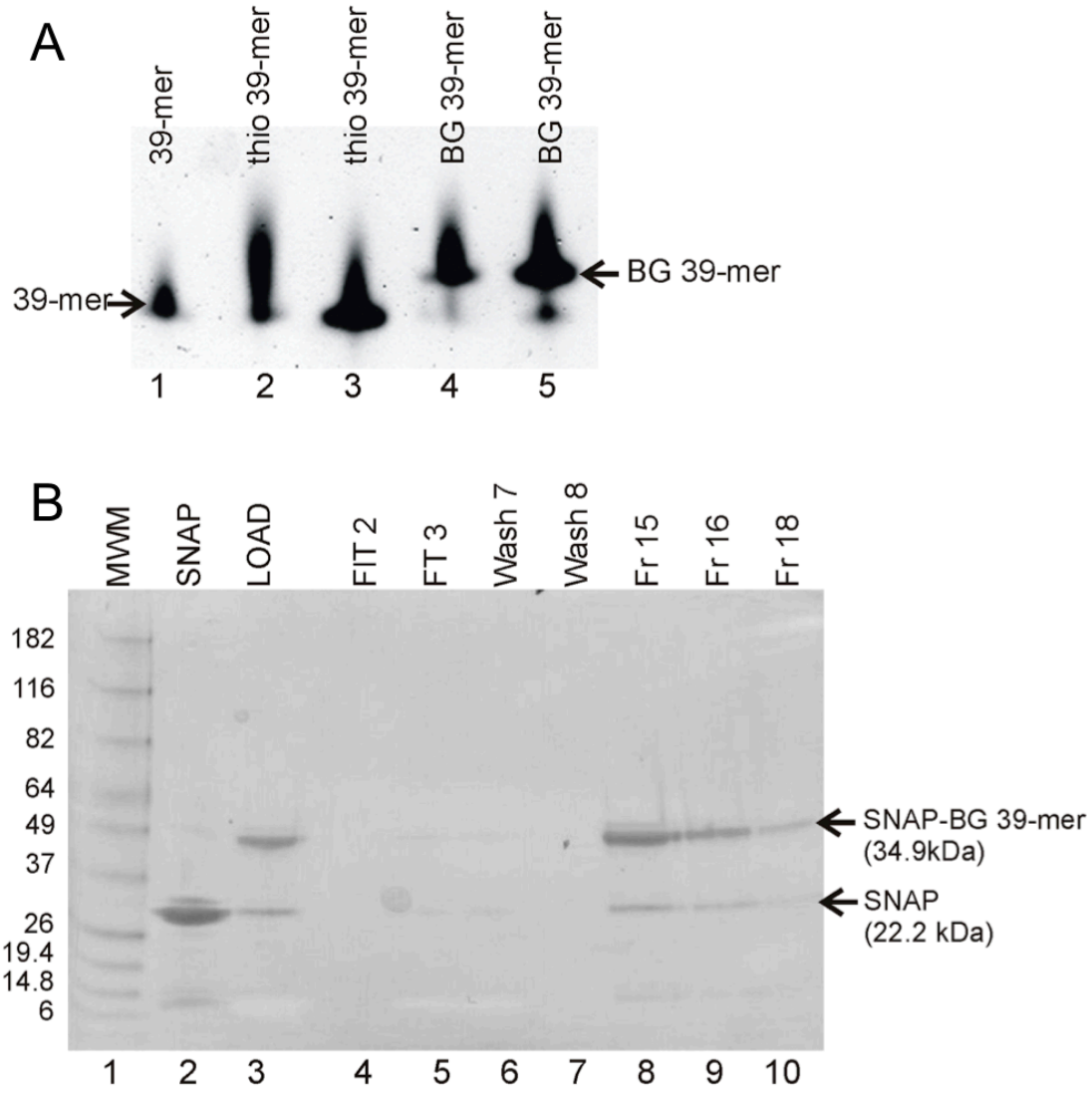

FIGURE A1.3
Analysis of products used to prepare the SNAP-conjugated blocking oligonucleotide. (A) Characterization of the BG-modified blocking oligonucleotide by 9% denaturing PAGE. A 39-mer (lane 1, 100 ng, no thiol group) was run beside unreacted thio 39-mer (lane 2,100 ng; lane 3, 200 ng) and BG-modified 39-mer (lane 4, 100 ng and lane 5, 200 ng). The molecular weight shift upwards indicated >90% of the thio 39-mer reacted with the benzylguanine maleimide. (B) Characterization of the SNAP-conjugated blocking oligonucleotide by SDS-PAGE (4-20% gradient). Lane1, molecular weight markers; lane 2, SNAP protein; lane 3, His_6-SNAP protein reacted with a 1.5-fold excess of benzylguanine 39-mer that was loaded onto an NTA column; lanes 4 and 5, flow-through fractions from the NTA column; lanes 6 and 7, column wash fractions; lanes 8, 9, 10; 400 mM imidazole-eluted SNAP-conjugated 39-mer fractions. Proteins were visualized by coomassie blue staining.

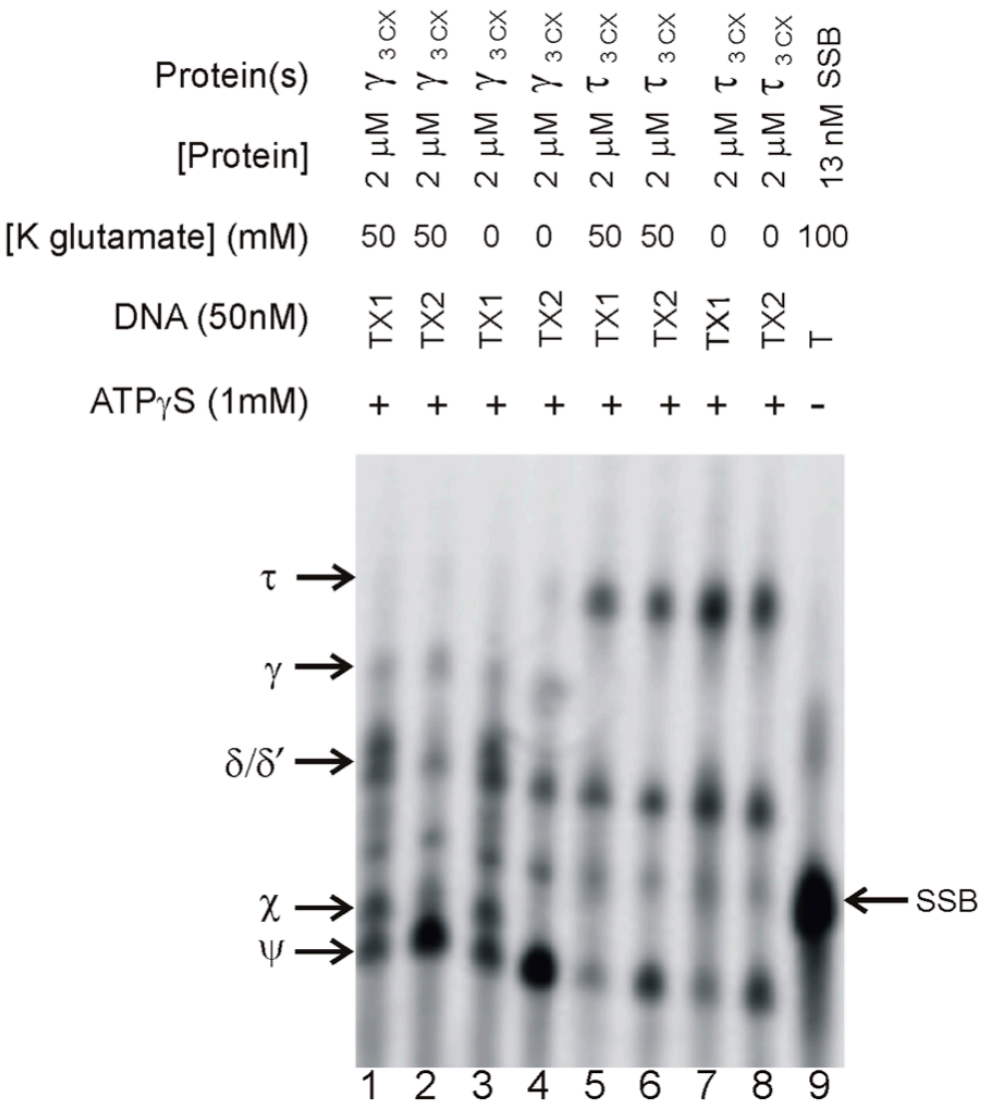

FIGURE A1.4
Photocrosslinking standards for the γ_3 complex and τ_3 complex. Denaturing polyacrylamide gel analysis of DnaX complex standards compared to SSB. Oligonucleotide constructs in Fig. 2.3A were combined with subunits and subunit complexes with the indicated nucleotide and potassium glutamate concentration, photo-cross-linked, and resolved as described under in section 2.3.7.

Table A1.1 Data for slow dissociation phase for experiments presented in Table 2.1

Injection	*Fast Phase* $t_{1/2}$ (s), [amplitude]	*Slow Phase* $t_{1/2}$ (s), [amplitude]	*Offset [% total amplitude]*
	4 nt gap template		
5'-OH DNA_{39} blocking oligo	30 [86%]	12,100 [3%]	[11%]
5' PO_4 RNA_{12}/DNA_{27} blocking oligo	60 [71%]	5,900 [7%]	[22%]
5' Tri-PO_4 DNA_{39} blocking oligo	80 [51%]	13,900 [7%]	[42%]
	5 nt gap template		
5'-OH DNA_{39} blocking oligo	40 [83%]	7,200 [3%]	[14%]
5' PO_4 RNA_{12}/DNA_{27} blocking oligo	70 [68%]	8,100 [7%]	[25%]
5' Tri-PO_4 DNA_{39} blocking oligo	90 [44%]	9,000 [9%]	[47%]

Table A1.2 Data for slow dissociation phase for experiments presented in Table 2.2

Injection	Gap size	*Fast Phase* 4 nt gap template $t_{1/2}$ (s), [amplitude]	*Slow Phase* $t_{1/2}$ (s), [amplitude]	*Offset [% total amplitude]*
Buffer	4	860 [12%]	16,300 [20%]	[68%]
dCTP	3	390 [69%]	15,000 [16%]	[15%]
ddCTP	3	660 [25%]	21,700 [24%]	[51%]
dCTP, dTTP	1	210 [62%]	13,800 [11%]	[28%]
dCTP, ddTTP	2	370 [36%]	15,300 [15%]	[49%]
dCTP, dTTP, dGTP	0	290 [55%]	9,600 [12%]	[33%]
dCTP, dTTP, ddGTP	0	110 [64%]	3,200 [12%]	[24%]
		5 nt gap template		
Buffer	5	620 [10%]	17,200 [20%]	[69%]
dCTP	3	360 [70%]	13,700 [14%]	[16%]
ddCTP	4	380 [26%]	18,000 [24%]	[51%]
dCTP, dTTP	1	190 [63%]	13,800 [10%]	[27%]
dCTP, ddTTP	2	350 [37%]	16,500 [15%]	[49%]
dCTP, dTTP, dGTP	0	180 [57%]	8,700 [12%]	[31%]
dCTP, dTTP, ddGTP	0	110 [63%]	3,600 [11%]	[26%]

Table A1.3 Data for slow dissociation phase for experiments presented in Table 2.3

Injection	*Fast Phase* 4 nt gap template $t_{1/2}$ (s), [amplitude]		*Slow Phase* $t_{1/2}$ (s), [amplitude]		*Offset [% total amplitude]*
ATP	990	[60%]	26,600	[27%]	[14%]
dNTPs	110	[64%]	3,200	[12%]	[24%]
dNTPs, 20/70-mer, ATP	30	[86%]	12,100	[3%]	[11%]
dNTPs, ATP	60	[75%]	3,900	[8%]	[17%]
20/70-mer, ATP	330	[52%]	24,500	[15%]	[33%]
dNTPs, 20/-70-mer	60	[80%]	3,900	[10%]	[10%]
dNTPs, 20/-70-mer, ATP, SSB_4	50	[77%]	200	[10%]	[13%]
dNTPs, 20/-70-mer, ATP, SSB_4, β_2	30	[64%]	500	[17%]	[19%]
dNTPs, 20/-70-mer, ATPγS	130	[68%]	6,800	[15%]	[18%]
	5 nt gap template				
ATP	920	[62%]	24,800	[29%]	[9%]
dNTPs	110	[63%]	3,600	[11%]	[26%]
dNTPs, 20/70-mer, ATP	40	[83%]	7,200	[3%]	[14%]
dNTPs, ATP	60	[77%]	5,100	[7%]	[16%]
20/70-mer, ATP	340	[51%]	18,400	[9%]	[40%]
dNTPs, 20/-70-mer	70	[77%]	4,300	[11%]	[11%]
dNTPs, 20/-70-mer, ATP, SSB_4	50	[73%]	200	[11%]	[16%]
dNTPs, 20/-70-mer, ATP, SSB_4, β_2	30	[59%]	400	[19%]	[22%]
dNTPs, 20/-70-mer, ATPγS	130	[67%]	8,100	[14%]	[18%]

A1.2 REFERENCES

1 Dohrmann, P. R., Manhart, C. M., Downey, C. D. and McHenry, C. S. (2011) The Rate of Polymerase Release upon Filling the Gap between Okazaki Fragments Is Inadequate to Support Cycling during Lagging Strand Synthesis. Journal of Molecular Biology, Elsevier Ltd **414**, 15–27.

APPENDIX 2*

Supplementary material for

Chapter 3

The PriA replication restart protein blocks replicase access prior to assembly and directs template specificity through its ATPase activity†

A2.1 SUPPLEMENTARY TABLES AND FIGURES

Varying lagging strand arm with 10 nt gap on leading strand

Lagging Strand Arm Length (nt)	[unwound DNA] (nM) in *Bsu*	[unwound DNA] (nM) in *Eco*
45	7.5	7.1
35	5.1	6.1
25	3.2	3.6
15	0.0	0.9
5	0.0	0.0

Varying parental duplex region with 10 nt gap on leading strand

Parental Duplex Length (nt)	[unwound DNA] (nM) in *Bsu*	[unwound DNA] (nM) in *Eco*
45	7.5	7.1
30	3.9	3.0

Varying leading strand duplex region with 10 nt gap on leading strand

Leading Strand Duplex Length (nt)	[unwound DNA] (nM) in *Bsu*	[unwound DNA] (nM) in *Eco*
35	7.5	7.1
30	0.0	0.3

TABLE A2.1
Determining the minimal substrate to sustain efficient helicase loading. Regions of the substrate in Fig. 3.1 were varied to determine the minimal substrate that can support an efficient helicase loading reaction. A replication fork consisting of a 45-mer lagging strand arm, a 45-mer parental duplex region, a 35-mer leading strand duplex region, and a 10 nucleotide gap are constructed from FT90, QT90, and P10g. Where regions were shortened, the sequences given in Fig. 3.1E were truncated from this starting substrate.

* I performed the entirety of the experimental work presented in this appendix.
† The contents in this appendix are the supplementary material for [1] and are presented here with few modifications.

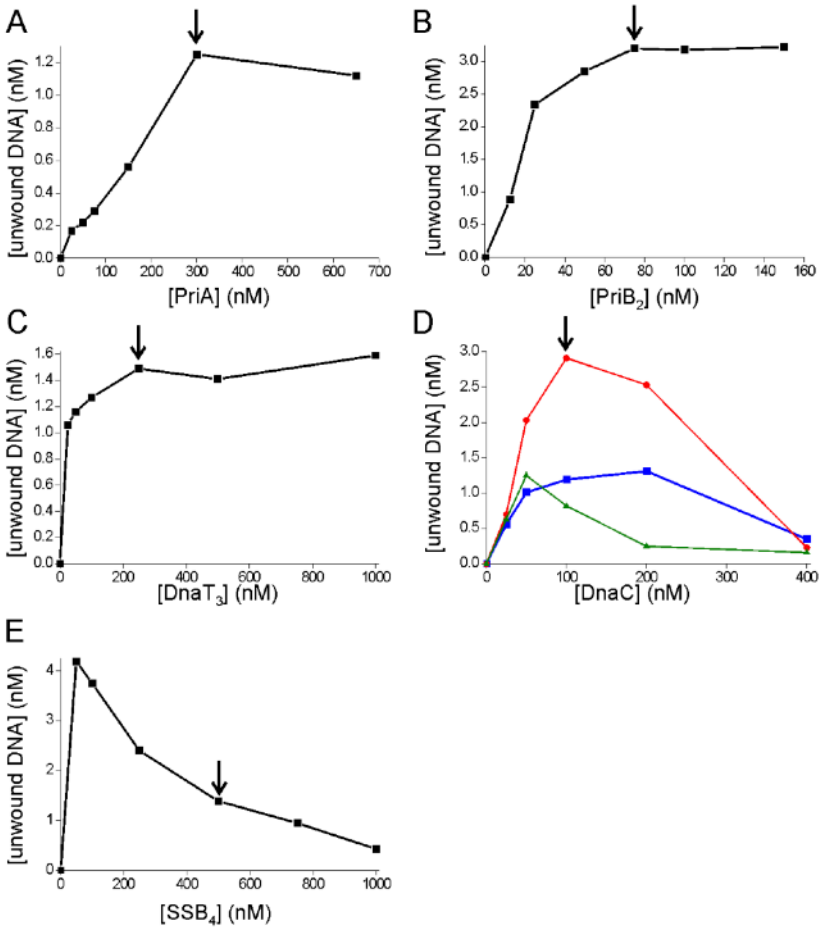

FIGURE A2.1
Optimization of *E. coli* helicase loading on 20 nM 0 nt gap forked template. Experiments were carried out as in Fig. 3.3. The starting conditions were: 50 nM $PriB_2$, 333 nM $DnaT_3$, 12 nM $DnaB_6$, 108 nM DnaC, and 500 nM SSB_4. The final optimized conditions (indicated by arrows) were: 300 nM PriA, 75 nM $PriB_2$, 250 nM $DnaT_3$, 12 nM $DnaB_6$, 100 nM DnaC, and 500 nM SSB_4. (A) PriA titration. (B) $PriB_2$ titration. (C) $DnaT_3$ titration. (D) DnaC titrated at three different $DnaB_6$ concentrations: 6 nM (green), 12 nM (red), and 24 nM (blue). (E) SSB_4 titration. To prevent the helicase self-loading reaction, 500 nM SSB_4 was chosen for future experiments.

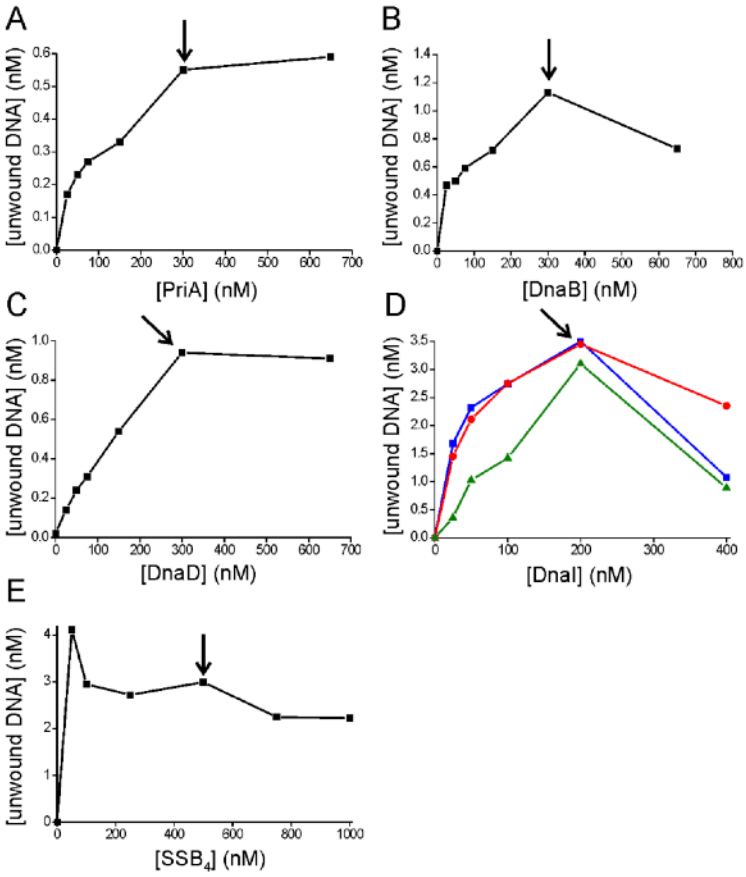

FIGURE A2.2
Optimizing *B. subtilis* helicase loading on 20 nM 0 nt gap forked template. Experiments were carried out as in Fig. 3.3. The starting conditions were: 300 nM DnaB, 300 nM DnaD, 12 nM $DnaC_6$, 100 nM DnaI, and 500 nM SSB_4. The final optimized conditions (indicated by arrows) were: 300 nM PriA, 300 nM DnaB, 300 nM DnaD, 12 nM $DnaC_6$, 200 nM DnaI and 500 nM SSB_4. (A) PriA titration. (B) DnaB titration. (C) DnaD titration. (D) DnaI titrated at three different $DnaC_6$ concentrations: 6 nM (green), 12 nM (red), and 24 nM (blue). (E) SSB_4 titration. To prevent the helicase self-loading reaction, 500 nM SSB_4 was used for future experiments

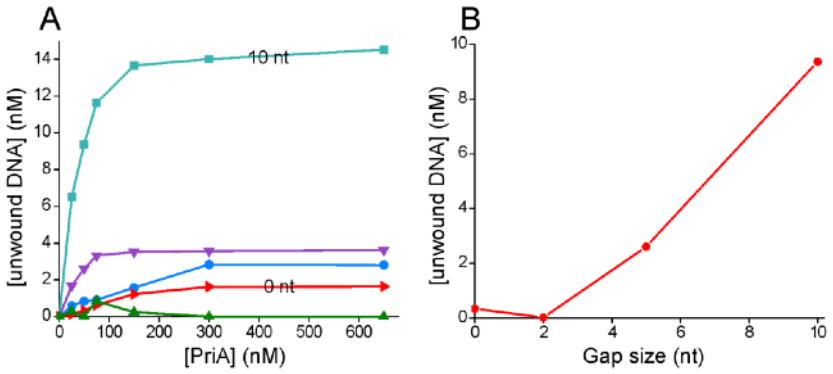

FIGURE A2.3
A larger gap on the leading strand is also preferred using the *E. coli* system under conditions optimized for the 0 nt gap forked template. Protein concentrations were those described in the legend to Fig. A2.1. (A) PriA titration on five unique substrates: unprimed forked template (blue), 0 nt gap forked template (red), 2 nt gap forked template (green), 5 nt gap forked template (purple), or 10 nt gap forked template (cyan). (B) Amount of DNA unwound plotted against gap size at 50 nM PriA.

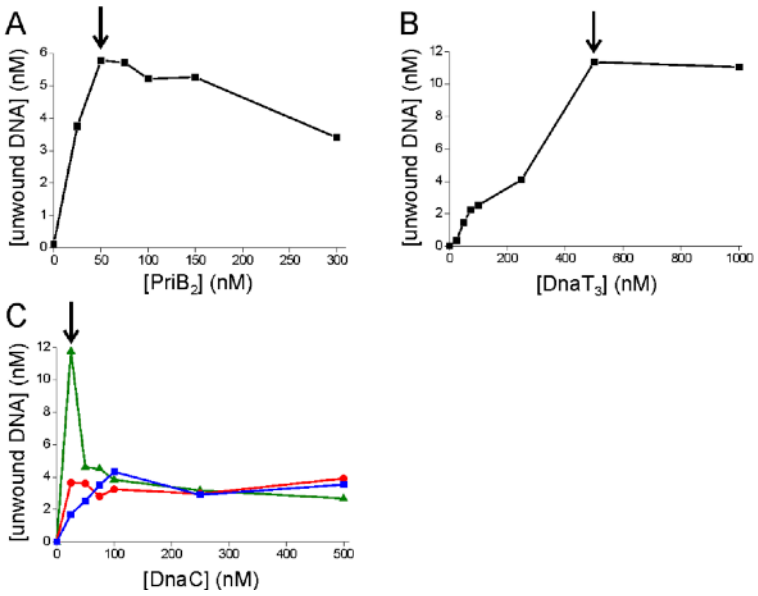

FIGURE A2.4
Optimization of protein levels on forked template bound to streptavidin beads. Radiolabeled, biotinylated primer/10 nt gap forked template was bound to streptavidin beads as described in section 3.3.4. After washing, the substrate (20 nM final concentration) was incubated with 2 mM ATP, 500 nM PriA, 500 nM SSB_4, and helicase and helicase-loading proteins for 15 min at room temperature. The reaction was quenched and the product was removed from the beads. The sample was resolved by 12 % native PAGE. PriA and SSB_4 were held constant at 500 nM. The remaining proteins were titrated sequentially in the order they appear here. For each, an optimum was chosen (as indicated by the arrow) and that concentration was used in subsequent titrations. The starting conditions for titration of the other helicase loading proteins and helicase were: 333 nM $DnaT_3$, 40 nM $DnaB_6$, and 200 nM DnaC. The final optimized conditions were: 50 nM $PriB_2$, 500 nM $DnaT_3$, 12 nM $DnaB_6$, and 25 nM DnaC. (A) $PriB_2$ titration. (B) $DnaT_3$ titration. (C) DnaC titrated at three different $DnaB_6$ concentrations: 12 nM (green), 40 nM (red), and 80 nM (blue).

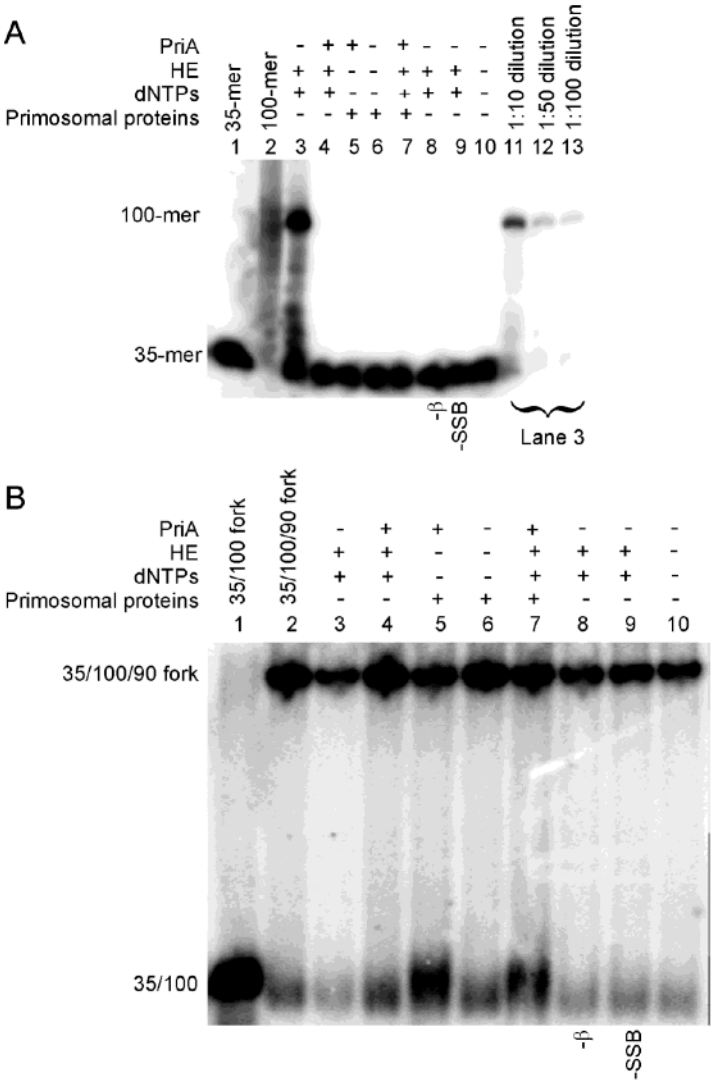

FIGURE A2.5
PriA and holoenzyme do not coexist on PriA-inhibited replication forks with a 20 nt gap. Substrate constructed from biotinylated primer 20 nt gap 5'-CT(biotin)ACGATCATTTGAAGATTCTTACATTAGCCGACA-3', FT100, and lagging strand template 90-mer. This experiment carried out as described for reactions on streptavidin beads under section 3.3.4 and in the legend for Fig. 3.7. (A) Denaturing gel analysis to monitor primer extension by *E. coli* Pol III (exo-). Lanes 11-13 are dilutions of the positive control lane 3 to establish detection limits. For both A and B, lanes 8 and 9 contain the full Pol III HE but in lane 8 the β_2 subunit was omitted and in lane 9 SSB was omitted. (B) Native gel analysis to monitor substrate unwinding by *E. coli* DnaB helicase. The upper band is the replication fork and 100/100 duplex for those reactions in which replication occurred. The lower band is the displaced leading strand primer-template. In lanes 5 and 7 ~50 % of the substrate was unwound by the helicase. In all other lanes, the amount of substrate unwound is not significantly above background.

A2.2 REFERENCES

1 Manhart, C. M. and McHenry, C. S. (2013) The PriA Replication Restart Protein Blocks Replicase Access Prior to Helicase Assembly and Directs Template Specificity through Its ATPase Activity. The Journal of Biological Chemistry **288**, 3989–99.

APPENDIX 3[*]

Supplemental material for

Chapter 4

Bacteriophage SPP1 DNA replication strategies promote viral and disable host replication *in vivo*[†]

A3.1 SUPPLEMENTARY MATERIALS AND METHODS: PURIFICATION OF SPP1 DNA REPLICATION PROTEINS

All proteins were expressed in *E. coli* overexpression vectors in which the encoding genes are the native genes without added tags. *B. subtilis* PriA, DnaD, DnaB, DnaI, DnaC helicase, DnaG primase, DnaE, PolC, τ, δ, δ', β and SSB were purified as described [1]. G*40*P was purified using pCB367 plasmid [2]. pCB367 is a pQE-11 (Qiagen) derivative containing wild-type gene *40* and the gene *39* carrying a hexa-histidine tag on its N-terminus, which allows the affinity purification of the native G*40*P. His_6-G*39*P stabilizes G*40*P and forms a complex with it only in the presence of ATP. Hence, in the presence of ATP, the co-expressed His_6-G*39*P-G*40*P complex is retained in a Ni-NTA column. Cells were grown at 37 ºC to an OD_{560} = 0.8, induced with 2 mM IPTG for 2 h, and harvested and stored at -20 ºC. Five g of cells were suspended in 25

[*] My experimental work is the FRET assay presented in Fig. A3.5 of this appendix. The remaining experimental work was performed by the co-authors of the corresponding publication [5].
[†] The contents of this appendix were published in [5] and are presented here with few modifications.

ml buffer A [50 mM sodium phosphate (pH 7.5), 10% (v/v) glycerol, 1mM $MgCl_2$, 0.1 mM ATP, 1 mM β-mercaptoethanol, 300 mM NaCl], lysed by sonication and centrifuged at 18,000 rpm in an SS-34 rotor for 45 min. The supernatant carrying G*40*P and G*39*P was brought to a concentration of 20 mM imidazole and loaded onto a Ni-NTA column (2 ml) equilibrated in buffer A carrying 300 mM NaCl and 20 mM imidazole. A gradient of fifty column volumes of buffer A containing 20– 500 mM imidazole and in the absence of ATP was applied and the last fractions, which contained G*40*P enriched with respect to G*39*P, were pooled and dialyzed against buffer B [50 mM Tris HCl (pH7.5), 10% (v/v) glycerol, 1mM $MgCl_2$, 50mM NaCl, 1mM β-mercaptoethanol] to be then loaded onto a Q-sepharose column. A linear gradient from 50 mM to 500 mM NaCl was applied and fractions enriched in G*40*P protein were pooled and loaded again onto a new Ni-NTA column (0.5 ml) in which the rest of the G*39*P forming a complex with G*40*P was retained. The flow-through containing pure G*40*P was dialyzed against buffer B and loaded onto a Q-sepharose column (0.5 ml) to elute 1 mg of G*40*P in the storage buffer [50 mM Tris HCl (pH 7.5), 50% (v/v) glycerol, 1 mM $MgCl_2$, 500 mM NaCl, 1 mM β-mercaptoethanol]. His_6-G*39*P was discarded because the His-tag affected the activity of the protein. To purify untagged G*39*P, plasmid pBT318 [3] was transformed into *E. coli* BL21(DE3)/pLysS, and cells were induced with 2 mM IPTG for 2 h, harvested and stored at -20 ºC. A total of 7.5 g of cells were suspended in 37.5 ml buffer C [50 mM Tris HCl (pH 7.5), 10% (v/v) glycerol, 1 mM dithiothreitol] containing 250 mM NaCl, lysed by sonication and centrifuged at 18,000 rpm in an SS-34 rotor for 30 min. Polyethylenimine (10% v/v, pH 7.5) was slowly added to the supernatant containing G*39*P to a final concentration of 0.25% (A_{260} = 120). The DNA and certain contaminating proteins were

pelleted by centrifugation (12,000 rpm in an SS-34 rotor, 10 min) and the pellet was discarded. Then proteins of the supernatant were precipitated by addition of solid ammonium sulfate to a final concentration of 80% saturation. The pellet containing G*39*P was resuspended in buffer C without salt and dialyzed against buffer C with 10 mM NaCl to be then loaded onto a Q-Sepharose column (2 ml). The protein eluted from the column in the 25 mM and 50 mM washes. These fractions were pooled and brought to 1.2 M ammonium sulfate to be then loaded onto a phenyl-Sepharose column. Serial washings of ten column volumes with buffer C and decreasing concentrations of ammonium sulfate from 1.2 to 0 were applied (1.2, 1, 0.8, 0.6, 0.4, 0.2 and 0 M ammonium sulfate) and the pure protein eluted in the 0.4 M and 0.2 M washing steps. Both fractions containing G*39*P were pooled and dialyzed against buffer B with 10 mM NaCl. A small Q-sepharose column (0.5 ml) was used to concentrate and elute 3 mg of G*39*P in the storage buffer (50 mM Tris HCl (pH 7.5), 50% (v/v) glycerol, 150 mM NaCl, 1 mM dithiothreitol).

G*38*P was purified from *E. coli* BL21(DE3)/pLysS cells carrying the plasmid pBT320 as described [3]. G*36*P was purified from *E. coli* BL21(DE3)/pLysS cells carrying the pCB596 plasmid. Plasmid pCB596 is a pET-3a (Novagen) derivative where gene *36* was cloned into the NdeI and BamHI restriction sites. Cells were grown to an OD_{560} = 0.8 at 37 ºC, 2 mM IPTG was added, and after 120 min cells were harvested by centrifugation and stored at -20 ºC. Five g of cells were resuspended in 25 ml buffer D [50 mM Tris HCl (pH 7.5), 1 mM dithiothreitol, 15% (v/v) glycerol] containing 150 mM NaCl. Lysis was accomplished by sonication and cell debris was removed by centrifugation (18,000 rpm in an SS-34 rotor, 30 min). DNA and G*36*P were precipitated

from the supernatant by addition of polyethylenimine (final concentration 0.25% v/v with A_{260} = 120) and centrifugation at 12,000 rpm in an SS-34 rotor for 10 min at 4 ºC. The protein was solubilized from the pellet in 25 ml buffer D containing 300 mM NaCl, and then precipitated by addition of ammonium sulfate to 30% saturation. Protein was re-dissolved in 25 ml of buffer D containing 300 mM NaCl and reprecipitated with 30% ammonium sulfate, rendering the protein almost pure. The pellet was resuspended in 25 ml buffer D containing 50 mM NaCl and extensively dialyzed. After dialysis, the sample was loaded onto a 1 ml Q-Sepharose column equilibrated with the same buffer. Serial washings of increasing concentrations of NaCl in ten column volumes were applied to the column and the pure protein eluted in the 150 and 200 mM NaCl washings steps. The pure protein was concentrated in another Q- Sepharose column and eluted in a single step with buffer D containing 500 mM NaCl. The G*36*P protein was dialyzed against storage buffer [50 mM Tris HCl (pH 7.5), 1 mM dithiothreitol, 50% (v/v) glycerol, 300 mM NaCl] and stored at -20 °C. The identity of the protein and the absence of *E. coli* SSB in the preparation were confirmed by MALDI-TOF. Plasmid pCB596 was used as a template to generate G*36*P variants lacking the last 9, 15 or 21 C-terminal residues that were purified following a protocol similar to the used for the wild type protein. The protein concentration was determined in all cases as previously described by measuring the absorbance of the peptide bond [4].

A3.2 SUPPLEMENTARY FIGURES

FIGURE A3.1
Alignment of the G*36*P and SsbA proteins. Identical residues have a black background and conserved residues gray.

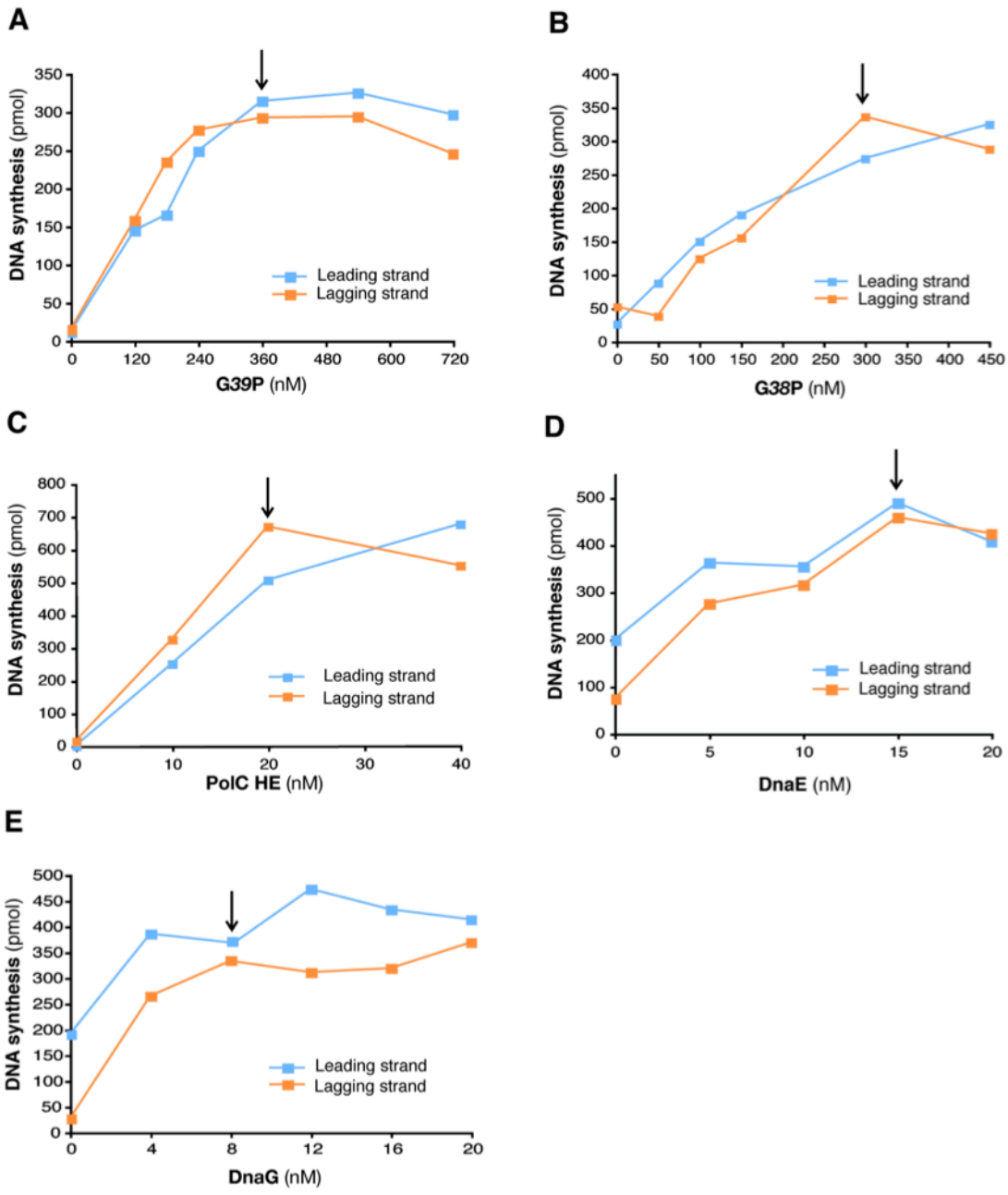

FIGURE A3.2
Optimization of SPP1 rolling circle replication. The reactions and the measurement of DNA synthesis on both leading and lagging strands were performed as described in Experimental Procedures. All the titrations were carried out in the presence of saturating levels of the other assay components and are the mean of at least two independent experiments. Titrations of (A) G*39*P, (B) G*38*P, (C) PolC, (D) DnaE, (E) and DnaG. An arrow indicates the concentration of protein chosen for subsequent experiments.

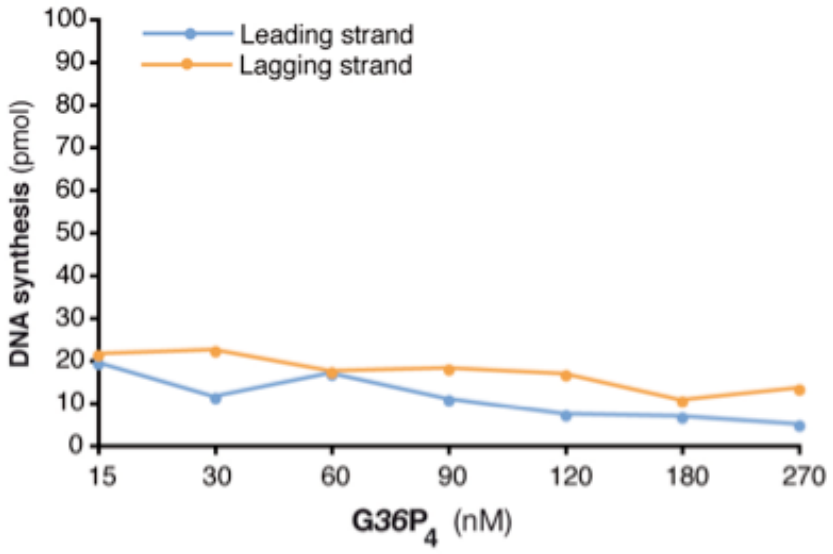

FIGURE A3.3
The *Bacillus subtilis* replisome can not be reconstituted in the presence of G*36*P. *B. subtilis* replication reactions were assembled with all host components except that $SsbA_4$ was replaced by increasing concentrations of G*36*P_4.

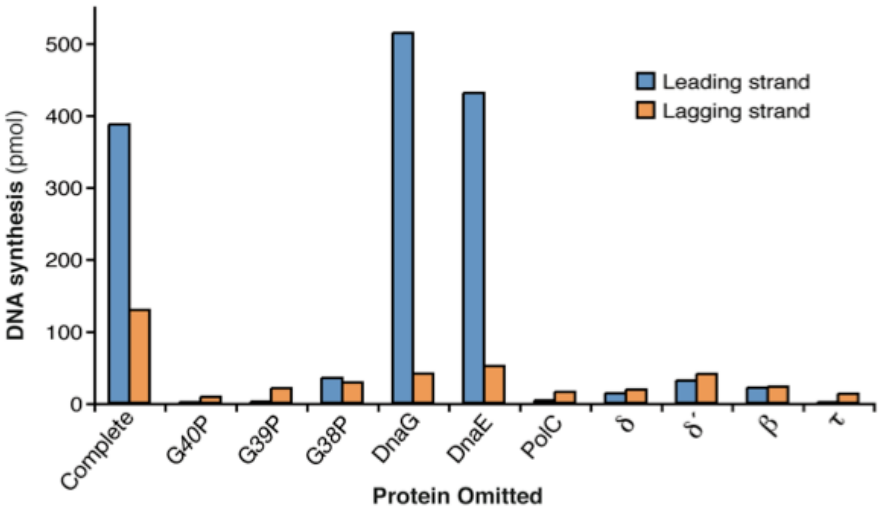

FIGURE A3.4
Protein requirements at high (180 nM) concentrations of G*36*P4. Leading and lagging strand synthesis were quantified by [α-^{32}P]dCTP or [α - ^{32}P]dGTP incorporation, respectively. The values represented are the mean of three independent experiments.

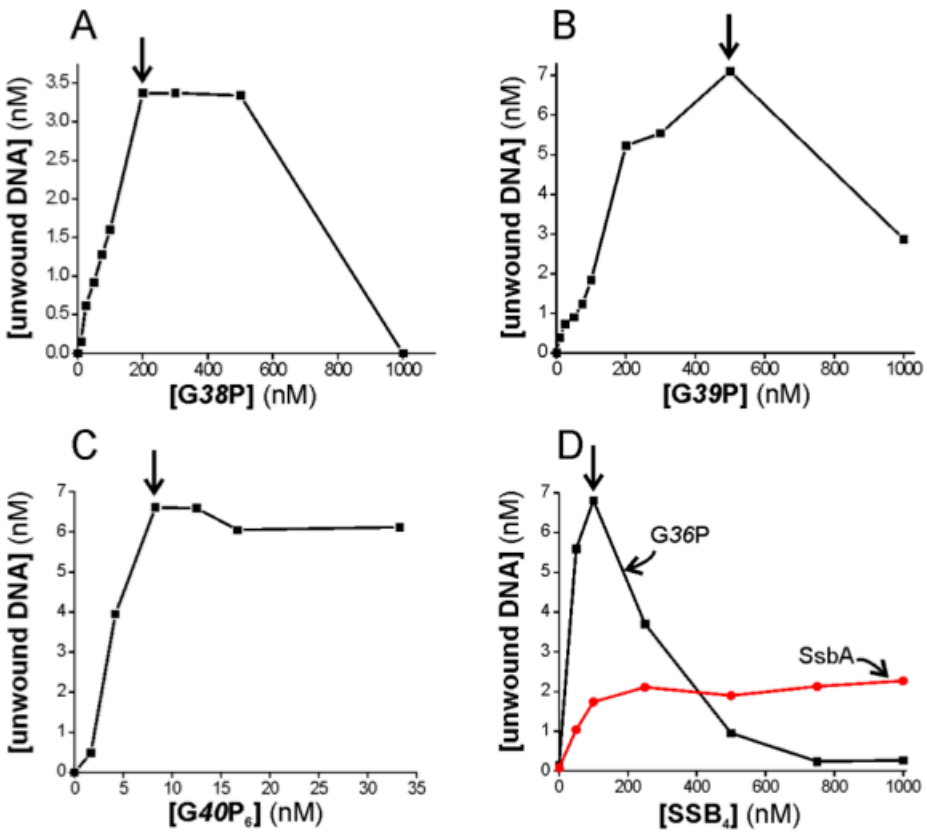

FIGURE A3.5
Optimization of SPP1 helicase assay. The substrate (see Figure 4.6A for diagram) was combined at 20 nM with SPP1 helicase and helicase loading proteins using the conditions described under section 4.3.3 for reactions with *B. subtilis* proteins. Helicase assembly proteins were titrated one at a time to optimize unwinding. (A) G*38*P titrated using 120 nM G*39*P, 15 nM G*40*P_6, and 100 nM G*36*P_4. (B) G*39*P titrated using 200 nM G*38*P, 15 nM G*40*P_6, and 100 nM G*36*P_4. (C) G*40*P titrated using 200 nM G*38*P, 500 nM G*39*P, and 100 nM G*36*P_4. (D) G*40*P requires an SSB to unwind forked substrates. G*36*P or SsbA titrated using 200 nM G*38*P, 500 nM G*39*P, and 10 nM G*40*P_6. The arrows indicate the concentration of protein chosen for subsequent experiments.

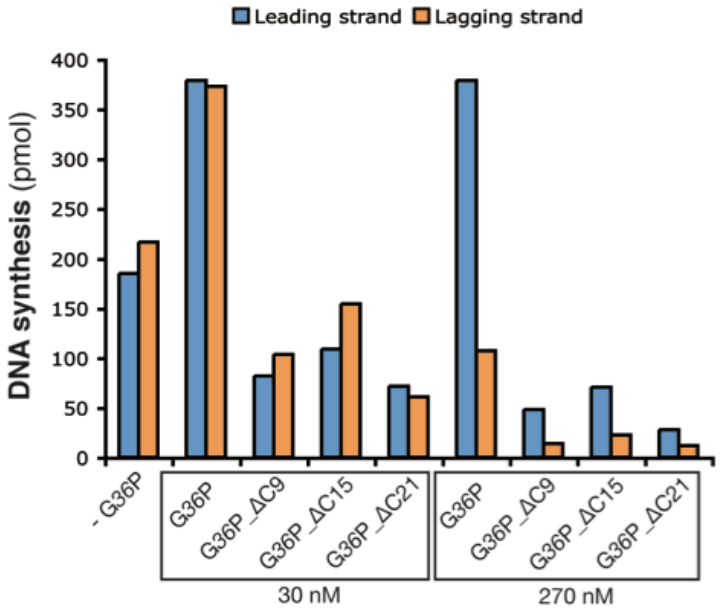

FIGURE A3.6
The C-terminal tail of G*36*P is required for efficient *in vitro* replication. Leading and lagging strand synthesis were quantified by [α-^{32}P]dCTP and [α -^{32}P]dGTP incorporation, respectively, in the presence of the serial C-terminal deletion mutants at low (30 nM) or high (270 nM) SSB_4 concentrations. The values represented are the mean of three independent experiments.

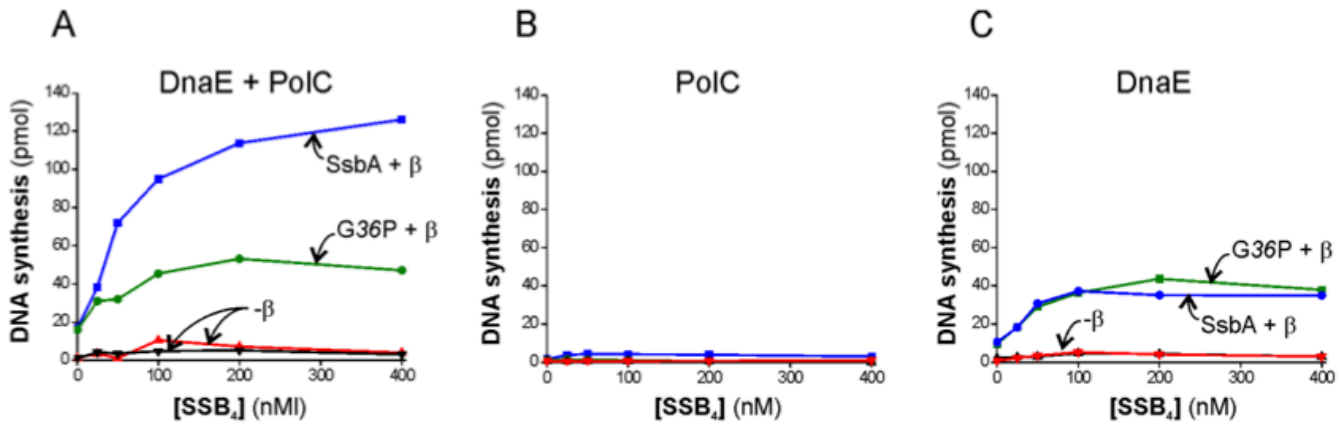

FIGURE A3.7
SsbA, but not G*36*P, stimulates RNA primer extension under conditions that require a handoff of the extended primer from DnaE to PolC in a reaction containing only *B. subtilis* proteins. Reactions were conducted as in Fig. 4.7 but contained RNA primers that cannot be elongated by PolC alone. (A) Extension of an RNA primer by both DnaE and PolC replicases using either SsbA or G*36*P. SsbA (blue and red lines) or G36P (green and black lines) was titrated in a reaction containing 0.5 nM DnaE and 2.5 nM PolC in the presence or absence of β_2 as indicated. Reactions were incubated at 30 ºC for 3 min. (B) Extension of an RNA primer by the PolC holoenzyme using either SsbA or G36P. Reactions were conducted as in (A) except DnaE was omitted from the reaction. (C) Extension of an RNA primer by the DnaE holoenzyme using either SsbA or G36P. Reactions were conducted as in (A) except PolC was omitted from the reaction.

A3.3 REFERENCES

1 Sanders, G. M., Dallmann, H. G. and McHenry, C. S. (2010) Reconstitution of the *B. subtilis* replisome with 13 proteins including two distinct replicases. Molecular Cell, Elsevier Ltd **37**, 273–81.

2 Mesa, P., Alonso, J. C. and Ayora, S. (2006) *Bacillus subtilis* bacteriophage SPP1 G*40*P helicase lacking the N-terminal domain unwinds DNA bidirectionally. Journal of Molecular Biology **357**, 1077–88.

3 Pedré, X., Weise, F., Chai, S., Lüder, G. and Alonso, J. C. (1994) Analysis of *cis* and *trans* acting elements required for the initiation of DNA replication in the *Bacillus subtilis* bacteriophage SPP1. Journal of Molecular Biology **236**, 1324–40.

4 Wolf, P. (1983) A critical reappraisal of Waddell's technique for ultraviolet spectrophotometric protein estimation. Analytical Biochemistry **129**, 145–55.

5 Seco, E. M., Zinder, J. C., Manhart, C. M., Lo Piano, A., McHenry, C. S. and Ayora, S. (2013) Bacteriophage SPP1 DNA replication strategies promote viral and disable host replication *in vitro*. Nucleic Acids Research **41**, 1711–21.

APPENDIX 4[*]

Supplemental material for

Chapter 5

Multiple C-terminal tails within a single *E. coli* SSB homotetramer coordinate DNA replication and repair[†]

A4.1 SUPPLEMENTARY MATERIALS AND METHODS

A4.1.1 Purification of linked-SSB proteins

The SSB-LD, SSB-LT, SSB-LD-Drl and SSB-LT-Drl proteins were overexpressed in BL21(DE3) cells and purified using a procedure similar to that described for *E. coli* SSB [1,2]. All further steps were carried out at 4 ˚C. 30 g of cell paste was resuspended in 150 mL lysis buffer (50 mM Tris-Cl, pH 8.0, 1 mM EDTA, 10 % sucrose, 0.2 M NaCl, 15 mM spermidine, 1 mM PMSF and 2x protease inhibitor cocktail) and lysed using an Avestin cell disrupter (Avestin Inc., Canada) and the lysate was clarified by centrifugation. The linked SSB protein and DNA in the clarified lysate were precipitated by adding polyethyleneimine (PEI) to 0.2% (final). The protein was resuspended from the PEI pellet using 200 ml of buffer $T^{0.4}$ (50 mM Tris-Cl, pH 8.0, 10 % glycerol, 1 mM EDTA, 0.4 M NaCl, 1 mM PMSF and 2x protease inhibitor cocktail). SSB from the PEI-

[*] The experimental work presented in this appendix was performed by the co-authors of the corresponding publication that is in preparation. This is included as a companion for the work in Chapter 5.

[†] The contents of this chapter are in preparation for publication in collaboration with Tim Lohman's lab at Washington University and are presented here with few modifications.

resuspension was precipitated by adding solid ammonium sulfate (144 g/L) (25% saturation) and the pellet containing >90 % pure SSB was resuspended in 200 ml buffer $T^{0.3}$ (50 mM Tris-Cl, pH 8.0, 15 % glycerol, 1 mM EDTA, 0.3 M NaCl, 1 mM PMSF and 2x protease inhibitor cocktail). The resuspended protein was loaded onto a ssDNA cellulose column (50 mL resin with ~3 mg/mL binding capacity) and eluted using 200 ml buffer T^2 (50 mM Tris-Cl, pH 8.0, 15 % glycerol, 1 mM EDTA, 2 M NaCl, 1 mM PMSF and 2x protease inhibitor cocktail). The linked SSB protein in the eluate was precipitated with 30.8% ammonium sulfate (170 g/L). The resulting precipitate was resuspended in 20 mL of storage buffer (30 mM Tris-Cl, pH 8.0, 50 % glycerol, 2 mM EDTA, 0.5 M NaCl, and 1x protease inhibitor cocktail) and stored as 5 mL aliquots at – 20˚C. Before performing experiments, theses proteins were further fractionated over a S200 size exclusion column in buffer $T^{0.5}$ (30 mM Tris-Cl, pH 8.0, 10 % glycerol, 1 mM EDTA, 0.5 M NaCl and 1x protease inhibitor cocktail). 3 ml fractions were collected throughout the procedure and the linked SSBs separate into distinct peaks. For the SSB-LD and SSB-LT, three distinct peaks are observed. The first peak corresponds to a higher order oligomeric species, the middle peak corresponds to an octamer and the last peak corresponds to a tetramer. For the SSB-LD-Drl and SSB-LT-Drl only the octameric and tetrameric species are observed. Once separated, the proteins do not redistribute into the higher order species at room temperature (Fig. A4.4). The tetrameric species was used for all the experiments described in this study. The fractions containing the tetramer were dialyzed into storage buffer (30 mM Tris-Cl, pH 8.0, 50 % glycerol, 2 mM EDTA, 0.5 M NaCl, and 1x protease inhibitor cocktail) and stored at -20 ˚C. The concentration of SSB was determined spectrophotometrically using the following

extinction coefficients (ε_{280} for 4-OB folds): SSB-WT, SSB-S1, SSB-LD and SSB-LT = 1.13 x10^5 $M^{-1}cm^{-1}$; SSB-LD-Drl = 1.08 x10^5 $M^{-1}cm^{-1}$ and SSB-LT-Drl = 9.53 x10^5 $M^{-1}cm^{-1}$.

A4.1.2 smFRET

The single-molecule fluorescence resonance energy transfer (smFRET) experiments were conducted with an objective-type total internal reflection (TIRF) microscope (Olympus IX71, IX2_MPITIRTL). A biotinylated DNA duplex/ssDNA having a SSB binding site $(dT)_{65}$ and a short hairpin containing a donor (cy3) and an acceptor (cy5) was generated by annealing a 5'-GCCTCGCTGCCGTCGCCA-biotin-3' with a 5'-TGGCGACGGCAGCGAGGC$(T)_{65}$ –Cy3-TGTGACTGAGACAGTCACTT-Cy5-T-3'). and immobilized onto the NeutrAvidin coated glass cover slip. The prepared slide was kept on a slide holder (Model BC-300A, 20/20 Technology, Canada) and its temperature was controlled by a Bionomic Controller BC-110 (20/20 Technology, Canada). The objective temperature was controlled by an objective heater system, Rev. 4 (Bioptechs, Inc., PA). The data collection and processing were done with software packages kindly provided by the Taekjip Ha (University of Illinois, Urbana Champaign) using IDL v.7.1 (Exelis Visual Information Solutions, CO) and Matlab v. 7.13 (MathWorks). The SSB binding site $(dT)_{65}$ was saturated with an 0.1 μM SSB solution (in 10 mM Tris pH 8.1, 0.1 mM Na_2EDTA, 0.5M NaCl - a salt concentration at which a single SSB protein is bound to $(dT)_{65}$) onto the channel and incubated for 5 to 10 minutes. Unbound (excess) SSB was removed by washing the channel with 200 ul or 20 channel volumes of an oxygen-deficient imaging buffer (10mM Tris (pH 8.1), 0.5 M NaCl, 0.1 mM Na_2EDTA, 2.5 mM

Trolox (6-hydroxy-2,5,7,8-tetramethylchroman-2-carboxylic acid, Sigma Aldrich)(3) , 0.8% w/v D-glucose, 0.1 mg/ml glucose oxidase (Type VII, from *Aspergillus*, Sigma Aldrich), 0.02mg/ml catalase (from bovine liver, Sigma Aldrich) (2,3)). At every spot, 2000 frames were collected with an exposure of 30 ms/frame at 25 C. Ten to forty spots were recorded all together. After corrections for leakage (from donor to acceptor) and detection efficiency, FRET traces for individual molecules were calculated. Molecules exhibiting anti-correlation changes in both donor and acceptors (FRET changes) were chosen for hidden Markov model (HMM) analysis to extract the transition rates between the FRET states. A histogram was created from the FRET traces (60 traces of SSB, 244 traces of SSB-LD-Drl, or 69 traces of SSB-LT-Drl) with a FRET efficiency bin-size of 0.01 and normalized to an area of 1.

A4.1.3 Amino Acid Composition of the various SSB proteins used in this study

(Note: The dotted lines denote deletions and the underlined sequence denote the various linkers. The amino acids in bold are the last 9 residues found in the C-terminus of the wild type SSB protein).

SSB-WT

MASRGVNKVILVGNLGQDPEVRYMPNGGAVANITLATSESWRDKATGEMKEQTEWH

RVVLFGKLAEVASEYLRKGSQVYIEGQLRTRKWTDQSGQDRYTTEVVVNVGGTMQM

LGGRQGGGAPAGGNIGGGQPQGGWGQPQQPQGGNQFSGGAQSRPQQSAPAAPS

NEPP**MDFDDDIPF**

SSB-S1

MASRGVNKVILVGNLGQDPEVRYMPNGGAVANITLATSESWRDKATGEMKEQTEWH

RVVLFGKLAEVASEYLRKGSQVYIEGQLRTRKWTDQSGQDRYTTEVVVNVGGTMQM

LGGRQGGGAPAGGNIGGGQPQGGWGQPQQPQGGNQFSGGAQSRPQQSAPAAPS

NEPP**MDFDDDIPF**TGASGT

SSB-D121-167

MASRGVNKVILVGNLGQDPEVRYMPNGGAVANITLATSESWRDKATGEMKEQTEWH

RVVLFGKLAEVASEYLRKGSQVYIEGQLRTRKWTDQSGQDRYTTEVVVNVGGTMQM

LGGRQGGG----------PP**MDFDDDIPF**

SSB-D131-167

MASRGVNKVILVGNLGQDPEVRYMPNGGAVANITLATSESWRDKATGEMKEQTEWH

RVVLFGKLAEVASEYLRKGSQVYIEGQLRTRKWTDQSGQDRYTTEVVVNVGGTMQM

LGGRQGGGAPAGGNIGGG----------PP**MDFDDDIPF**

SSB-D163-167

MASRGVNKVILVGNLGQDPEVRYMPNGGAVANITLATSESWRDKATGEMKEQTEWH

RVVLFGKLAEVASEYLRKGSQVYIEGQLRTRKWTDQSGQDRYTTEVVVNVGGTMQM

LGGRQGGGAPAGGNIGGGQPQGGWGQPQQPQGGNQFSGGAQSRPQQSAPAA-----

--PP**MDFDDDIPF**

SSB-LT-Drl

MASRGVNKVILVGNLGQDPEVRYMPNGGAVANITLATSESWRDKATGEMKEQTEWH

RVVLFGKLAEVASEYLRKGSQVYIEGQLRTRKWTDQSGQDRYTTEVVVNVGGTMQM

LQLGTQPELIQDAGGGVRMSGAGTASRGVNKVILVGNLGQDPEVRYMPNGGAVANIT

LATSESWRDKATGEMKEQTEWHRVVLFGKLAEVASEYLRKGSQVYIEGQLRTRKWTD

QSGQDRYTTEVVVNVGGTMQMLASHMASRGVNKVILVGNLGQDPEVRYMPNGGAV

ANITLATSESWRDKATGEMKEQTEWHRVVLFGKLAEVASEYLRKGSQVYIEGQLRTRK

WTDQSGQDRYTTEVVVNVGGTMQMLQLGTQPELIQDAGGGVRMSGAGTASRGVNK

VILVGNLGQDPEVRYMPNGGAVANITLATSESWRDKATGEMKEQTEWHRVVLFGKLA

EVASEYLRKGSQVYIEGQLRTRKWTDQSGQDRYTTEVVVNVGGTMQMLGGRQGGG

APAGGNIGGGQPQGGWGQPQQPQGGNQFSGGAQSRPQQSAPAAPSNEPP**MDFDD**

DIPF

SSB-LD-Drl

MASRGVNKVILVGNLGQDPEVRYMPNGGAVANITLATSESWRDKATGEMKEQTEWH

RVVLFGKLAEVASEYLRKGSQVYIEGQLRTRKWTDQSGQDRYTTEVVVNVGGTMQM

LQLGTQPELIQDAGGGVRMSGAGTASRGVNKVILVGNLGQDPEVRYMPNGGAVANIT

LATSESWRDKATGEMKEQTEWHRVVLFGKLAEVASEYLRKGSQVYIEGQLRTRKWTD

QSGQDRYTTEVVVNVGGTMQMLGGRQGGGAPAGGNIGGGQPQGGWGQPQQPQG

GNQFSGGAQSRPQQSAPAAPSNEPP**MDFDDDIPF**

SSB-LD

MASRGVNKVILVGNLGQDPEVRYMPNGGAVANITLATSESWRDKATGEMKEQTEWH

RVVLFGKLAEVASEYLRKGSQVYIEGQLRTRKWTDQSGQDRYTTEVVVNVGGTMQM

LGGRQGGGAPAGGNIGGGQPQGGWGQPQQPQGGNQFSGGAQSRPQQSAPAAPS

NEPPMDFDDDIPFTGASGTASRGVNKVILVGNLGQDPEVRYMPNGGAVANITLATSES

WRDKATGEMKEQTEWHRVVLFGKLAEVASEYLRKGSQVYIEGQLRTRKWTDQSGQD

RYTTEVVVNVGGTMQMLGGRQGGGAPAGGNIGGGQPQGGWGQPQQPQGGNQFS

GGAQSRPQQSAPAAPSNEPP**MDFDDDIPF**

SSB-LT

MASRGVNKVILVGNLGQDPEVRYMPNGGAVANITLATSESWRDKATGEMKEQTEWH

RVVLFGKLAEVASEYLRKGSQVYIEGQLRTRKWTDQSGQDRYTTEVVVNVGGTMQM

LGGRQGGGAPAGGNIGGGQPQGGWGQPQQPQGGNQFSGGAQSRPQQSAPAAPS

NEPPMDFDDDIPFTGASGTASRGVNKVILVGNLGQDPEVRYMPNGGAVANITLATSES

WRDKATGEMKEQTEWHRVVLFGKLAEVASEYLRKGSQVYIEGQLRTRKWTDQSGQD

RYTTEVVVNVGGTMQMLGGRQGGGAPAGGNIGGGQPQGGWGQPQQPQGGNQFS

GGAQSRPQQSAPAAPSNEPPMDFDDDIPFTGPWIDASRGVNKVILVGNLGQDPEVRY

MPNGGAVANITLATSESWRDKATGEMKEQTEWHRVVLFGKLAEVASEYLRKGSQVYI

EGQLRTRKWTDQSGQDRYTTEVVVNVGGTMQMLGGRQGGGAPAGGNIGGGQPQG

GWGQPQQPQGGNQFSGGAQSRPQQSAPAAPSNEPPMDFDDDIPFTGDVPRASRGV

NKVILVGNLGQDPEVRYMPNGGAVANITLATSESWRDKATGEMKEQTEWHRVVLFGK

LAEVASEYLRKGSQVYIEGQLRTRKWTDQSGQDRYTTEVVVNVGGTMQMLGGRQGG

GAPAGGNIGGGQPQGGWGQPQQPQGGNQFSGGAQSRPQQSAPAAPSNEPP**MDFD**

DDIPF

A4.2 SUPPLEMENTARY TABLE AND FIGURES

Number	Plasmid Name	Ability to Complement
1	pEW-WT-*t*	Helper plasmid
2	pEW-WT-*a*	Positive Control - YES
3	pEW-SSB-S1-*a*	Negative Control - NO
4	pEW-SSB-ΔC8	Negative Control - NO
5	pEW-SSB-LD-Drl-*a*	YES
6	pEW-SSB-LD-*a*	YES
7	pEW-SSB-LT-Drl-*a*	Dominant Negative
8	pEW-SSB-LT-*a*	Dominant Negative
9	pEW-SSB-LT-*a*	
10	pEW-SSB-Δ121-167-*a*	YES
11	pEW-SSB-Δ131-167-*a*	YES
12	pEW-SSB-Δ146-167-*a*	YES
13	pEW-SSB-Δ163-167-*a*	YES
14	pEW-SSB-LD-Δ121-167-*a*	Partial Complementation
15	pEW-SSB-LD-Δ146-167-*a*	NO
16	pEW-SSB-LD-Δ163-167-*a*	NO

TABLE A4.1
Plasmids used in this study. (-*a* or –*t* denotes plasmids carrying resistance to either ampicillin or tetracycline respectively).

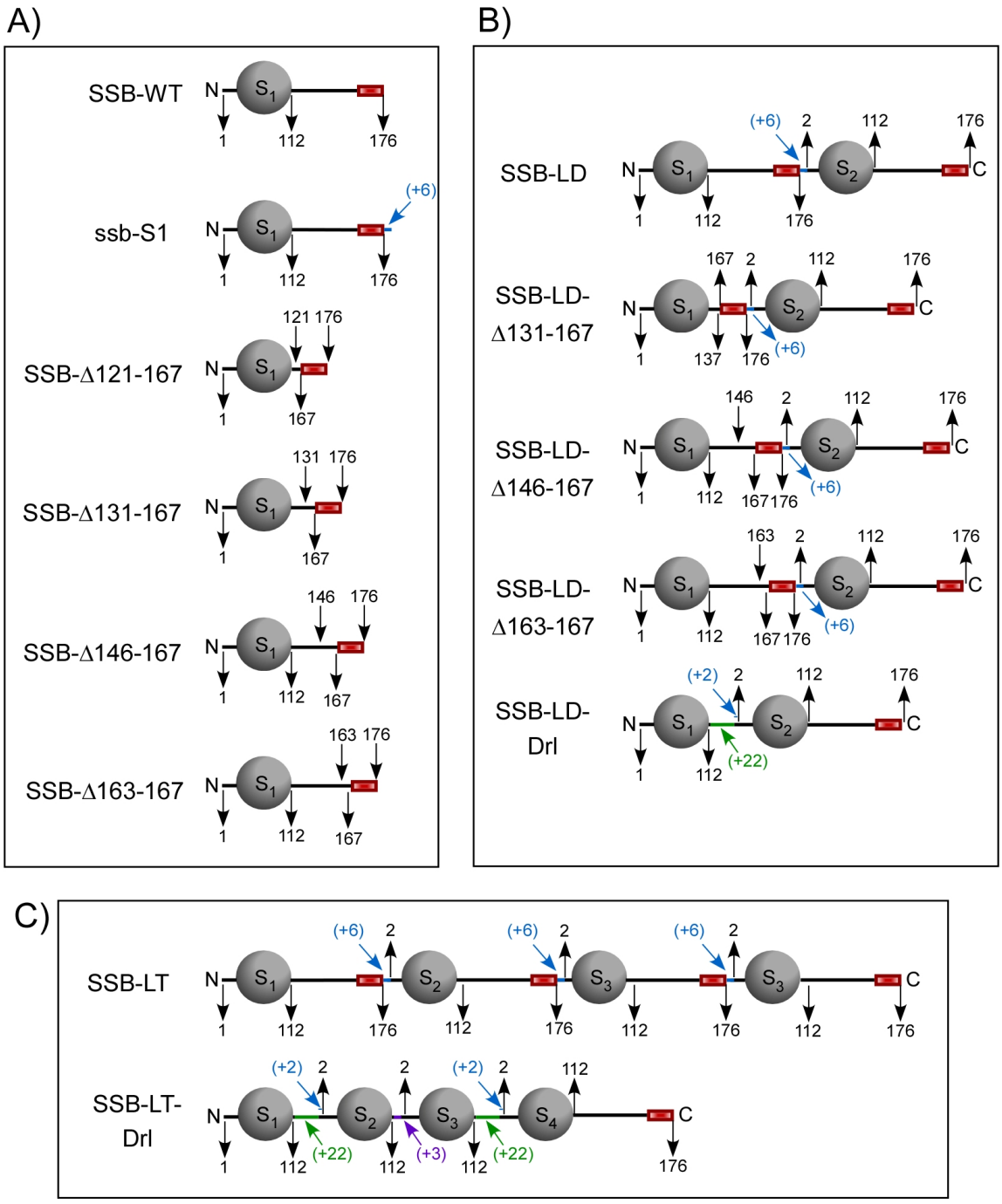

FIGURE A4.1
Schematic representation of the various constructs used in this study. A) Constructs in which the loop region between the DNA binding core and the SIP interaction motif (9 amino acids) have been deleted to various lengths. B) Linked dimers with various linkers between the two linked DNA binding domains. C) Linked tetramers with either the full length linker or the Drl linker between the DNA binding domains.

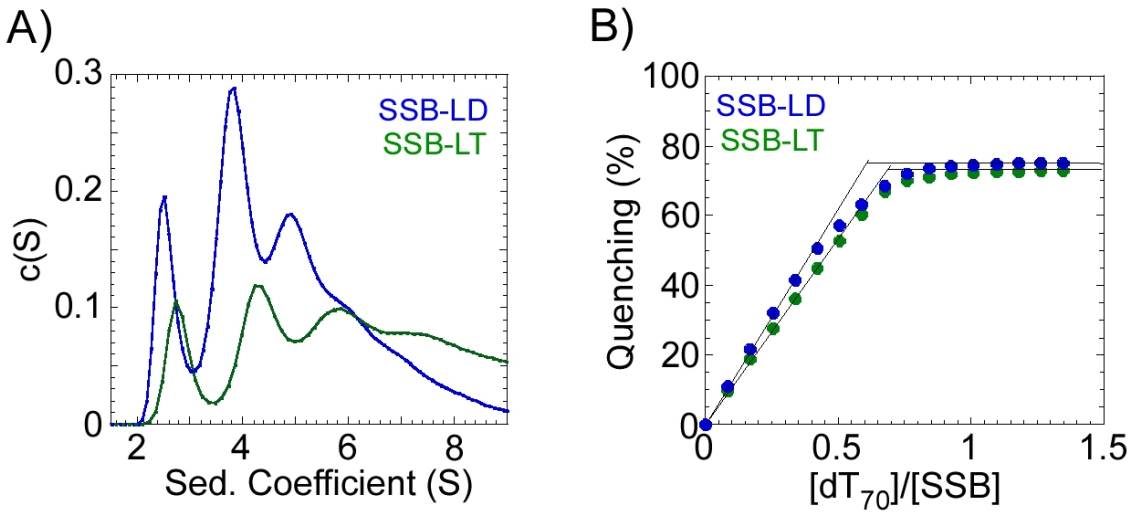

FIGURE A4.2
A) Analytical sedimentation experiments showing the presence of three or more species in the SSB-LD and SSB-LT protein preps. The predicted molecular weights correspond to a tetrameric, octameric and higher species in the reaction. B) Binding of the SSB-LD and SSB-LT proteins to $(dT)_{70}$. Protein preps containing a mixture of tetramers, octamers and higher order species are able to bind almost stoichiometrically to a $(dT)_{70}$ DNA substrate.

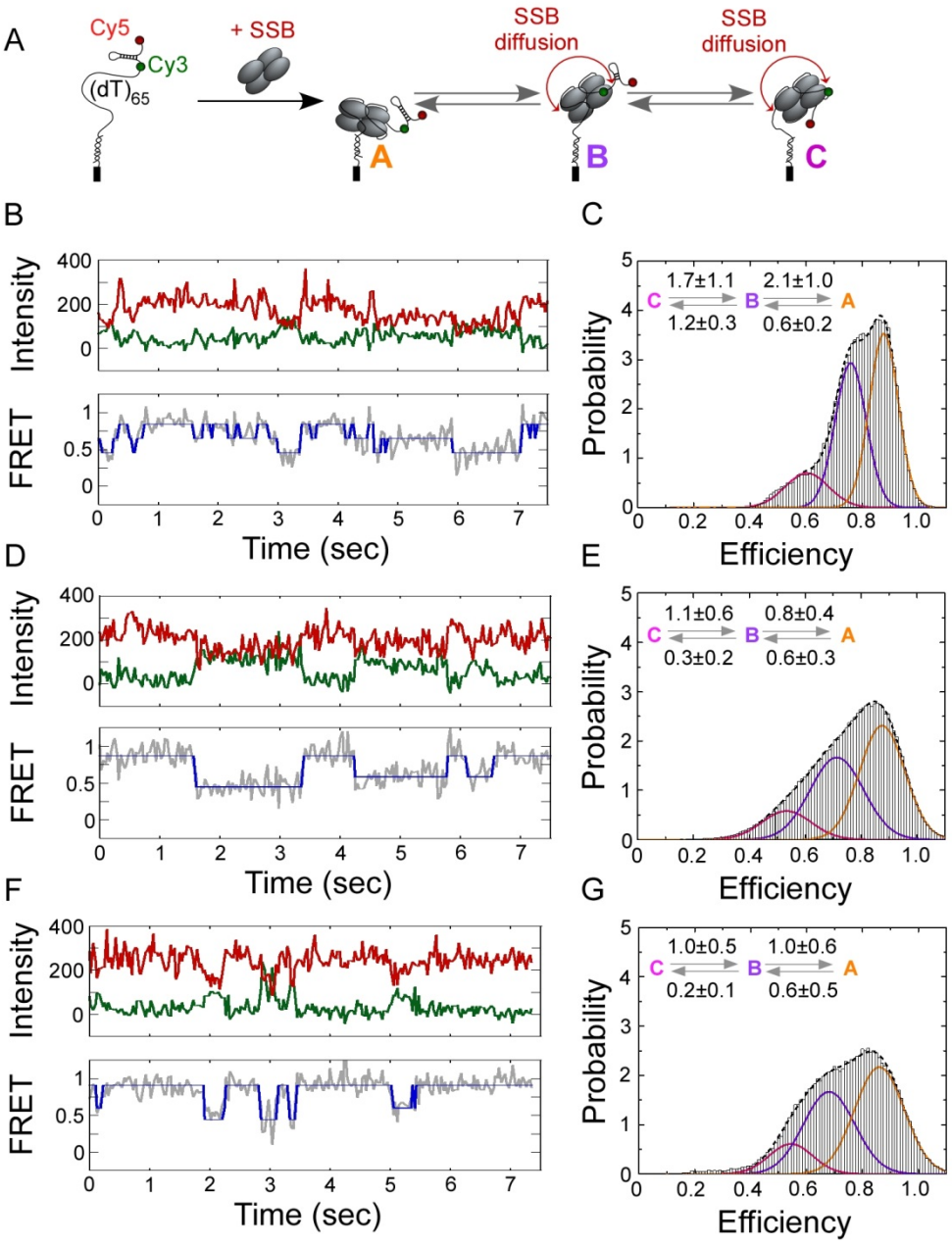

FIGURE A4.3
smFRET analysis showing diffusion and duplex melting activities of SSB tetramers. A) Schematic of DNA substrate used to monitor DNA melting associated with diffusion of SSB on ssDNA. The three predicted FRET states are also shown as A, B and C. Individual fluorescence changes in the donor (green) and acceptor (red) are sown along with the resulting change in FRET (grey) for SSB-WT (B), SSB-LD-Drl (D) and SSB-LT-Drl (F). The blue line denotes a Hidden Markov Model analysis of the FRET traces to identify distict states upon SSB diffusion and melting of the hairpin. C, E and G are histograms showing the presence of various FRET efficiencies for the SSB-WT, SSB-LD-Drl and SSB-LT-Drl tetramers respectively. The forward and backward rates for the transitions between the three states for each experiment are also depicted.

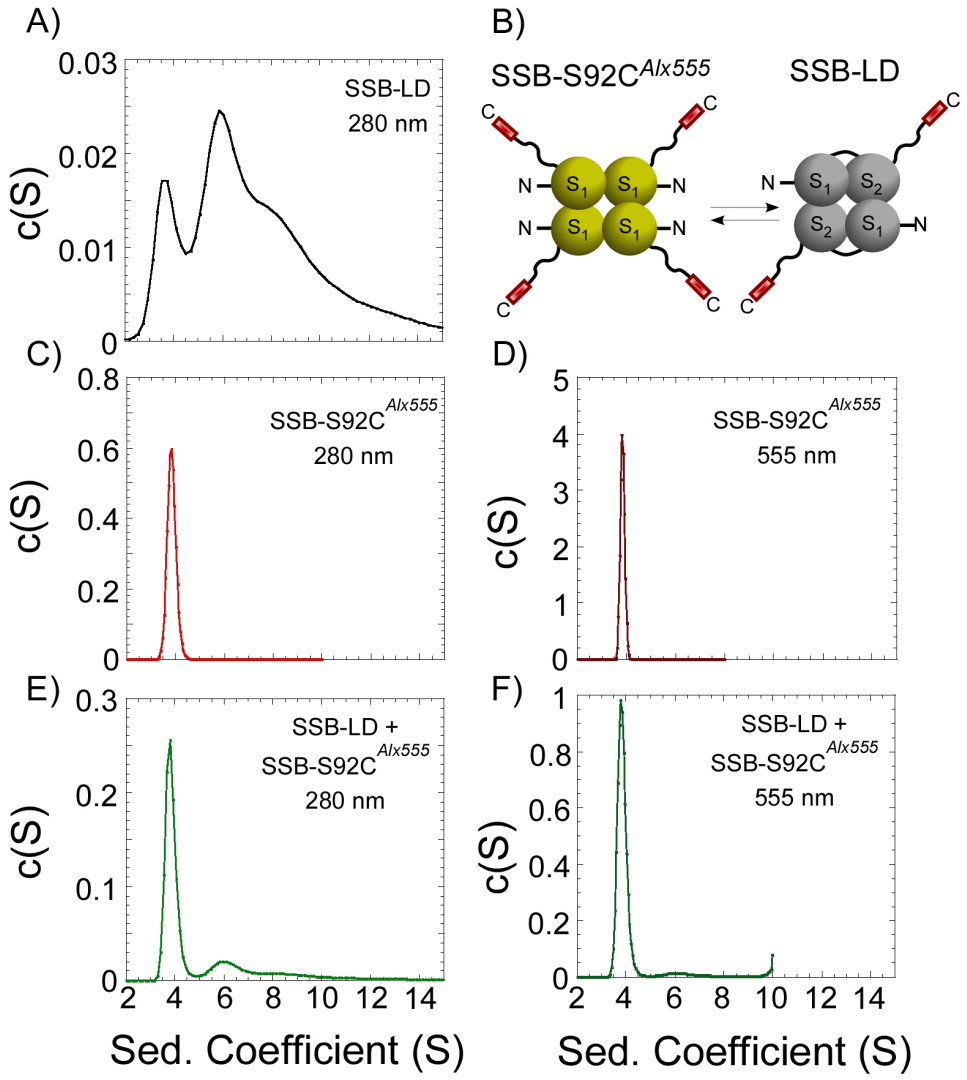

FIGURE A4.4
Stability of linked SSB tetramers. The mixed oligomeric pool of the purified linked SSB proteins after were mixed with unlinked SSB proteins labeled with alexa-555. After 3 days of incubation at 25 ˚C, we tested the stability of the olgigomeric proteins by analyzing the mixture using sedimentation velocity experiments and monitoring the absorbance at both 280 nm and 555 nm. A) Shows the various oligomeric states of the SSB-LD protein. B) Is a schematic for the mixing experiment. C) and D) show a single tetrameric species for the labeled unlinked SSB protein at 280 nm and 555 nm respectively. E) and F) show the 280 nm and 555 nm absorbance profiles for the mixed experiment showing that the labeled-unlinked SSB subunits have not exchanged with SSB-LD protein oligomeric mixtures.

A4.3 Transition states of SSB sliding

Using Hidden Markov Model analysis (HMM), we identified the distinct FRET states, and calculated the rate of the transitions among the states which reflects SSB diffusion and DNA melting [3]. The rates of the transitions among the three states are comparable for the SSB-LD-DrI [k_{CB} = 1.1±0.6, k_{BA} = 0.8±0.4, k_{AB} = 0.6±0.3 and k_{BC} = 0.3±0.2 respectively (Fig. A4.3)] and SSB-LT-DrI [k_{CB} = 1±0.5, k_{BA} = 1±0.6, k_{AB} = 0.6±0.5 and k_{BC} = 0.2±0.1 complexes (Fig. A4.3)]. However, they are slightly slower than the rates measured for wt SSB [k_{CB} = 2.1±1, k_{BA} = 1.7±1.1, k_{AB} = 1.2±0.3 and k_{BC} = 0.6±0.2 (Fig. A4.3)]. These data indicate that the reduced number of C-terminal tails does not affect the ability of SSB to diffuse along ssDNA, although the rates are reduced slightly.

A4.4 REFERENCES

1 Bujalowski, W. and Lohman, T. M. (1991) Monomers of the Escherichia coli SSB-1 mutant protein bind single-stranded DNA. Journal of molecular biology **217**, 63–74.

2 Lohman, T. M. (1986) Kinetics of protein-nucleic acid interactions: use of salt effects to probe mechanisms of interaction. CRC critical reviews in biochemistry **19**, 191–245.

3 Roy, R., Kozlov, A. G., Lohman, T. M. and Ha, T. (2007) Dynamic structural rearrangements between DNA binding modes of E. coli SSB protein. Journal of molecular biology **369**, 1244–57.

APPENDIX 5*

Determining points of contact between Pol III α and template downstream of the primer terminus in *E. coli*

A5.1 BACKGROUND

On the lagging strand, the polymerase operates in a discontinuous manner despite the polymerase's ability to replicate more than 150 kilobases without dissociating [1,2]. The polymerase progresses on single-stranded DNA templates at approximately 600 nucleotides per second [3]. This is also the approximate rate of replication fork progression [4]. Very little time remains for the polymerase to dissociate from the DNA, bind to a new primer at the replication fork, and begin synthesis of a new Okazaki fragment. Thus, a processivity switch is needed to increase the off-rate of the polymerase on the lagging strand.

Two non-exclusive models for a processivity switch have been proposed. In the collision model, it is hypothesized that the polymerase replicates to approximately the last nucleotide and collides with the 5'-end of the preceding Okazaki fragment. Sensing a completed Okazaki fragment triggers the release of the polymerase [5]. In the signaling model, synthesis of a new primer by primase at the replication causes the replicase to dissociate whether or not the Okazaki fragment is complete [6].

* All mass spectrometry procedures and analysis were performed by William Old of the Mass Spectrometry facility at the University of Colorado Boulder. I performed the remaining experimental work.

A kinetic assessment of the collision model indicates that such a mechanism alone is insufficient to support the physiological off-rate of the polymerase (Chapter 2). On primed template, an initiation complex was observed to have a half-life of ~15 min (Chapter 2). Reducing the gap size to 1 nucleotide on a model substrate with a blocking oligonucleotide mimicking a preceding Okazaki fragment, increased the off-rate by ~2.5-fold (Chapter 2). Converting the gap to a nick increased the rate another 3-fold, giving a half-life of ~2 min (Chapter 2). Providing an exogenous primer-template and ATP can increase the off-rate even further ($t_{1/2}$ ~ 30 s) (Chapter 2). This remains too slow to support the less than 0.1 s available for the polymerase to cycle.

Efforts to increase the off-rate proved inadequate to substantiate the collision model, but it is important to note that the replicase was destabilized when the last nucleotide was added, forming a nick (Chapter 2). Despite being too slow for replication, this model may provide insight into other functions of the polymerase where it needs to release from substrate. It is likely significant in Pol III-dependent repair pathways, such as mismatch repair and long patch repair.

Using a non-specific photo-crosslinker (phenyldiazirine), it is shown that α makes direct contact with the primer terminus, single-stranded DNA ahead of the primer terminus, and the duplex region near the 5'-end of a preceding Okazaki fragment on model substrates (Chapter 2). α is in position to sense duplex DNA ahead of the nucleotide incorporation site triggering cycling. Sensing such road blocks may trigger conformational changes, disrupting interactions, ultimately leading to polymerase release.

Global conformational changes take place within α when primer-template is bound [7]. In particular, the β_2 binding domain moves to a position where it can more efficiently interact with β_2 [7]. The single-stranded portion of the template in the active site is spatially constrained. When the template becomes double-stranded, insertion of the last nucleotide may become energetically unfavorable. Double-stranded DNA may decrease affinity between the active site of α and the DNA substrate, causing these conformational changes to reverse and the polymerase switching to a low processivity mode. The entire polymerase may act as a sensor for the end of elongation.

A5.2 RESEARCH GOALS

To identify residues that are positioned to sense duplex DNA ahead of the site for nucleotide incorporation, photo-crosslinking coupled with mass spectrometry is used. Phenyldiazirine was chosen to probe residues in α, due to its lack of specificity. A further description of this substrate and its use is provided in Chapters 2 and 6.

Studies have been done that show the feasibility of identifying peptides with mass shifts corresponding to photo-crosslinkers [8–11]. The ultimate goal of this work was to map out residues that photo-crosslink on α to determine candidate residues that contact template DNA downstream of the primer terminus. Using these data, a proposal could be made concerning the sensor α uses to differentiate between single-stranded and duplex DNA.

Due to the potential problems (sample heterogeneity) associated with working with a non-specific photo-crosslinker, a method for separating modified peptides was

optimized using SNAP-tag protein as a simplified control. The methods developed for this project were optimized with this system and are presented here.

SNAP-tag is O^6-alkylguanine-DNA alkyltransferase—a DNA repair protein that will recognize lesions in DNA and repair them. Its substrate O^6-methylguanine (BG-GLA) is commercially available, as is SNAP-tag protein. The N-hydroxysuccinimide form of the substrate can be attached to an amine modified oligonucleotide and HPLC-purified. This oligonucleotide can then be reacted with SNAP-tag protein. SNAP-tag will recognize O^6-methylguanine as a lesion and repair it. C145 of the protein will act as a nucleophile, attacking the lesion thereby forming a covalent bond to the substrate. This creates a mimic to the phenyldiazirine photo-crosslinking method of forming a covalent bond between a protein and template DNA. With SNAP-tag, a specific bond is formed between C145 of the protein and the position modified on the oligonucleotide. This method has the advantage of being able to modify >90% of the SNAP-tag protein. Also I can predict which tryptic peptide will have a mass shift corresponding to the digested nucleotide. Initially, this method was used to establish proof of concept to later be applied to photo-crosslinking the α subunit of Pol III.

A5.3 MATERIALS AND METHODS

A5.3.1 Reagents

BG-GLA-NHS and SNAP-tag were purchased from New England BioLabs. Protein components were purified as described for Pol III [12], ε [13], τ [14], δ [15], δ'

[15], χ [16], ψ [16], and β_2 [17]. DnaX protein complex with stoichiometry $\tau_3\delta\delta'\chi\psi$ was purified as described previously [18,19]. The ε subunit was mutated at D12A and E14A to eliminate endogenous 3' to 5' exonuclease activity, which degrades the primer [20].

All oligonucleotides were obtained from IDT. 60-mer template oligonucleotide: 5'-GCGACTACAGGCTCACTGATGG/iAmMC2T/CCCAAAACAGCCTATGCGCGTGA TCTGTACACATCTG-biotin-3' where iAmMC2T is amino-modifier C2 dT phosphoramidite from Glen Research. 30-mer primer oligonucleotide: 5'-CAGATGTGTACAGATCACGCGCATAGGCTG-3'. 20-mer blocking oligonucleotide: 5'-ATCAGTGAGCCTGTAGTCGC-biotin-3'.

A5.3.2 Preparations of SNAP-tag control samples

A solution of 0.1 M BG-GLA-NHS was prepared in anhydrous N,N-dimethylformamide. A 0.88 μmol portion of this sample was reacted with 20 nmol of amine-modified 60-mer template oligonucleotide in a 0.1 M $Na_2B_4O_7 \cdot 10H_2O$ buffer at pH 8.5. The reaction was incubated at room temperature overnight.

The sample was purified by HPLC. A Waters brand XBridge OST C_{18} column with dimensions 4.6 x 50 mm and a pore size of 2.5 μm is used with a 0.1 M triethylammonium acetate pH 7.0 mobile phase. The sample was applied in 100% of the previously mentioned buffer and eluted with 100% acetonitrile increasing by 1.54%/min up to 30%. Absorbance was monitored at 265 nm for the oligonucleotide.

SNAP-tag protein (New England BioLabs) was then combined with a five-fold molar excess of purified 60-mer oligonucleotide containing the BG-GLA substrate (100

pmol of SNAP-tag and 500 pmol of substrate) in a buffer containing 50 mM Tris-HCl pH 7.5, 100 mM NaCl, 0.1% Tween-20, 1 mM DTT, and 10 mM $Mg(OAc)_2$. The reaction mixture was allowed to incubate overnight at 4 ºC per the manufacturer's instructions. A negative control without oligonucleotide was included.

Using conditions independently optimized, 200 units of Phosphodiesterase I (3' to 5' exonuclease) (Sigma-Aldrich), 200 units of Nuclease P1 (ssDNA endonuclease) (Sigma-Aldrich), and 150 units of $RecJ_f$ (5' to 3' exonuclease) (New England BioLabs) were added to completely digest the oligonucleotide-portion of the sample. The reaction was incubated overnight at 37 °C in a buffer with 50 mM NaCl, 10 mM Tris-HCl 10 mM $MgCl_2$, and 1 mM DTT at pH 7.9.

The samples were resolved by 4-20% SDS-PAGE. The gel was stained using Coomassie G-250 to visualize. The bands containing SNAP-tag (bound to nucleotide and unbound) were excised and de-stained as described [21]. An in-gel trypsin digest was then performed as described [21] using a 1:2 w/w ratio of trypsin to substrate.

One half of the digested sample containing nucleotide was subjected to a TiO_2 enrichment step to isolate the phosphate-containing portion of the sample as described [22].

A5.3.3 Mass spec methods/analysis of SNAP-tag control samples

Samples were analyzed by high-resolution tandem mass spectrometry analysis on a LTQ-Orbitrap mass spectrometer (Thermo) interfaced with an Eksigent nanoLC-2D HPLC. Peptide mixtures (10 μL) were loaded and separated on a Acclaim PepMap100

C18 (15 cm x 75 mm) nanocolumn (Dionex) by a linear gradient from 95% Buffer A (0.1% formic acid) to 40% Buffer B (0.1% formic acid, 80% acetonitrile) over 90 min at flow rate 300 nL/min. Parent ion masses were determined in the Orbitrap and the top 5 most intense precursors were selected for fragmentation by collision induced dissociation in the LTQ ion trap. Automatic gain control was $1x10^4$ for ion trap MS/MS and $1x10^6$ for Orbitrap parent scans.

Tandem mass spectra (MS/MS) were extracted and searched using Mascot (v2.1, Matrix Science) against the SNAP-Tag protein sequence (below) with a 20 ppm parent mass tolerance and a 0.6 Da fragment mass tolerance, and a variable modification of 635.1992 Da addition to C residues (addition of $C_{27}H_{34}N_5O_{11}P$), corresponding to modification of cysteine by the single nucleotide analog containing the crosslinker. All MS/MS peptide assignments were manually verified.

SNAP-tag sequence:

MDKDCEMKRTTLDSPLGKLELSGCEQGLHEIKLLGKGTSAADAVEVPAPA
AVLGGPEPLMQATAWLNAYFHQPEAIEEFPVPALHHPVFQQESFTRQVLW
KLLKVVKFGEVISYQQLAALAGNPAATAAVKTALSGNPVPILIPCHRVVS
SSGAVGGYEGGLAVKEWLLAHEGHRLGKPGLGPAGIGAPGS

A5.3.4 Preparations of Pol III photo-crosslinked samples

2 nmol of amine-modified 60-mer template oligonucleotide was derivatized with the phenyldiazirine photo-crosslinker (Chapter 2). The sample was HPLC-purified as

described (Chapter 2). The product was annealed to equimolar 30-mer primer oligonucleotide and 20-mer blocking oligonucleotide as described previously (Chapter 2). The oligonucleotide substrate is identical to the T+8 in Fig. 2.3 of this thesis.

4 μM annealed substrate was combined with 4 μM Pol III core, 4 μM DnaX complex, and 4 μM β_2 in a buffer containing 50 mM HEPES pH 7.5, 100 mM potassium glutamate, 20% glycerol, 0.02% Nonidet-P40, 10 mM DTT, 10 mM $Mg(OAc)_2$, and 2 mM ATP. The reaction was irradiated for 1 h at 350 nm as described in Chapters 2 and 6.

Nuclease digestion, SDS-PAGE, protease digestion, and TiO_2 enrichment steps were performed as described for SNAP-tag samples, with the exception that DNaseI was substituted for Nuclease P1.

A5.3.5 Mass spec methods/analysis of Pol III photo-crosslinked samples

Analyses of Pol III digests were performed with the same high-resolution mass spectrometry method (LC/MS/MS) used for SNAP-Tag. Analysis included: Mascot database search against Pol III sequence with various phenyldiazarine modifications, i.e. addition of C23H26N4O10P F3 (+606.133865 Da). Error tolerant Mascot database search, which involves a first pass search with no specified variable modifications, followed by iterative searching of unassigned MS/MS allowing for each PTM in the database, which included all modifications in the Unimod database as well as the 10 nucleotide variants that would result from the diazirine crosslinking. Open modification search, which allows for any mass modification shift, using MS-Alignment [23]. Search

for expected neutral losses (-320, -196, -98) that were seen with the SNAP-Tag, to find those MS/MS that might be candidates, followed by manual de-novo sequencing. Only 10-15 cases were analyzed out of 100s of possible MS/MS due to time limitations.

A5.4 PRELIMINARY RESULTS

For preparing the SNAP-tag control samples, nucleases were chosen that give a product with a 5'-phosphate. This was done so that a TiO_2 enrichment step could be performed to select for phosphate-containing moieties. In both reactions with and without the TiO_2 enrichment step, a modified variant of the predicted tryptic peptide (TALSGNPVPILIPCHR) was observed. In each, this variant had an addition of 635.21 ±1 Da. This mass is congruent to the predicted structure in Fig. A5.1 which has a mass of 635.56 Da. Mass spectrometry data is included in Fig. A5.2.

Pol III crosslink digests were analyzed with the same high-resolution mass spectrometry method (LC/MS/MS) used for SNAP-Tag analyses. Several methods for identifying post-translational modified peptides were attempted. The expected phosphorylated and dephosphorylated products are in Fig. A5.3. Initially, candidate crosslinks mapped to R272 (located in the junction between the PHP and palm domains), Y15 (in the PHP domain), and T520 (located in the palm domain) were identified as having masses shifted by 604 Da, 525 Da, and 525 Da, respectively in the trypsin digested samples.

After closer inspection, no nucleotide crosslinked peptides assigned with high confidence were found. The difficulty with this type of crosslinker is that the addition can

occur at any residue, which results in massive search spaces and lowered sensitivity. Although many assignments to MS/MS with masses consistent with a nucleotide-peptide crosslink were found (including the above mentioned residues), they were ultimately deemed false positives, because the spectral evidence lacked sufficient coverage over the peptide backbone or expected ions were missing.

The success with the SNAP-tag control samples shows proof of concept for this type of sample preparation and separation for use in identifying modified amino acids by mass spectrometry. It also shows high selectivity for peptides with crosslinked nucleotides containing a 5'-phosphate with the success of the TiO_2 enrichment step. Future experiments with Pol III should be scaled up to offset issues with heterogeneity.

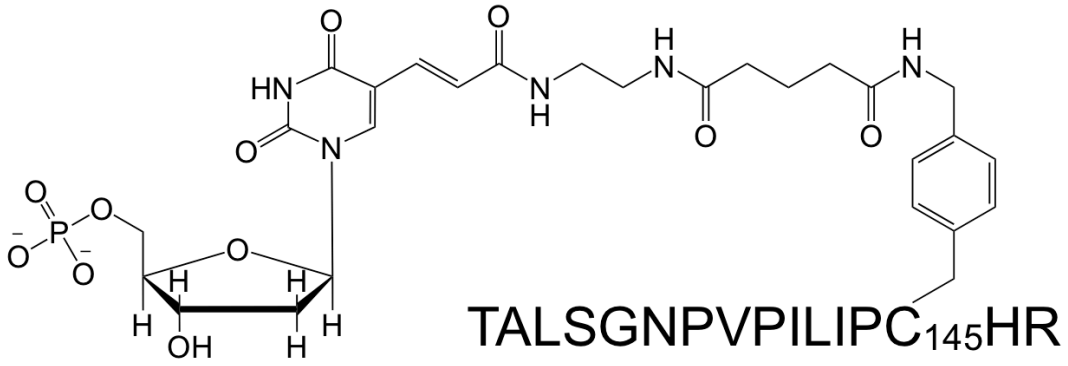

FIGURE A5.1
Expected nuclease product attached to C145 of SNAP-tag (tryptic peptide).

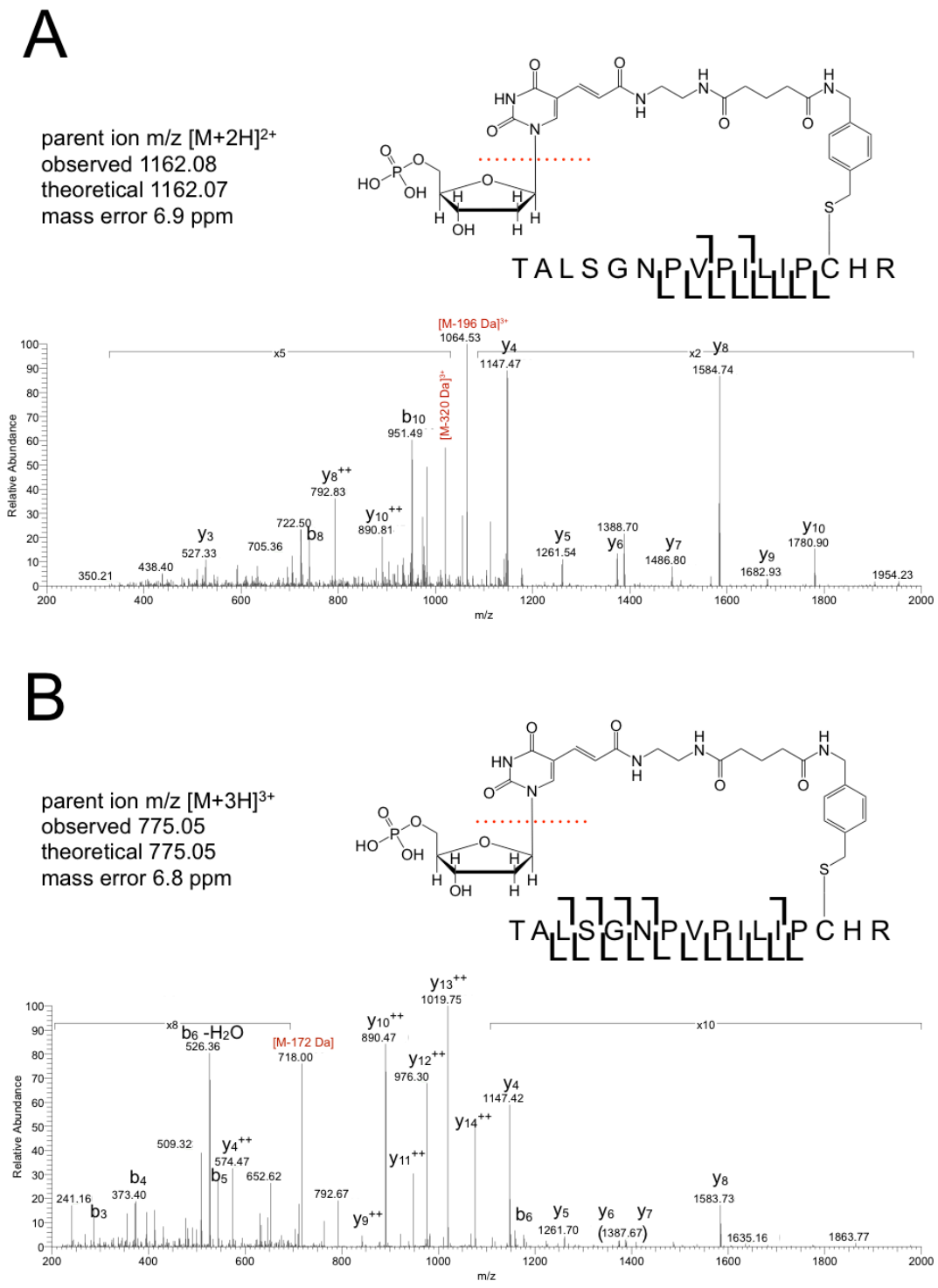

FIGURE A5.2
Mass spectrometry spectra for SNAP-tag control experiment. The expected structure is shown attached to sulfur of C145 of the peptide. The characteristic neutral loss of the sugar is indicated by the red dotted line. (A) doubly charged ion, (B) triply charged ion.

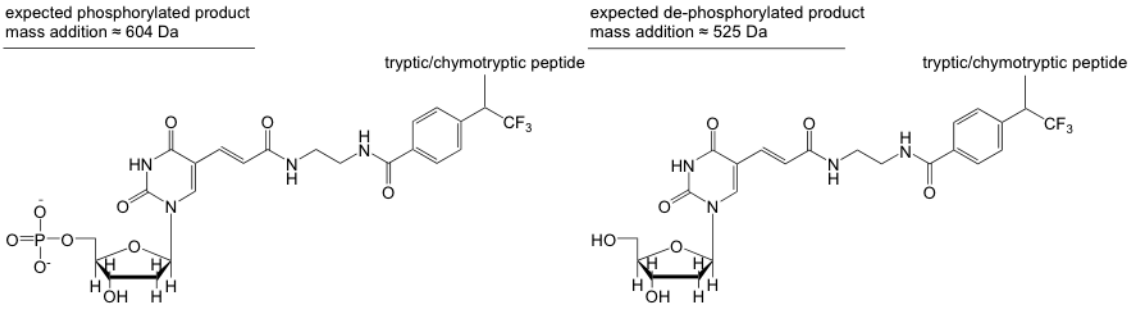

FIGURE A5.3
Expected phosphorylated (left) and dephosphorylated (right) products of nuclease digestion and corresponding mass additions to proteolysis products.

A5.5 REFERENCES

1 Mok, M. and Marians, K. J. (1987) Formation of rolling-circle molecules during ΦX174 complementary strand DNA replication. The Journal of Biological Chemistry **262**, 2304–9.

2 Mok, M. and Marians, K. J. (1987) The *Escherichia coli* preprimosome and DNA B helicase can form replication forks that move at the same rate. The Journal of Biological Chemistry **262**, 16644–54.

3 Johanson, K. O. and McHenry, C. S. (1982) The β subunit of the DNA polymerase III holoenzyme becomes inaccessible to antibody after formation of an initiation complex with primed DNA. The Journal of Biological Chemistry **257**, 12310–5.

4 Breier, A. M., Weier, H.-U. G. and Cozzarelli, N. R. (2005) Independence of replisomes in *Escherichia coli* chromosomal replication. Proceedings of the National Academy of Sciences of the United States of America **102**, 3942–7.

5 Leu, F. P., Georgescu, R. and O'Donnell, M. (2003) Mechanism of the *E. coli* τ processivity switch during lagging-strand synthesis. Molecular Cell **11**, 315–27.

6 Wu, C. A., Zechner, E. L., Reems, J. A., McHenry, C. S. and Marians, K. J. (1992) Coordinated leading- and lagging-strand synthesis at the *Escherichia coli* DNA replication fork. V. Primase action regulates the cycle of Okazaki fragment synthesis. The Journal of Biological Chemistry **267**, 4074–83.

7 Wing, R. A, Bailey, S. and Steitz, T. A. (2008) Insights into the replisome from the structure of a ternary complex of the DNA polymerase III α-subunit. Journal of Molecular Biology **382**, 859–69.

8 Golden, M. C., Resing, K. A., Collins, B. D., Willis, M. C. and Koch, T. H. (1999) Mass spectral characterization of a protein-nucleic acid photocrosslink. Protein science : a publication of the Protein Society **8**, 2806–12.

9 Gomes, A. F. and Gozzo, F. C. (2010) Chemical cross-linking with a diazirine photoactivatable cross-linker investigated by MALDI- and ESI-MS/MS. Journal of Mass Spectrometry : JMS **45**, 892–9.

10 Krivos, K. L. and Limbach, P. A. (2010) Sequence analysis of peptide:oligonucleotide heteroconjugates by electron capture dissociation and electron transfer dissociation. Journal of the American Society for Mass Spectrometry **21**, 1387–97.

11 Steen, H., Petersen, J., Mann, M. and Jensen, O. N. (2001) Mass spectrometric analysis of a UV-cross-linked protein-DNA complex: tryptophans 54 and 88 of *E.*

coli SSB cross-link to DNA. Protein science : a publication of the Protein Society **10**, 1989–2001.

12 Kim, D. R. and McHenry, C. S. (1996) *In vivo* assembly of overproduced DNA polymerase III. Overproduction, purification, and characterization of the α, α-ε, and α-ε-θ subunits. The Journal of Biological Chemistry **271**, 20681–9.

13 Wieczorek, A. and McHenry, C. S. (2006) The NH_2-terminal php domain of the alpha subunit of the *Escherichia coli* replicase binds the ε proofreading subunit. The Journal of Biological Chemistry **281**, 12561–7.

14 Dallmann, H. G., Thimmig, R. L. and McHenry, C. S. (1995) DnaX complex of *Escherichia coli* DNA polymerase III holoenzyme. Central role of τ in initiation complex assembly and in determining the functional asymmetry of holoenzyme. The Journal of Biological Chemistry **270**, 29555–62.

15 Song, M. S., Pham, P. T., Olson, M., Carter, J. R., Franden, M. A., Schaaper, R. M. and McHenry, C. S. (2001) The δ and δ' subunits of the DNA polymerase III holoenzyme are essential for initiation complex formation and processive elongation. The Journal of Biological Chemistry **276**, 35165–75.

16 Olson, M. W., Dallmann, H. G. and McHenry, C. S. (1995) DnaX complex of *Escherichia coli* DNA polymerase III holoenzyme. The χψ complex functions by increasing the affinity of τ and γ for δ.δ' to a physiologically relevant range. The Journal of Biological Chemistry **270**, 29570–7.

17 Johanson, K. O., Haynes, T. E. and McHenry, C. S. (1986) Chemical characterization and purification of the β subunit of the DNA polymerase III holoenzyme from an overproducing strain. The Journal of Biological Chemistry **261**, 11460–5.

18 Pritchard, A. E., Dallmann, H. G. and McHenry, C. S. (1996) *In vivo* assembly of the τ-complex of the DNA polymerase III holoenzyme expressed from a five-gene artificial operon. Cleavage of the τ-complex to form a mixed γ-τ-complex by the OmpT protease. The Journal of Biological Chemistry **271**, 10291–8.

19 Glover, B. P. and McHenry, C. S. (2000) The DnaX-binding subunits δ' and ψ are bound to γ and not τ in the DNA polymerase III holoenzyme. The Journal of Biological Chemistry **275**, 3017–20.

20 Fijalkowska, I. J. and Schaaper, R. M. (1996) Mutants in the Exo I motif of *Escherichia coli* dnaQ: defective proofreading and inviability due to error catastrophe. Proceedings of the National Academy of Sciences of the United States of America **93**, 2856–61.

21 Huynh, M.-L., Russell, P. and Walsh, B. (2009) Tryptic digestion of in-gel proteins for mass spectrometry analysis. Methods in Molecular Biology (Clifton, N.J.) **519**, 507–13.

22 Richter, F. M., Hsiao, H.-H., Plessmann, U. and Urlaub, H. (2009) Enrichment of protein-RNA crosslinks from crude UV-irradiated mixtures for MS analysis by on-line chromatography using titanium dioxide columns. Biopolymers **91**, 297–309.

23 Tsur, D., Tanner, S., Zandi, E., Bafna, V. and Pevzner, P. A. (2005) Identification of post-translational modifications by blind search of mass spectra. Nature Biotechnology **23**, 1562–7.